The Synthesis and Photophysical Properties of New Phosphorus-Containing Macromolecules

by

Benjamin Walter Rawe

MSci., The University of Bristol, 2011

A THESIS SUBMITTED IN PARTIAL FULFILLMENT OF

THE REQUIREMENTS FOR THE DEGREE OF

DOCTOR OF PHILOSOPHY

in

THE FACULTY OF GRADUATE AND POSTDOCTORAL STUDIES

(Chemistry)

THE UNIVERSITY OF BRITISH COLUMBIA

(Vancouver)

August 2017

Abstract

The thesis outlines the synthesis and photophysical properties of novel macromolecules that contain phosphorus atoms. Significantly, the fluorescence properties of the polymers prepared in this thesis are dependent on the chemical environment at phosphorus. These materials have the potential to be useful sensors for analytes that react with the phosphine moieties in these polymers.

Chapter 1 introduces conjugated polymers and details known examples of phosphorus-containing polymers of this class that have been previously reported. A particular focus is the synthesis of these materials, as well as their photophysical properties. The known examples of molecular phosphine sensors are also presented.

Chapters 2 and 3 focus on the anionic polymerization of phosphaalkene monomers to make novel poly(methylenephosphine)s, (PMPs) that contain fluorescent polyaromatic substituents. The synthesized polymers exhibited "turn on" fluorescence upon oxidation of the phosphorus centres. Notably, the C-pyrenyl PMP synthesized in Chapter 3 was also fluorescent in the solid state when the phosphine centres were oxidized.

Chapter 4 describes the synthesis and photophysical properties of poly(*p*-phenylenediethynylene phosphine)s, PPYPs, a new class of phosphorus-containing macromolecule. The polymers were prepared using a nickel-catalyzed coupling between phenyldichlorophosphine and dialkynes. The resulting materials displayed photophysical characteristics consistent with a degree of conjugation through the phosphorus centres within the polymer. Upon oxidation of the phosphorus atoms in PPYPs, "turn on" emission was observed. Remarkably oxidized PPYPs were also fluorescent in the solid state and therefore may have application as solid-state sensors or as OLEDs.

Chapter 5 describes the study of a fluorene-containing PPYP as a fluorescent sensor for metal analytes. Remarkably the polymer exhibited a substantial fluorescence increase upon coordination to gold and mercury ions whereas exposure of the polymer to other ions resulted in no fluorescence increase.

Chapter 6 provides a summary of the work contained within this thesis, and future directions for these projects are postulated.

Lay Summary

This thesis details the synthesis and characterization of new polymers that contain phosphorus atoms within the polymer backbone. There are only a few examples of such materials as they are difficult to prepare. This is because the methodology to make these materials is far less established compared to well-known polymers. Phosphorus-containing polymers are of interest as they are a unique class of chemical active polymer. The properties of these materials can be easily modified by the addition of chemicals that react with the phosphorus atoms within the polymer. Of particular focus is the change of the fluorescent properties of these materials when the phosphorus atoms within the polymer are reacted with analytes. Such materials have potential as chemical sensors to detect the presence of precious or heavy metals that bind to the polymer.

Preface

Sections of this work have previously been published in peer reviewed academic journals. Chapter 1 has sections of which have been published in *Chemical Society Reviews* in a review article featuring the synthesis and properties of main group-containing polymers. It was written in collaboration with Dr. Andrew M. Priegert, Dr. Spencer C. Serin and our supervisor Prof. Derek P. Gates. Andrew, Spencer and I contributed equally to the writing of the manuscript and the order of the authors in this publication is given alphabetically. Andrew M. Priegert, Benjamin W. Rawe, Spencer C. Serin and Derek P. Gates. Polymers and the p-block elements. *Chem. Soc. Rev.* **2016**, 45, 922.

Chapter 2 has been published as a full paper in *Chemical Science*. All synthetic work was carried out by myself apart from the phosphaalkene MesP=C(Phen)Ph (**2.1b**) and corresponding poly(methylenephosphine) (**2.2b**) which was prepared by Cindy P. Chun, a former member of the Gates group. Data to determine the molecular structures of **2.1a-2.1c** by X-ray crystallography was collected and solved by Dr. Joshua I. Bates and Amber M. Juilfs. I wrote manuscript, with guidance from my supervisor Prof. Derek P. Gates. Cindy P. Chun was consulted upon finalization of the manuscript. Benjamin W. Rawe, Cindy P. Chun and Derek P. Gates. Anionic polymerisation of phosphaalkenes bearing polyaromatic chromophores:phosphine polymers showing "turn-on" emission selectively with peroxide. *Chem. Sci.* **2014**, *5*, 4928.

Chapter 3 has been published as a full paper in *Organometallics*. This manuscript was written in collaboration with my supervisor, Prof. Derek P. Gates. Our collaborator Prof. Graham J. Bodwell (MUN) was consulted upon finalization of the manuscript. All synthesis and characterization of the reported materials was carried out by myself, apart from a portion of 1-

benzoylpyrene, which was prepared by Marc R. Mackinnon (MUN). I performed the computational calculations. All photophysical measurements were carried out by myself apart from the solid state fluorescence characterization of **3.2**·O, which was performed by Christopher M. Brown. Data to determine the molecular structure of **3.1** by X-ray crystallography was collected by Dr. Spencer C. Serin and solved by Dr. Brian O. Patrick. Benjamin W. Rawe, Christopher M. Brown, Marc R. MacKinnon, Brian O. Patrick, Graham J. Bodwell and Derek P. Gates, A C-Pyrenyl Poly(methylenephosphine): Oxidation "Turns On" Blue Photoluminescence in Solution and the Solid State. *Organometallics* **2017,** *36*, 2520.

Chapter 4 is written as a full paper for submission in a peer reviewed journal in due course. Sections of this chapter have been published as a communication in *Angewandte Chemie International Edition* and *Angewandte Chemie*. This manuscript was written in collaboration with Prof. Derek P. Gates. All synthesis was performed by myself, apart from polymers **4.1c,** **4.1c**·O and model compound **4.3c**·O, which were made by Michael R. Scott, an undergraduate working under my supervision. I performed the computational calculations. Christopher M. Brown performed the solid-state photophysical characterization of the reported materials within this chapter. The crystal for X-ray determination of **4.2a** was grown by Harvey K. MacKenzie while working under my supervision. The data to determine the molecular structure of **4.2a**·O and **4.3b**·O and **4.3c**·O by X-ray crystallography was collected and solved by Dr. Spencer C. Serin, Zeyu Han and Dr. Brian O. Patrick. Benjamin W. Rawe and Derek P. Gates, Poly(*p*-phenylenediethynylene phosphane): A Phosphorus-Containing Macromolecule that Displays Blue Fluorescence Upon Oxidation. *Angew. Chem. Int. Ed.* **2015**, *54*, 11438; *Angew. Chem.* **2015**, *127*, 11600.

Chapter 5 is being written as a communication for submission in a peer reviewed journal and will be submitted in due course. All the work presented in this chapter was undertaken by myself, apart from the synthesis of **5.2**·AuCl which was prepared by Harvey K. MacKenzie. The data to determine the molecular structure of $(Ph\text{-}C{\equiv}C)_2PhPAuCl$ by X-ray crystallography was collected by Harvey K. MacKenzie and Michael R. Scott

Chapter 6 was written by myself.

Table of Contents

List of Tables

List of Figures

List of Schemes

List of Abbreviations and Symbols

Å	angstrom (1×10^{-10} metres)
acac	acetylacetonate
APT	attached Proton Test (NMR spectroscopy)
Ar	aryl
b	block (copolymer)
Bn	benzyl
br	broad (NMR spectroscopy)
Bu	butyl
c	concentration
ca.	circa (about)
calc	calculated
cat.	catalytic
CCD	charge-coupled device
CCDC	Cambridge Crystallographic Data Centre
cf.	compare
cis	same side
co	copolymer
cod	cyclooctadiene
d	day(s)
	doublet (NMR spectroscopy)
dba	dibenzylideneacetone

DCM	dichloromethane
DEPT	distortionless enhancement by polarization transfer (NMR spectroscopy)
δ	chemical shift in parts per million (ppm)
DFT	density functional theory
DHB	2,5-dihydroxybenzoic acid
DMSO	dimethylsulfoxide
DP_n	number average degree of polymerization
DSF	dynamic sheet formed
Đ	dispersity
E	entgegen (configuration)
E_a	activation energy
ed.	edition
Ed. Eds.	editor(s)
EI	electron impact
Elem.	elemental
ε	molar extinction coefficient
equiv	equivalents
eV	electron volt
exo	outside
f	oscillator strength
Fc	ferrocenyl
FW	free weight

fwhm	full width at half maximum
GPC	gel permeation chromatography
$\{^1H\}$	proton decoupled (NMR spectroscopy)
HMBC	heteronuclear multiple bond correlation (NMR spectroscopy)
HSQC	heteronuclear single quantum correlation (NMR spectroscopy)
HOMO	highest occupied molecular orbital
HRMS	high resolution mass spectrometry
Hz	Hertz
i	iso (as in *i*-Pr)
in silico	by computational methods
in situ	in place or in the reaction
in vacuo	in a vacuum
init.	initiator
J	coupling constant (NMR spectroscopy)
K	Kelvin
Kα	spectral line
λ	wavelength
λ_{em}	wavelength of emission
λ_{ex}	wavelength of excitation
λ_{max}	maximum wavelength
λ_{onset}	onset of absorbance
LLS	laser light scattering

LRMS	low resolution mass spectrometry
LUMO	lowest unoccupied molecular orbital
μ	micro (10^{-6})
m/z	mass-to-charge ratio
m	milli (10^{-3})
	meter
	multiplet (NMR spectroscopy)
M	mega (10^{6})
	molarity (moles per liter)
M/I	monomer to initiator ratio
MALDI-TOF	matrix-assisted laser desorption/ionization-time of flight (mass spectrometry)
MALS	multi angle light scattering
Me	methyl
Mes	2,4,6 trimethylbenzene
Mes*	2,4,6 tri-*tert*-butylbenzene
MHz	megahertz
Min	minute
M_n	number average molecular weight
M_w	weight average molecular weight
MW	molecular weight
mol	mole(s)
n	normal (as in *n*-BuLi)

	principle quantum number
	number
n	nano
Naph	napthyl
NMR	nuclear magnetic resonance
o	ortho
OLED	organic light emitting diode
p	para
Φ	quantum yield
P / g	phosphorus per gram
PA	polyacetylene
PAni	polyaniline
PET	photoinduced electron transfer
Ph	phenyl
Phen	phenanthryl
ρ	density
PI	polyisoprene
PMP	poly(methylenephosphine)
PPE	poly(*p*-phenyleneethynylene)
ppm	parts per million
PPP	poly(*p*-phenylenephosphaalkene)
PPV	poly(*p*-phenylenevinylene)

PPYP	poly(*p*-phenylenediethynylene phosphine)
PT	poly(thiophene)
Pyr	pyrenyl
R	generic substituent
R_h	hydrodynamic radius
rf	retention factor
ROP	ring opening polymerization
RT	room temperature
S	Siemens
SADABS	Siemens area detector absorption correction program
SCE	saturated calomel electrode
t	tertiary
	triplet
τ	excited state lifetime
τ_{sld}	excited state lifetime in solid state
τ_{soln}	excited state lifetime in solution
TBAF	tert-*n*-butylammonium fluoride
TEM	transmission electron microscope
TEMPO	(2,2,6,6-tetramethylpiperidin-1-yl)oxyl
THF	tetrahydrofuran
tht	tetrahydrothiophene
TMP	thermomechanical pulp

TMSA	trimethylsilylacetylene
TNT	2,4,6-trinitrotoluene
trans	opposite side
UBC	University of British Columbia
UV	ultraviolet
UV/Vis	ultraviolet/visible
VAZO	1,1′-azobis(cyclohexanecarbonitrile)
vide infra	see below
w/w	weight to weight ratio
Z	zusammen (configurational)
Z	number of units in a cell (X-ray)

Acknowledgements

I thank Prof. Derek P. Gates for his insight, passion and encouragement throughout my years of study. Your attention to detail and out of the box ideas has made me a more complete scientist.

To the past and previous members of the Gates group, in particular Khatera Hazin, Michael Scott, Harvey MacKenzie, Anna Bennett, Andrew Priegert, Spencer Serin, Thomas W. Hey and Saeid Sadeh. You have each made the lab a more amicable place to work.

Thanks to Christopher Brown for collaborating with me on some of my projects. Your insight pushed these projects further.

I would like to thank Michael Scott, Harvey MacKenzie, Jeffery Suen and Ania Sergenko for your efforts while under my supervision. You have made me a better leader and decision maker.

I would like to thank the numerous support staff within the chemistry department, without which carrying out my research would be immeasurably more difficult. In particular, Brian Patrick, Paul Xia, Maria Ezhova, Marshall Lapawa, Emily Seo and Jane Cua.

I would like to thank Paloma Prieto for your support while writing, not to mention your help proofreading.

Dr. Natalie Fey and Dr. Gareth Owen for your mentorship in my first forays into chemical research. Sue Turrell and Jenny Varley for igniting my interest in chemistry.

My friends outside of the lab have kept me somewhat sane, in particular Stuart and Martina Chambers, Matthew and Zoe Beavis, Nicolas and Jessica McGregor, Leigh Renwick and Tim Smytheman.

My twin brother, Tom should be thanked for always supporting and believing in my ability to achieve great things.

My parents should probably get a mention as well. Much of who I am today is influenced by you both.

Here's to the ones who dream,

Chapter 1: Introduction

Without synthetic polymers, the world we live in would be unrecognizable. When the first fully synthetic polymer, Bakelite,[1] was discovered in 1907, a new class of man-made materials known as plastics was born. This initial discovery formed the foundation for the "modern plastic age" and these materials are widely regarded as one of the great scientific success stories of the 20th century. Through decades of synthetic development, many polymers have been invented that have desirable properties. Many of these materials have become commercial successes due to their unique properties and thus, have become ubiquitous in everyday life. Synthetic polymers are used in a wide range of applications including tires, lubricants, packaging materials, electronics and coatings, etc. Such is the demand for synthetic materials that an estimated 311 million metric tonnes of plastics were produced globally in 2015.[2] In spite of the ever increasing use of synthetic polymeric materials, most of their chemical structures only contain carbon, nitrogen, oxygen, and hydrogen.[3] To date, only two main group-containing polymers, polyphosphazene[4] and polysiloxane[5] (Figure 1.1) have been commercialized.

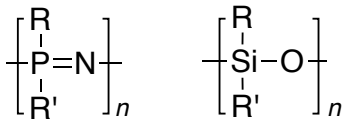

Figure 1.1: The chemical structure of polyphosphazene and polysiloxane. The substituents on phosphorus and silicon influence the physical and chemical properties of these polymers.

The incorporation of heteroatoms within macromolecules is of interest due to the interesting properties that may be imparted from elements that can have a diverse range of oxidation states and coordination number. The ability to easily modify the chemical environment of heteroatoms within a polymer may lead to materials with fascinating characteristics which

Versions of sections of this chapter have been published. Andrew M. Priegert, Benjamin W. Rawe, Spencer C. Serin and Derek P. Gates. Polymers and the p-block elements. *Chem. Soc. Rev.* **2016**, *45*, 922-953

find use in specialty applications.[6] The incorporation of phosphorus (III) atoms into polymers is of particular interest. This is because the chemically active nature of the P atoms (via the P lone pair) may give rise to a class of "functional" materials that respond to chemical stimuli. It is the goal of this research project to synthetize new phosphorus-containing macromolecules that are photophysically active. It is our hypothesis that such materials may have intriguing sensing properties as their photophysical properties may change upon modification of the phosphorus chemical environment.

1.1 π-Conjugation within Polymers

One of the most fascinating advances in materials science over the last 30 years has been the development of π-conjugated organic polymers. Each atom involved in the conjugated system is sp^2 (or sp) hybridized and has at least one p-orbital involved in π bonding. As each of these p-orbitals have the same symmetry, the electrons involved in π bonding are delocalized over the whole conjugated system rather than restricted to individual bonds. As π conjugation increases over a larger number of atoms, the energy difference between the π and π* levels decreases. The result is that the energy to promote an electron from the highest occupied molecular orbital (HOMO) to the lowest unoccupied molecular orbital (LUMO) decreases as the conjugated system increases in length. When this HOMO-LUMO energy difference becomes low enough, electrons can transition easily between these states and the material behaves as a semiconductor. Figure 1.2 depicts the relative energy levels of the π-π* transition in ethene and the longer chain *trans* alkenes (i.e. oligomers of *trans* polyacetylene) as determined by density functional theory. The HOMO-LUMO gap decreases from 5.63 eV in ethene (n = 1) to 3.17 eV in hexatriene (n = 3).[7] As the alkene chain increases in length, the HOMO-LUMO energy decreases until a limit is

reached. For *trans* polyacetylene this limit is reached at a chain length of 32 repeat units. At this point the energy between the HOMO and LUMO is 1.32 eV.

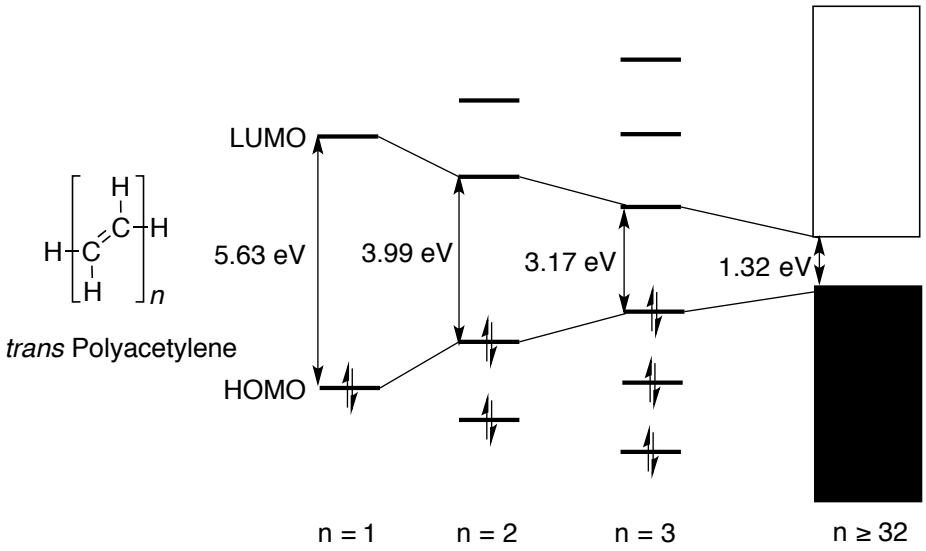

Figure 1.2: Energy levels (π and π^* only) of n=1, n=2, n=3 and n≥32 of *trans* polyacetylene.

As the chain length of a conjugated polymer increases the HOMO-LUMO energy difference may decrease so that its magnitude may approach the energy of visible light. This means that the polymer can absorb photons and an electron can be excited from the HOMO to the LUMO. As the polymer absorbs visible light it becomes coloured. An electron in an excited state can relax back to the ground state through fluorescence. A variety of conjugated polymers have been developed to fashion materials with a range of interesting and useful electronic properties. The most studied of these are described in the following section.

1.1.1 Common Organic Conjugated Polymers

Polyacetylene (**PA**, Figure 1.3) was the first example of a semi-conducting organic material. By using a Ziegler-Natta catalyst, acetylene gas molecules were polymerized to make a solid flexible film.[8] Upon doping with iodine, the resulting material underwent a substantial increase in conductivity (up to 3800 S m^{-1}). At the time (in 1977), this was an unprecedented phenomenon for organic materials (*cf.* conductivity of polyethylene ≈ 1×10^{-15} S cm^{-1},[9] conductivity of metals ≈

1×10^{6}-1×10^{8} S cm^{-1}). Unfortunately, **PA** has low processability and chemical stability, which has precluded its usefulness. It is completely insoluble in organic solvents and reacts with atmospheric oxygen upon exposure to air.[10] Nevertheless, Heeger, MacDiarmid and Shirakawa were recognized with the Nobel prize for chemistry in 2000 "for the discovery and development of conductive polymers."[11] Following the discovery of the novel electronic characteristics displayed by doped **PA**, efforts have focused on developing conjugated polymers that display similar semiconducting properties but are solution processable. To this end, several polymer systems have been discovered and tested for a variety of different electronic applications. Figure 1.3 contains the generic chemical structures of the most studied conjugated polymers.[12-14] It should be noted that all of these macromolecules contain backbones that are composed of organic functionalities only (with the exception of **PT**, which contains a single sulfur atom in its repeat unit).

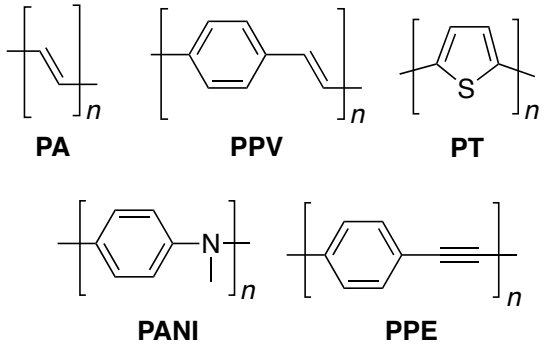

Figure 1.3: Heavily studied organic π-conjugated polymers

The most studied conjugated polymers are poly(*p*-phenylenevinylene)s (**PPV**), and polythiophenes (**PT**), (Figure 1.3). Historically **PPV** found fame as it was the first polymer used to construct an organic light emitting diode (OLED) in 1990[15] and since this time a variety of **PPV** derivatives have been made that exhibit electroluminescence across the whole visible spectrum.[16] Derivatives of **PT** have been used to make a plethora of electrochemical devices, but

special attention has been focused on its incorporation into photovoltaic devices.[17-19] Polyaniline, **PANI** is a conjugated macromolecule that features sp^2 hybridized nitrogen atoms in the main chain. As the nitrogen atoms have a trigonal planar geometry, their lone pair electrons are delocalized throughout the π system in the polymer backbone. Polyanilines are attractive materials for chemosensing applications as they can be easily oxidized or reduced and each oxidation state has distinctly different colours.[20, 21] **PANI** derivatives are highly conductive and therefore have been studied for use as antistatic coatings,[22-24] or as flexible electrode materials.[25-27] Poly(*p*-phenylene ethynylene)s, (**PPE**s) are "rigid rod" polymers due to the linear nature of the alkyne groups.[28] These materials have been incorporated into OLED devices[29] and show a promising application as colormetric chemosensors.[30, 31] An example of this is the incorporation of **PPE**s in the Fido® explosives trace sensor, which can detect explosives in parts per quadrillion.[32]

The preceding paragraphs give merely a snapshot into the diverse field of conjugated polymers. Their intriguing electronic properties have led to their study across many fields of science and engineering. The fascinating chemical and physical characteristics imparted by the presence of inorganic groups may yield materials with exciting properties that are not attainable to purely organic systems. Given the significant promise of these materials, it is somewhat surprising that the development of new structures that incorporate main group elements within polymer structures has been sluggish. Perhaps the largest reason for the slow development of conjugated polymers that incorporate main group elements is the significant difficulty in synthesizing these materials. Often well-established polymerization protocols to synthesize organic polymers are incompatible with main group element-containing species. This is often due to the synthetic difficulty of preparing appropriate monomers for polymerization or the

incompatibility of the polymerization reaction conditions with main group functionalities. Overcoming this significant synthetic barrier is a crucial first step in developing new materials. Once the synthesis of the polymer has been achieved, the role that main group elements have on the properties of these new materials can be better understood. Of particular interest is the incorporation of phosphorus atoms within a conjugated polymer. This is because the unique functionality of the phosphorus moieties may be exploited to make a chemically active material with easily modifiable electronic properties.

1.2 Goals of the Project

The key objective of the projects contained in this thesis was to synthesize and characterize new phosphorus-containing polymers with photophysical properties that are dependent on the chemical environment of the phosphorus atoms. The project necessitated the development of new synthetic routes to P-containing polymers in an effort to synthesize materials containing new functionalities and unprecedented structural motifs. Upon success of these goals, this project would make a significant contribution to synthetic main group polymer chemistry. It was also a goal to investigate these new polymers to gain an understanding of what regulates the photophysical properties of P-based materials. This would enable a future worker to develop these projects further towards application driven sensing targets.

1.3 Phosphorus-Containing Conjugated Polymers

In contrast to the aforementioned conjugated polymers and derivatives that have received a lot of attention since the discovery of **PA** (Figure 1.3), the synthesis of conjugated polymers that incorporate phosphorus atoms into the backbone remains a relatively unexplored avenue of research. This is partly due to the slow development of synthetic routes to make such materials. The following sections will review the known examples of phosphorus-containing polymers that

exhibit electronic delocalization throughout the main chain. The work contained in this thesis adds to these known examples.

Broadly speaking, electronic delocalization through phosphorus atoms is achieved through the implementation of one of two different structural motifs. One motif features unsaturated phosphorus-carbon or phosphorus-phosphorus bonds. Analogous to traditional conjugated organic polymers (i.e. those described in section 1.1.1), these polymers have a π system throughout the backbone that incorporates phosphorus atoms (depicted in Figure 1.4a). The other motif involves phosphorus atoms that are singly bonded to an adjacent π system (depicted in Figure 1.4b, 1.4c and 1.4d). An overriding consensus in the literature on which orbitals contribute to this conjugation has not been found. Common hypotheses are that the phosphorus lone pair can contribute into the π system (Figure 1.4b),[33-36] or that the P-C σ (or σ*) orbitals can overlap with the adjacent π framework (Figure 1.4c and d). This is possible by the greater radial extension of phosphorus' atomic (and therefore molecular) orbitals compared to carbon.[37, 38] σ-σ* orbital interactions are commonly observed in the bonds formed by main group elements,[39, 40] perhaps most famously with polysilanes. It is the presence of a σ-σ* framework that which gives rise the intriguing electronic properties in these polymers.[6] It should also be noted that phosphorus ligands are well known to undergo π backbonding from filled metal d orbitals into P-C σ* orbitals.[41]

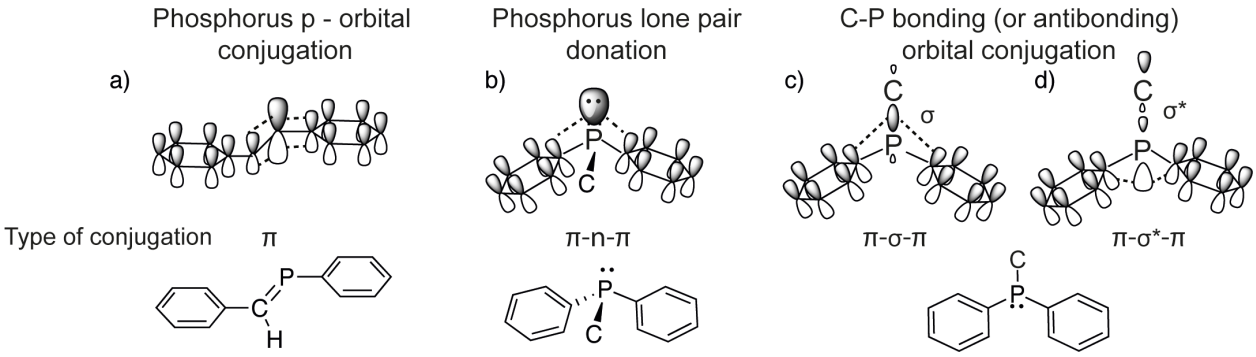

Figure 1.4: Electronic conjugation involving phosphorus atoms.

a) π – conjugation involving a purely p-orbitals through an unsaturated system b) π-n-π conjugation; donation of the phosphine lone pair into adjacent π systems c) π-σ-π conjugation; contribution of P-C σ bond into the π system. d) π-σ*-π conjugation; contribution of P-C σ* orbital into the π system.

1.3.1 Phosphorus-Containing Macromolecules Possessing π-Delocalization Through the Main Chain.

A polymer that incorporates phosphorus atoms within a π-conjugated framework requires the presence of P=C or P=P bonds throughout the main chain. The weak bond strength of these π bonds, due to the poor overlap of 3p-2p (P=C) / 3p-3p (P=P) orbitals makes the synthesis of compounds incorporating these functionalities a formidable synthetic challenge. Without a large substituent on phosphorus, the double bond is thermodynamically and/or kinetically unstable and breaks, resulting in dimerization or oligomerization.[42] Despite this difficulty, polymers featuring P=C and P=P bonds throughout the main chain have been reported.

The first example of a linear polymer containing multiple bonds involving a low-valent heavier main group element was poly(*p*-phenylenephosphaalkene) (PPP), a phosphorus analogue of poly(*p*-phenylenevinylene) (PPV) (Scheme 1.1).[43] Heating 1,4-bis(disilylphosphino)benzene and tetramethylterephthaloyl chloride afforded **1.1a** with an approximately equal ratio of *E*- to *Z*-configurations at the P=C bonds. Employing a monomer with a bulkier substituent on phosphorus allowed for significantly greater stereoselectivity, such that polymer **1.1b** was

isolated exclusively in the *Z*-configuration.[44] The air-sensitivity of **1.1a** and **1.1b** precluded determination of the absolute molecular weight by GPC, however end-group analysis by ^{31}P NMR integration revealed modest molecular weights (M_n = 2,900 – 10,500 g mol^{-1}). Interestingly, the UV/Vis spectra of **1.1a** (328 - 338 nm) and **1.1b** (394 nm) are bathochromically shifted with comparison to model compounds, consistent with a degree of π-conjugation throughout the backbone. Polymer **1.1a** exhibited weak fluorescence at 445 nm, however the emissive properties of **1.1b** were not reported.

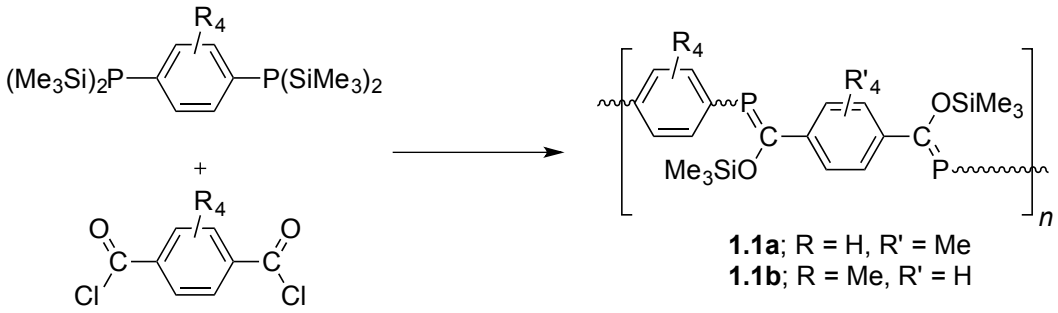

Scheme 1.1: Synthesis of poly(*p*-phenylenephosphaalkene)s by employing the Becker reaction of a bis(disilylphosphine) and a diacyl chloride).

Phosphaalkene-containing PPV analogues have also been accessed by employing the phospha-Wittig reaction as the P=C bond forming step (Scheme 1.2).[45] In this approach, a bis(dichlorophosphine) was first treated with PMe_3 in the presence of zinc to generate a phospha-Wittig reagent. Subsequent addition of a dialdehyde afforded polymer **1.2** with phosphaalkene moieties in predominantly the *E*-configuration. The molecular weights of the synthesized polymers were determined by end-group analysis (M_n = 6,500 g mol^{-1}). PPP **1.2** has an absorbance maximum of 445 nm that is substantially red-shifted by comparison to **1.1a** and **1.1b** and exhibits weak fluorescence at approximately 540 nm.

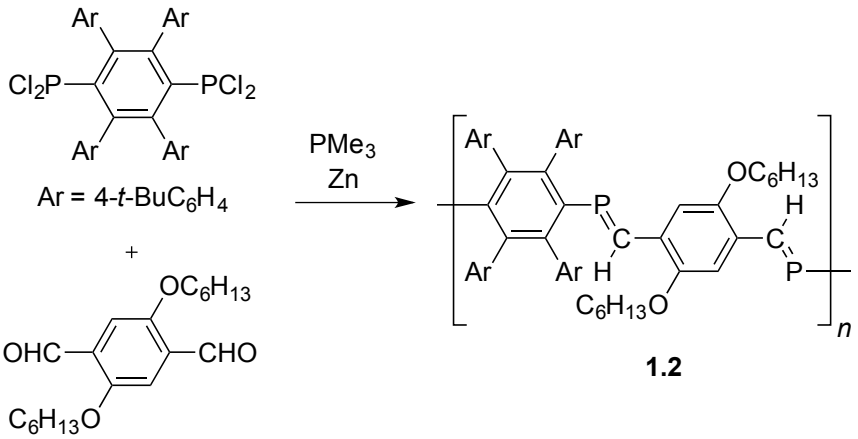

Scheme 1.2: Synthesis of a poly(*p*-phenylenephosphaalkene) by the phospha-Wittig reaction.

The phospha-Wittig reaction has also been used to synthesize the fascinating diphosphene-containing polymer **1.3**, the first example of a polymer containing a multiple bond between heavy main group elements within the backbone.[46] In this case, the phospha-Wittig intermediate was either photolyzed or thermolyzed to afford **1.3** (Scheme 1.3, M_n = 5,900 g mol^{-1}, Đ = 2.1). Intriguingly, photophysical measurements revealed that unlike **1.2,** this red coloured polymer was not fluorescent in solution.

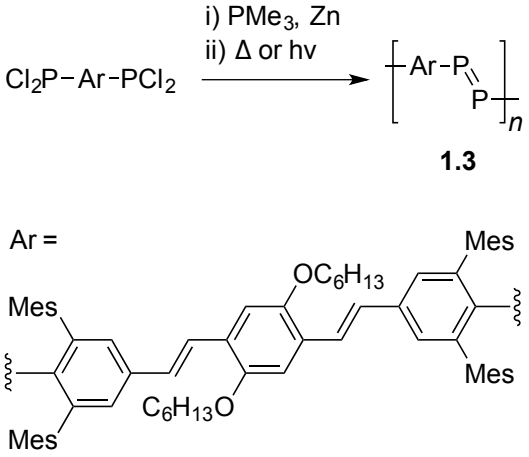

Scheme 1.3: Synthesis of a diphosphene-containing polymer by a phospha-Wittig reaction.

In addition to polymers, a variety of molecular conjugated phosphaalkenes have been synthesized to form photophysically active materials. A particularly common motif is the incorporation of a phosphaalkene moiety adjacent to alkynes to make highly conjugated

materials that incorporate phosphorus atoms. An example of this is **1.4**, a diphosphaalkene, where each phosphaalkene unit is separated by four alkynes.[47] In the first synthetic step, a single phosphaalkene is made by base-induced elimination. Deprotection of the alkyne followed by copper mediated homocoupling results in product (Scheme 1.4). Compound **1.4** shows an absorbance maximum at 485 nm. Like the aforementioned polymers (**1.1-1.3**) the absorbance maxima of **1.4** is bathochromically shifted when compared to its precursors and related smaller conjugated systems. Based on electrochemical measurements the authors predicted that the electron density in the LUMO resided on the phosphaalkene moieties, indicating the important role of the P=C bond on the molecule's electronic properties.

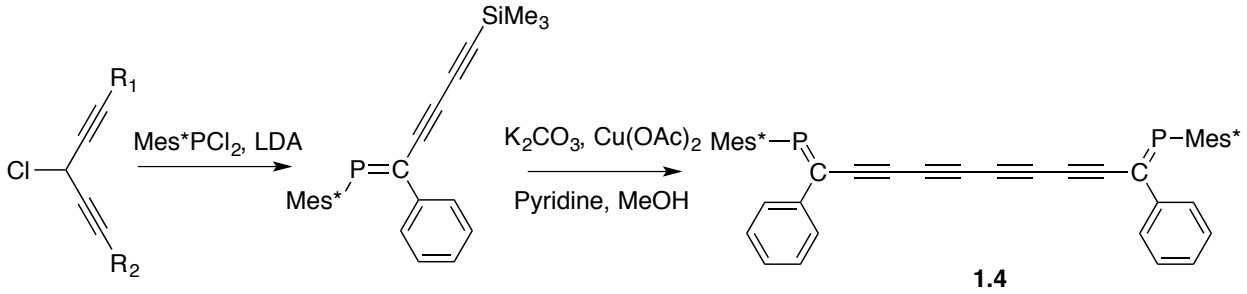

Scheme 1.4: The synthesis of conjugated molecular diphosphaalkene 1.4.

Similar derivatives (**1.5a-1.5d,** Figure 1.5) have been synthesized, which feature an aromatic substituent between the second and third alkyne units. The resulting materials are highly coloured, and have absorption properties are directly correlated to the identity of the linker, with the anthracenyl ($\lambda_{max} \approx 515$ nm) and napthyl ($\lambda_{max} \approx 445$ nm) derivatives (**1.5c** and **1.5d**) having the highest wavelength absorptions.[48] The authors report that the *para*-substituted bridged phosphaalkenes (i.e. **1.5b-1.5d**) have absorption maxima that are bathochromically shifted compared to their alkyne monomers and precursors, indicating the importance of the phosphaalkene moiety on the absorption properties. **1.5a-1.5d** are non emissive at room

temperature. A similar coupling strategy has been used to make **1.6** and **1.7**. In this case the phosphaalkene moieties are *exo*-substituents.[49]

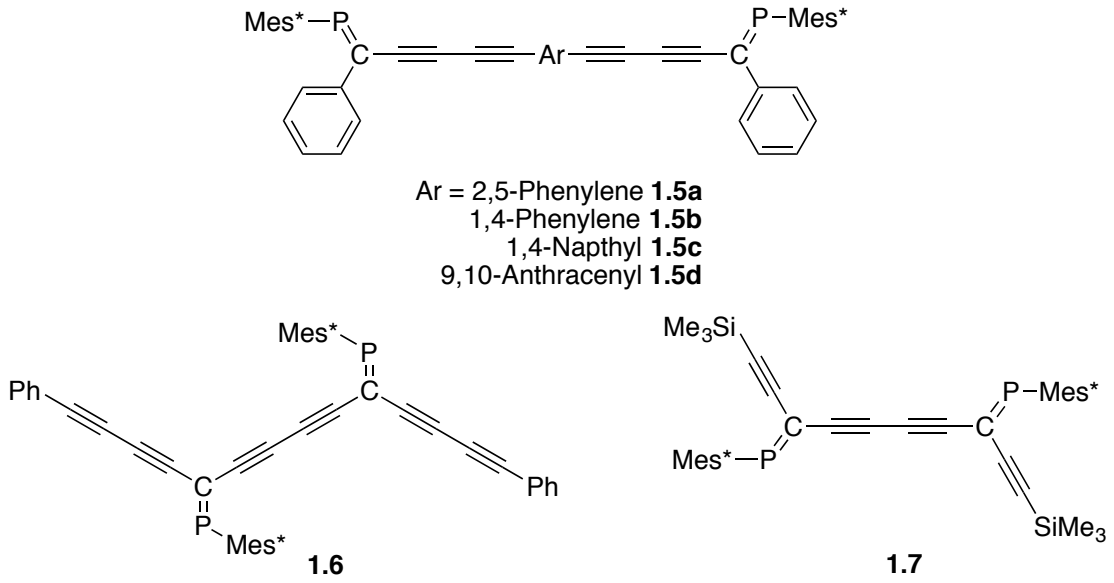

Figure 1.5: Examples of molecular conjugated phosphaalkenes

1.3.2 Other Phosphorus-Containing Conjugated Polymers.

The following section details the synthetic strategies that have been used to make phosphorus-containing polymers where the P atoms within the polymer backbone are not formally π-bonded to other atoms. Many of these polymers are of interest to this project as they have intriguing photophysical properties. Where appropriate these details will be mentioned.

1.3.2.1 Poly(arylene/vinylene/ethynylene phosphine)s

Polymer **1.8**, the first well-characterized example of a poly(arylenephosphine), was prepared by using nickel-catalyzed homocoupling (Scheme 1.5, M_n = 15,300 g mol^{-1}, Đ = 1.65).[50] Similar polymers have been synthesized by nucleophilic aromatic substitution reactions.[51, 52] Transition metal-catalyzed hydrophosphorylation has also been used to prepare polymers with both arylenephosphine and vinylenephosphine moieties in the main chain.[53]

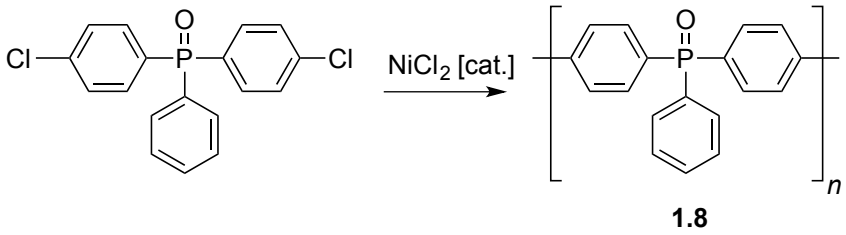

1.8

Scheme 1.5: Nickel-catalyzed homocoupling of bis(4-chlorophenyl)phenylphosphine oxide to afford a poly(arylenephosphine oxide).

The first true phosphorus analogue of polyaniline, poly(*p*-phenylenephosphine) **1.9**, was synthesized by palladium(0)-catalyzed cross-coupling of 1,4-di-iodobenzene with a primary phosphine to afford low molecular weight materials (Scheme 1.6, M_n = 1,300 – 3,100 g mol^{-1}, Đ = 1.3 – 1.5).[33, 34] This approach was extended to the synthesis of a series of poly(*p*-phenylenephosphine)/polyaniline copolymers.[35]

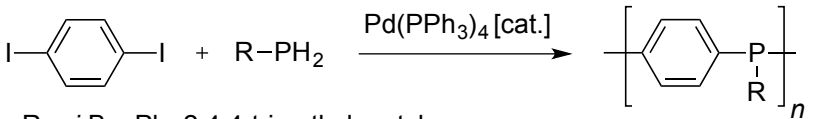

R = *i*-Bu, Ph, 2,4,4-trimethylpentyl

1.9

Scheme 1.6: Synthesis of poly(*p*-phenylenephosphine)s by palladium-catalyzed cross-coupling.

These materials have received considerable attention due to their fascinating photophysical and electronic properties. Interestingly, in each case a bathochromic shift of absorbance was observed compared to model compounds. The authors concluded that this was due to electronic delocalization through the phosphine moiety. Upon chemical oxidation of the phosphine to the phosphine oxide the same shift was not observed. This indicates that the phosphine lone pair electrons are involved in conjugation throughout the polymer. This example illustrates the dependence of the chemical environment of phosphorus on the polymers electronic properties.

Related macromolecules that incorporate unsaturated organic moieties next to phosphorus atoms include macromolecules composed of alkenylphosphine backbones. The

anionic ROP of a phosphirene afforded poly(vinylenephosphine) **1.10**, the first example of a polymer containing only vinylene and phosphine units in the main chain (Scheme 1.7 M_n = 1,700 – 18,000 g mol^{-1}, Đ = 1.23 – 1.58).[54]

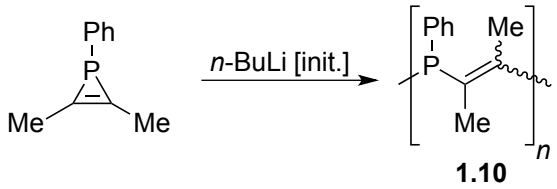

1.10

Scheme 1.7: Anion-initiated ROP of a phosphirene to yield a poly(vinylenephosphine).

Subsequently, an alternate methodology was developed to produce poly(vinylenephosphine)s. Treatment of *cyclo*-(PMe)$_5$ with phenylacetylene in the presence of the radical initiator AIBN resulted in polymer **1.11** (Scheme 1.8, M_n = 2,500 g mol^{-1}, Đ = 1.25).[55] This strategy was adapted from earlier work on the synthesis of polymers containing heavier group 15 congeners, however, lower molecular weights were observed for the phosphorus-containing polymer.

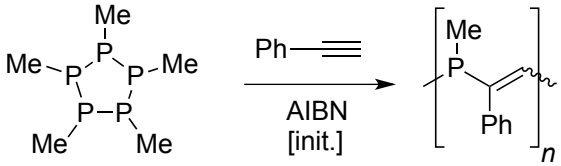

1.11

Scheme 1.8: Radical copolymerization of a cyclo-pentaphosphine with a primary alkyne to generate a poly(vinylenephosphine).

1.3.2.2 Poly(phosphole)s

The incorporation of phosphole moieties into extended π-conjugated structures has received considerable attention due to the fascinating photophysical and electronic properties imparted by this P-heterocycle. Such is the excitement in these compounds, that a large number of

optoelectonic devices have been developed that contain phosphole derivatives as their photoactive layer.[56]

The first phosphole-containing polymer (**1.12**) was synthesized by oxidative coupling using zirconocenes (Scheme 1.9).[57] The resulting metallacycle-containing polymer was subsequently treated with dichlorophenylphosphine to generate the phosphole-containing macromolecule with moderate regioselectivity (M_n = 6,200 g mol^{-1}, Đ = 2.6). Polymer **1.12** was found to be fluorescent in solution (λ_{ex} = 308 nm, λ_{em} = 470 nm), albeit with a moderate quantum yield (Φ = 0.09).

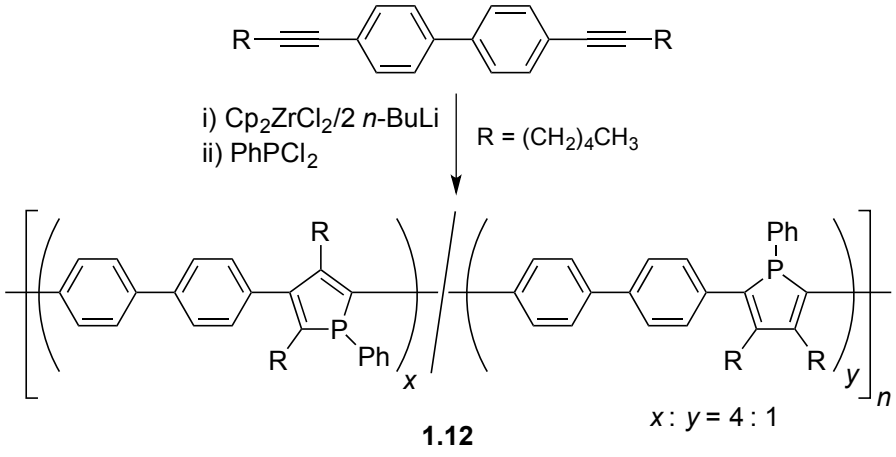

Scheme 1.9: Synthesis of a phosphole-containing polymer by zirconocene-mediated oxidative coupling.

A more common strategy is to synthesize and isolate the phosphole-containing monomer first, rather than forming the phosphole moieties in the polymerization step. Zirconocene coupling to make the phosphole-containing monomer, followed by a Sonogashira coupling was used to afford a series of arylenephosphole-alkynylarene polymers **1.13a-1.13c** (M_n = 6,800 – 10,200 g mol^{-1}, Đ = 1.3 – 1.5, Scheme 1.10).[58] Each derivative had similar absorption properties (λ_{max} = 382-414 nm) but substantially different Stokes shifts. Alkoxy derivatives **1.13a** and **1.13b** showed bright blue-green coloured emission (λ_{em} = 487 and 490 nm) at a higher wavelength than

the fluorenyl-containing derivative **1.13c** (λ_{em} = 435 nm) demonstrating that the emission of these materials can be tuned by varying the identity of the aryl comonomer.

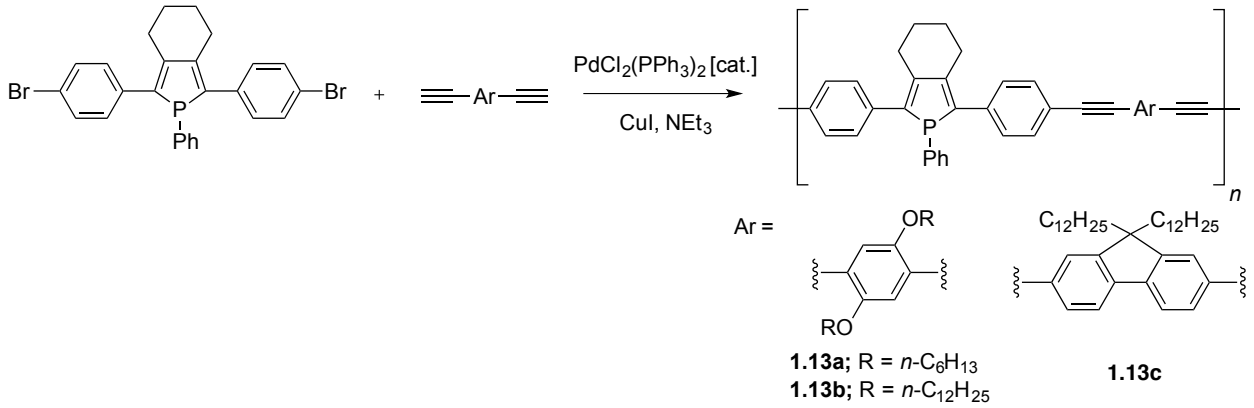

Scheme 1.10: Synthesis of a phosphole-containing polymer by Sonogashira coupling.

Classic synthetic routes to polythiophenes such as electropolymerization are not compatible with phosphole functionalities. This has prompted researchers to turn their attention towards synthesizing hybrid systems that combine the properties of phospholes with the well-developed chemistry of thiophenes. This has been demonstrated by synthesizing 2,5-bis(2-thienyl)phospholes followed by electropolymerization to yield insoluble polymeric films (**1.14**) (Scheme 1.11).[59, 60] The polymer bearing non-functionalized phosphole moieties was initially only accessible by the decomplexation of gold(I)-coordinated polymer **1.14e**.[61] However, in a subsequent report, it was found that a non P-functionalized 2,5-bis(3,4-ethylenedioxythiophene)phosphole derivative could successfully be electropolymerized.[62] In each of these derivatives it was found that both the absorption and emission properties of **1.14a-1.14e** were considerably different from each other. Specifically, the authors noted a significant bathochromic shift of the UV-Vis spectra ($\Delta\lambda_{onset}$ = 38 nm) when comparing **1.14b** to the parent phosphine polymer, and suggested the use of these polymers as elemental chalcogenide sensors.[61] It is clear that the chemical environment of the phosphorus atoms has an important effect on the photophysical properties of these materials.

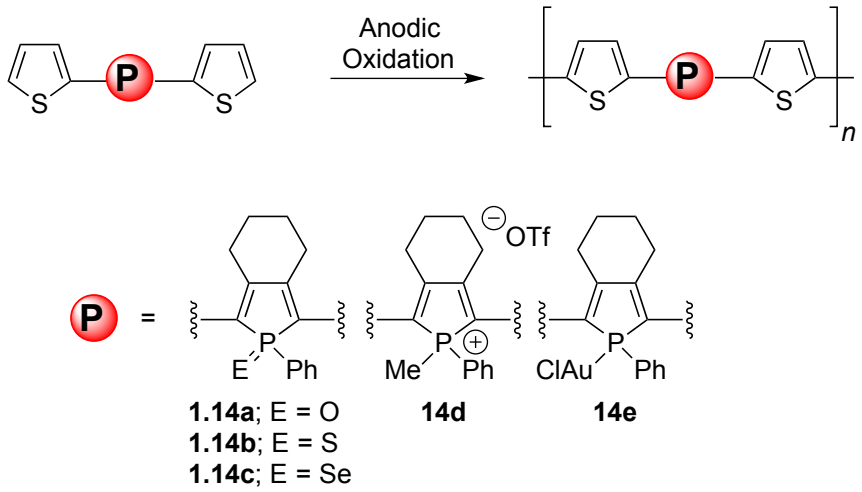

Scheme 1.11: Electropolymerization of 2,5-bis(2-thienyl)phospholes.

Dithienophospholes, in which two thiophene rings are annulated to a phosphole core, can be incorporated into polymers to provide novel fluorescent materials such as **1.15** (Figure 1.6).[63, 64] Polymers incorporating this rigid tricyclic system have been synthesized in high molecular weights (up to M_w = 871,000 g mol^{-1}). The two bis(thienyl)phosphole moieties in **1.15** emit two different colours (orange, λ_{em}= 601 nm, and blue, λ_{em}= 460 nm). When the amino moieties in **1.15** are protonated, the attached bis(thienyl)phosphole unit emits green coloured emission (λ_{em}= 524 nm). The different coloured emission from each chromophore has been utilized to make a polymeric material that emits close to white light in both solution and solid state with a high fluorescence quantum yield (up to Φ = 0.74).[64]

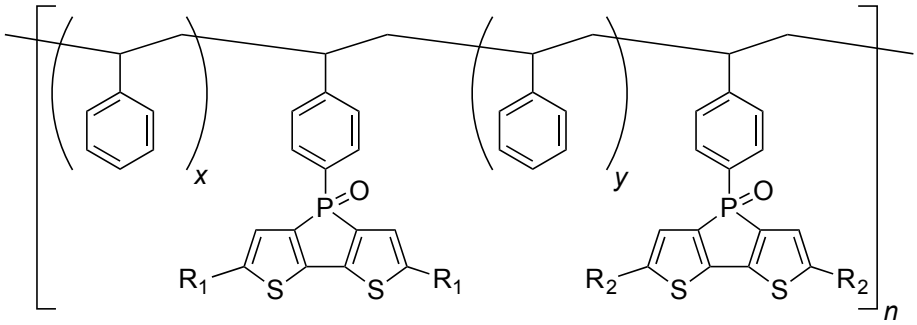

R_1 = TBDMS; R_2 = 4-(NMe_2)C_6H_4

1.15

Figure 1.6: Multi chromophore-containing styrene-dithienophosphole copolymer.

Using a series of transition metal catalyzed coupling strategies including Stille coupling,[65] platinum-catalyzed dehydrocoupling,[66] and Suzuki coupling,[67] polymers containing dithienophosphole units in the main chain have been accessed (**1.16-1.18**, Scheme 1.12). In some cases poor solubility precluded extensive molecular weight analysis of the polymers, however the Suzuki coupling route afforded **1.18** in moderate molecular weight and dispersity (M_w = 9,800 g mol^{-1}, Đ = 1.7). Polymers **1.16-1.18** showed absorption at higher wavelengths than their corresponding model compounds and exhibited fluorescence in the visible region (λ_{em} = 555 (**1.16**), 459 (**1.17**) and 485 nm (**1.18**)). Polymer **1.18** also exhibited green-coloured fluorescence in the solid state and the wavelength of absorbance and emission maxima are red shifted when compared to solution. This shift was attributed to intermolecular π-stacking interactions.

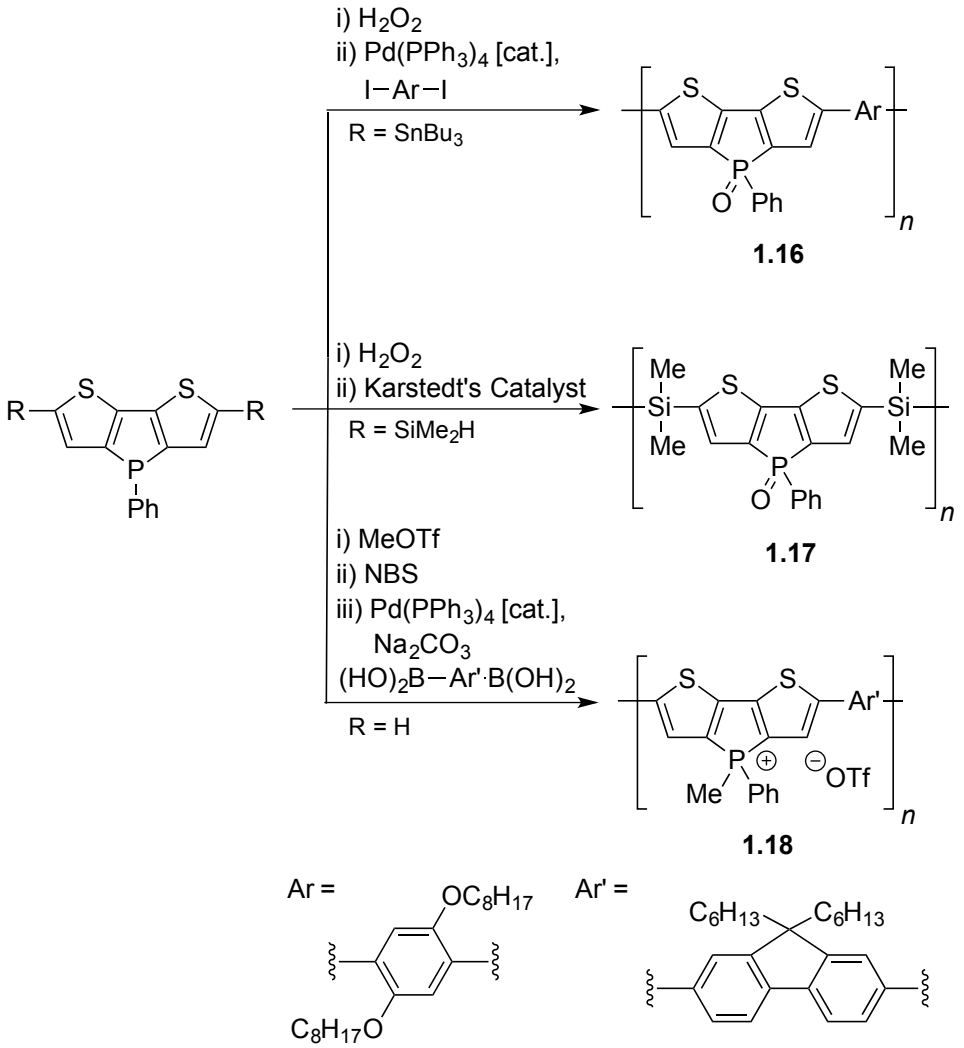

Scheme 1.12: Synthetic routes to polymers containing the dithienophosphole motif.

The phosphorus analogue of fluorene, dibenzophosphole, remains a relatively underexplored motif in main-group polymer chemistry. In a singular study, dibenzophosphole/fluorene copolymers were synthesized by Suzuki coupling (Scheme 1.13, M_n = 9,500 – 15,400 g mol^{-1}, Đ = 1.1 – 2.3).[68] The degree of incorporation of dibenzophosphole oxide units into the polymer was calculated by integration of the ^1H NMR spectrum and was determined to be 7 mol% in **1.19**. The absorbance spectra of **1.19** and its oxidized derivative revealed a slight red shift by comparison to the homo-fluorene polymer, suggesting that the presence of dibenzophosphole moities did not inhibit conjugation. Both **1.19** and its oxide were

fluorescent and exhibited near identical wavelength maxima (λ_{max} = 438, 462 and 492 nm) and good quantum yields (Φ = 0.52-0.53). Polymer **1.19** also exhibits blue coloured electroluminescence whereas **1.19**·O showed weaker white coloured emission.

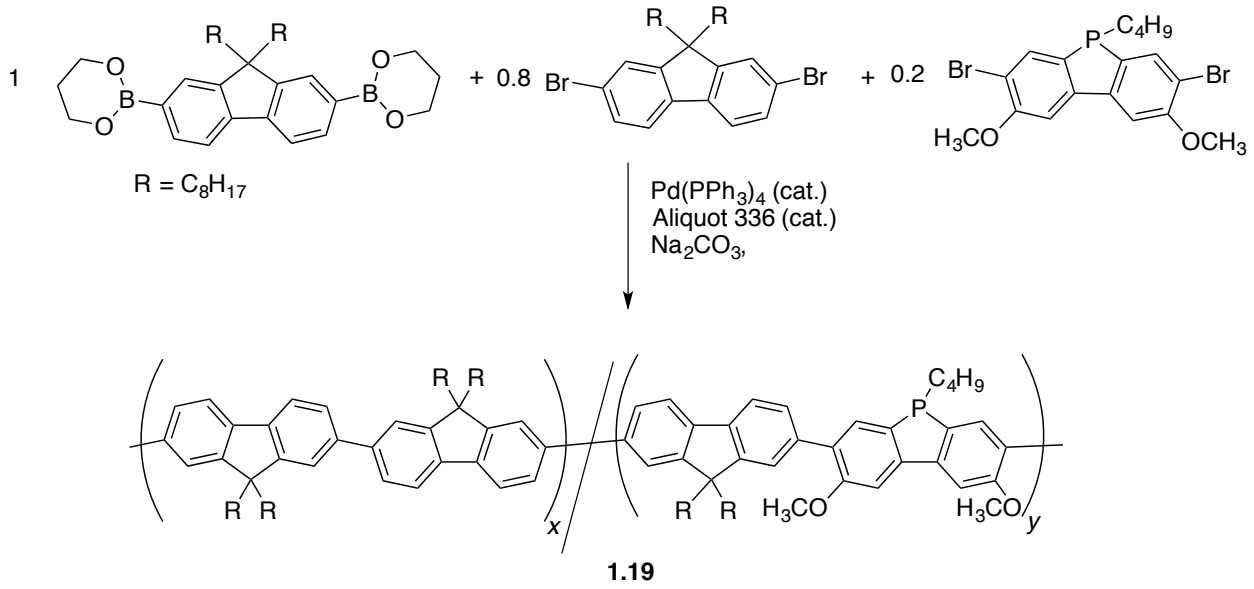

1.19

Scheme 1.13: Synthetic pathway to dibenzophosphole-containing copolymer 1.19

Recently, in a landmark study, the first example of a homopolymer containing only *P*-oxide phosphole rings, **1.20**, was reported.[69, 70] This material was prepared by Stille-type cross-coupling of phosphole oxide comonomers affording the moderate molecular weight polymer (M_n = 13,000 g mol^{-1}, Đ = 2.3, Scheme 1.14). Efforts to reduce the phosphorus(V) moiety to phosphorus(III) were unsuccessful. The deep blue coloured polymer **1.20** undergoes a broad absorption at 655 nm, a substantially higher wavelength than the related dimeric (λ_{max} = 463 nm) and trimeric (λ_{max} = 511 nm) phospholes. Unlike these model compounds the poly(phosphole oxide) was non-fluorescent in solution. In a related study, the analogous homopolymerization of *P*-alkanesulfonylimide phosphole provided access to poly(phosphole)s with P=NR rather than P=O moieties and shows similar photophysical properties.[70]

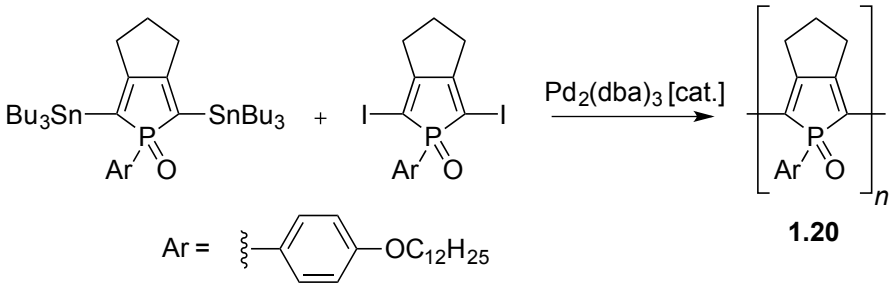

Scheme 1.14: Synthesis of a poly(phosphole oxide) 1.20 by Stille-type cross-coupling.

1.4 Poly(methylenephosphine)s

The following section discusses the synthesis and chemical properties of poly(methylenephosphine)s (PMPs). Although these polymers are not conjugated, the synthesis of PMPs with fluorescent pendent groups provides fascinating materials whose photophysical properties can be modulated based on the chemical environment of the phosphorus atoms. This work forms the basis of the experimental material in Chapters 2 and 3 and is described in the following section.

1.4.1 Synthesis of PMPs

The most important method of producing commodity polymers is by the addition polymerization of the C=C bond of olefins. The addition polymerization of a P=C bond in a phosphaalkene was accomplished in 2003 by Gates *et al.*[71] Specifically, the polymerization of MesP=CPh_2 afforded poly(methylenephosphine) (PMP, **1.21**). Polymer **1.21** was first isolated from the residue that remained after the distillation of the phosphaalkene monomer. In the same report, the radical- and anion-initiated polymerizations afforded samples of **1.21** with near-identical spectroscopic properties (Scheme 1.15). Shortly after, the radical-initiated copolymerization of MesP=CPh_2 and styrene (**1.22**, Scheme 1.15)[72] was reported to make random copolymers.

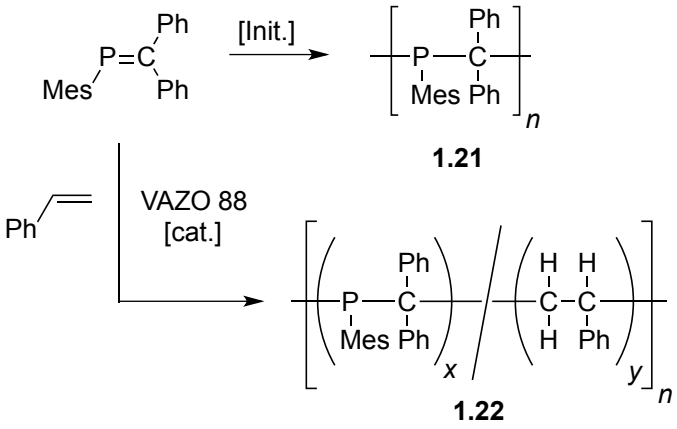

Scheme 1.15: Addition homo- and copolymerization of MesP=CPh$_2$ to yield poly(methylenephosphine) 1.21 and poly(methylenephosphine)-*co*-polystyrene 1.22.

Mass spectrometric investigations of oligomers prepared by treating MesP=CPh$_2$ with MeLi as initiator (25 mol%) provided the first evidence for chain growth polymerization in solution at ambient temperature.[73] Subsequently, the room temperature anionic-initiated polymerization of phosphaalkenes using *n*-BuLi was shown to follow a living mechanism. PMPs **1.23a-1.23b** were prepared with controlled molecular weights and low dispersity (M/I = 25:1-100:1, M_n = 8,900 – 29,600 g mol^{-1}, Đ = 1.04 – 1.15) (Scheme 1.16).[74] Employing living polystyrene as the anionic initiator afforded polystyrene-block-poly(methylenephosphine) copolymers (**1.24**, Scheme 1.17). These novel copolymers were made into films (Figure 1.7). Detailed studies of the kinetics of the living anionic polymerization of MesP=CPh$_2$ allowed for the determination of the activation energy for propagation (E_a = 14.0 ± 0.9 kcal mol^{-1}), one of the largest recorded for an addition polymerization.[75]

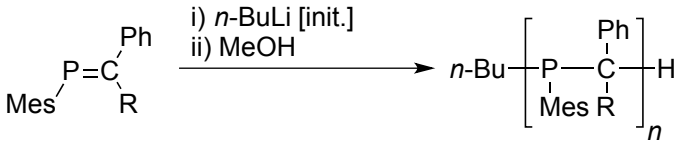

Scheme 1.16: Anionic polymerization of substituted phosphaalkenes.

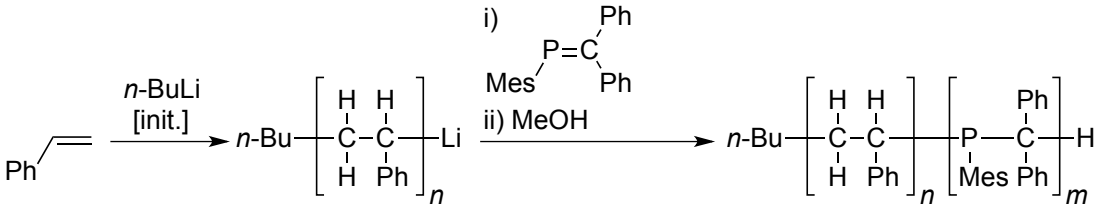

Scheme 1.17: Preparation of polystyrene-block-poly(methylenephosphine) by living anionic polymerization.

Figure 1.7: Film cast from a block copolymer of phosphaalkene and styrene. Photograph provided courtesy of Dr. E. Conrad.

As long as the phosphorus carbon bond is kinetically stabilized with sterically encumbering substituents, phosphaalkenes bearing a variety of functional substituents can be polymerized. To this end, the ferrocene-containing monomer, MesP=C(Fc)Ph, has been anionically polymerized to afford the novel redox-active PMP **1.23c** (M_n = 9,500 g mol^{-1}, Đ = 1.21, $\Delta E_{1/2}$ = 0.41 V vs. SCE, Scheme 1.16).[76] Another example illustrating the structural diversity possible for PMPs is the polymerization of enantiomerically pure phosphaalkenes.

Specifically, the chiral phosphaalkene-oxazoline[77] was copolymerized with styrene to give a phosphine-containing polymer bearing enantiomerically pure substituents (**1.25**: M_w = 7,400 g mol^{-1}, Đ = 1.15) (Scheme 1.18).[78] The phosphaalkene incorporation in copolymer **1.25** was estimated by elemental analysis to be 13 mol% and the optical rotation found to be –14.0°. Copolymers of **1.25** with varied comonomer ratios have been shown to react with $[Rh(cod)_2]BF_4$ to form [**1.25**·Rh(cod)]BF_4. In this case up to 93% of the phosphine centres can be bound to rhodium atoms as determined by ^{31}P NMR spectroscopy.[79] This discovery potentially opens the door towards polymer-supported catalysis for enantiomerically pure organic transformations in the future.

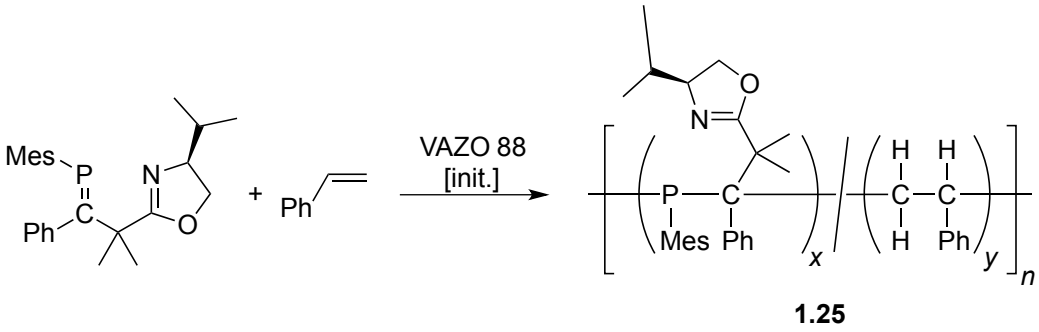

1.25

Scheme 1.18: Copolymerization of an enantiomerically pure phosphaalkene-oxazoline and styrene.

1.4.2 Exploring the Functionality of PMPs.

A unique feature of PMPs is their chemical functionality through the phosphorus lone pairs. Homopolymer **1.21** can be oxidized with either H_2O_2 or S_8 (**1.26a** and **1.26b**),[71] coordinated to either gold(I) (**1.26c**),[80] borane (**1.26e**)[81] or alkylated to yield an ionomer (**1.26d**) (Scheme 1.19).[81] In the case of borane and gold(I), uncoordinated phosphorus moieties could not be observed by ^{31}P NMR spectroscopy indicating complete conversion to the phosphine-gold or phosphine-borane adducts. In contrast, the phosphonium ionomer **1.26d** could not be obtained in higher than 50% conversion, possibly due to ionic repulsion. In all cases, molecular weight analysis by GPC of the resulting polymers showed no degradation of the polymer chain, but only

the expected increase in molecular weight. For example, gold(I) complex **1.26c**, synthesized from a sample of polymer **1.21** (M_n = 38,900 g mol^{-1}), was found to have an M_n of 71,600 g mol^{-1}.

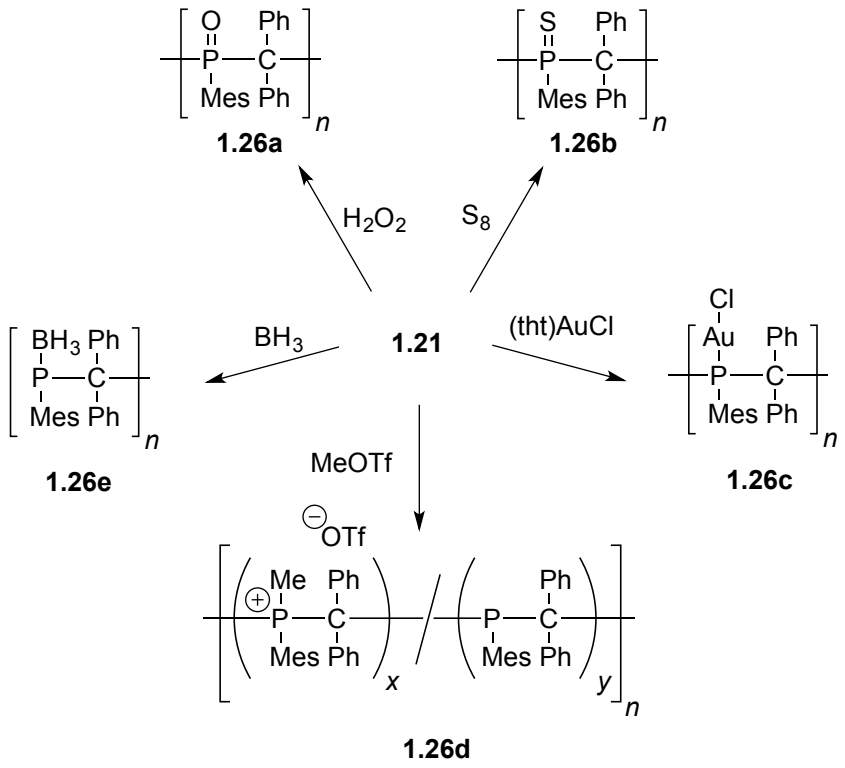

Scheme 1.19: The functionalization of poly(methylenephosphine)s.

When coordinated to Au(I) ions, amphiphilic phosphaalkene-isoprene block copolymers, $[PI]_{404}$-*b*-$[PMP]_{35}$ formed self-assembled nanostructures in a block-selective solvent [R_h = 5 nm (THF), 82 nm (*n*-heptane)].[82] Transmission electron microscopy (TEM) analysis of samples obtained from dilute *n*-heptane revealed spherical nanostructures (28-32 nm) that were attributed to micelles with a PMP·AuCl core and polyisoprene corona. Remarkably, increasing the PMP block length in the copolymer afforded worm-like gold nanostructures with high aspect ratio.

The use of phosphaalkene/styrene random copolymers in polymer-supported palladium catalysis has been demonstrated.[72] Specifically, the copolymer **1.22** (9 mol% P; M_w = 7,000 g mol^{-1}, Đ = 1.7) has been employed in combination with $Pd_2(dba)_3$ as a catalyst for the Suzuki coupling of

phenylboronic acid and bromobenzene. The biphenyl product was isolated in high yield (90%) and purity by simple precipitation of a THF solution into hexanes and without the need for chromatography.

The use of poly(methylenephosphine)s as flame retardants has been reported recently (Figure 1.8).[83] Paper samples were treated with homopolymer **1.21** and its oxide **1.26a** and subjected to flame testing and both were found to be competent flame retardants (limiting oxygen index = 25.9%), with the oxidized homopolymer performing slightly better. Importantly, after leaching with water no loss of flame retardancy was observed.

Figure 1.8: Top: Dynamic sheet formed (DSF) paper made from thermomechanical pulp (TMP), coated with poly(methylenephosphine oxide) 1.26a (0.8 mmol P / g) and ignited with a lighter in air. This flame retardant paper is self-extinguishing. Bottom: An untreated DSF TMP sheet was ignited in air and burns completely. Picture courtesy of Dr. A. Priegert.

Recently, detailed spectroscopic analysis of the homopolymer previously formulated as **1.21** synthesized by radical-initiated polymerization revealed the presence of an unexpected microstructure **1.27.** This microstructure resulted from an isomerization polymerization (Scheme 1.20).[84] After the addition of the radical species to P atom in MesP=CPh_2, a carbon based radical

was formed. A hydrogen atom subsequently migrated from the *o*-Me of the mesityl group to this carbon radical. This means that a benzylic radical was formed at the *o*-Me position that functioned as the propagating species and accounts for the microstructure **1.27** (*x* >> *y*).

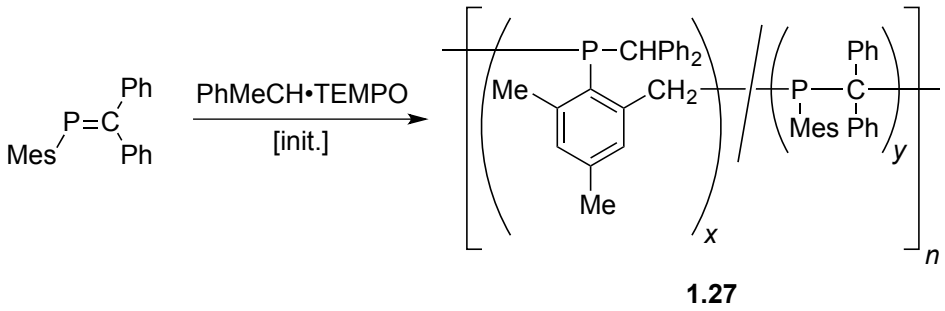

1.27

Scheme 1.20: Alternative microstructure of poly(methylenephosphine) using a nitroxide-mediated radical polymerization initiator.

Although the synthesis and chemistry of PMPs has been studied, the photophysical properties of these polymers have not been investigated to date. As the phosphorus atoms within the polymer are chemically active, it may be possible to fashion materials where the photophysical properties of the polymer can be tuned by the addition of analytes. The investigation of the photophysical properties of PMPs is detailed in Chapters 2 and 3.

1.5 Chemical Sensing

Chemosensors are materials that undergo a detectable change in properties upon exposure to an external stimulus. Fluorescence as a detection method in chemical sensing is particularly prevalent due to its high sensitivity, ease of detection and, numerous measurable transduction outputs (e.g. fluorescence intensity, lifetimes and energy transfer). Common targets for chemical sensing include explosives (such as TNT),[85-87] toxic metals (such as Hg(I) and Hg(II) ions),[88] platinum group metals[89] and biological targets.[90]

Traditional chemosensors are typically multidentate ligands that contain N, O and S heteroatoms that bind to Lewis acidic analytes (such as metal cations).[86, 91] In order to prepare a solid device, the sensor molecule is entrapped within a polymer matrix to prevent leaching into the sensing medium. There are a number of disadvantages to using this matrix immobilization approach. It can be difficult to identify a polymer matrix that has compatibility with the sensing material and the sensing medium. Another drawback is that leaching of the sensing material is commonly encountered and as a result the effectiveness of the sensor often decreases over time.[92]

The physical properties associated with polymers often make them useful as support materials. Due to their prominent fluorescence characteristics, chemosensors based on π-conjugated polymers (i.e. polymers in section 1.1.1) have been thoroughly investigated.[86, 90, 93, 94] Although the backbone structure of these molecules typically contain carbon and hydrogen only, the incorporation of receptor sites featuring N, O and S atoms can be achieved by the addition of side groups. These heteroatoms can bind to analytes causing a photophysical response. A famous example is **1.28**, a PPE (Figure 1.9) that contains crown ether side groups with an affinity to cations. In the absence of an analyte, the polymer is fluorescent. As a substoichiometric amount of cation binds to the crown ether, the fluorescence of the whole polymer is quenched (Scheme 1.21).[95, 96] The amplification of fluorescence quenching is due to the inability of the excited photon to migrate though the chain of the polymer. Subsequent derivatives of PPEs have been developed to detect other analytes[31, 97] and even commericalized as detectors that can measure the presence of explosives at femtogram levels.[98]

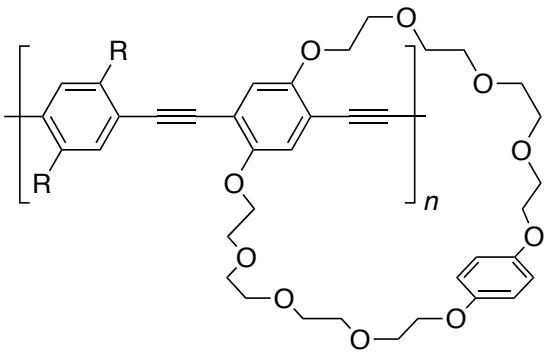

1.28

Figure 1.9: a) Poly(phenyleneethynylene) that exhibits amplified fluorescence quenching upon binding of K^+ cations.

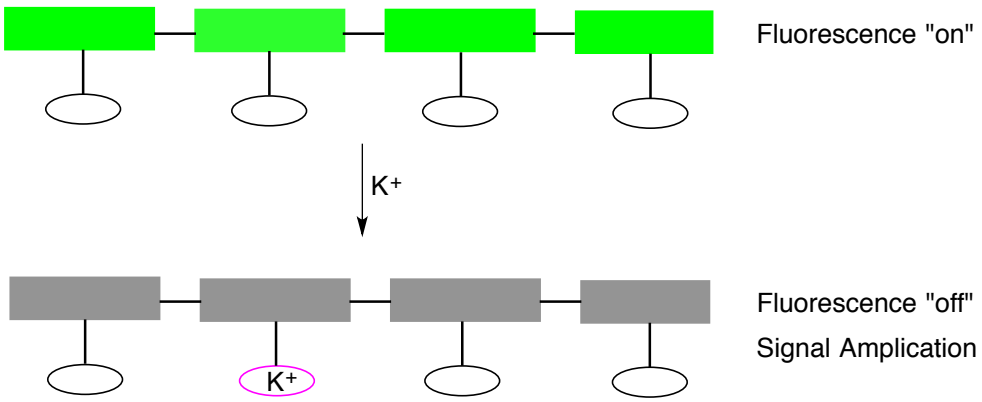

Scheme 1.21: A diagram demonstrating fluorescence quenching upon binding of K^+ ions to a receptor in the polymer.

Phosphorus-containing materials may be excellent candidates for the sensing of analytes that can bind to the P lone pair. As detailed in the examples in the following section, analyte binding to phosphorus can dramatically change the photophysical properties of the overall material. It is well established that low valent phosphine-containing compounds tend to be non-emissive.[99] This is because fluorescence is quenched by a photoinduced electron transfer (PET) mechanism involving the P lone pair electrons. Coordination or oxidation of these electrons by an analyte results in increased fluorescence as PET is suppressed. (Scheme 1.22).

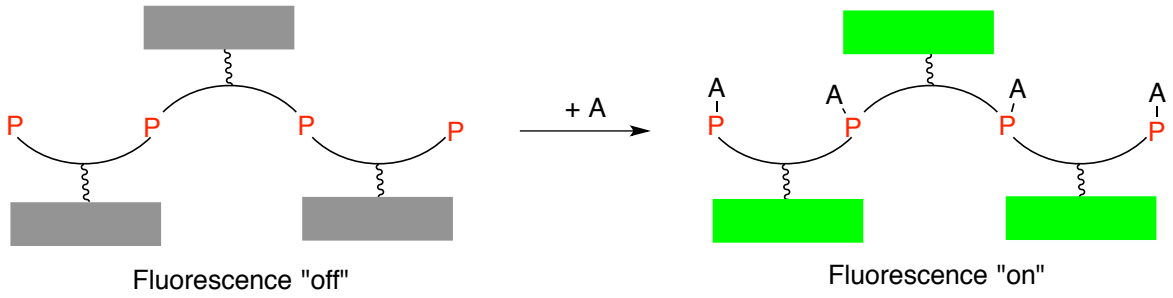

Scheme 1.22: A hypothesis of the "turn on" luminescence of phosphorus polymers upon coordination of an analyte to the P centres.

Despite the fact that phosphine ligands have been widely utilized in the areas of coordination chemistry and catalysis,[100] sensors based on phosphorus-containing receptors are uncommon.[99, 101] The known examples are presented in the following section. As displayed throughout this introduction, the photophysical properties of phosphorus-containing polymers are dependent on the environment at phosphorus. Previous reports have hinted at the potential sensing applications for P-based polymeric materials[61] but to date there are extremely limited examples of definitive sensing studies in the literature.

1.5.1 Phosphorus-Containing Materials that show Sensing Behaviour

Early reports in the literature suggest that arylphosphines and arylphosphine oxides have rather different photophysical properties.[102-105] While the parent phosphines are not fluorescent, oxidation of the P centre by the addition of a hydroperoxide or molecular oxygen resulted in "turn on" fluorescence. This is an alternative mechanism of action compared to traditional oxygen sensors, which are fluorescent metal complexes that undergo fluorescence quenching upon exposure to molecular oxygen due to triplet quenching.[106-108]

The emission colour of phosphorus-based sensors is dependent on the identity of the fluorophore. In particular, two aryldiphenylphosphines, diphenyl-1-pyrenylphosphine (**1.29**) and 3-perylene diphenylphosphine (**1.30**) (Figure 1.10) are of interest as they exhibit blue coloured

emission upon phosphine oxidation. This has led to the application of both receptor molecules as monitors for hydroperoxide formation within lipoproteins.[109-116]

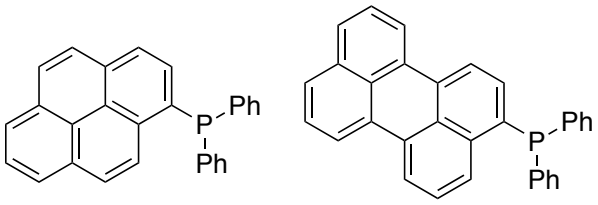

1.29 **1.30**

Figure 1.10: Fluorescent probes 1.29 and 1.30 that show turn on emission upon oxidation with hydroperoxides.

A cited drawback of the aryldiphenylphosphine systems is that their excitation and emission maxima are outside of the visible region (λ_{ex} = 352 nm, λ_{em} = 380 nm). Their photophysical properties also share similarities to some biomatrices, a problem that has hindered their incorporation into devices.[117] Thus, alternative organophosphorus oxide compounds, which undergo fluorescence at higher wavelengths may be more useful. To this end, three probes, **1.31**,[118] **1.32**,[119] and **1.33**[120] have been reported (Figure 1.11). The oxides undergo fluorescence well into the visible region (λ_{max} = 449 nm (**1.31**·O), 520 nm (**1.32**·O), 515 nm (**1.33**·O) whereas the parent phosphines are far less emissive. Each system consists of a phosphine moiety tethered away from a fluorophore. Photoinduced electron transfer (PET) from the P lone pair was speculated to be the cause of fluorescence quenching. The presence of phosphorus atoms was crucial to the emissive properties of the sensor; similar derivatives with no P atoms were highly fluorescent. Oxidation of **1.31-1.33** using a lipid hydroperoxide was performed to demonstrate their potential application in biological systems.[118-120]

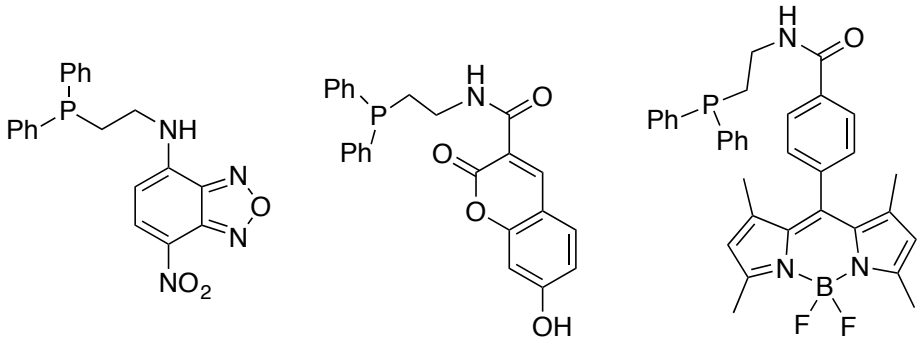

Figure 1.11: Phosphine sensors based on a photoinduced electron transfer mechanism.

In addition to oxidation sensors, phosphines have also been used as sensors for other analytes. A coumarin-phosphine dye, **1.34**, exhibited fluorescence upon exposure to S-nitrosothiols. The reaction of two equivalents of the dye with a S-nitrosothiol generated one equivalent of phosphine oxide **1.34**·O, and an azaylide intermediate, which was readily hydrolyzed to form another equivalent of **1.34**·O (Scheme 1.23). The phosphine oxide exhibits blue coloured fluorescence with a high quantum yield (λ_{em} = 489 nm, Φ = 0.79) unlike the starting material (λ_{em} = 486 nm, Φ = 0.033).[121]

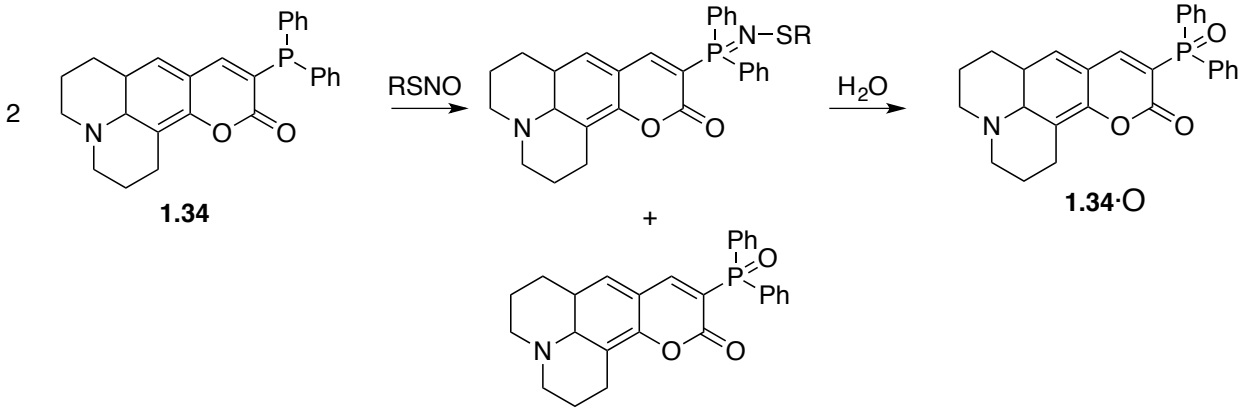

Scheme 1.23: Phosphine sensor that undergoes fluorescence upon reacting with S-nitrosothiols.

Recently, phosphinofluorescein compound **1.35** (Figure 1.12) was shown to undergo a substantial emission enhancement (λ_{max} = 549 nm) when coordinated to Au(I), Au(III) or Ag(I) ions in aqueous solution.[122] Interestingly, this emission enhancement was selective; when other

heavy metals [e.g. Rh(I)/Rh(III), Ir(III), Pd(0)/Pd(II), Pt(II)/Pt(IV)] were added to **1.35,** no emission increase was observed. Similarly, the coordination of an Au(I) ion to phenanthrene phosphine **1.36** resulted in phosphorescent emission ($\lambda_{max} \approx 500$ nm, $\Phi_P = 0.06$) even at room temperature. The unoxidized phosphine, **1.36**, was non emissive. Last year, the synthesis of phosphine bodipy ligand **1.37** was reported. The emissive properties of the gold-ligand complexes formed were measured *in situ* to probe the mechanism of the reaction of alkynes with gold complexes by ligand displacement.[123]

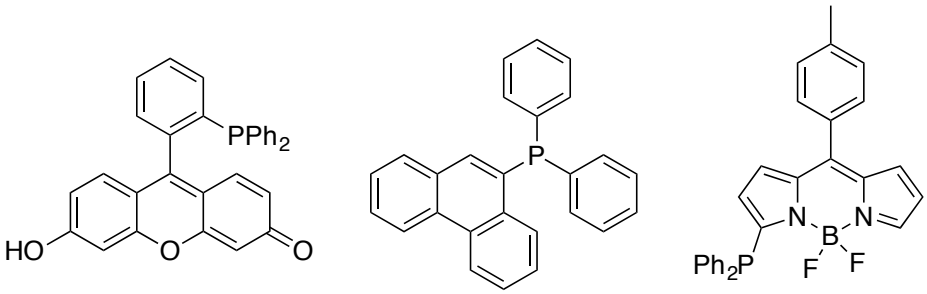

1.35 **1.36** **1.37**

Figure 1.12: Compounds that undergo emission enhancement upon coordination to Au (I) ions.

A "turn on" fluorescence sensor for palladium based on a phosphine-rhodamine conjugate has been reported (**1.38**, scheme 1.24). Addition of one equivalent of common palladium catalysts ($PdCl_2$(cod), $Pd(PhCN)_2Cl_2$, $Pd_2(dba)_3$, $Pd(PPh_3)_4$, K_2PdCl_4) to **1.38** resulted in a significant fluorescence enhancement and distinct colour changes. The authors also showed that the addition of Na_2S to **1.38**·$PdCl_2$ resulted in regeneration of free ligand **1.38**. Competitive binding studies with other metal ions showed that the binding of the ligand to Pd(0) and Pd(II) was highly selective, suggesting a potential application of **1.38** is the detection of palladium species in drug chemical synthesis.[124]

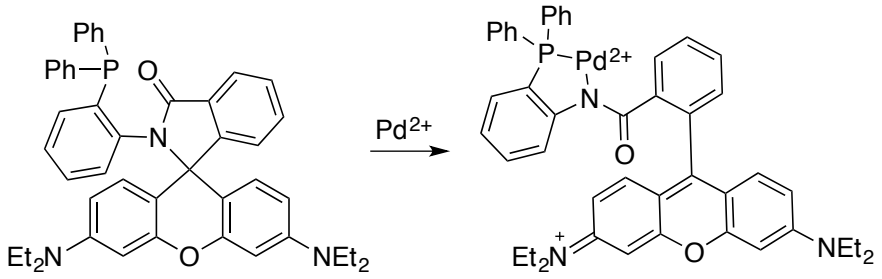

1.38

Scheme 1.24: Phosphine based dye that undergoes turn on fluorescence upon exposure to Pd(II) complexes.

A tridentate phosphine oxide ligand was reported which sensed Eu(III) ions in water (**1.39**, scheme 1.25).[125, 126] The authors prepared europium complexes with the ligand separately and showed that two equivalents of the ligand **1.39** bind to Eu(III) ions making an 8-coordinate centre (with two chloro- ligands). Complexes of the ligand **1.39** with other lanthanides were non-fluorescent. The authors showed that the immobilized ligand can be could be coated on an optical probe and retain functionality as an Eu(III) sensor.

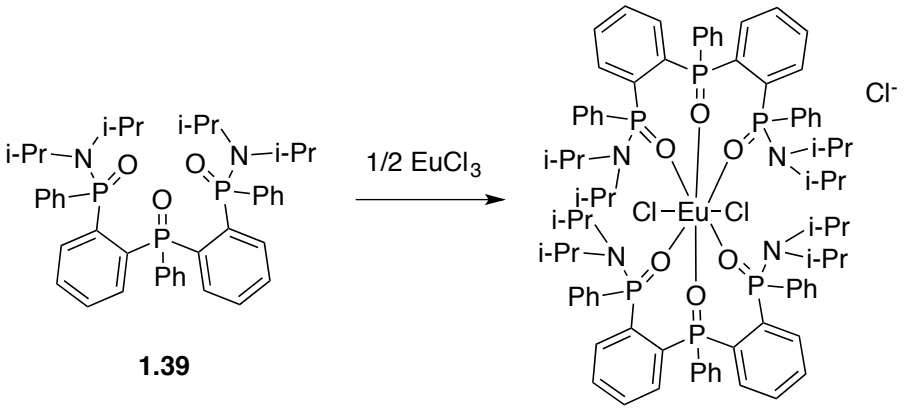

1.39

Scheme 1.25: Reaction of phosphine oxide ligand 1.39 with $EuCl_3$.

The described examples provide the starting point for the field of phosphorus-based sensory materials. Of note is the ability of phosphorus-based compounds to change their photophysical properties upon oxidation or binding to specific metals or metal ions. The study of phosphine polymers as sensory materials is at a very primitive stage due to limited number of polymers where phosphorus has been incorporated into the main chain. It is the hope during this

thesis to amalgamate phosphine polymers and chemical sensors and investigate some truly fascinating materials.

1.6 Outline of Thesis

This thesis is split into an introduction, four chapters of original research and a conclusion. The research chapters are split into two major themes. Chapters 2 and 3 detail the synthesis of four new phosphaalkenes that each contain a polyaromatic substituent. Three of these phosphaalkenes were polymerized by anionic initiation to make PMPs. The absorption and emissive properties of the synthesized materials were explored and turn-on fluorescence was observed upon oxidation of the phosphorus centres in the PMP in each case. Notably, the oxidized C-pyrenyl PMP displayed solid-state fluorescence. The second theme of the original research chapters focuses on the synthesis of novel phosphorus-containing polymers, poly(*p*-phenylenediethynylene phosphine)s (PPYPs). Chapter 4 details the synthesis and characterization of this new class of polymer. It was found that PPYPs exhibit photophysical properties consistent with a degree of electron delocalization through the phosphorus centres in the backbone. It was also discovered that as with PMPs, the environment of the phosphorus atoms dictates the emissive properties of the polymer. Chapter 5 features a sensing study using a fluorenyl-containing PPYP, that was found undergo fluorescence upon coordination to Au(I) and Au(III) ions selectively. Chapter 6 concludes the thesis by summarizing the research and suggesting new directions of study for these projects.

Chapter 2: Synthesis and Polymerization of P- Mesityl Phosphaalkenes bearing Fluorescent Substituents

2.1 Introduction

Macromolecules with phosphorus atoms in the main chain are of broad interest due to their unique properties, chemical functionality and the prospect of finding specialty applications.[127] Beyond the ubiquitous and important polyphosphazenes,[4] several new classes of phosphorus-containing polymers have attracted considerable recent attention, such as: poly(ferrocenylphosphine)s;[128-133] π-conjugated phosphole-containing polymers;[58, 61, 69, 70, 134] polyphosphines with arylene[33-35] and/or vinylene[135, 136] spacers; polyphosphinoboranes;[137-139] and π-conjugated phospha- and diphospha-PPVs with P=C or P=P bonds in the main chain.[43, 44, 46, 140] Despite this growth in phosphorus polymer chemistry, the incorporation of phosphorus atoms into long chains still presents a formidable synthetic barrier. For example, ring-opening routes require access to suitably strained rings whereas commonly used step growth methods require high purity monomers in precise stoichiometries to achieve reasonable molecular weights. Perhaps surprisingly, addition polymerization, being the most general and widespread method of organic polymer synthesis, has been largely unexplored for hetero-element multiple bonds. For more than three decades, the synthesis and reactivity of compounds featuring genuine (p–p) π bonds involving the heavier p-block elements has been a central theme within main group chemistry.[39, 40, 141] Phosphaalkenes, which contain a (2p–3p) π bond, represent one of the most well studied classes of unsaturated main group compounds and remain an intensely active area of research, particularly in the areas of π conjugation and ligand design.[47, 48, 142-149]

Of particular interest is the close analogy between the molecular chemistry of the P=C

Versions of sections of this chapter have been published. Benjamin W. Rawe, Cindy P. Chun and Derek P. Gates. *Chem. Sci.* **2014**, 5, 4928.

bond of phosphaalkenes and the C=C bonds of olefins.[150, 151] Over the past decade, our group has been interested in expanding the P=C/C=C analogy to polymer science.[152] To this end, we reported the first addition polymerization of a heavy element multiple bond in 2003.[71] Namely, MesP=CPh_2 was polymerized in the melt to afford poly(methylenephosphine) (PMP), a new class of phosphorus-containing macromolecule. The polymerization of MesP=CPh_2 can be accomplished by employing either radical or anionic methods of initiation. Radical-initiated copolymerization of MesP=CPh_2 with styrene permits the development of randomly enchained copolymers that can be employed as catalyst-supports.[72] In contrast, the anionic polymerization of MesP=CPh_2 can be performed in a "living" fashion and provides access to block copolymers that self assemble in block selective solvents.[74, 75, 82] The versatile chemical functionality of the P(III) moiety within PMPs, which can be oxidized to P(V) or coordinated to metals or Lewis acids, is of considerable interest.[80, 81] As detailed in Chapter 1, molecular phosphines bearing π-conjugated chromophores are widely used as fluorescent probes since they exhibit "turn-on" emission upon oxidation or coordination.[109-116, 118-122, 124-126] Therefore, it is hypothesized that similar behaviour may be observed for PMPs to provide sensory-type behaviour for these novel materials. Herein, the synthesis and full characterization of phosphaalkenes **2.1a–2.1c** bearing aromatic chromophores are reported. The anionic polymerization of two of these monomers to afford PMPs **2.2a** and **2.2b** is also detailed. The fact that anionic polymer **2.2a** adopts an alternative microstructure that involves an addition–isomerization mechanism similar to that reported recently for the radical polymerization of MesP=CPh_2 is of particular significance.[84] Remarkably, naphthyl-substituted **2.2a** exhibits "turn-on" emission selectively towards peroxide oxidation.

2.2 Results and Discussion

2.2.1 Synthesis of Phosphaalkenes

New phosphaalkenes bearing π-conjugated C-substituents such as 1-napthyl, 9-phenanthryl and 5-dibenzosuberenyl were targeted for the present study. Our group,[77, 153] and others[154, 155] have exploited the phospha-Peterson reaction as a general and convenient route to phosphaalkenes from silylphosphines and ketones. The P=C bond is formed by reaction of the ketone either directly with a lithium silylarylphosphide or indirectly with a mixture of $RP(SiMe_3)_2$ and a base catalyst (e.g. KOH). The milder base-catalyzed method was suitable for the preparation of **2.1c** whilst the standard phospha-Peterson reaction was employed to access **2.1a** and **2.1b** due the sluggish rate of the base-catalyzed version (> 2 weeks to completion) (Scheme 2.1). In each case, ^{31}P NMR spectroscopic analysis of the reaction mixture suggested that the desired phosphaalkenes were formed cleanly and quantitatively [**2.1a**: 238 ppm (30%, *E*), 250 ppm (70%, *Z*); **2.1b**: 238 ppm (40%, *E*), 252 ppm (60%, *Z*); **2.1c**: 249 ppm].

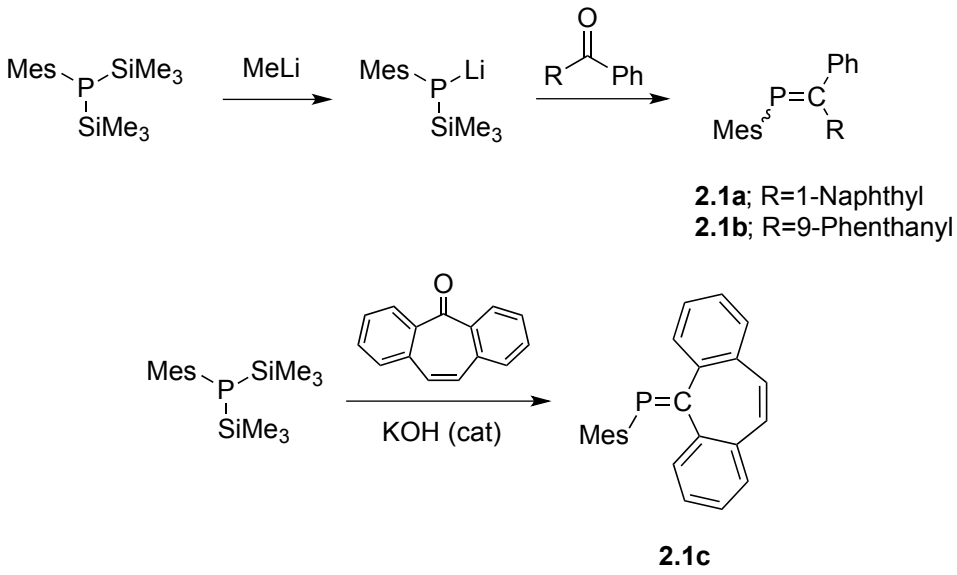

Scheme 2.1: Synthetic routes to 2.1a-2.1c

The first step in the synthesis of **2.1a** and **2.1b** involves treating a THF solution of $MesP(SiMe_3)_2$ with MeLi (1 equiv.) in Et_2O to afford $MesP(SiMe_3)Li$ (^{31}P NMR shift = –187 ppm). Subsequent addition of the corresponding ketone to the Et_2O solution of $MesP(SiMe_3)Li$ at –78 °C affords a mixture of *E/Z* phosphaalkene with the *Z* isomer corresponding to the major product. Interestingly, recrystallization of the crude phosphaalkenes revealed that the minor stereoisomer in solution (*E*-**2.1a**) crystallized preferentially as determined by ^{31}P NMR spectroscopy and X-ray crystallography (*vide infra*). In contrast, the major *Z*-isomer of the phenanthryl phosphaalkene **2.1b** was crystallized exclusively. In addition to ^{31}P NMR and X-ray crystallography, both new phosphaalkenes were characterized by ^{1}H and $^{13}C\{^{1}H\}$ NMR spectroscopy, mass spectrometry and elemental analysis (**2.1b** only). A very slow *E/Z*-isomerization is observed by ^{31}P NMR spectroscopy when crystals of pure *E*-**2.1a** or *Z*-**2.1b** are dissolved in $CDCl_3$ and spectra of this solution recorded daily (Figure 2.1). The interconversion of *E*- and *Z*-isomers in solution is commonly observed for phosphaalkenes, however this process often requires UV irradiation to occur.[156-158]

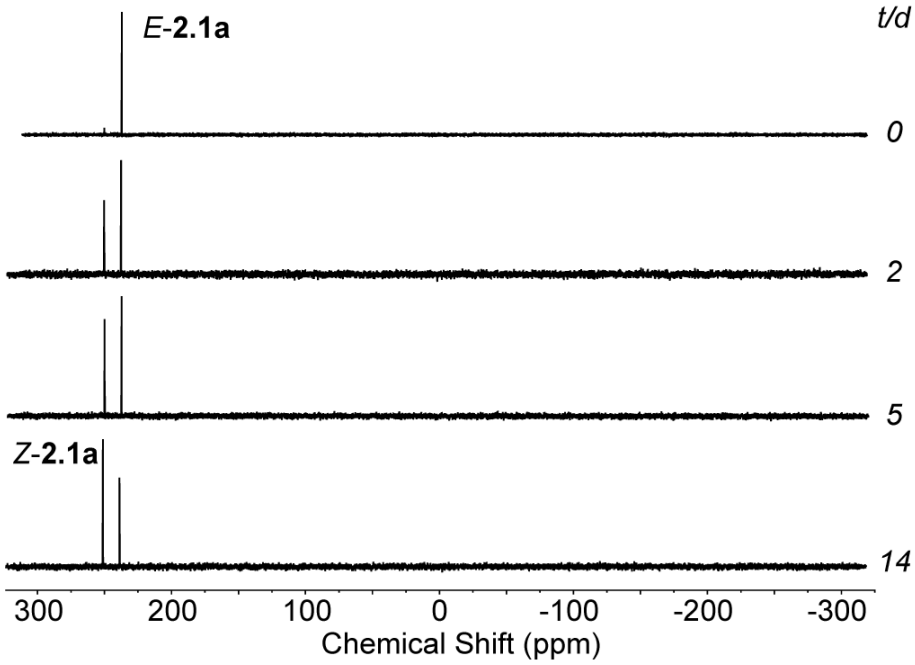

Figure 2.1: ^{31}P NMR spectra ($CDCl_3$, 121 MHz) showing the isomerization of pure *E*-2.1a to a mixture of *E/Z*-2.1a over a period of 14 d.

Due to the potential reactivity of the alkene bond in 5-dibenzosuberenone, the milder base-catalyzed phospha-Peterson reaction was employed to prepare **2.1c**. To a stoichiometric mixture of $MesP(SiMe_3)_2$ and 5-dibenzosuberenone in THF solvent was added KOH (10 mol%). The reaction mixture was monitored by ^{31}P NMR spectroscopy and, over a period of two days, the signal assigned to $MesP(SiMe_3)_2$ (–161 ppm) diminished in intensity in favour of a new signal assigned to the desired phosphaalkene **2.1c** (249 ppm). Yellow crystals of compound **2.1c** (yield = 57%) were isolated from a saturated hexanes solution and the identity of the product was confirmed by X-ray crystallography (section 2.2.2). Additional evidence of the identity of **2.1c** was provided by ^{1}H and $^{13}C\{^1H\}$ NMR spectroscopy, mass spectrometry and elemental analysis.

2.2.2 Structural and Electronic Properties of Phosphaalkenes

The molecular structures of phosphaalkenes **2.1a-2.1c** are shown in Figure 2.2 with selected metrical parameters being given in Table 2.1. Selected data collection parameters, cell constants and refinement details are given in Appendix A (Table A1). The P=C bond lengths in **2.1a-2.1c** [avg. 1.691(4) Å] are on the longer side of that expected for C-substituted phosphaalkenes (1.61–1.71 Å),[159] but are characteristic of phosphaalkenes bearing P-Mes substituents (1.67–1.70 Å).[153, 160, 161] In contrast, the P–C_{Mes} bonds [avg. 1.829(4) Å] lie at the shorter end of the range typical of P–C single bonds (1.85-1.90 Å).[162] Previous reports from the Gates group have suggested that the slight elongation of the P=C bond accompanied by the shortening of the P–C_{Mes} bond suggests a degree of π-conjugation between the Mes group and the P=C bonds.[153] The C–C_{trans} and C–C_{cis} bond lengths in **2.1a**–**2.1c** (ca. 1.49 Å) are shorter than typical C–C single bonds (1.54 Å) but are typical of C_{sp2}–C_{Ar} (1.48 Å) bonds,[162] perhaps also reflecting π-conjugative effects between the P=C bond and the C-substituents. Of course, more insight into the nature of π-conjugation within these phosphaalkenes may be gathered by evaluation of the angles between the planes of the substituents and that of the P=C bond.

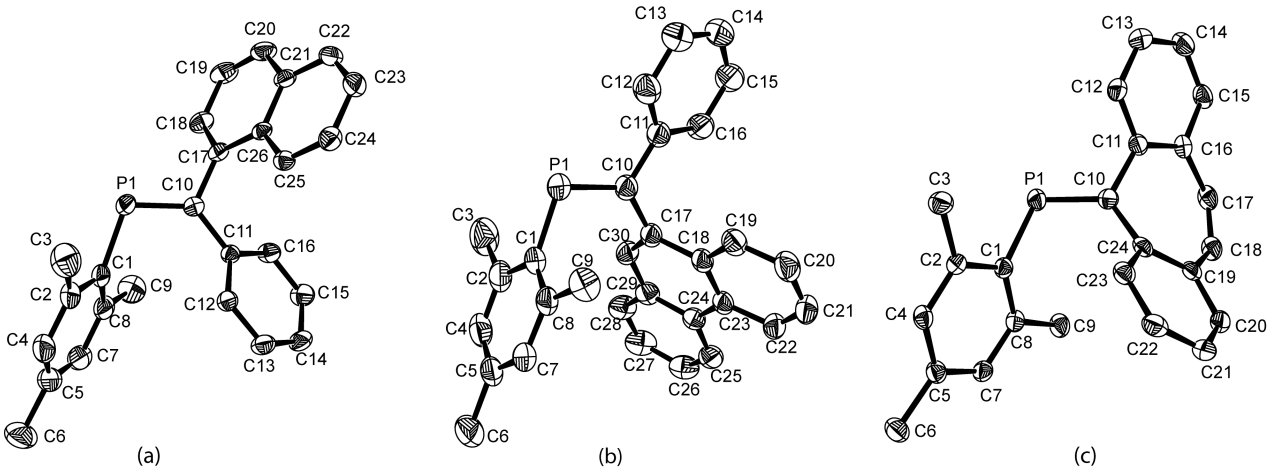

Figure 2.2 Molecular structure of *E*-2.1a (a), *Z*-2.1b (b) and 2.1c (c)

(thermal ellipsoids are displayed at 50% probability level). Hydrogen atoms are omitted for clarity.

In P-Mes phosphaalkenes the angle between the P=C bond and the Mes group is consistently ca. 71°.[153] It is therefore striking that the present systems, bearing large aromatic C-substituents, show significantly different angles between the plane of the P=C bond and the Mes substituent (*E*-**2.1a**: 64.8°, *Z*-**2.1b**: 85.3°, **2.1c**: 66.4°). Although this may simply be due to crystal packing effects, it is consistent with a higher degree of π-conjugation between the Mes group and the P=C bond in *E*-**2.1a** and **2.1c** and a lower degree of conjugation in *Z*-**2.1b**. Interestingly, the *cis*-configured 9-phenanthrenyl moiety in *Z*-**2.1b** is similarly bent out of the best plane of the P=C bond by 63.2°. This is accompanied by smaller than usual $\angle C_{Mes}$–P=C and $\angle$P=C–C_{cis} angles as the mesityl and phenanthrenyl substituents are slightly bent towards one another. In addition, there are clear intermolecular interactions between the phenanthrenyl moieties of adjacent *Z*-**2.1b** molecules in the solid state (Figure 2.3). A similar intermolecular arrangement has also been observed in the crystal structure of phenanthrene itself.[163]

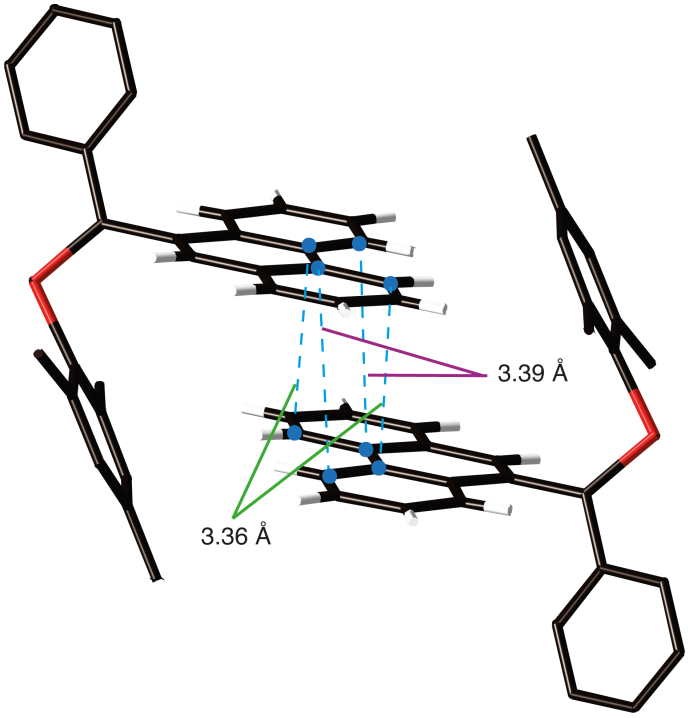

Figure 2.3: A portion of the crystal structure of *Z*-2.1b showing intermolecular distances between the planes of 9-phenanthryl moieties of adjacent molecules.

Table 2.1: Selected metrical parameters for phosphaalkenes bearing P-Mes and C–Ar substituents

Compound	***E*-2.1a**	***Z*-2.1b**	**2.1c**	**MesP=CPh$_2$**	**MesP=CPh$_2$**
Bond lengths (Å)					
P=C	1.688(2)	1.693(2)	1.691(3)	1.692(3)	1.693(2)
P-C_{Mes}	1.831(2)	1.827(2)	1.829(3)	1.828(3)	1.830(2)
C-C_{trans}	1.493(2)	1.483(3)	1.492(4)	1.491(5)	1.493(5)
C-C_{cis}	1.482(2)	1.482(3)	1.476(4)	1.487(4)	1.489(2)
Bond angles (°)					
∠C_{Mes}-P=C	108.37(7)	105.76(9)	108.5(2)	107.5(2)	107.6(2)
∠P=C-C_{trans}	114.2(1)	117.7(1)	114.4(2)	116.2(2)	118.0(2)
∠P=C-C_{cis}	129.2(1)	123.9(1)	126.6(2)	127.2(2)	124.8(2)
∠C_{cis}-C-C_{trans}	116.6(1)	118.1(2)	119.0(3)	116.6(2)	117.1(3)
Angles between planes (°)[a]					
Mes	64.79	85.33	66.41	71	72.2
Ar_{trans}	59.33	20.45	55.71	36.6	21.4
Ar_{cis}	41.82	63.16	53.61	42.9	59.2
Reference	This work	This work	This work	160	161

[a]The angle between the mean plane of the specified aryl ring atoms to the best plane of C_{Mes}–P=C–(C_{trans})(C_{cis}).

In *E*-**2.1a**, the naphthyl and phenyl moieties are twisted out of the plane of the P=C bond by 59.3° and 41.8°, respectively. Similarly, 5-dibenzosuberene-substituted **2.1c** shows significant twisting of the C-aryl moieties with respect to the plane of the P=C bond and one another. For instance, the angles between the P=C bond plane and the *cis* and *trans* C-aryl moieties are 53.6°

and 55.7°, respectively. In addition, the seven-membered suberene ring is not planar with the benzo moieties lying on two different planes twisted by 41° with respect to one another. In the Mes*P=C($C_{14}H_{10}$) analogue,[164] this angle is significantly larger (49°) whilst in 5-dibenzosuberenone the analogous angle is 37°.[165] These data for **2.1b** and **2.1c** are consistent with moderate π-conjugation between the C-substituents and the P=C bond.

To gain further insight into the π-conjugative effects in **2.1a**–**2.1c**, the electronic properties of these new phosphaalkenes were investigated by UV/Vis spectroscopy. The absorption spectra are shown in Figure 2.4. Emission spectra were also recorded but no emission was observed for any of the monomers. Remarkably, each of the absorption spectra show quite similar features with one fairly sharp band (λ_{max}: 298 nm, **2.1a**; 302 nm, **2.1b**; 294 nm, **2.1c**) that overlaps with a broad lower energy band (ca. 330–360 nm). Noting that the extinction coefficients (>10^4 M^{-1} cm^{-1}) for the sharper band in **2.1a**–**2.1c** are significantly greater than those of the substituents alone (e.g. naphthalene, phenanthrene or derivatives: 10^3–10^4 M^{-1} cm^{-1}),[166] these bands are most likely attributable mainly to the π–π* and n–π* transitions involving the P=C bond. For comparison, the absorption spectrum of MesP=CPh_2 was also recorded and shows bands at 285 nm and 326 nm which are similar to those reported previously by Bickelhaupt.[167]

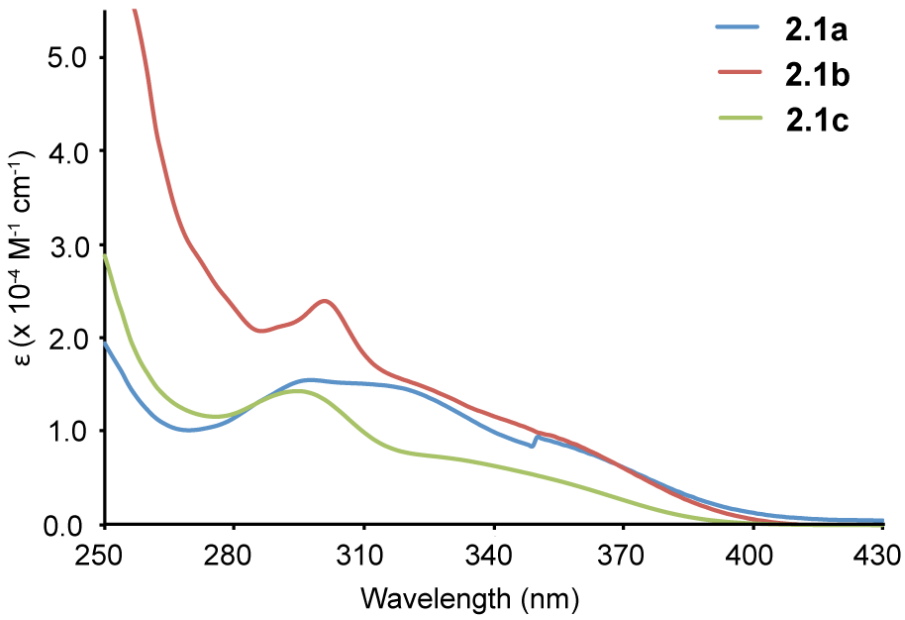

Figure 2.4: UV/Vis spectra of 2.1a, 2.1b and 2.1c in THF solution (c = 2 x 10^5 mol L^{-1}).

The artefact at 350 nm in the spectra of 2.1a is due to source changeover of the UV lamp.

It is noteworthy that the absorbance maxima in phosphaalkenes undergo a red shift of the high energy band in the order MesP=CPh_2, **2.1a** and **2.1b**. This trend is perhaps reflective of the increasing π-conjugation between the phosphorus carbon double bond and the aryl substituents as they increase in size (i.e.phenyl, naphthyl, phenanthyl). Similar π-conjugative effects on UV/Vis absorption spectra have been observed with related aryl- or alkynyl-substituted systems as referred to in Chapter 1.[43-45, 47, 48, 146, 168]

2.2.3 Anionic Polymerization of Monomers

The polymers resulting from **2.1a–2.1c** are of interest due to the prospect that the emissive properties of the fluorophore may be sensitive to functionalization of the phosphine moiety. Following procedures developed for the anionic polymerization of MesP=CPh_2,[74, 75] monomer **2.1a** was treated with *n*-BuLi (5 mol%) in THF in a glovebox (Scheme 2.2). The addition of the initiator to the pale yellow monomer solution resulted in a deep red solution

analogous to that observed for MesP=CPh_2 polymerization. After 5 d, the ^{31}P NMR spectrum of the reaction mixture revealed that signals assigned to *E/Z*-**2.1a** were replaced by a broad resonance at –9 ppm. This signal was assigned to polymer **2.2a**. The addition of three drops of methanol to the red polymerization mixture afforded a yellow coloured solution. After concentration of the THF solution, the polymer was precipitated with hexanes. The precipitation was repeated (×2) to afford the colourless solid polymer **2.2a** (yield = 53%). Analysis of **2.2a** using gel permeation chromatography (GPC) equipped with a multi-angle light scattering (MALS) detector revealed a narrow, monomodal molecular weight distribution (M_n = 15,100 g mol^{-1}; Đ = 1.14, $DP_n \approx 41$).

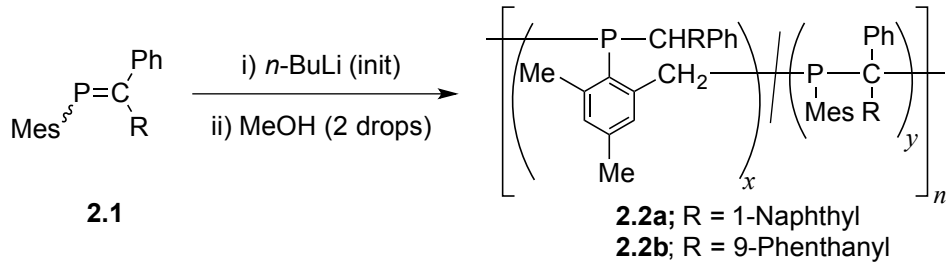

2.1

2.2a; R = 1-Naphthyl
2.2b; R = 9-Phenthanyl

Scheme 2.2: The anionic polymerization of 2.1a and 2.1b to afford PMPs 2.2a and 2.2b, respectively.

The observed molecular weight is significantly higher than that predicted from the monomer-to-initiator ratio [M_n (calc.) = 7,400 g mol^{-1}, n = 20]. It is speculated that a portion of the initiator was consumed by traces of electrophilic impurities present in the monomer **2.1a** and the solvent used for the polymerization resulting in a larger monomer-to-initiator ratio. It should be noted that monomer **2.1a**, although spectroscopically pure, did not meet the stringent standards of purity that are required for the anionic polymerization of MesP=CPh_2 to be living.

The polymerization of 9-phenanthryl phosphaalkene **2.2b** followed a similar procedure to that described above with the only difference being that the monomer to initiator ratio was 67:1 rather than 20:1 for **2.1a** (Scheme 2.2). Over the course of several days the dark red coloured

reaction mixture became increasingly viscous. The progress of polymerization was monitored by ^{31}P $\{^{1}H\}$ NMR spectroscopy. After five days the spectrum revealed only a broad resonance at –10 ppm assigned to polymer **2.2b** and sharp signals assigned to *E/Z*-**2.1b** with a conversion ratio of *ca*. 73% (by integration of ^{31}P NMR signals; see Figure 2.5a). After an additional two days the ratio of monomer to polymer was unchanged and, consequently, the polymerization reaction was terminated with MeOH (3 drops). A concentrated THF solution of the crude polymerization mixture was precipitated into hexanes (×3) to afford **2.2b** free from monomer (Figure 2.5b). GPC analysis of the isolated **2.2b** revealed a monomodal polymer of molecular weight (M_n = 27,100 g mol^{-1}; Đ = 1.37). Coincidently, this M_n is close to that predicted from the monomer-to-initiator ratio [M_n (calc) = 27,900 g mol^{-1}].

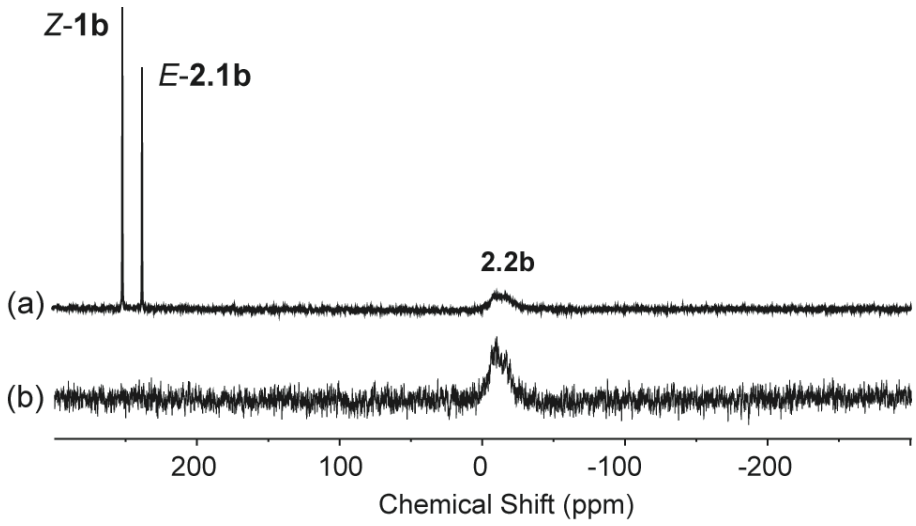

Figure 2.5: $^{31}P\{^{1}H\}$ NMR spectra (121 MHz, THF) of: a) the crude reaction mixture in the *n*-BuLi-initiated polymerization of *E*/*Z*-2.1b {[M]:[I] = 50:1} in THF (ca. 73% monomer conversion after 5 d.); b) poly(methylenephosphine) (2.2b) (M_n = 27,100 g mol^{-1}; Đ = 1.37) isolated after precipitation.

Efforts to polymerize 5-dibenzosuberenyl-substituted **2.1c** using *n*-BuLi as initiator have thus far proven unsuccessful. The presence of the strained seven-membered ring of the dibenzosuberene group suggested an alternate ring-opening metathesis polymerization pathway might be available. In an NMR-scale experiment, a solution of **2.1c** in C_6D_6 was treated with Grubb's (generation 1) catalyst, $RuCl_2(PCy_3)_2(=CHPh)$ (6 mol%). Analysis of the reaction mixture by ^{1}H and ^{31}P NMR spectroscopy showed only unreacted phosphaalkene, even after several days of heating to 70 °C.

In 2011, it was discovered that the radical-initiated polymerization of $MesP=CPh_2$ affords PMP with an alternative microstructure to that initially reported.[84] It was therefore of interest to investigate the microstructure of the polymer **2.2a** derived from **2.1a** using an anionic initiator. The microstructure of **2.2a**, as depicted in Scheme 2.3, shows both the alternating P–C–P–C structure and the alternate structure where the mesityl group is part of the main chain, presumably resulting from an isomerization process. The key experiments that permitted the elucidation of this alternative microstructure (of the polymer derived from $MesP=CPh_2$) resulted from ^{13}C APT and ^{1}H-^{13}C HSQC NMR experiments performed on a 600 MHz NMR spectrometer equipped with a cryoprobe. Analogous experiments were performed with polymer **2.2a** in $CDCl_3$ solution. Significantly, the ^{1}H-^{13}C HSQC NMR spectrum (Figure 2.6) reveals cross-correlations that are assigned to $–CH_2–$ and –CH(Naph)Ph groups of the alternative microstructure. Thus, we conclude that a similar isomerization polymerization occurs with the anionic polymerization of **2.1a**. However, these experiments do not permit quantification of the ratio of *x* to *y* in polymer **2.2a** and furthermore the quaternary carbon atom ($P–CPh_2–P$) will likely be quite difficult to identify spectroscopically especially if present in small quantities. Unfortunately, insufficient sample of **2.2b** was available and, consequently, analogous

experiments could not be performed with the phenanthryl-polymer. However, it should be noted that the ^{1}H NMR spectrum of **2.2b** has very similar features to that shown in Figure 2.6 for **2.2a**.

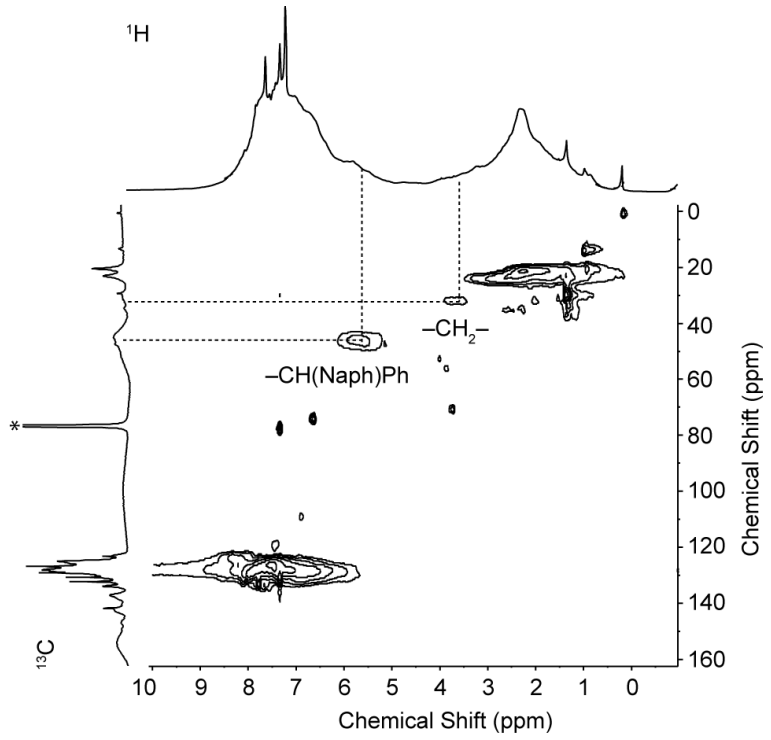

Figure 2.6: ^{1}H–^{13}C HSQC NMR spectrum (600 MHz for ^{1}H, $CDCl_3$) of poly(methylenephosphine) 2.2a. The ordinate axis shows the ^{13}C{^{1}H} NMR spectrum and the abscissa axis shows the ^{1}H NMR spectrum. * indicates $CDCl_3$.

2.2.4 Investigation of the Chemical Functionality of 2.2a

The presence of phosphine moieties within the polymer backbone bestows unique chemical functionality and properties upon PMPs when compared to typical organic polymers. With this in mind, naphthyl-substituted **2.2a** was treated with H_2O_2 and S_8 to afford the phosphine oxide and phosphine sulfide **2.2a**·O and **2.2a**·S, respectively (Scheme 2.3). The resultant polymers were characterized by ^{31}P{^{1}H} and ^{1}H NMR spectroscopy.

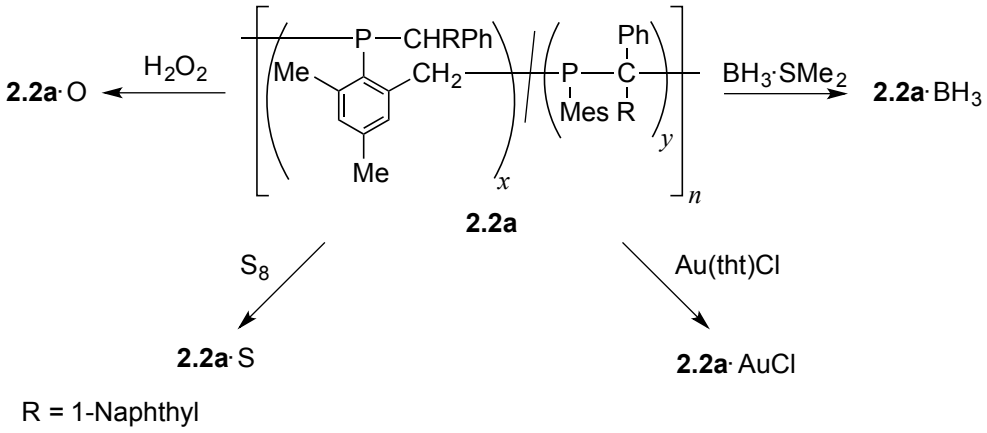

Scheme 2.3. Chemical functionalization of naphthyl-substituted poly(methylenephosphine) 2.2a.

The $^{31}P\{^{1}H\}$ NMR spectra, shown in Figure 2.7, reveal signals assigned to the oxide **2.2a**·O (48 ppm) and **2.2a**·S (53 ppm) that are shifted downfield with respect to unoxidized **2.2a** (–9 ppm). The sulfurization of **2.2a** with S_8 required reflux conditions in toluene for 22 h and still a small amount of unoxidized **2.2a** (ca. 10%) remains as suggested by the ^{31}P NMR spectrum. It is also interesting that the signals assigned to **2.2a**·O and **2.2a**·S, albeit still broad (fwhm=445 Hz and 590 Hz, respectively), are significantly sharper than that assigned to **2.2a** (fwhm=1210 Hz). Similar spectral features were observed for PMPs derived from $MesP{=}CPh_2$.[71, 80] The coordination complexes of polymer **2.2a** with gold(I) and borane were also prepared (Scheme 2.3) and characterized by ^{31}P and ^{1}H NMR spectroscopy. The ^{31}P NMR spectra of the reaction mixtures are shown in Fig. 7 and are consistent with the assigned products (**2.2a**·BH_3: 27 ppm; **2.2a**·AuCl: 24 ppm). Interestingly, the reaction of **2.2a** with Au(tht)Cl (1 equiv) proceeded smoothly at room temperature whilst a large excess of $BH_3{\cdot}SMe_2$ (10 equiv) was required to achieve full conversion to **2.2a**·BH_3. Furthermore, prolonged heating of the borane adduct **2.2a**·BH_3 (ca. 12 h at 60 °C) *in vacuo* resulted in loss of borane and reformation of uncomplexed **2.2a**.

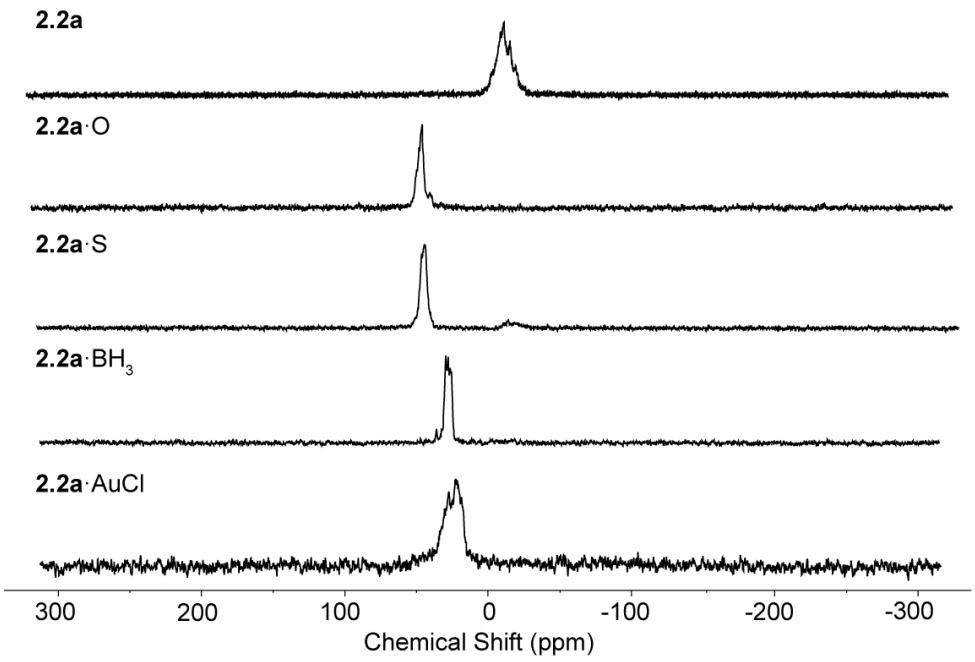

Figure 2.7: $^{31}P\{^{1}H\}$ NMR spectra (121 MHz) of reaction mixtures showing the formation of PMPs: 2.2a from 2.1a and *n*-BuLi (5 mol%) in THF; 2.2a·O from 2.2a and H_2O_2 (aq) in CH_2Cl_2; 2.2a·S from 2.2a and S_8 in toluene; 2.2a·BH_3 from 2.2a and $BH_3{\cdot}SMe_2$ in THF; 2.2a·AuCl from 2.2a and Au(tht)Cl in CH_2Cl_2.

Each of the new polymers were analyzed by GPC-MALS in THF solution to determine their molecular weights. Expectedly, the molecular weight of **2.2a** (M_n = 15,100 g mol^{-1}) increased upon oxidation (**2.2a**·O: M_n = 17,500 g mol^{-1}) and coordination to gold(I) (**2.2a**·AuCl: M_n = 26,000 g mol^{-1}) or borane (**2.2a**·BH_3: M_n = 23,100 g mol^{-1}). In contrast, the sulfurization of **2.2a** resulted in a polymer with a lower molecular weight (**2.2a**·S: M_n = 12,800 g mol^{-1}). This suggests that there may be some degradation of the polymer chain due to the forcing conditions necessary to achieve ca. 90% sulfurization. It is gratifying that all functionalized polymers have relatively narrow dispersity (Đ = 1.07-1.13) consistent with their precursor **2.2a**.

2.2.5 Photophysical Properties of 2.2a and Derivatives.

The absorption and emission properties of naphthyl polymer **2.2a** and its derivatives were evaluated to assess the impact of the phosphorus chemical environment on the electronic

properties of the naphthyl chromophore. The UV/Vis spectra of naphthyl-substituted polymer **2.2a** and its derivatives are shown in Figure 2.8 (top). Very similar features and absorption profiles are observed for each polymer. In particular, the absorbance maximum (λ_{max} = 286 nm) is identical for each polymer and is very similar to 1-methylnaphthalene (λ_{max} = 283 nm).[166] Moreover, the extinction coefficients for the polymers are much lower than that observed for monomer **2.1a** due to the absence of the strongly absorbing P=C moiety in the polymers. Therefore, it is speculated that the polymer absorbances mainly result from π-π* transitions within the naphthyl substituent. A broad absorbance between 320 and 400 nm is observed for **2.2a** that is not observed in any of the P-functionalized polymers. This broad absorbance is possibly associated with an electronic transition involving the P-lone pair although such bands in molecular phosphines typically show smaller molar extinction coefficients.[169]

It is well established that trivalent organophosphines bearing fluorescent substituents are not emissive due to photoinduced electron transfer involving the P-lone pair.[102-105, 124, 170-172] Upon oxidation or coordination of the P-lone pair, such systems often become emissive. Thus, the emission spectra for each of the new naphthyl-containing PMP polymers were recorded and are shown in Figure 2.8 (bottom). Expectedly, the unfunctionalized polymer **2.2a** showed no significant emission when irradiated at the absorbance maximum (λ_{ex} = 286 nm). Remarkably, only the oxide polymer **2.2a**·O showed a strong emission (λ_{em} = 342 nm) upon irradiation at 286 nm. This observation of selective "turn-on" emission is particularly exciting and hints at a strong potential for sensor applications for PMPs. The lack of emission from the other functionalized derivatives of **2.2a** is surprising but it should be noted that many P-functionalized molecular species are also non emissive.

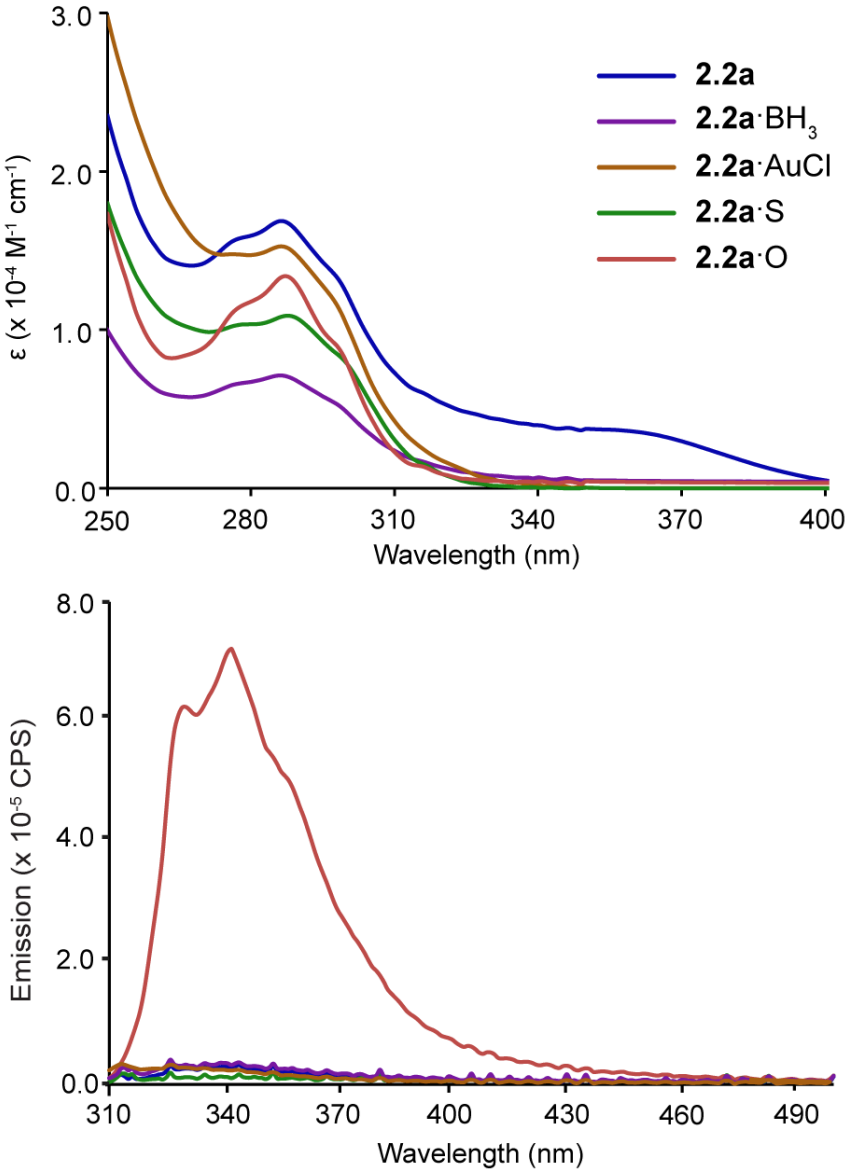

Figure 2.8 Top: UV/Vis absorption spectra of 2.2a and derivatives in THF ($c = 3\times10^{-5}$ mol L^{-1}). Bottom: Emission spectra of 2.2a and derivatives in THF (λ_{ex} = 286 nm; $c = 3\times10^{-5}$ mol L^{-1}).

2.3 Conclusions

Phosphaalkenes that incorporate emissive chromophores as the C-substituents are monomers that are amenable to anionic polymerization. Detailed characterization of the naphthyl-substituted polymer shows that its microstructure results from the isomerization of a proton from the *ortho*-

Me group of Mes to the $-CPh_2$ anion after initial anion addition across the P=C bond. This implies a highly unusual polymerization mechanism for phosphaalkenes. Despite this complex mechanism, the phosphine moiety of naphthyl-substituted PMP **2.2a** displays a high degree of chemical functionality through either oxidation or coordination. Perhaps most interesting, this novel PMP shows selective "turn-on" emission upon oxidation to **2.2a**·O by using hydrogen peroxide. This exciting observation points towards potential sensor properties for PMPs bearing emissive chromophores, a subject that is pursued in Chapter 3.

2.4 Experimental

2.4.1 Materials and Methods

All manipulations of air- and/or water-sensitive compounds were performed under a nitrogen atmosphere by using standard Schlenk or glovebox techniques. Hexanes and dichloromethane were deoxygenated with nitrogen and dried by passing through a column containing activated alumina. Tetrahydrofuran (THF) was dried over sodium and benzophenone. 1-bromonaphthalene, 9-bromophenanthrene, dibenzosuberenone, chlorotrimethylsilane, benzaldehyde and borane dimethylsulfide complex were purchased from Aldrich and used as received. Hydrogen peroxide was purchased as a 50% solution with water from Aldrich and used as received. Methyllithium and *n*-butyllithium were purchased from Aldrich and used as recieved and titrated by using *N*-benzylbenzamide.[173] $MesP(SiMe_3)_2$,[174] Au(tht)Cl,[175] 1-benzoylnaphthalene,[176] and 9-benzoylphenanthrene[177] were made following literature procedures.

2.4.2 Equipment

^1H, $^{31}P\{^1H\}$, $^{13}C\{^1H\}$ NMR spectra were recorded at 25 °C on Bruker Avance 300, 400 or 600 MHz spectrometers. H_3PO_4 (85%) was used as an external standard ($\delta = 0$ for ^{31}P). ^1H NMR

spectra were referenced to residual protonated solvent signal and $^{13}C\{^{1}H\}$ NMR spectra were referenced to the deuterated solvent signal. Elemental analyses were performed in the University of British Columbia Chemistry Microanalysis Facility. Mass spectra were recorded on a Kratos MS 50 instrument in EI mode (70 eV). Polymer molecular weights were determined by triple detection gel permeation chromatography (GPC-MALS) using an Agilent liquid chromatograph equipped with an Agilent 1200 series isocratic pump, Agilent 1200 series standard autosampler, Phenomenex Phenogel 5 μm narrow bore columns (4.6 × 300 mm) 10^4 Å (5,000 – 500,000 g mol^{-1}), 500 Å (1,000 – 15,000 g mol^{-1}), and 10^3 Å (1,000 – 75,000 g mol^{-1}), Wyatt Optilab rEx differential refractometer (λ = 658 nm, 40 °C), Wyatt TriStar miniDAWN (laser light scattering detector at λ = 690 nm) and a Wyatt ViscoStar viscometer. A flow-rate of 0.5 mL min^{-1} was used and samples were dissolved in THF (ca. 2 mg mL^{-1}). The molecular weights were determined using 100% mass recovery methods from Astra software version 5 with each polymer sample being run at least three times. Solution absorption spectra were obtained in THF on a Varian Cary 5000 UV-Vis-near-IR spectrophotometer using a 1 cm quartz cuvette. Fluorescence and excitation spectra were obtained in THF on a Horiba scientific fluoromax-4 fluorospectrometer using a 1 cm quartz cuvette.

2.4.3 X-Ray Crystallography

Crystal data and refinement parameters are listed in Table A1. All single crystals were immersed in oil and mounted on a glass fibre. Data were collected on a Bruker X8 APEX II diffractometer with graphite-monochromated $Mo_{K\alpha}$ radiation. Data were collected and integrated using the Bruker SAINT software package and corrected for absorption effects using SADABS. All structures were solved by direct methods and subsequent Fourier difference techniques. Unless noted, all non-hydrogen atoms were refined anisotropically, whereas all hydrogen atoms were

included in calculated positions but not refined. All data sets were corrected for Lorentz and polarization effects. All refinements were performed using SHELXL-97[178, 179] via the WinGX interface.[180]

2.4.4 Synthesis

2.4.4.1 Preparation of 2.1a

To a stirred solution of $MesP(SiMe_3)_2$ (8.0 g, 27 mmol) dissolved in THF (100 mL) was added MeLi (18 mL, 28 mmol, 1.6 M) in ether. The reaction mixture was heated under reflux overnight. An aliquot removed for analysis by ^{31}P NMR spectroscopy revealed a single resonance at –187 ppm, which was assigned to $MesP(SiMe_3)Li$. The reaction mixture was cooled to -78 °C, after which a solution of 1-benzoylnaphthalene (6.4 g, 28 mmol) was added dropwise to the reaction mixture. After 5 min, the reaction mixture was warmed to room temperature and was stirred for a further 20 min over which time the reaction mixture turned yellow. An aliquot was taken for ^{31}P NMR spectroscopy, which indicated an *E*/*Z*-mixture of phosphaalkene (δ = 250 and 239). The reaction mixture was cooled to -78 °C and $SiMe_3Cl$ (4.1 mL, 32 mmol) was added to quench $LiOSiMe_3$. The solvent was removed in vacuo leaving an orange residue. To this residue was added hexanes (3 × 100 mL) and the suspension was filtered and the solvent removed *in vacuo*. The residue was heated (55 °C) *in vacuo* for 6 h to remove other volatiles e.g. $(Me_3Si)_2O$ from the reaction mixture. From the resulting residue, small yellow crystals of **2.1a** formed from the slow evaporation of a saturated hexanes solution (while maintaining a nitrogen atmosphere) over 1 week. Yield = 2.5 g (25%).

^{31}P NMR (162 MHz, $CDCl_3$): δ 250 (70%, *Z*-**2.1a**), 238 (30%, *E*-**2.1a**); ^{1}H NMR (400 MHz, $CDCl_3$): (*E*-**2.1a**) δ 7.91 – 6.82 (m, 14H, aryl H), 2.46 (s, 6H, *o*-CH_3), 2.31 (s, 3H, *p*-CH_3); $^{13}C\{^{1}H\}$ NMR (101 MHz, $CDCl_3$): (*E*-**2.1a**) δ 191.1 (d, *J* = 44 Hz, P=*C*), 143.3 (d, *J* = 15 Hz, aryl

C), 141.7 (d, J = 27 Hz, aryl C), 140.5 (d, J = 7 Hz, aryl C), 138.9 (aryl C), 136.7 (d, J = 40 Hz, *i*-Mes), 134.1 (aryl C), 132.0 (aryl C), 129.4 – 124.8 (m, aryl C), 22.2 (d, J = 9 Hz, *o*-*C*H$_3$), 21.3 (*p*-*C*H$_3$); LRMS (EI, 70eV): *m*/*z* (%): 368, 367, 366 (2, 21, 91) [M$^+$]; 365 (100) [M$^+$– H], 246 (21) [M$^+$–H–Mes], 119 (8) [M$^+$–H–Mes–Naph].

2.4.4.2 Preparation of 2.1b

A stirred solution of MesP(SiMe$_3$)$_2$ (2.4 g, 8.0 mmol) in THF (10 mL) was treated with MeLi in Et$_2$O (5.35 mL, 1.5 M, 8 mmol) at 25 ºC. After heating the reaction mixture at under reflux for 12 h, analysis of an aliquot removed from the reaction by ^{31}P NMR spectroscopy suggested the complete lithiation of the starting material to MesP(SiMe$_3$)Li (−187 ppm). To this reaction mixture was added 9-benzoylphenanthrene (2.3 g, 8.0 mmol) dissolved in THF (*ca.* 10 mL) at −78 ºC. After 10 min an aliquot was taken for analysis by ^{31}P NMR spectroscopy, which indicated an *E*/*Z*- mixture of phosphaalkene (252 and 238 ppm). The reaction mixture was then treated with Me$_3$SiCl (1.0 mL, 8.0 mmol) to quench LiOSiMe$_3$. After the removal of solvent, the crude oil was extracted with hexanes (3 × 40 mL) and filtered through Celite. The solvent was removed *in vacuo* to afford a red oil. Yellow crystals of **2.1b** suitable for X-ray diffraction were obtained from the slow evaporation of a concentrated hexanes solution. Yield = 0.50 g (15%).

^{31}P NMR (162 MHz, CDCl$_3$): δ 252 (60%, *Z*-**2.1b**), 238 (40%, *E*-**2.1b**); ^{1}H (400 MHz, C$_6$D$_6$) (*Z*-**2.1b**) δ 8.36 – 7.02 (m, 14H, aryl H), 6.53 (br s, 1H, Mes-*H*), 5.08 (br s, 1H, Mes-*H*), 2.45 (br s, 3H, *o*-C*H*$_3$), 2.02 (br s, 3H, *o*-C*H*$_3$), 1.56 (s, 3H, *p*-C*H*$_3$); ^{13}C{^{1}H} NMR (101 MHz, CDCl$_3$): (*E*/*Z*–**2.1b**) δ 193.7 (d, J = 44 Hz, P=*C*), 191.0 (d, J = 44 Hz, P=*C*), 144.2 (d, J = 24 Hz, aryl C), 142.7 (d, J = 15 Hz, aryl C), 140.5 (d, J = 6 Hz, aryl C), 140.1 (d, J = 28 Hz, aryl C), 138.9 (aryl C), 138.1 (aryl C), 138.0 (aryl C), 136.6 (aryl C), 140.7 (aryl C), 136.6 (d, J = 40 Hz, *i*-Mes), 135.9 (d, $^1J_{CP}$ = 41 Hz, *i*-Mes), 131.6 – 122.5 (m, aryl C), 22.6 (br, *o*-*C*H$_3$), 22.6 (*o*-*C*H$_3$), 21.3 (s,

p-CH_3), 21.0 (s, *p*-CH_3). LRMS (EI, 70eV): *m*/*z* (%): 418, 417, 416 (3, 29, 98) [M^+], 415 (100) [M^+–H], 296 (29) [M^+–H–Mes], 220 (5) [M^+–Mes–Phen], 119 (13) [M^+–H–Mes–Phen]; Anal. Calcd for $C_{30}H_{25}P$: C, 86.51; H, 6.05; Found: C, 86.27; H, 6.12.

2.4.4.3 Preparation of 2.1c

To a solution of dibenzosuberenone (1.4 g, 6.7 mmol, 1.0 equiv) in THF (20 mL) was added $MesP(SiMe_3)_2$ (2.0 g, 6.7 mmol, 1 equiv) and KOH (0.042 g, 10 mol%). After 1 h the reaction mixture appeared dark green. After 3 d the ^{31}P NMR spectrum of the reaction mixture showed complete consumption of starting material, which was replaced by a new resonance at 249 ppm. The solvent was removed *in vacuo* and the product was extracted using hexanes. The hexanes were removed under reduced pressure to leave a yellow solid. Crystals of **2.1c** were isolated from a saturated hexanes solution on standing. Yield = 1.3 g (57%).

^{31}P NMR (121.5 MHz, C_6D_6): δ 249; ^1H NMR (300 MHz, C_6D_6): δ 7.72–6.35 (m, 12H, aryl H + alkene H), 2.3 (s, 6H, *o*-CH_3) 2.2 (s, 3H, *p*-CH_3); $^{13}C\{^1H\}$ (75.5 MHz, C_6D_6) δ 194.0 (d, *J* = 45 Hz, P=*C*), 143.2 (d, *J* = 28 Hz, aryl C), 141.6 (d, *J* = 14 Hz, aryl C), 141.3 (d, *J* = 11 Hz, aryl C), 139.8 (aryl C), 138.0 (aryl C), 135.7 (d, *J* = 45 Hz, aryl C), 133.9 (d, *J* = 11 Hz, aryl C), 131.9 (aryl C), 131.5 (aryl C), 131.4 (aryl C), 128.7 – 127.6 (m, aryl C), 127.0 (aryl C), 22.0 (m, *o*-CH_3), 20.9 (*p*-CH_3); LRMS (EI,7 0eV): m/z (%): 342, 341, 340 (4, 29, 100) [M^+], 339 (22) [M^+-H], 220 (12) [M^+-Mes–H], 189 (23) [M^+–PMes–H]; Anal. Calcd for $C_{24}H_{24}P$: C, 84.68; H, 6.22; Found: C, 84.78; H, 6.24.

2.4.4.4 Preparation of 2.2a

The polymerization was performed in a glovebox. To a stirred solution of **2.1a** (2.6 g, 7.1 mmol) in THF, *n*-BuLi (0.22 mL, 1.6 M, 0.36 mmol) was added. Upon the addition of initiator the reaction mixture turned dark red immediately. The reaction mixture was stirred at room

temperature for 5 d. At this time an aliquot was taken for ^{31}P NMR spectroscopy, which revealed the replacement of phosphaalkene signals with a very broad signal centred at –9 ppm, indicative of polymer formation. The polymer was quenched with degassed methanol (3 drops) to which the reaction mixture turned yellow. Polymer **2.2a** was purified by precipitation from THF into ice cold hexanes (3 × 25 mL) and dried *in vacuo*. Yield = 1.4 g (53%).

^{31}P {^{1}H} NMR (121.5 MHz, $CDCl_3$): δ –9 (br); ^{1}H NMR (600 MHz, $CDCl_3$): δ 9.01 – 6.47 (br, 14H, aryl H), 6.48 – 5.01 (br, 1H, C*H*(Naph)Ph), 4.24 – 2.82 (br, 2H, CH_2), 2.75 – 0.52 (br, 6H, CH_3); ^{13}C{^{1}H} (151 MHz, $CDCl_3$): δ 147 (br, aryl C), 142.5 (br, aryl C), 137.0 (br, aryl C), 133.9 (br, aryl C), 128.0 (br, aryl C), 124.9 (br, aryl C), 122.8 (br, aryl C), 46.1 (br, *C*H(Naph)Ph), 29.3 (s, *C*H_2), 23.1 (br, CH_3), 20.6 (br, *C*H_3). Assignments are made with the assistance of APT and 2D correlation NMR experiments. GPC-MALS (THF): M_n=15,100 g mol^{-1}, Đ = 1.14.

2.4.4.5 Preparation of 2.2b

The polymerization of **2.2b** was performed inside a glovebox. A stirred solution of **2.1b** (0.39 g, 1.3 mmol) dissolved in THF (3 mL) was treated with *n*-BuLi (1.2 M, 16 μL, 0.019 mmol). The reaction mixture was stirred at room temperature and monitored by ^{31}P NMR spectroscopy, which showed the gradual increase in intensity of a broad signal (centred at –10 ppm) over 8 d. The viscous reaction mixture was subsequently removed from the glovebox and quenched with methanol (3 drops). The solvent was removed in vacuo, leaving an orange oil. Polymer **2.2b** was dissolved in minimal THF and isolated by hexanes precipitation (3 × 100 mL), then dried in a vacuum oven for 24 h. Yield = 0.12 g (32%).

^{31}P{^{1}H} NMR (121.5 MHz, $CDCl_3$): δ –10 (br); ^{1}H (300 MHz, $CDCl_3$): δ 9.11 – 4.89 (br m, aryl H + C*H*(Phen)Ph), 3.48 – 0.51 (m, Mes-CH_3 + Mes-CH_2). GPC-MALS (THF): M_n = 27,100 g mol^{-1}, Đ =1.39.

2.4.4.6 Preparation of 2.2a·O

To a rapidly stirred solution of **2.2a** (0.14 g, 0.37 mmol P) in CH_2Cl_2 (2 mL), H_2O_2 (30%. 1.5 ml) was added dropwise at RT. The reaction was stirred rigorously for 1 h, at which time a ^{31}P NMR spectrum of the reaction mixture revealed quantative conversion to a new product. An additional 5 mL of CH_2Cl_2 was added and the organic layer was taken to give **2.2a**·O as an off-white solid that was dried in a vacuum oven for 24 h. Yield = 0.13 g (98%).

$^{31}P\{^1H\}$ NMR (121.5 MHz, $CDCl_3$): δ 48 (br); ^1H NMR (300 MHz, $CDCl_3$): δ 9.02 – 6.37 (br, 14H, aryl H), 6.41 – 5.54 (br, 1H, C*H*(Naph)Ph), 3.52 – 2.74 (br, 2H, Mes-CH_2), 2.66 – 0.81 (br, 6H, Mes-CH_3); GPC-MALS (THF): M_n = 17,500 g mol^{-1}; Đ =1.07.

2.4.4.7 Preparation of 2.2a·S

To a toluene (*ca.* 5 mL) solution of (0.14 g, 0.38 mmol P) was added S_8 (0.08 g, 0.31 mmol) and the reaction mixture was stirred under reflux for 2 h. An aliquot of the reaction mixture was taken and analyzed by ^{31}P NMR which revealed almost quantitative formation of a new product (53 ppm) with a small ~10% of starting material present. Heating the reaction mixture for a further 22 h failed to complete the reaction. After this time the reaction mixture was cooled to room temperature and the solvent was removed under reduced pressure. The reaction mixture was dissolved in minimal (1 mL) CH_2Cl_2 and precipitated into hexanes (15 mL). The precipitate was filtered and dried under reduced pressure to afford **2.2a**·S. Yield = 0.13 g (73%).

$^{31}P\{^1H\}$ NMR (121.5 MHz, $CDCl_3$): δ 53 (br); ^1H NMR (300 MHz, $CDCl_3$): δ 9.04 – 6.51 (br, 14H, aryl H), 6.46 – 5.0 (br, 1H, C*H*(Naph)Ph), 3.01 – 2.48 (br, 2H, Mes-CH_2), 2.46 – 1.03 (br, 6H, Mes-CH_3); GPC-MALS (THF): M_n = 12,800 g mol^{-1}, Đ =1.09.

2.4.4.8 Preparation of 2.2a·BH_3

To a THF (*ca*. 3 mL) solution of **2.2a** (0.20 g, 0.55 mmol P) was added $BH_3 \cdot SMe_2$ (0.26 mL, d = 0.80 g mL^{-1}, 2.8 mmol, 5 equiv) at −78 ºC. The reaction mixture was allowed to warm slowly to room temperature. After 24 h a ^{31}P NMR spectrum of an aliquot from the reaction mixture showed the presence of a new broad resonance (27 ppm, 50%) in addition to starting material. The reaction mixture was treated with additional $BH_3 \cdot SMe_2$ (0.26 mL, 2.8 mmol) at RT and was stirred for 36 h. $^{31}P\{^1H\}$ NMR analysis at this time showed complete conversion to product. The reaction mixture was filtered and subsequently precipitated into hexanes (25 mL) to afford **2.2a**·BH_3 as a white solid. Yield = 0.14 g (67%).

$^{31}P\{^1H\}$ NMR (162 MHz, $CDCl_3$): δ 27 (br); ^1H NMR (400 MHz, $CDCl_3$): δ 9.03 – 5.48 (br, 15H), 2.98–0.45 (br, 11H); GPC-MALS (THF): M_n = 23,100 g mol^{-1}; Đ = 1.13

2.4.4.9 Preparation of 2.2a·AuCl

To a CH_2Cl_2 (4 mL) solution of **2.2a** (0.080 g, 0.22 mmol P) was added Au(tht)Cl (0.075 g, 0.23 mmol) at RT. The reaction mixture was stirred for 2.5 h, at which time $^{31}P\{^1H\}$ NMR analysis of the reaction mixture revealed the presence of a new broad resonance at 24 ppm and complete consumption of the starting material. A further 2 mL of CH_2Cl_2 was added and **2.2a**·AuCl was precipitated into hexanes (25 mL) and dried under vacuum for 24 h. Yield = 0.12 g (93%).

$^{31}P\{^1H\}$ NMR (162 MHz, $CDCl_3$): δ = 27 (br); ^1H NMR (300 MHz, $CDCl_3$): δ 9.23 – 6.48 (br, 14H, aryl H), 6.45 – 5.17 (br, 1H, C*H*(Naph)Ph), 3.01–0.95 (br, 8H, Mes-CH_2 + Mes-CH_3); GPC-MALS (THF): M_n = 26,000 g mol^{-1}, Đ =1.10.

Chapter 3: A C-Pyrenyl Poly(methylenephosphine): Oxidation "Turns On" Blue Photoluminescence in Solution and the Solid State.

3.1 Introduction

The development of polymers featuring main group elements in the backbone is a rapidly growing interdisciplinary area of research.[127, 181-185] The unique oxidation states and coordination numbers of heteroatoms in the main chain impart chemical functionality, semi-conducting, optoelectronic and physical properties that are often quite different from their organic counterparts. Specifically, phosphorus-containing π-conjugated polymers have garnered widespread attention due to the fact that their electronic properties are dependent on the readily modifiable chemical environment at phosphorus.[127, 152, 186-189] Noteworthy classes of π-conjugated phosphorus polymers include (Figure 3.1): poly(phosphole)s (**A**),[58, 59, 61, 69, 134, 190-192] poly(arylene phosphine)s (**B**),[33-35] phospha[43-45]- and diphospha[46]-PPVs (**C** and **D**) and poly(*p*-phenylenediethynylene phosphine)s (**E**).[193] The exciting prospects for P-containing hybrid organic-inorganic materials are illustrated by the fact that devices have been fabricated for optoelectronic applications from π-conjugated molecular P-containing compounds.[194-197]

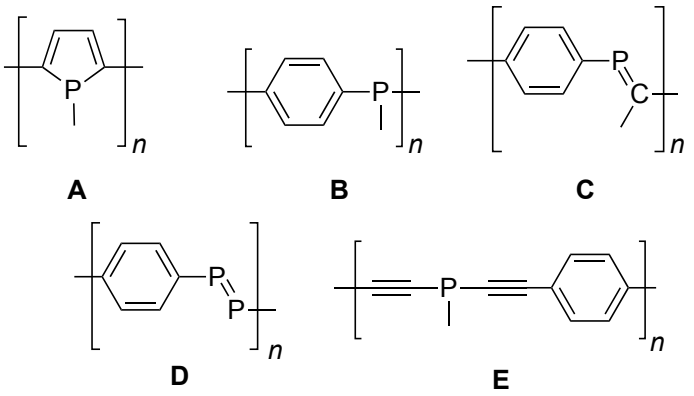

Figure 3.1: π-Conjugated phosphorus-containing polymers.

Versions of sections of this chapter have been published. Benjamin W. Rawe, Christopher M. Brown, Marc R. MacKinnon, Brian O. Patrick, Graham J. Bodwell and Derek P. Gates, *Organometallics* **2017,** *36*, 2520.

A particular interest within our research group involves the striking analogy between the polymer chemistry of olefins and that of phosphaalkenes. In 2003, we reported the addition polymerization of $MesP{=}CPh_2$ as a route to poly(methylenephosphine)s (PMPs), a new class of chemically functional P-polymers.[71] Living anionic methods of initiation may be employed to afford homo- and block co-polymers with controlled architectures.[74, 75]Additionally, the P moieties within PMPs can be functionalized to give materials that undergo self-assembly in block selective solvents. Radical-initiated copolymerization of phosphaalkenes with styrene can be achieved to access random copolymers that are effective ligands for Pd-catalyzed Suzuki-Miyaura cross-coupling reactions.[72] Recently, we have shown that PMP copolymers derived from an enantiomerically pure phosphaalkene and styrene can be used as chiral macromolecular ligands for rhodium(I).[79]

Chapter 2 of this thesis described initial investigations into the photophysical properties of PMPs. The synthesized *C*-naphthyl-substituted PMP that exhibited "turn on" emission upon oxidation of the phosphorus atoms in the polymer. Remarkably, other P-functionalized derivatives (e.g. S, BH_3 and AuCl) were non-emissive. Despite the observed selectivity towards oxygen, a limitation is that much of the emission occurs in the UV region and therefore cannot be seen with the naked eye. For this reason, a C-pyrenyl PMP was envisaged. It was hypothesized that the incorporation of pyrene units would provide access to a chemically functional hybrid organic-inorganic material that emits in the visible region.

Herein, we report a C-pyrenyl PMP that displays blue-fluorescence upon oxidation. Remarkably, strong emission is only observed upon complete oxidation suggestive of a communicative effect where even traces of unoxidized phosphine moieties lead to long range intramolecular fluorescence quenching (inverse amplification of fluorescence).

3.2 Results and Discussion

3.2.1 Monomer Synthesis

Phosphalkene **3.1** was synthesized by utilizing the well-established phospha-Peterson reaction (Scheme 3.1).[198] $MesP(SiMe_3)_2$ was treated with MeLi (1 equiv) and heated to reflux for 2 h to afford $MesP(SiMe_3)Li$ quantitatively as determined by ^{31}P NMR spectroscopy. The dropwise addition of a THF solution of 1-benzoylpyrene to the phosphide at –78 °C resulted in the quantitative formation of a diastereometric mixture of **3.1** [^{31}P NMR: 252 ppm, 80% (*Z*-**3.1**); 242 ppm, 20% (*E*-**3.1**)]. Me_3SiCl was added at –78 °C to quench anionic byproducts (e.g. $LiOSiMe_3$). After removal of volatiles *in vacuo*, *Z*-**3.1** was recrystallized selectively from toluene or THF to afford a bright yellow crystalline solid. Like many phosphaalkenes, when crystals of *Z*-**3.1** were dissolved in $CDCl_3$ an *E/Z*-**3.1** mixture formed in the presence of ambient light at RT over a few hours. The absence of light slows down this process considerably.[153, 156, 199]

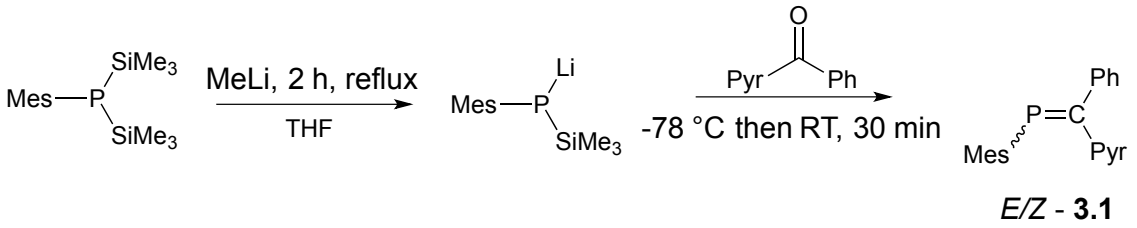

Scheme 3.1: Synthesis of *E/Z*–3.1

Crystals suitable for analysis by X-ray crystallography of *Z*-**3.1** were grown from a solution of hexanes and dichloromethane. The molecular structure is shown in Figure 3.2 (see Appendix A, table A1 for data collection parameters). The P=C bond length [avg. 1.689(9) Å] is on the longer side of that expected for *C*-aryl phosphaalkenes but is typical of *P*-Mes bearing phosphaalkenes[153, 161]

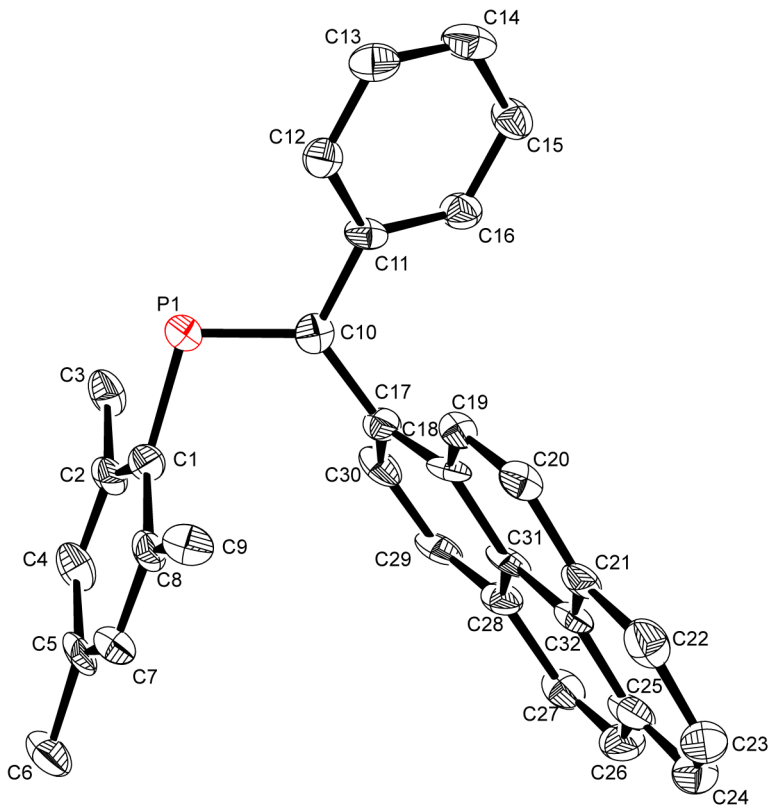

Figure 3.2: Molecular structure of *Z*-3.1

(thermal elipsoids are displayed at the 50% probability level) Hydrogen atoms are omitted for clarity. The unit cell contains three distinct conformations of *Z*-3.1 only one is displayed here.

The P-C_{Mes} single bond (avg. 1.83 Å) is shorter than that of a typical P-C single bond (1.85-1.91 Å) which suggests a small degree of π-conjugation between the *P*-Mes substituent and the P=C bond. Similarly, the bond length of =C–C_{Pyr} (avg. 1.49 Å) is slightly shorter than a typical C-C single bond which is consistent with the expected effect of conjugation of the *C*-Aryl substituents with the P=C π bond. Another indicator of the degree of π conjugation in **3.1** is the angle between the aryl moieties and the best plane of the P=C bond. The angle between the *P*-Mes and the P=C bond (*ca.* 71°) is typical for *P*-Mes phosphaalkenes (*cf.* MesP=CPh_2 = 71° [160] or 72°).[161]

Interestingly, the *trans* configured phenyl moiety is only slightly twisted with respect to the P=C bond (34°). In contrast, the angle between the *cis*-1-pyrenyl group and the P=C bond is far greater (*ca*. 64°). Previously, it has been suggested that intermolecular π-stacking of a *cis*-aryl substituent can account for large differences in plane angles between the P=C bond and the *cis* and *trans* substituents. Specifically, MesP=CPh_2 has been obtained in two crystallographic forms. One has similar plane angles (Ph_{trans} = 37°, Ph_{cis} = 43°)[160] and no π-stacking whereas the other has different plane angles (Ph_{trans} = 21°, Ph_{cis} = 59°)[161] and intermolecular dimers are observed via π-stacking of the *cis*-Ph. Likewise, for *Z*-MesP=CPh(Phen) (*Z*-**2.1b**) the angles are quite different (Ph_{trans} = 20°, $Phen_{cis}$ = 63°) and intermolecular π-stacking is observed for the Phen moieties. Inspection of the crystal packing of *Z*-**3.1** (Figure 3.3) suggests a considerable intermolecular interaction between adjacent pyrene substituents. The molecules of *Z*-**3.1** adopt a dimeric structure with the distance between the planes of the pyrene substituents is consistently *ca.* 3.6 Å. For comparison, the distance between planes of Phen substituents in *Z*-**2.1b** is *ca.* 3.4 Å. It should also be noted that π stacking in pyrene and between pyrenyl substituents in a variety of compounds is well-established within the literature.[200, 201]

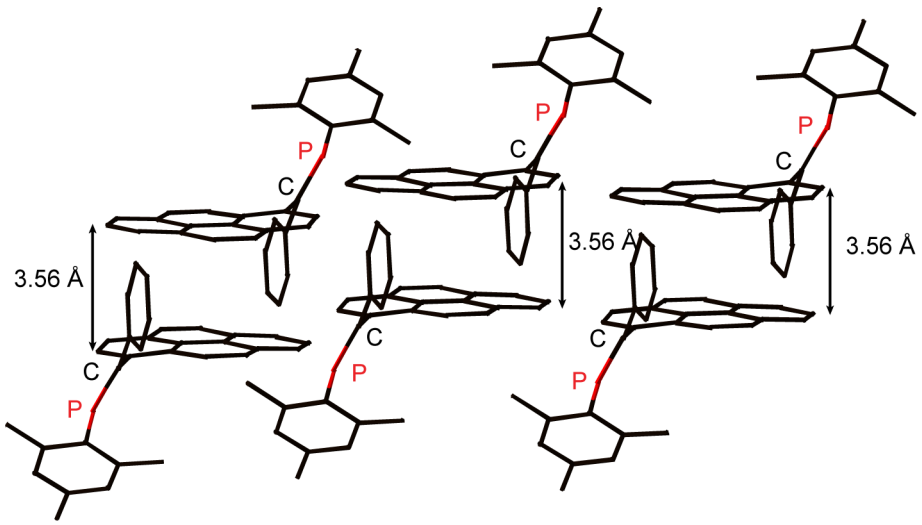

Figure 3.3: A portion of the crystal structure of *Z*-3.1 showing intermolecular packing of pyrene moieties.

3.2.2 Polymer Synthesis

The polymer derived from **3.1** is of interest for its potentially novel photophysical properties. Following procedures developed for the anionic polymerization of MesP=CPh_2 and derivatives,[74] Monomer **3.1** was treated with 10 mol% *n*-BuLi in a glove box at RT (Scheme 3.2). Upon addition of initiator the reaction mixture turned a dark blue color immediately. The reaction mixture was stirred at RT for 7 days in a sealed vessel within a glovebox under an N_2 atmosphere. The reaction progress was monitored by ^{31}P NMR spectroscopy which revealed the depletion of the signals corresponding to *E/Z*-**3.1** (252 & 241 ppm) and their replacement by a broad signal at –11 ppm, which was assigned, to PMP **3.2**. The polymerization was terminated by the addition of degassed methanol (2 drops) upon which the reaction mixture turned a yellow color. The reaction mixture was added to a vigorously stirred ice-cold hexanes solution from which the polymer precipitated as an off-white solid. The material was purified by two further precipitations and dried *in vacuo*.

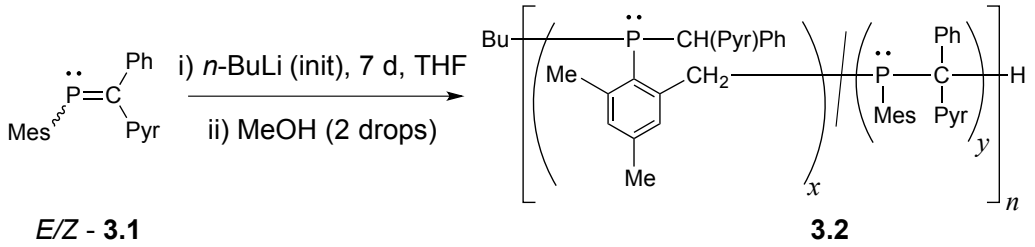

E/Z - **3.1** **3.2**

Scheme 3.2: Synthesis of Poly(methylene phosphine) 3.2

Analysis of *C*-1-pyrenyl-substituted PMP by gel permeation chromatography featuring a multi-angle light scattering detector (GPC-MALS) revealed **3.2** to be a polymer of M_n = 4,800 g mol^{-1} and Đ = 1.56. The molecular weight is close to the expected value for the monomer to initiator ratio used (M_n calcd = 4,400 g mol^{-1}). Recently, we reported that the microstructure of the PMP made from the polymerization of MesP=CPh$_2$ with a radical initiator featured an Ar-CH$_2$-P-CHPh$_2$ linkage.[84] Multinuclear NMR spectroscopy using a 600 MHz spectrometer with a cryoprobe was used to investigate the microstructure of **3.2**. ^{1}H NMR spectroscopic analysis of **3.2** revealed two broad signals from 5.4-9.3 and 0.5-4.0 ppm with two broad shoulders at 5.4-6.5 and 2.6-4.0 ppm which are assigned to the PyrC*H*Ph and Mes-C*H*$_2$ protons respectively with the aid of HSQC and ^{13}C-APT experiments (see Appendix C for spectra). These assignments are in good agreement with the ^{1}H NMR spectra of the model compounds Bn(Mes)P-CH(Pyr)Ph (see Figure 3.4a) and Bn(Mes)P-CHPh$_2$.[84] The obtained NMR spectra for **3.2** exhibit similarities to C-naphthyl PMP **2.2a** synthesized by anionic initiation. The mechanism to explain the microstructure of PMPs synthesized by anion initiation is of ongoing study within our group.

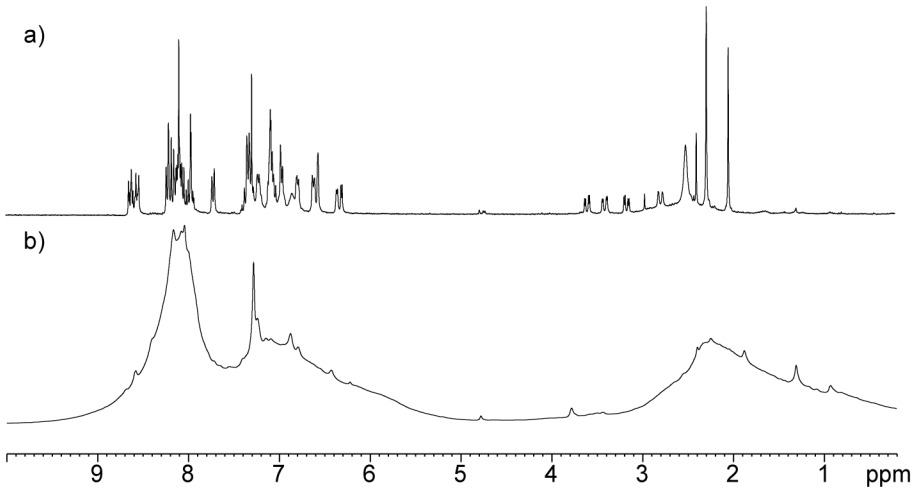

Figure 3.4: a) ^{1}H NMR (300MHz, $CDCl_3$) spectra of Bn(Mes)P-CH(Pyr)Ph; b) ^{1}H NMR (300MHz, $CDCl_3$) spectrum of 3.2.

Oxidized polymer **3.2**·O was prepared by the addition of an aqueous hydrogen peroxide solution (30% w/w) to a solution of **3.2** in dichloromethane. The resultant polymer, **3.2**·O displays a broad resonance in its ^{31}P NMR spectrum in $CDCl_3$ at 47 ppm but, analogous to previously reported PMP-oxide polymers, has a narrower line width than **3.2**.[71] The highly fluorescent nature of **3.2**·O appears to interfere with the GPC analysis of **3.2**·O using MALS detection. Thus, molecular weights were determined by conventional GPC (*vs.* polystyrene standards). Similar molecular weight estimates for **3.2**·O (M_n = 2,100 g mol^{-1}; Đ = 1.4) and **3.2** (M_n = 2,400 g mol^{-1}; Đ = 1.4) were obtained. Presumably, the apparent decrease in molecular weight for the oxidized polymer resulted from the increased polarity of phosphine oxide **3.2**·O, which might lead to a tighter coil size in solution (vs. polystyrene). It should also be noted that the molecular weight of **3.2** was also underestimated when using polystyrene as a standard. This is expected since the repeating unit for the former is much higher than styrene of an equal chain length.

3.2.3 Photophysical Properties

The absorption spectra (Figure 3.5) recorded show that **3.1**, **3.2** and **3.2**·O had large extinction coefficients ($\varepsilon \sim 10^5$ M^{-1} cm^{-1}) and contain several maxima typical for polyaromatics. Each spectrum displayed three sets of overlapping signals (λ_{max} = 248 nm, 281 nm and 351 nm for **3.2**) assigned to vibronic spacing of the π-π* transition of the pyrene substituent. The observed spectra are analogous to those of 1-methylpyrene and similar derivatives.[166] In addition to these three sets of signals, a higher wavelength broad absorption was observed (*ca.* 390 nm) for **3.1** only. This low energy band is tentatively assigned to an π-π* transition involving the P=C bond. DFT calculations revealed that the HOMO was primarily π-type with contributions from phosphorus and the pyrene. The LUMO was of π* nature with a major contribution from the P=C moiety and a minor contribution from pyrene. The HOMO and LUMO are shown in Figure 3.6. TD-DFT was also used to aid UV/Vis assignments. The HOMO-LUMO transition was calculated to be the first excited state, with an energy of 370 nm (3.35 eV), f = 0.61.

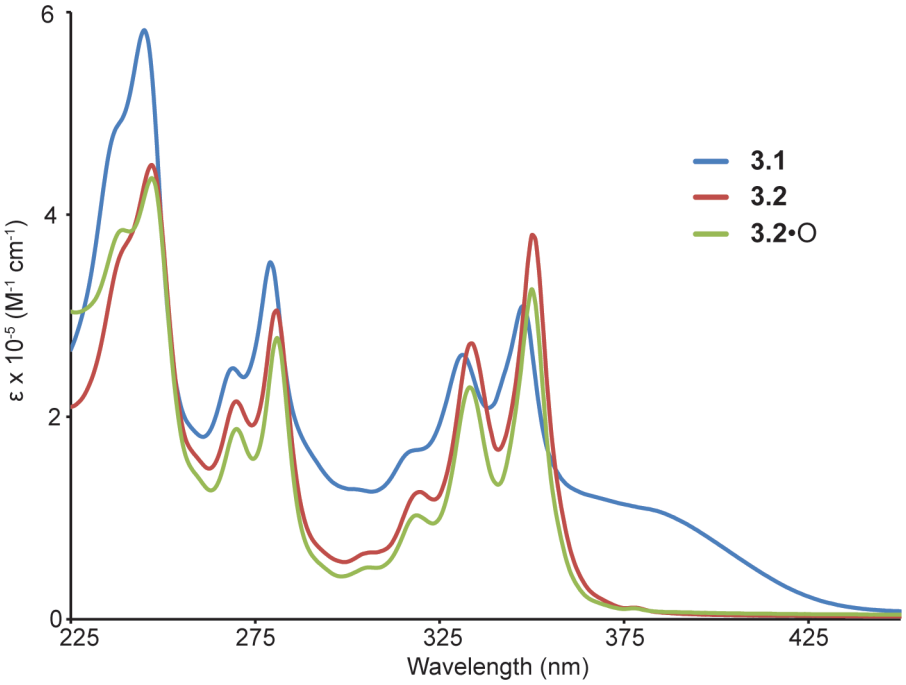

Figure 3.5. Absorption Spectra of 3.1, 3.2 and 3.2·O (solvent = THF, c = 1.0 × 10^{-6} M in phosphorus).

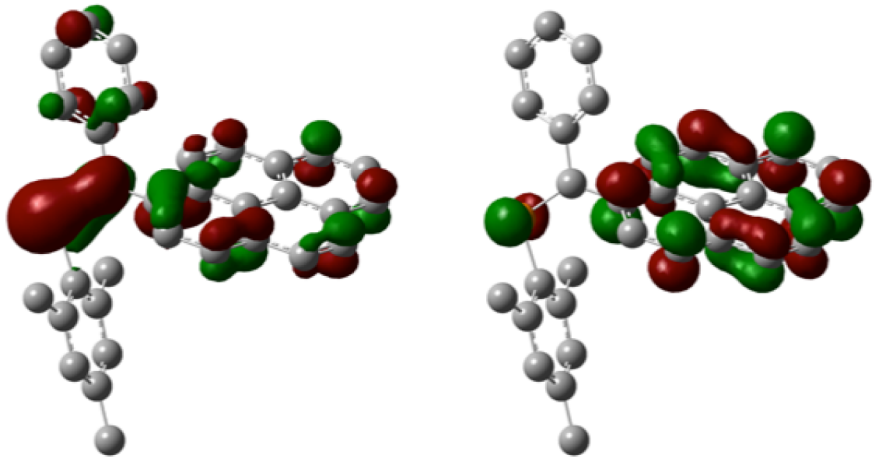

Figure 3.6. Calculated MO of HOMO (MO 116) and LUMO (MO 117) for 3.1.

Interestingly, the absorption maxima for monomer **3.1** and polymers **3.2** and **3.2**·O were virtually identical. This suggests that π-conjugation between the aromatic system and the P=C bond is minimal. Upon isomerization of pure *Z*-**3.1** to *E/Z*-**3.1** there was no change in the UV/Vis spectrum suggesting there was a minimal change in π-conjugation between the *trans*-configured pyrenyl moiety and the P=C bond in *E*-**3.1**.

Investigations of the emission properties of **3.2**·O in THF solution revealed three emission maxima (λ_{max}= 379, 389 and 400 nm) and a shoulder (423 nm) tailing into the blue region (>450 nm; Figure 3.7) The appearance of the spectrum shares similarities to 1-methylpyrene and other substituted derivatives of pyrene[202] albeit with a lower quantum yield (Φ = 0.05 for **3.2**·O). These observations potentially reflect the heavy atom quenching effect of the phosphorus atoms.[203]

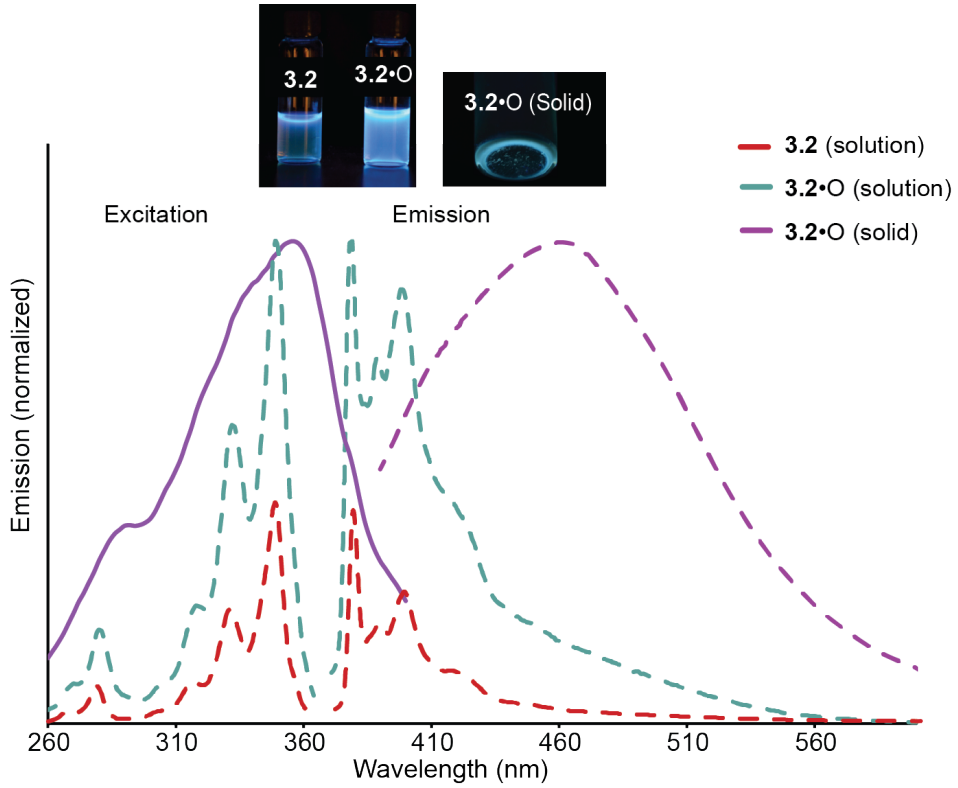

Figure 3.7: Emission and excitation spectra of 3.2·O in the solution (solvent=THF, c = 1.0×10^{-6} M in phosphorus) and solid state.

Inset (left): THF solutions of 3.2 (left) and 3.2·O (right) under a UV lamp (c ≈ 1 mg/mL, λ_{ex} = 365 nm). Inset (right): A solid sample of 3.2·O irradiated with a UV lamp (λ_{ex} = 365 nm).

Phosphine oxide polymer **3.2**·O also exhibited blue emission in the solid state. In this case, the emission band was much broader, lacked fine structure, and was bathochromically shifted (λ_{max} = 460 nm, Φ = 0.07) from that observed in the solution spectrum of **3.2**·O. The breadth and wavelength of this emission band is typical of that observed for pyrene excimers in the solid state.[204-206] Similar behavior has been noted for pyrene-containing polymers[207-209] and dendrimers.[210, 211]

The lifetimes of emission from both solution and solid states were measured. Each state had three distinct short-lived fluorescence emissions (τ_{soln} = 3.1 ns, 6.2 ns, 12.3 ns; τ_{sld} = 1.2 ns, 5.7 ns, 25.6 ns). The excitation spectra of **3.2**·O (Figure 3.7) indicated that both solid- and

solution-state emission originated mainly from the lowest energy set of absorption signals (i.e. λ_{max} = 351 nm in the absorption spectrum described above). The other absorption bands resulted in far less emission.

It should be noted that THF solutions of **3.1** and **3.2** were far less emissive than solutions of oxidized **3.2**·O. This phenomenon can be observed spectroscopically and also by irradiation with a UV lamp, which revealed a strong blue emission for **3.2**·O (Figure 3.6, inset). Blue emission is quite desirable since it is one of the primary colors but is rarely observed for conjugated polymers. For example, a few derivatives of PPV exhibit blue photoluminescence but require exotic substituents or bulky groups to limit the extent of π-conjugation.[212-215] It should be noted that there are examples of conjugated boron-containing polymers that are blue emitting but have limited stability towards air.[216, 217]

Another fascinating property of PMP **3.2** is its "turn on" fluorescence when the P-centres are oxidized. A series of experiments were performed to understand the relationship between the degree of oxidation of the polymer and its emission properties. Specifically, substoichiometric amounts of hydrogen peroxide were added to a solution of **3.2** in order to afford polymers where the phosphorus centres are partially oxidized. $^{31}P\{^{1}H\}$ NMR spectroscopic analysis of each isolated polymer revealed signals assigned to either phosphine (–11 ppm) and phosphine oxide (47 ppm) units (Figure 3.8).

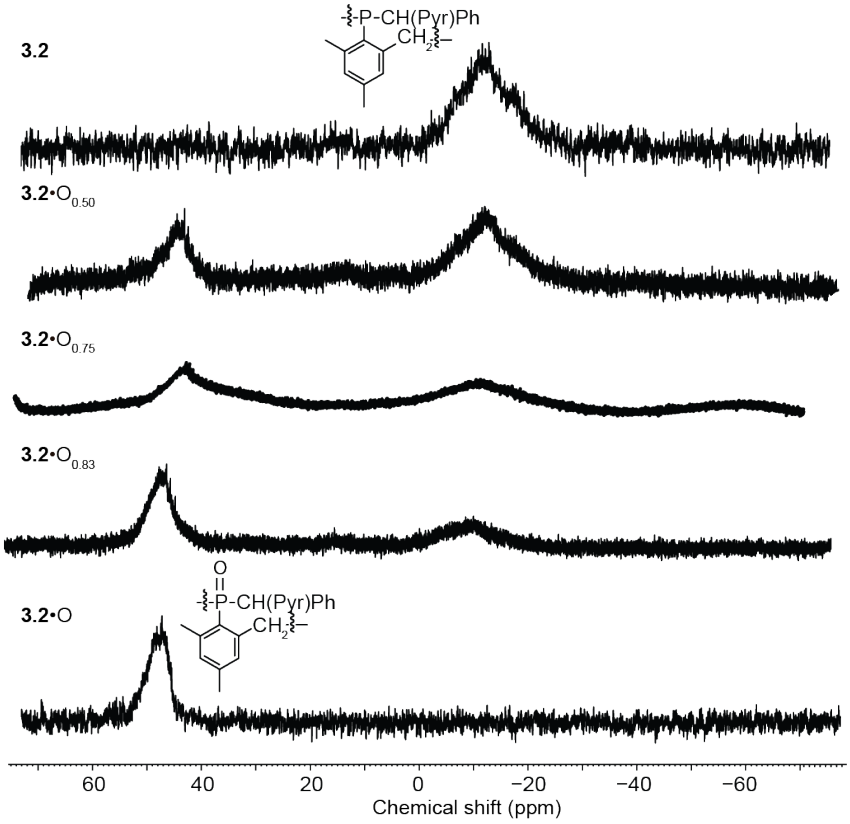

Figure 3.8: $^{31}P\{^{1}H\}$ NMR spectra of 3.2, 3.2·O and partially oxidized polymers $3.2\cdot O_{0.50}$ $3.2\cdot O_{0.75}$ and $3.2\cdot O_{0.83}$.

The degree of oxidation was estimated by integration of these signals. The emission spectra of unoxidized **3.2**, fully oxidized **3.2**·O, and samples with 50%, 75% and 83% oxidation are shown in Figure 3.9. As the degree of oxidation was increased, an increase in fluorescence was expected. It was therefore remarkable to observe that the partially oxidized polymers showed similar emission intensity to unoxidized **3.2**. By comparison, the fully oxidized **3.2**·O was substantially more emissive, thereby indicating that "turn on" emission occurred only at very high degrees of oxidation. The increase of emission upon oxidation is possibly due to the absence of photoinduced electron transfer of the phosphorus lone pair as a quenching mechanism[99] and has been documented previously for molecular P-containing chromophores.[118, 119, 122, 124]

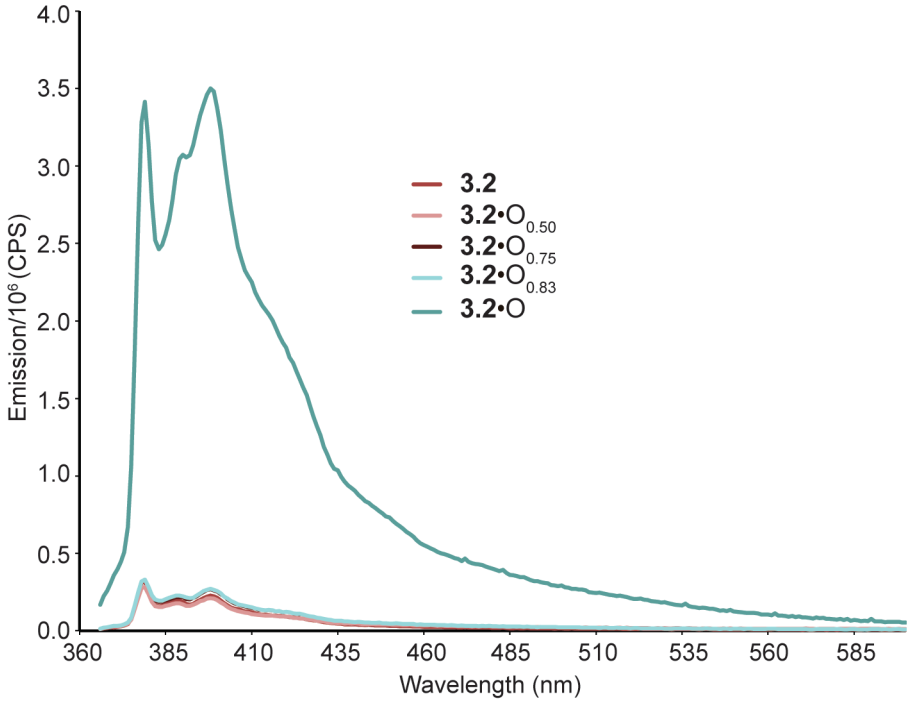

Figure 3.9: Emission spectra of 3.2, 3.2·O and partially oxidized derivatives (solvent=CH_2Cl_2, c = 1.0×10^{-6} M in phosphorus, λ_{ex} = 351 nm).

Molecular phosphines bearing pyrene moieties have been used extensively for solution-based peroxide-sensing applications.[111-114] In contrast to polymeric **3.2**, the emission of molecular systems increases linearly with oxide concentration. In partially oxidized **3.2**·O, there appears to be an unexpected cooperative or communicative effect where the fluorescence of the oxide units within a chain is quenched, presumably by phosphines, until extremely high degrees of oxidation are reached. For comparison, the fluorescence intensity of a mixture of **3.2** (0.5 μM) and **3.2**·O (0.5 μM) (i.e. 50% oxidized) was greater than that of partially oxidized **3.2**·O (50% oxidized, 1.0 μM) and comparable to fully oxidized **3.2**·O (0.5 μM). Furthermore, the same observations were made with more concentrated solutions of **3.2** (10 μM), **3.2**·O (10 μM) and a 50:50 mixture (10 μM). Therefore, we conclude that the amplification of quenching observed for partially oxidized PMPs is intramolecular (i.e. within the chain) rather than intermolecular (i.e.

between chains). Given the proliferation of applications for oxygen sensors,[218-224] the potential for sensor applications for these unique materials based on PMP **3.2** is of interest.

3.3 Summary

This chapter features the synthesis and polymerization of a new phosphaalkene bearing a C-pyrenyl substituent. The resultant poly(methylenephosphine) possessed intriguing photophysical properties in solution and in the solid state. The solid state emission spectrum suggested that the broad emission is due to pyrene excimer formation. In solution, a weak blue fluorescence was observed that was greatly enhanced when the phosphorus centres are oxidized using H_2O_2. Notably, this fluorescence enhancement was only observed upon complete oxidation of the phosphorus atoms within the chain. It appears as though a small number of phosphine moieties within a chain intramolecularly quench the fluorescence of all the pyrene units in the chain. This cooperative or amplification of quenching of fluorescence is quite unusual. Thus, future studies on these and related phosphorus polymer will investigate their potential use as novel sensory or switching materials.

3.4 Experimental Section

3.4.1 Materials and Methods

All manipulations of air- and/or water-sensitive compounds were performed under a nitrogen atmosphere by using standard Schlenk or glovebox techniques. Hexanes and dichloromethane were deoxygenated with nitrogen and dried by passing through a column containing activated alumina. Tetrahydrofuran (THF) was dried over sodium and benzophenone and was distilled prior to use. Hydrogen peroxide was purchased as a 30% solution with water from Aldrich and was used as received and titrated against $KMnO_4$. Methyllithium and *n*-butyllithium were

purchased from Aldrich and used as received and titrated by using *N*-benzylbenzamide.[173] $MesP(SiMe_3)_2$[174] was made following literature procedures.

3.4.2 Equipment

^1H, $^{31}P\{^1H\}$, $^{13}C\{^1H\}$ NMR spectra were recorded at 25 °C on Bruker Avance 300, 400 or 600 MHz spectrometers. H_3PO_4 (85%) was used as an external standard ($\delta = 0$ for ^{31}P). ^1H NMR spectra were referenced to residual protonated solvent signal and $^{13}C\{^1H\}$ NMR spectra were referenced to the deuterated solvent signal. Elemental analyses were performed in the University of British Columbia Chemistry Microanalysis Facility. Mass spectra were recorded on a Kratos MS 50 instrument in EI mode (70 eV). Polymer molecular weights were determined by triple detection gel permeation chromatography (GPC-MALS) using an Agilent liquid chromatograph equipped with an Agilent 1200 series isocratic pump, Agilent 1200 series standard autosampler, Phenomenex Phenogel 5 μm narrow bore columns (4.6 × 300 mm) 10^4 Å (5,000 – 500,000), 500 Å (1,000 – 15,000), and 10^3 Å (1,000 – 75,000), Wyatt Optilab T-rEx differential refractometer ($\lambda = 658$ nm, 40 °C), Wyatt TriStar miniDAWN (laser light scattering detector at $\lambda = 690$ nm) and a Wyatt ViscoStar viscometer. A flow-rate of 0.5 mL min^{-1} was used and samples were dissolved in THF (ca. 2 mg mL^{-1}). The molecular weights were determined using 100% mass recovery methods from Astra software version 5. Solution absorption spectra were obtained in THF on a Varian Cary 5000 UV-Vis-near-IR spectrophotometer using a 1 cm quartz cuvette. Fluorescence and excitation spectra were obtained in THF on a Horiba scientific fluoromax-4 fluorospectrometer using a 1 cm quartz cuvette. The solution state quantum yield of **2**·O was determined using anthracene as a standard ($\Phi = 0.27$ in ethanol). Solid state emission spectra and quantum yield measurements were recorded on a Photon Technology International QuantaMaster 50 fluorimeter fitted with an integrating sphere, double monochromator and utilizing a 75W Xe

arc lamp as the source. Emission lifetime data were collected using a Horiba Yvon Fluorocube TCSPC apparatus. A 370 nm NanoLED source pulsing at a repetition rate of 50 - 100 kHz was used for excitation. Broadband emission was monitored by a CCD detector at wavelengths > 400 nm using a low pass filter. Data were fitted using the DAS6 Data Analysis software package.

3.4.3 X-Ray Crystallographic Studies

All single crystals were immersed in oil and mounted on a glass fiber. Data were collected on a Bruker X8 APEX II diffractometer with graphite-monochromated $Mo_{K\alpha}$ radiation. All structures were solved by direct methods and subsequent Fourier difference techniques. All non-hydrogen atoms were refined anisotropically with hydrogen atoms being included in calculated positions but not refined. All data sets were corrected for absorption effects (SADABS), Lorentz, and polarization effects.[225] All calculations were performed using SHELXL-2014 crystallographic software package from Bruker AXS.[179] Additional crystal data and details of data collection and structure refinement are given in Appendix A, table A1. Crystallographic data for *Z*-**3.1** has been deposited with the Cambridge Structural Database, CCDC 1530414.

3.4.4 Computational Details

Density functional theory calculations were performed in Gaussian 09 (Revision D.01).[226] Initial geometry optimizations using the crystal structure geometry of **3.1** were performed using the 6-31G*+ basis set and the B3LYP functional.[227-229] Molecular orbital and TD-DFT[230] calculations were performed using the 6-311G**++ basis set and CAM-B3LYP functional.[231] Additionally, solvation corrections were implemented using the Polarizable Continuum Model[232] using tetrahydrofuran ($\varepsilon = 7.43$) as solvent.

3.4.5 Synthesis

3.4.5.1 Preparation of 1-Benzoylpyrene

Pyrene (2.0 g, 9.9 mmol) and benzoyl chloride (1.7 g, 1.4 mL, 12 mmol) were dissolved in CH_2Cl_2 (100 mL). To this solution was added $AlCl_3$ (1.6 g, 12 mmol) in one portion and the reaction mixture was stirred at rt under a N_2 atmosphere for 3 h. The reaction mixture was poured into H_2O (100 mL) and extracted with CH_2Cl_2 (2 × 50 mL). The combined organic layers were dried, filtered and concentrated under reduced pressure. The resulting residue was subjected to column chromatography (25% CH_2Cl_2/hexanes) to yield 1-benzoylpyrene as yellow solid. Yield = 2.5 g (82%).

^{1}H NMR (300 MHz, $CDCl_3$): δ 8.42 (d, *J* = 9.3 Hz, 1H, aryl H), 8.21 -8.32 (m, 4H, aryl H), 8.20-8.02 (m, 4H, aryl H), 7.9 (m, 2H, aryl H), 7.61 (tt, *J* = 7.4, 1.5 Hz, 1H, aryl H), 7.38-7.51 (m, 2H, aryl H); ^{13}C{^{1}H} NMR (75 MHz, $CDCl_3$): δ 198.4 (*C*=O), 138.7 (aryl C), 133.2 (aryl C), 133.1 (aryl C), 133.0 (aryl C), 131.1 (aryl C), 130.6 (aryl C), 130.5 (aryl C), 129.7 (aryl C), 129.1 (aryl C), 128.8 (aryl C), 128.4 (aryl C), 127.2 (aryl C), 126.9 (aryl C), 126.4 (aryl C), 126.0 (aryl C), 125.9 (aryl C), 124.8 (aryl C), 124.7 (aryl C), 124.4 (aryl C), 123.7; Mp 124-125 °C; HRMS (APCI-(+)) calcd for $C_{23}H_{14}O$: *m/z* = 306.1045, found: *m/z* 306.2148.

3.4.5.2 Preparation of 3.1

To a stirred solution at RT of $MesP(SiMe_3)_2$ (1.0 g, 3.4 mmol) dissolved in THF (30 mL) was added MeLi (2.1 mL, 3.5 mmol, 1.60 M) in ether. The reaction mixture was heated under reflux overnight. An aliquot removed for analysis by ^{31}P spectroscopy revealed a signal resonance at –187 ppm, which was assigned to $MesP(SiMe_3)Li$. The reaction mixture was cooled to -78 °C, after which a solution of 1-benzoylpyrene (1.1 g, 3.4 mmol) was added dropwise to the reaction mixture. After 5 min, the reaction mixture was warmed to room temperature and was stirred for a

further 25 min. An aliquot was taken for ^{31}P NMR spectroscopy that indicated that an *E/Z* mixture of phosphaalkene **3.1** had been formed quantitatively (252 ppm, *Z*-**3.1**, 80%, 241 ppm, *E*-**3.1**). The solvent was removed *in vacuo* leaving an orange residue. To the residue was added ether (3 × 30 mL) and the suspension was filtered and the solvent removed *in vacuo*. The residue was heated (55 °C) under reduced pressure for 4 h to remove other volatiles from the reaction mixture. From the resulting residue, bright yellow crystals suitable for x-ray diffraction were formed from the slow evaporation of solvent from a dichloromethane/hexanes mixture. Crystals can also be grown from a saturated solution of toluene or THF. In all cases *Z*-**3.1** crystallized preferentially. Yield = 1.15 g, (76%).

^{31}P NMR (C_6D_6, 121MHz): δ 252 (*Z*-**3.1**), 241(*E*-**3.1**); ^{1}H (C_6D_6, 300MHz): (*Z*-**1**) δ 8.21-7.04 (m, 14H, aryl H), 6.88 - 5.78 (br, 2H, Mes-*H*), 3.04 - 1.82 (br, 6H, *o*-C*H*$_3$), 1.71 (s, 3H, *p*-C*H*$_3$); $^{13}C\{^{1}H\}$ NMR ($CDCl_3$, 101 MHz) *Z*-**1** only: δ 194.0 (d, *J* = 44 Hz, P=*C*), 145.1 (d, *J* = 24 Hz, aryl C), 138.1 (aryl C), 137.9 (aryl C), 135.6 (d, *J* = 42 Hz C_{ipso}-P), 131.1 (aryl C), 130.7 (aryl C), 130.6 (aryl C), 128.8 (d, *J* = 5.1 Hz, aryl C), 128.5 (aryl C), 128.1 (aryl C), 127.4 (aryl C), 127.1 (aryl C), 126.8 (aryl C), 126.1 (aryl C), 126.0 (aryl C), 125.9 (aryl C), 125.1 (aryl C), 125.0 (aryl C), 124.9 (aryl C), 124.0 (aryl C), 22.3 (br, *o*-*C*H$_3$), 20.5 (s, *p*-*C*H$_3$); MS (EI, 70 eV): 441, 440 [7, 100; M^+]; 426, 425 [3, 75; M^+-CH_3]; 78, 77 [2, 11; Ph^+]. Anal. Calcd. for $C_{32}H_{25}P$: C, 87.25; H, 5.72. Found: C, 87.15; H, 5.80.

3.4.5.3 Preparation of 3.2

The polymerization of **3.1** was performed in a glovebox. To a stirred solution of **3.1** (1.20 g, 2.7 mmol) in THF, *n*-BuLi (85 μL, 5 mol%) was added. Upon the addition of initiator the reaction mixture turned dark blue immediately. The reaction mixture was stirred at RT for 7 d. At this time an aliquot was taken for $^{31}P\{^{1}H\}$ NMR spectroscopy, which revealed the replacement of

phosphaalkene signals with a very broad signal centreed at –11 ppm, indicative of polymer formation. The reaction mixture was removed from the glovebox and quenched with degassed methanol (3 drops) to which a yellow solution was formed. The polymer was purified by precipitation from minimal THF into ice-cold hexanes (3 x 25 ml) and dried in a vacuum oven overnight. Yield = 0.61 g (51%).

$^{31}P\{^{1}H\}$ NMR ($CDCl_3$, 121MHz): δ –11 (br). ^{1}H NMR ($CDCl_3$, 600 MHz): δ 9.61-7.63 (br, 9H, aryl H), 7.56-6.21 (br, 7H, aryl H), 6.17-5.33 (br, 1H, P-C*H*(Pyr)Ph), 4.21-3.04 (br, 2H Mes-C*H*$_2$) 2.7-0.3 (br, 6H, Mes-C*H*$_3$). $^{13}C\{^{1}H\}$ NMR ($CDCl_3$, 151 MHz): δ 149.2-134.7 (br m, aryl C), 132.8-121.6 (br m, aryl C) 49.9-41.5 (br, P-*C*H(Pyr)Ph), 36.2-27.4 (br, Mes-*C*H$_2$), 26.9-15.7 (br, Mes *o*-*C*H$_3$), 14.6-13.1 (br, Mes *p*-*C*H$_3$). Assignments are made with the assistance of APT and 2D correlation NMR experiments. GPC (THF, MALS): M_n = 4 800 g·mol^{-1}, Đ = 1.56; *dn/dc* = 0.276.

3.4.5.4 Preparation of 3.2·O

To a rapidly stirred solution of **3.2** (100 mg, 0.23 mmol) in CH_2Cl_2 (2 mL), H_2O_2 (1.5 mL, 30% in H_2O) was added dropwise at RT. The reaction was stirred rigorously for 1 h, at which time a $^{31}P\{^{1}H\}$ NMR spectrum of the reaction mixture revealed quantitative conversion to a new product. An additional 5 mL of CH_2Cl_2 was added and the organic layer was taken to give an off white solid which was dried in a vacuum oven overnight. Yield: 81 mg, (78%).

$^{31}P\{^{1}H\}$ NMR ($CDCl_3$, 121 MHz): δ 47 (br). ^{1}H NMR ($CDCl_3$, 300 MHz): δ 9.62-7.73 (br, 11H, aryl H), 7.71-6.83 (br, 3H, aryl H), 6.77-5.59 (br, P-C*H*(Pyr)Ph), 4.03-2.47 (br, 2H, Mes-C*H*$_2$), 2.46-0.32 (br, 6H, Mes-C*H*$_3$). Assignments are tentative. GPC (vs. Polystyrene) M_n = 2,100 g mol^{-1}; Đ: 1.4).

3.4.5.5 Preparation of Bn(Mes)PC(Pyr)PhH

A stirred solution of $PhCH_2Li$ (11.5 mL, 0.166 M, 1.91 mmol) in THF was prepared and cooled to -78 °C. To this solution was added **3.1** (0.70 g, 1.59 mmol) and the reaction mixture immediately turned dark blue. Upon warming to RT the reaction mixture was stirred for a further 1 h. The ^{31}P NMR spectrum of an aliquot revealed that the signal assigned to starting material had been consumed. Two new signals at –10 ppm were assigned to stereoisomers of Bn(Mes)P-C(Pyr)PhLi. Degassed water (1 mL) was added to quench the reaction. The solvent was removed *in vacuo* to leave an orange residue. To this residue was added dichloromethane (2 × 30 mL) and the suspension was filtered and the volatiles removed *in vacuo*. Attempts to crystallize this compound were unsuccessful.

^{31}P NMR ($CDCl_3$, 121 MHz): δ –3, –5 (diastereomers of Bn(Mes)PC(Pyr)PhH); ^{1}H and $^{1}H\{^{31}P\}$ NMR ($CDCl_3$, 300 MHz): Spectra and tentative assignments of key signals are shown in the Appendix (Figure C8); MS (EI, 70eV): 534, 533, 532 [8, 41, 100; M^+]; 441 [7; M^+-$PhCH_2$]; 292, 291 [39, 100; $PyrPhCH^+$], 91 [26, $PhCH_2^+$].

3.4.5.6 In situ preparation of partially oxidized derivatives of 3.2·O

To a rapidly stirred solution of **3.2** (40 mg, 91 μmol) in CH_2Cl_2 (1.8 mL), H_2O_2 (45 μL, 44 μmol, 0.98M in H_2O) was added at RT using a microsyringe. The reaction was stirred rigorously for 1 h, at which time the solvent was removed and minimal $CDCl_3$ added to dissolve all products. A $^{31}P\{^{1}H\}$ NMR spectrum was taken which showed 2 broad signals at –11 and 47 ppm assigned to P and P=O moieties within the polymer. The NMR experiment was performed with a long delay time (2 s) between scans to allow integration of each region to be quantitative. The contents of the NMR tube were added back into the reaction flask and the solvent was removed. The off white solid formed was redissolved in CH_2Cl_2 (1.8 mL) and 50 μL was taken from the solution

and diluted to make a 1.0 μM solution in CH_2Cl_2 to be measured by fluorescence spectroscopy. To the bulk solution further H_2O_2 was added and the process repeated to make a total of three partially oxidized polymers (50, 75 and 83% oxidation) and **3.2**·O.

$^{31}P\{^1H\}$ NMR ($CDCl_3$, 121 MHz): δ 47 (br, R_3P=O), -11 (br, R_3P).

Chapter 4: Poly(*p*-phenylenediethynylene phosphine)s: Synthesis, Characterization and Photophysical Properties

4.1 Introduction

The development of phosphorus-containing macromolecules is a highly active research area lying at the interface of main group chemistry and polymer science. Inspired by the prospect of finding materials with novel chemical functionality and properties, researchers are attracted by the wide range of coordination numbers, oxidation states and bonding environments that are uniquely provided by phosphorus.[4, 127, 152, 189, 196] Perhaps resulting from the synthetic difficulty to incorporate phosphorus atoms into long chains, the major classes of organophosphorus polymers (Figure 4.1) remain limited to polyphosphazenes (**A**),[4] poly(phosphole)s (**B**),[58, 61, 69, 70, 134, 192] poly(arylene/vinylene phosphine)s (**C** and **D**),[33-35, 54, 55, 135, 136] poly(*p*-phenylene phosphaalkene)s (**E**)[29, 43-45] and poly(*p*-phenylene diphosphene) (**F**),[46] poly(methylenephosphine)s (**G**).[71, 72, 74, 78, 79, 82, 84] poly(ferrocenylphosphine)s (**H**),[128-131] and polyphosphinoboranes (**I**).[137-139, 233] A major thrust in this area has involved incorporating phosphorus moieties within extended π-conjugated organic frameworks. The ready oxidation or coordination of the phosphorus moiety has the potential to finely tune or modulate the electronic properties.

Versions of sections of this chapter have been published. Benjamin W. Rawe and Derek P. Gates, *Angew. Chem. Int. Ed.* **2015**, *54*, 11438; *Angew. Chem.* **2015**, *127*, 11600.

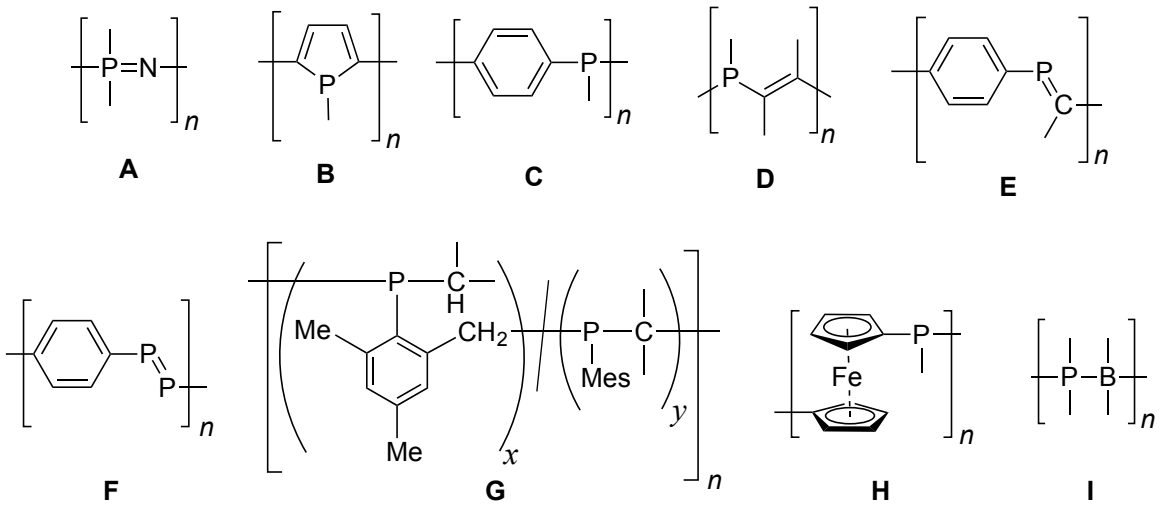

Figure 4.1: Major classes of phosphorus-containing polymers

Poly(*p*-phenylene ethynylene)s (PPEs), represent a widely studied class of organic π-conjugated polymer, which possess useful photophysical properties and potential applications as sensors.[234] There has been growing interest in combining alkyne functionalities with phosphine or phosphaalkene moieties as building blocks in molecular chemistry.[47-49, 147, 235-244] Although researchers have proposed more extended structures, polymers possessing P-alkyne functionalities in the main chain have not been realized until now.

Herein, we provide an efficient synthetic route to a fascinating class of "turn-on" luminescent and chemically functional phosphorus-containing macromolecule. Namely, we report the synthesis and characterization of poly(*p*-phenylenediethynylene phosphine)s (PPYPs) the first di-yne-substituted phosphine macromolecule.

4.2 Results and Discussion

4.2.1 Synthesis of New Polymers.

A modified Ni-coupling procedure[245] was utilized in our attempts to synthesize the target PPYPs. This coupling method was chosen as it has been shown to be a convenient and high yielding route to many tertiary substituted alkynyl phosphines. Furthermore, this synthetic method does not require the use of highly reactive organometallic compounds (such as alkynyllithium reagents) that may be tricky to prepare and utilize for the synthesis of PPYPs. As the prototypical PPYP, we focused our initial investigations on the unsubstituted **4.1a** even though such a rigid system would be expected to be insoluble. A reaction vessel was charged with 1,4-diethynylbenzene, $PhPCl_2$ (both 1 equiv.), NEt_3 (6 equiv.), $Ni(acac)_2$ (5 mol%) and toluene as solvent. The reaction mixture was heated at 85 °C and was stirred overnight. The next day, the orange reaction mixture had substantially increased in viscosity and had darkened in colour. A large amount of dark red coloured precipitate had formed. An aliquot was removed from the reaction mixture and analyzed by ^{31}P NMR spectroscopy. Importantly, analysis of this soluble portion showed no signal corresponding to starting material (161 ppm). Instead, a single resonance was observed at –61 ppm, which was assigned to **4.1a**. For comparison, $(Ph\text{-}C{\equiv}C)_2PPh$, prepared by ourselves (see experimental section) and others[246] shows a similar chemical shift of –60 ppm. It must be noted that the majority of the reaction product was insoluble in common organic solvents (e.g. THF, DMSO, toluene etc.). Attempts to work-up the polymeric material **4.1a** were thwarted by its low solubility. This material was analyzed by MALDI-TOF MS (DHB matrix) which revealed a series of ions with spacing corresponding to $[(M+H)_n]^+$(233 g mol^{-1}) of a polymer with the structure of **4.1a**. This MALDI-TOF MS spectrum can be found in Appendix D (Figure D1).

Buoyed with optimism that a polymer with the desired structure had been achieved, efforts were focused on synthesizing a solution processable PPYP. A common strategy to increase solubility of π-conjugated organic polymers with rigid structures involves installing aliphatic substituents in the side chain structure. With this in mind, polymers **4.1b-4.1e** were envisaged as synthetic targets. The incorporation of hexyl/alkyloxy substituents was achieved through substitution on the di-yne comonomer. Each of the di-ynes were chosen since they are readily accessible using literature procedures.[247-249]

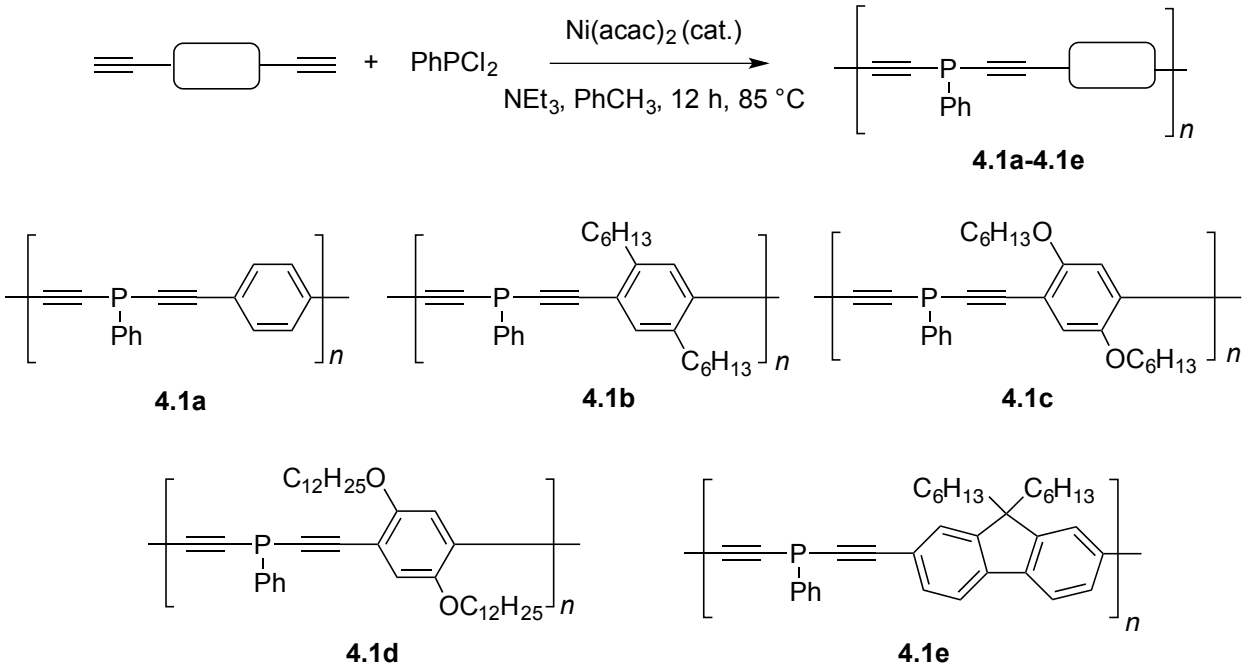

Scheme 4.1: Synthesis of PPYPs 4.1a-4.1e

The syntheses of polymers **4.1b-4.1e** were performed under similar conditions to that of **4.1a** (Scheme 4.1). ^{31}P NMR spectroscopy was employed to monitor the reaction progress over time. As the reaction progresses the starting material (161 ppm) was consumed and, in each case, was replaced by a new signal, which was assigned to the growing polymer chain (**4.1b**: –61 ppm; **4.1c**: –59 ppm; **4.1d**: –59 ppm, **4.1e**: –60 ppm). A stack-plot of ^{31}P NMR spectra over time for the reaction to synthesize **4.1b** is shown in Figure 4.2. Unlike a typical stepwise polymerization,

where monomer is consumed early in the reaction, $PhPCl_2$ is observed in the reaction mixture until very late in the polymerization.[250] The intensity of the signal assigned to the -C≡C-P(Ph)Cl (51 ppm) end-group remained low throughout the reaction, which suggested that these chain ends, when formed, are highly reactive. It should also be noted that only a few reports for compounds that contain -C≡C-P(R)Cl functionalities exist and in these reports they have been described as unstable in storage or heating.[251] The slow consumption of monomer, combined with the fast depletion of -C≡C-P(R)Cl moieties is unusual for a simple step growth polymerization is which all functional groups have similar reactivities. These experimental observations suggest that the polymerization proceeds with chain ends of unequal reactivity (i.e. -C≡C-P(Ph)Cl chain ends react faster than -C≡CH). This suggests that the end groups on the polymer are terminal alkynes only. In the $^{31}P\{^{1}H\}$ NMR spectrum of the isolated polymers **4.1b-4.1e**, no signals corresponding to P-Cl moieties are observed.

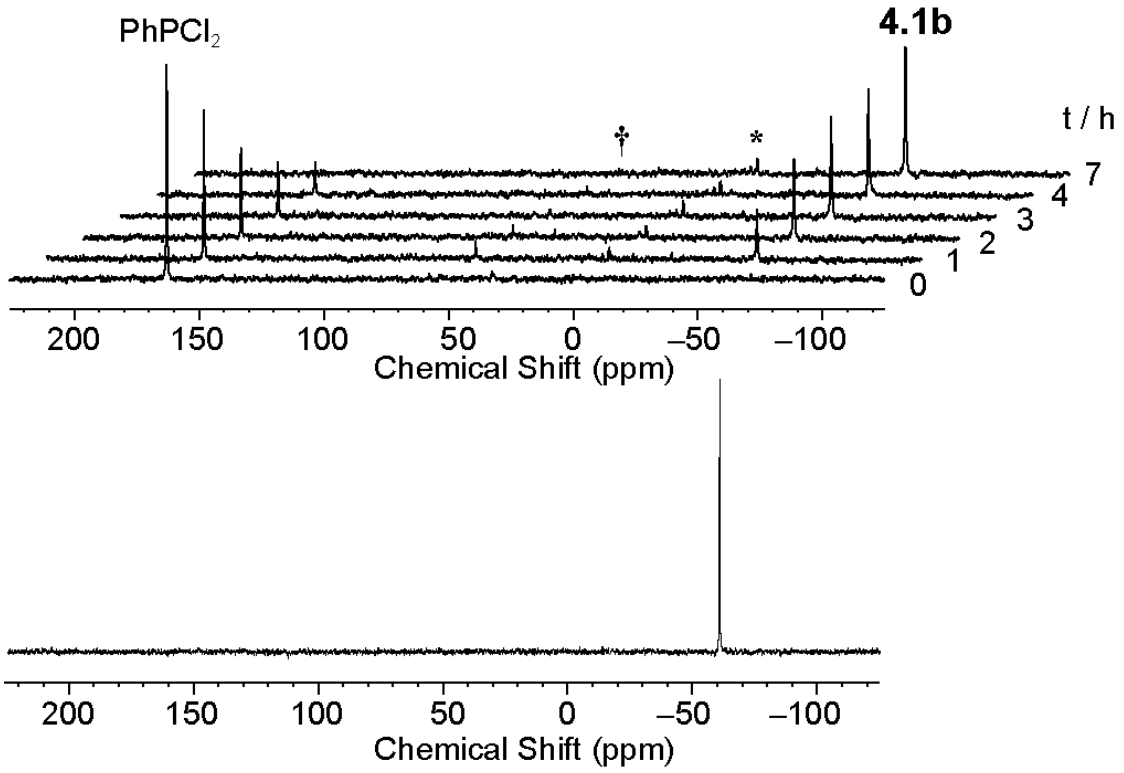

Figure 4.2. a) Selected ^{31}P NMR spectra (121 MHz, toluene, 358K) showing: the progress of the polymerization of $PhPCl_2$ and 1,4-diethynyl-2,5-di-*n*-hexylbenzene using $Ni(acac)_2$ (5 mol%) as catalyst and NEt_3 (6 equiv) as base. b) ^{31}P NMR spectrum (121 MHz, $CDCl_3$, 358 K) of isolated polymer 4.1b after precipitation.

The measurement times are given in hours. [†] indicates signals assigned to –P(Ph)–Cl moieties. The signals marked with [*] result from hydrolysis of $PhPCl_2$ by traces of water found in the nickel(II) catalyst.

Upon completion of each polymerization, the solvent was removed under reduced pressure and, in each case, left a dark red gummy residue of **4.1b-4.1e**. The addition of a small amount of THF (*ca*. 2 mL) to each residue caused significant swelling suggesting the presence of polymeric material. The polymers were dissolved in a minimal amount of THF and the concentrated solutions were precipitated with degassed methanol or ethanol to afford a sticky gum (**4.1b**) or solid (**4.1c-4.1e**). This process was repeated twice more and PPYPs **4.1b-4.1e** were isolated as deep red solids in each case. Each of the polymers **4.1b-4.1e** have been fully

characterized by ^{1}H, $^{13}C\{^{1}H\}$, APT and 2D NMR spectroscopy and gel permeation chromatography (GPC) (*vide infra*).

The new PPYPs (**4.1b-4.1e**) were oxidized to the corresponding phosphine oxide polymers (denoted hereafter as **4.1b**·O-**4.1e**·O) by treating a CH_2Cl_2 solution of the polymer with aqueous hydrogen peroxide (15% w/w). The oxidation reaction is facile and can easily be followed by $^{31}P\{^{1}H\}$ NMR spectroscopy (*ca.* –19 ppm) in each case. Alternatively, PPYPs can be oxidized upon exposure to air in either the solution or the solid state over the course of a few hours. It should be noted that the phosphine oxide polymers **4.1b**·O-**4.1e**·O showed significantly less solubility in common organic solvents (THF, DCM, toluene) than the corresponding phosphine polymers. Each of the oxidized polymers have also been characterized by ^{1}H and $^{13}C\{^{1}H\}$ NMR spectroscopy (**4.1b**·O-**4.1d**·O only) and GPC.

Polymers **4.1b-4.1e** were analyzed by gel permeation chromatography (GPC). The obtained molecular weights (*vs.* polystyrene) are shown in Table 4.1. As expected for a stepwise polymerization, modest molecular weights and dispersity were obtained (M_w = 6,600-12,000 g mol^{-1}, Đ = 1.4-2.1). Unfortunately, while each polymer showed moderate solubility in THF, some material was insoluble. In each case a higher molecular weight material was likely obtained, but the limited solubility of larger chain polymers in THF precluded their analysis by GPC. This is especially true for **4.1e**, which exhibited the lowest solubility in THF out of polymers **4.1b-4.1e**. Nevertheless, its solubility is still far higher than **4.1a**, which was not amenable to GPC analysis.

Table 4.1 Molecular weight data for polymers 4.1b-4.1e

Polymer	M_n / g mol^{-1}	M_w / g mol^{-1}	Đ
4.1b	6600	12000	1.8
4.1c	4800	6600	1.4
4.1d	5700	9600	1.7
4.1e	3400	7400	2.1

When isolating longer chain PPYPs by precipitation, some shorter chain oligomers are soluble in the precipitation solvent (methanol or ethanol). When these short oligomers were analyzed by GPC, the traces of each polymer showed resolved maxima, which were assigned to oligomers of different lengths (up to n = 5). This assignment was aided by determining the exact elution times of pure **4.2b**·O-**4.2d**·O and the dialkyne monomer for each polymer. The GPC traces of these oligomers and isolated **4.1b** are shown in Figure 4.3. By comparing the calculated molecular weight (*vs.* polystyrene) with the formula weight for each oligomer, it was possible to determine a correction factor for each polymer. A plot of GPC M_w (*vs.* polystyrene) and actual M_w for each polymer is shown in Figure 4.4. Notably, the plot for each series showed a strongly linear correlation (R≥0.997 in each case). A near-zero intercept for each plot was observed which demonstrates unambiguously that the assignment of each oligomer is correct. Moreover, the observed overestimation of the actual M_w by GPC (*vs.* polystyrene) is expected for rigid rodlike PPYPs and has been studied with PPEs.[252-254] Due to their rod-like structure, PPYPs show shorter retention times (i.e. higher MWs) on the size-exclusion column than the corresponding coil-like polystyrene reference materials. The magnitude of the gradient of each plot provides information about the rigidity of the polymer in solution (**4.1b**: 0.69; **4.1c**: 0.75; **4.1d**: 0.67; **4.1e**: 0.65). The smallest gradient and hence the largest overestimation of MW is seen for **4.1e**. This is perhaps due to it being derived from the fluorene dialkyne, which is more rigid than the other

dialkyne monomers. A greater, non-linear overestimation of MW is observed for PPEs.[252-254] This is perhaps due to the higher rigidity of the alkynyl framework throughout the backbone compared to PPYPs that incorporate a more flexible P-moiety.

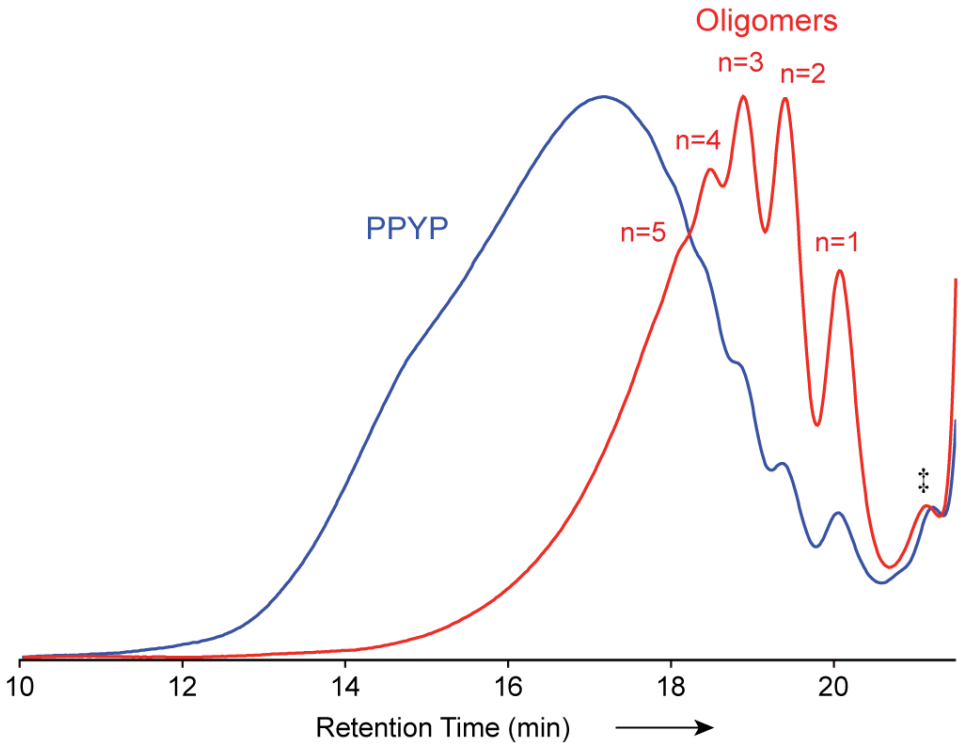

Figure 4.3: Gel permeation chromatography (GPC) traces of PPYP (4.1b) M_n = 5000 g mol^{-1}; Đ = 2.0, vs. polystyrene standards] and the methanol-soluble fraction containing oligomers of 4.1b (*n* = 1–5 are resolved; X = H–C≡C–; Y = –$C_6H_2R_2$–C≡C–H). The assignments are tentative. [‡] assigned to monomer 1,4-diethynyl-2,5-di-*n*-hexylbenzene by comparison to the GPC trace of an authentic sample.

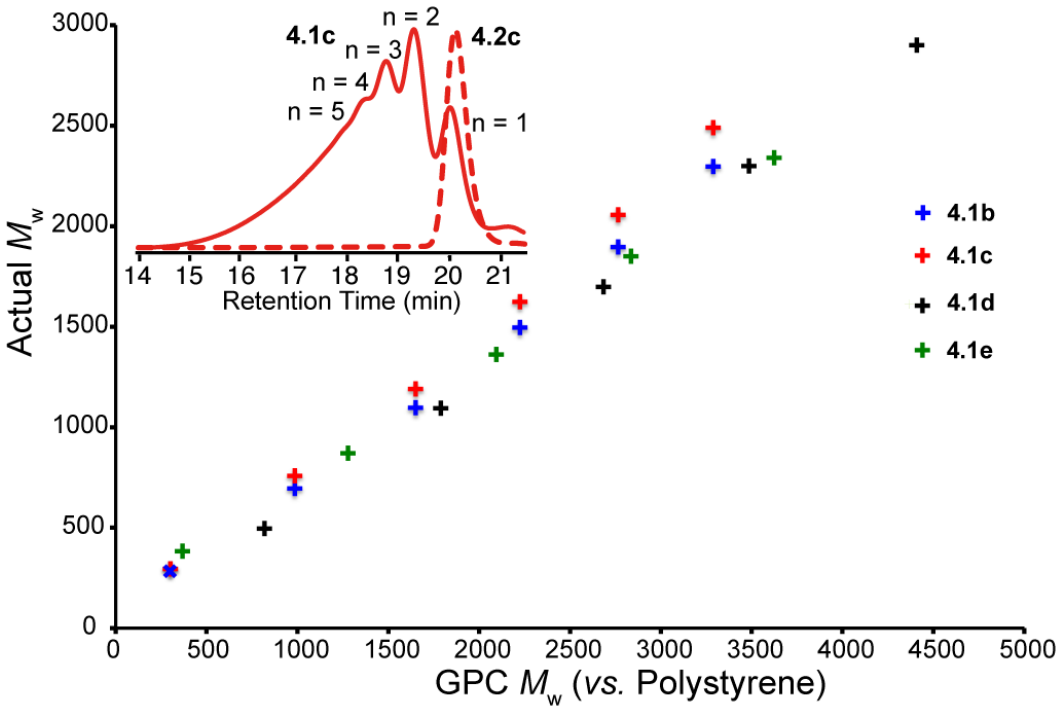

Figure 4.4. A plot of GPC M_w vs actual M_w for polymers 4.1b-4.1e. (n = 1-5). The dialkyne monomer is also plotted in each case. The gradient of each plot is as follows 4.1b: 0.69; 4.1c: 0.75; 4.1d: 0.67; 4.1e: 0.65. Inset: GPC trace of low M_w sample of 4.1c (solid line), 4.2c·O (dashed line).

4.2.2 Synthesis of Model Compounds to Aid Polymer Characterization

In order gain insight into the π-conjugative effects within PPYPs and to assist in the spectroscopic and structural characterization, several small molecule model compounds were synthesized (Figure 4.5). Compounds **4.2a**·O-**4.2d**·O were prepared by reacting two equiv. of a monodeprotonated dialkyne with $PhPCl_2$ at –78 °C, followed by facile oxidation of the phosphine to the phosphine oxide using a H_2O_2 solution after work up (Scheme 4.2). As the polymerization reactions proceed to fashion PPYPs with alkyne end group only, compounds **4.2a**·O-**4.2d**·O are the smallest size (oxidized) polymers that can be formed in the synthesis of **4.1a-4.1c** and **4.1e**.

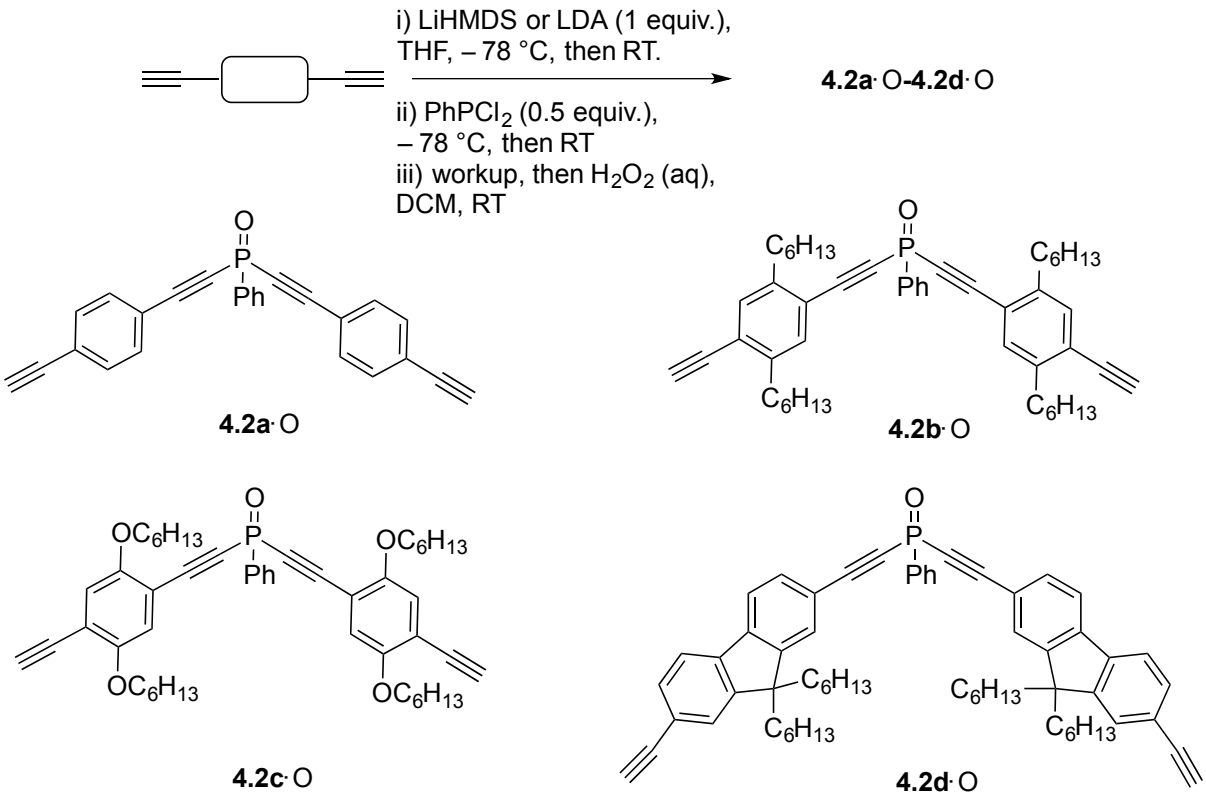

Scheme 4.2: Synthesis of model compounds 4.2a·O-4.2d·O

Compounds **4.2e**·O and **4.3a**·O-**4.3d**·O were synthesized following a modified nickel catalyzed coupling procedure,[245] similar to the synthesis of the polymers (Scheme 4.3). Full experimental details for the synthesis of each model compound are given in the experimental section. Each compound has been characterized by ^{31}P, ^{1}H and $^{13}C\{^{1}H\}$ NMR spectroscopy, in addition to low- and high-resolution mass spectrometry (all apart from **4.3d**·O) and elemental analysis (**4.2c**·O, **4.2e**·O and **4.3b**·O only).

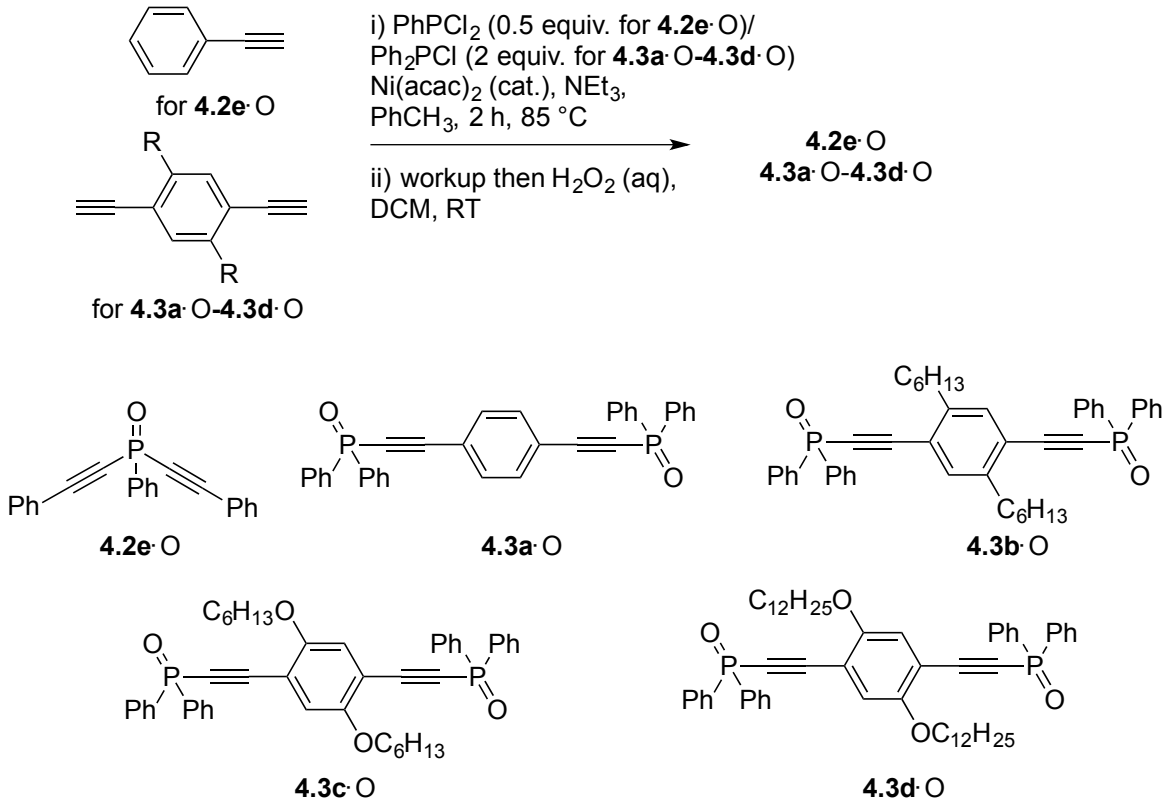

Scheme 4.3: Synthesis of model compounds 4.2e·O and 4.3a·O-4.3d·O

In addition to GPC analysis, each polymer has also been characterized fully by ^{1}H and $^{13}C\{^{1}H\}$ NMR spectroscopy. The ^{1}H NMR for each polymer is broader compared to the model compounds, indicative of polymeric material. In agreement with the assigned structure, the only resonances that were observed correspond to aryl and alkyl protons. Additionally, for each polymer, a small signal corresponding to an alkynyl C-*H* proton can be observed [3.30 ppm (**4.1b**); 3.36 ppm (**4.1c**), 3.35 ppm (**4.1d**) 3.18 ppm (**4.1e**)] which was assigned to the end group of the polymer. A signal assigned to the alkynyl C-H was also observed in model compounds **4.2a**·O-**4.2d**·O, and, as expected, is absent from model compounds **4.3a**·O-**4.3d**·O, which do not contain alkyne protons.

Table 4.2: NMR data for synthesized compounds.

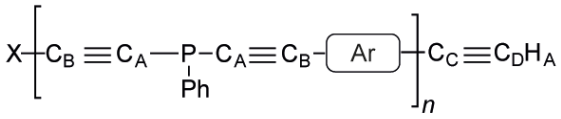

	δ C_A / $^1J_{PC}$ (Hz)	δ C_B / $^2J_{PC}$ (Hz)	δ C_C (ppm)	δ C_D (ppm)	δ H_A (ppm)
4.1b	87.6	104.9	82.8	81.8	3.30
4.1b·O	88.0	102.5	82.9	81.7	3.36
4.1c	88.4	102.5	79.8	82.1	3.36
4.1c·O[b]	89.2	104.3	79.4	83.6	3.40
4.1d	88.2	102.6	79.9	82.7	3.35
4.1d·O[b]	88.7	100.4	79.4	83.6	3.39
4.1e[b,c]	83.0	107.5	84.5	77.2	3.18
4.2a·O	84.8 / 201	103.0 / 38	82.6	80.5	3.25
4.2b·O	87.5 / 202	102.7 / 38	82.8	81.8	3.37
4.2c·O	88.1 / 203	100.4 / 39	79.4	83.6	3.40
4.2d·O	83.6 / 202	104.8 / 38	84.3	77.8	3.19
4.2e·O	83.2 / 202	103.7 / 38	N/A	N/A	N/A
4.3a·O	85.7/ 165	103.6 / 29	N/A	N/A	N/A
4.3b·O	88.1 /167	103.1 / 29	N/A	N/A	N/A
4.3c·O	88.6 /169	101.2 / 30	N/A	N/A	N/A
4.3d·O	88.7 /168	101.3 / 30	N/A	N/A	N/A

[a] NMR solvent was $CDCl_3$ in each case. [b] assignments are tentative due to poor resolution of spectrum due to low solubility of polymer in $CDCl_3$. X= C≡C-Ar-C≡CH. [c] A $^{13}C\{^1H\}$ NMR of **1e**·O was not obtained due to low solubility. Measurable *J*- couplings were not observed for the polymers as the signals in these spectra were broad.

The synthesized polymers along with their corresponding model compounds have also been characterized by $^{13}C\{^1H\}$ NMR spectroscopy. Selected data are given in Table 4.2 and the $^{13}C\{^1H\}$ NMR spectra of **4.1c** and **4.2c**·O are shown in Figure. 4.5. The $^{13}C\{^1H\}$ NMR spectra of each polymer showed little change upon oxidation (i.e. **4.1b** and **4.1b**·O have very similar chemical shifts). Two broad alkynyl resonances corresponding to P-C_A≡C_B carbons within the polymer [e.g. 87.6 ppm (C_A) and 104.9 ppm (C_B) (**4.1b**); 88.0 ppm (C_A) and 102.5 ppm (C_B) **4.1b**·O] are also observed. Due to the breadth of these signals, P-C coupling was not observed.

The assignment of each carbon signal was made with reference to the model compounds **4.2a**·O-**4.2e**·O and **4.3a**·O-**4.3d**·O [84.4-88.7 ppm (C_A) and 100.4-103.7 ppm (C_B)]. The C_A and C_B atoms were assigned based on the substantially larger coupling constant observed for C_A (J_{PC} = 168-203 Hz) compared to C_B (J_{PC} = 29-39 Hz). For each polymer, two additional signals were observed in the alkynyl region, which were assigned to the alkyne end group carbon atoms, Ar-C_C≡C_DH [e.g. for **4.1b**·O: 82.9 ppm (C_C) and 81.7 ppm (C_D)]. These signals compare favorably to model compounds (e.g. **4.2b**·O: 82.8 ppm (C_C) and 81.8 ppm (C_D)]. The aforementioned assignments of the C-H alkynyl end-groups in PPYPs have been confirmed by HSQC and APT experiments for each compound.

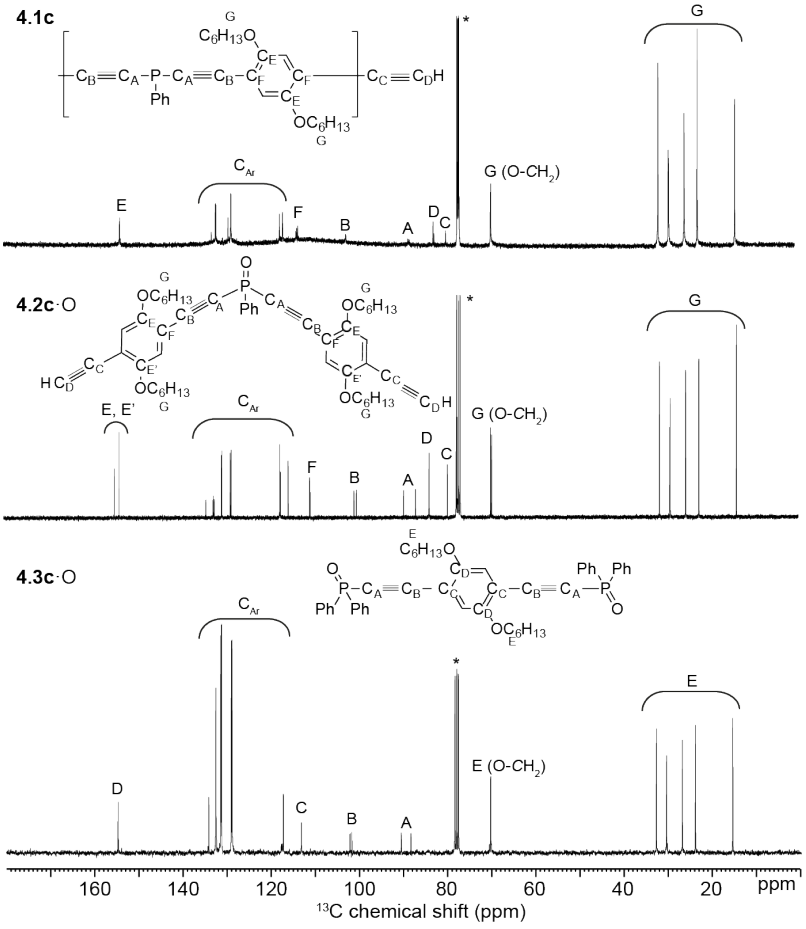

Figure 4.5: $^{13}C\{^1H\}$ NMR (101MHz, $CDCl_3$) spectra of 4.1c (top), 4.2c·O (middle) and 4.3c·O (bottom). *$CDCl_3$ Assignments are made with assistance of 2D and APT NMR experiments.

4.2.3 Electronic Properties Within PPYPs and their Corresponding Model Compounds.

A multifaceted approach was used to elucidate the nature of the π-system within the new PPYPs synthesized for this study. Preliminary insight into their electronic structure was gained from the arrangement of the aryl and alkynyl moieties within the molecular structures of the model alkynyl phosphines as determined using X-ray crystallography. Crystals suitable for X-ray diffraction were obtained for three of the model compounds: **4.2a**·O (from $CDCl_3$), **4.2e**·O (from ethyl acetate), and **4.3b**·O (from a 1:1 ethyl acetate:hexane mixture). The molecular structures of each of these are shown in Figure 4.6. The three crystal structures show many structural similarities and each is consistent with extended π-conjugation involving the P-moiety and backbone alkyne and arylene moieties. For example, the P-C≡C alkyne bond lengths [**4.2a**·O 1.203(2) and 1.217(2) Å; **4.2e**·O 1.203(6) Å; **4.3b**·O 1.196(4) Å] are on the longer side of that expected for alkyne bonds (*ca*. 1.18 Å)[162] whilst the P-C_{sp} single bonds (**4.2a**·O 1.745(2) and 1.752(2) Å; **4.2e**·O 1.750(4) Å; **4.3b**·O 1.746(3) Å) are significantly shorter than that of a typical P-C single bond (1.84 Å).[162] Similar trends have been observed with other alkynyl phosphines such as $CH_3PhC{\equiv}CPOPh_2$,[255] $P(C{\equiv}CPh)_3$.[256] and $Mes_2PC{\equiv}CPh$.[257]

In addition to the change in bond lengths, the two phenyl rings in **4.2a**·O and **4.2e**·O show only slight twisting from co-planarity (angle between planes: **4.2a**·O: 15.7° **4.2e**·O: 9.1°). In contrast, the phenyl-P substituent lies almost totally perpendicular to the aforementioned phenyl planes (angle between planes: **4.2a**·O 82.6° and 81.8°; **4.2e**·O 79.9° and 88.5°). In diphosphine **4.3b**·O, one of the P-phenyl rings lies far more planar to the central phenyl ring than the other (angle between planes: 23.6° and 82.3°). The coplanar nature of the backbone aryl moieties combined with the lengthening of the C≡C bonds and shortening of the P-C bonds may be reflective of the π-conjugation within the main chain.

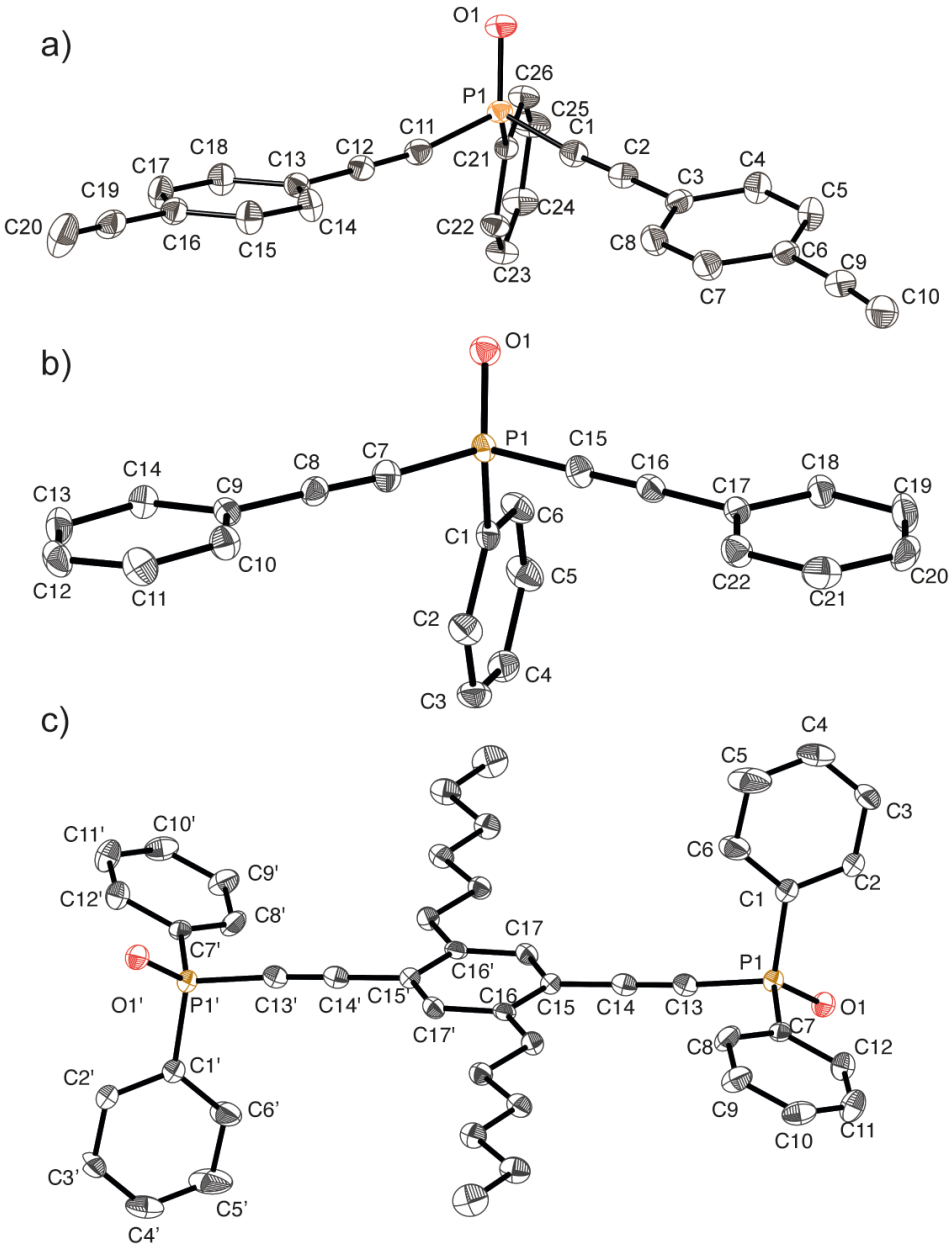

Figure 4.6 a). Molecular structure of 4.2a·O b) 4.2e·O c) 4.3b·O Thermal ellipsoids are displayed at a 50% probability level. Hydrogen atoms are omitted.

Crystal packing may also affect the relative orientation of the phenyl moieties. In the unit cell of **4.2a**·O, parallel-displaced π-stacking of the alkynyl phenyl moieties is observed. The distance between benzene rings in **4.2a**·O are *ca.* 3.8 Å, which is on the longer side for π-π interactions involving carbon atoms and is larger than twice its calculated VDW radii (3.54

Å).[258] No π-stacking is observed in **4.2e**·O and **4.3b**·O with the closest intermolecular contacts being long-range interactions between the oxygen atom and P-phenyl hydrogens in **4.2e**·O (2.39 Å) and the oxygen with hexyl-CH_2 hydrogens in **4.3b**·O (2.49 Å). These observations suggest that the near-planar orientation of the arylene moieties within the model compounds is more likely to reflect π-conjugation in the backbone rather than intermolecular ordering.

Additional insight into the electronic structure of PPYPs was gained by studying their UV-Vis absorbance spectra. The spectra are shown in Figure 4.7 and, for comparison, both the polymer and its corresponding model compound are overlaid (e.g. **4.1b**·O and **4.2b**·O). Although spectra are only shown for the phosphine oxides, the spectra of the unoxidized phosphines are virtually identical.

Each of the polymers showed similar features to its corresponding model compound with an expected red shift in the absorbance maxima for the polymers. In the case of the 2,5-alkyl-substituted system, each band observed in the spectrum of polymer **4.1b**·O is consistently bathochromically shifted by 10-12 nm with respect to model **4.2b**·O. In contrast, when 2,5-alkoxy-substituents are employed the magnitude of the red shift was more pronounced for low energy bands (Δλ = 6 nm; e.g. 365 nm in **4.2c**·O to 371 nm, in **4.1c**·O) than for high energy bands (Δλ = 2 nm; e.g. 284 nm in **4.2c**·O to 286 nm in **4.1c**·O]. Likewise, the magnitude of the red shift for fluorenyl-containing polymer **4.1e**·O was higher for low energy bands (Δλ = 12 nm; e.g. 344 nm in **4.2d**·O to 356 nm in **4.1e**·O) than for high energy bands (Δλ = 4 nm; e.g. 309 nm in **4.2d**·O to 313 nm in **4.1e**·O). Presumably, the greater red shift for the lower energy bands is reflective of more significant changes in the energy levels of the frontier orbitals when the π-conjugation length is increased (i.e. in a polymer). We also note that a small tail or shoulder extends into the visible region that was also red shifted for the polymers with respect to the

models (**4.1b**·O-**4.2b**·O: Δλ = 24 nm; **4.1c**·O-**4.2c**·O: Δλ = 14 nm; **4.1e**·O-**4.2d**·O: Δλ = 11 nm). We tentatively assign this lowest energy band to the HOMO→LUMO transition (*vide infra*). Importantly, this feature seems to involve the phosphine moiety since the di-yne monomers show all features of the corresponding polymer or model compound except for this shoulder.

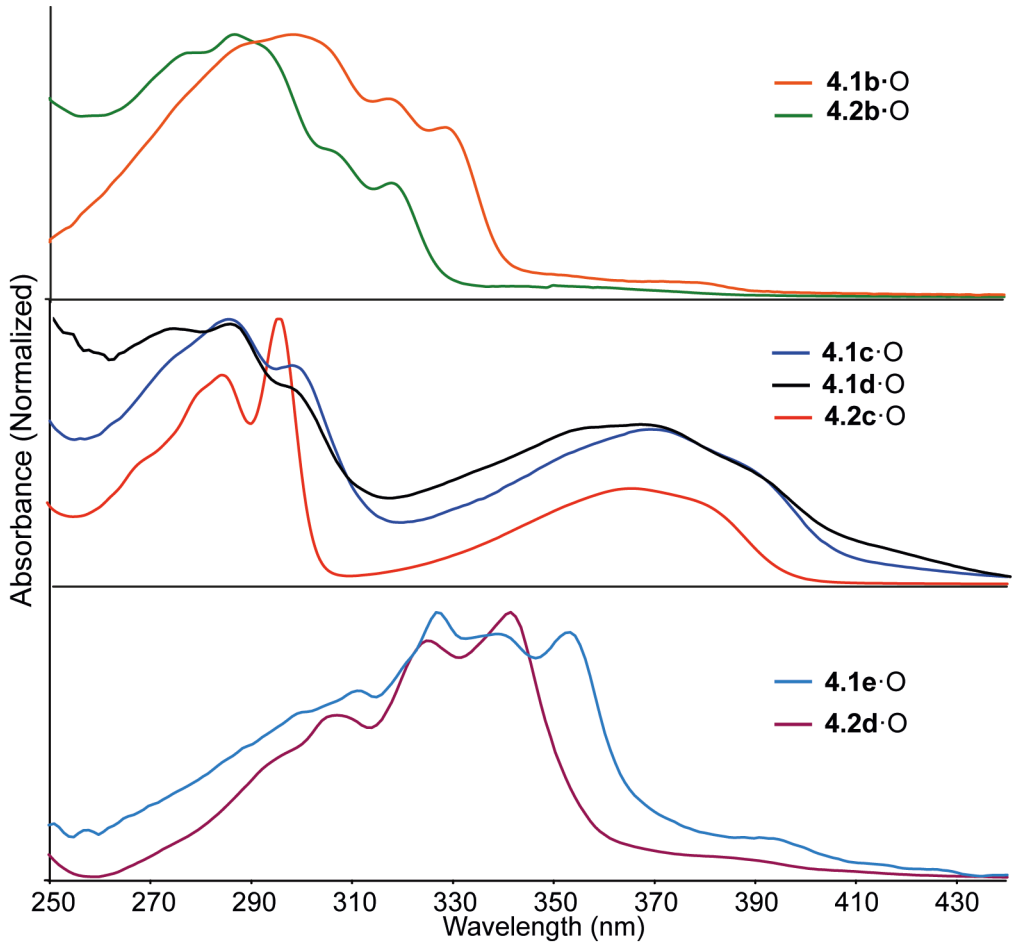

Figure 4.7: UV/Vis spectra of 4.1b·O, and 4.2b·O (top), 4.1c·O, 4.1d·O and 4.2c·O (middle); 4.1e·O and 4.2d·O (bottom), Solvent = THF, c = 10 µM

To aid in the assignment of the aforementioned UV-Vis absorbance spectra, time dependent density functional theory (TD-DFT) calculations were performed on optimized structures using Gaussian 09.[226] The model chosen was similar to **4.2b·O** with methyl rather than

hexyl substituents in the 2- and 5-positions of the dialkyne substituted phenyl rings and is denoted as **M4.2b**·O. Computational details are provided in the experimental section.

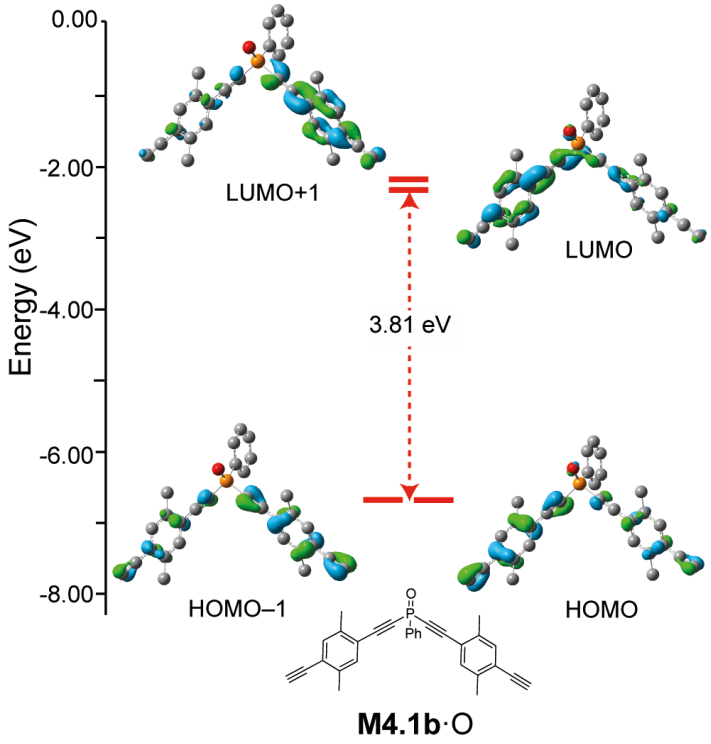

Figure 4.8: Computed HOMO-1, HOMO, LUMO and LUMO+1 of computed model M1b·O.

Remarkably, the calculated absorptions for **M4.2b**·O (318, 307, 306, 290 and 287 nm) almost exactly matched the experimental UV-Vis absorption spectra for **4.2b**·O (λ_{max}: 318, 307, 287, 277 nm). The absorptions at 318 and 307 nm consist of major contributions from a HOMO–1→LUMO transition (86 and 98% respectively) and a small contribution from the HOMO→LUMO+1 (14% and 2%) transition. The molecular orbital mapping diagram is shown in Figure 4.8 and shows the HOMO–1, HOMO, LUMO and LUMO+1 orbitals. In each case, these frontier orbitals reveal that there is electron density spread across the entire π-system. Notably, the LUMO appears to involve a π-type bonding overlap involving the C-P-C moiety. The lowest energy absorbance calculated for **M4.2b**·O (325 nm, 3.81 eV, f=0.65) is purely the

HOMO→LUMO transition and corresponds to the broad shoulder observed for **4.2b**·O (358 nm, 3.46 eV).

4.2.4 Emissive Properties of PPYPs

The emissive properties of the synthesized compounds were investigated. Polymers **4.1b-1e** showed either very weak to no emission in dilute THF solutions. Although there are some notable exceptions,[259] phosphorus (III) compounds tend to be non-emissive. This has been attributed to a photo-induced electron transfer (PET) mechanism[99] involving the phosphorus lone pair electrons, which quenches fluorescence (see refs [112, 118, 119, 122, 124, 260] for examples). Remarkably, upon the oxidation of the phosphine centres in **4.1b-4.1e**, a blue-coloured fluorescence was observed in each case. The vastly different emissive properties of PPYPs upon oxidation can be observed by the use of a UV lamp (Figure 4.9). This observed turn-on of fluorescence upon phosphine functionalization is potentially exciting because it may form the basis for sensing applications for PPYP materials. This is explored in Chapter 5 of this thesis.

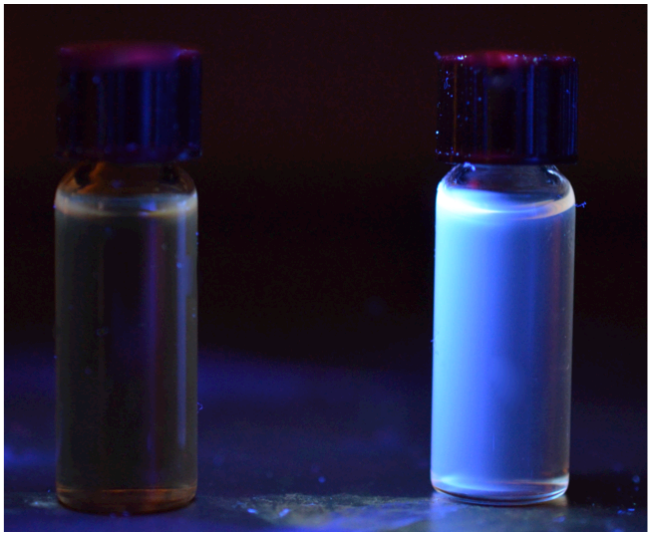

Figure 4.9: Vials containing 4.1b (left) and 4.1b·O (right) under a UV lamp (λ = 365 nm) (c of solns 1mg/ml)

The solution emission spectra of the oxidized polymers are shown in Figure 4.10. Similar to PPEs,[28] the presence of strongly electron donating 2,5-alkyloxy groups appeared to redshift

the polymer emission in comparison to 2,5-alkyl substituents (for example λ_{max} **4.1c**·O: 415 nm; **4.1b**·O: 339 nm). Since **4.1c**·O and **4.1d**·O had very similar emission wavelength maxima and emission band shapes, the length of the alkyl side group had little effect on their emissive properties in solution. Polymer **4.1e**·O exhibited fluorescence with three maxima (λ_{max} 363, 382 nm and 404 nm). Similar features have been observed for other conjugated fluorene-containing polymers and oligomers.[261, 262] An excitation spectrum was measured for each of the oxidized polymers which suggested that emission in each case is derived from a strongly absorbing band in each polymers' absorption spectrum.

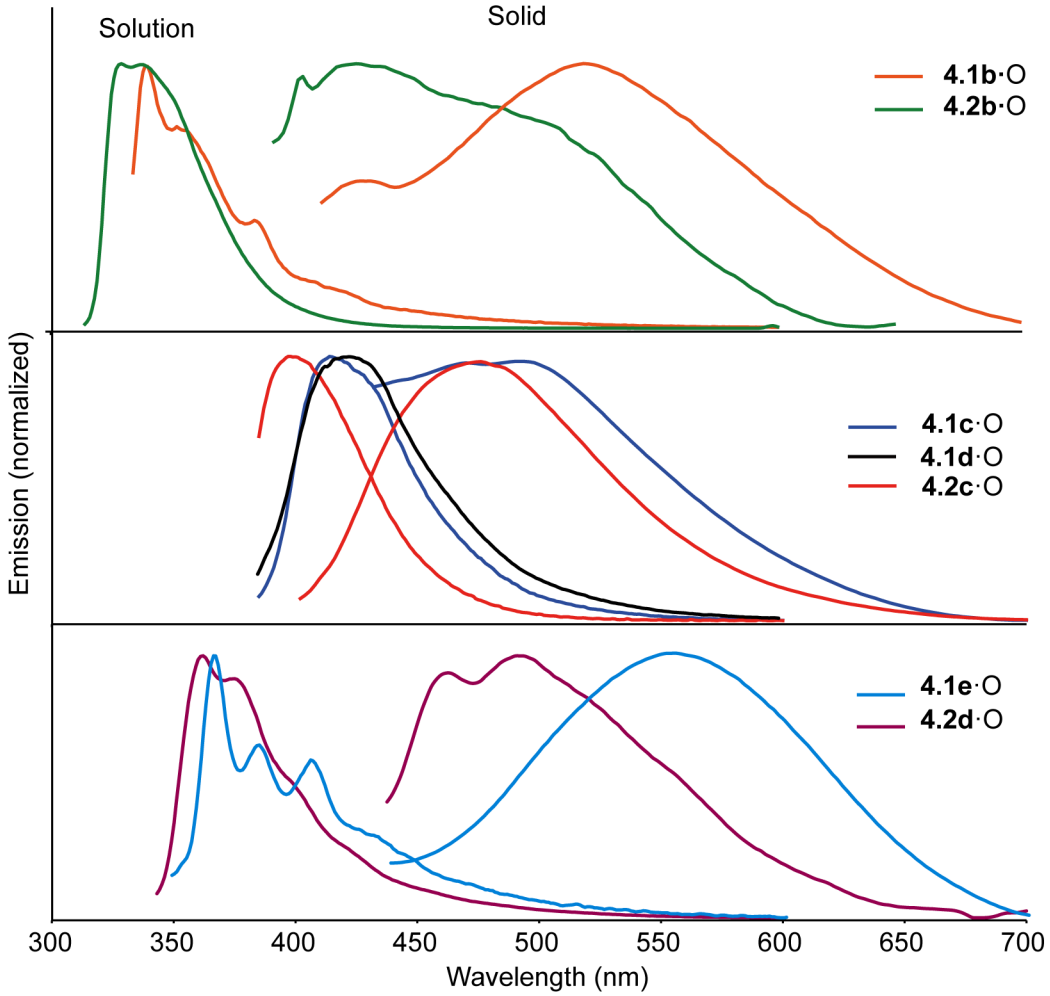

Figure 4.10: Emission spectra of 4.1b·O-4.1e·O and 4.2b·O-4.2d·O in the solution and solid state. The solid-state emission spectrum of 4.1d·O is not shown due to being only weakly emissive.

The solution quantum yield of each of the oxidized polymers was determined (Φ = 0.12-0.28) relative to that of anthracene (Φ = 0.27).[263] These quantum yields are modest compared to organic conjugated polymers such as PPEs,[264] which can have have quantum yields >0.90 or polyfluorenes which typically have quantum yields typically over 0.40.[265] The lower quantum yield in oxidized PPYPs is potentially due to heavy atom quenching effects,[266, 267] which are often regarded as the cause of low emission in P-containing polymers.[45, 46, 140, 168] The quantum yields determined here are higher, or at least comparable, to most previously reported fluorescent phosphorus-containing macromolecules. There are limited examples of P-polymers that do have higher quantum yields (up to Φ = 0.53) but these examples either do not feature P atoms in every polymer repeat unit[68, 268] or are very short chain oligomers.[269] Other reported fluorescent polymers that incorporate P atoms contain polyphosphole moieties with thiophene,[270] arylene[57, 271] or alkynylarylene[58] spacers in the polymer main chain and have lower quantum yields than those reported here (Φ = 0.01-0.14). Other mildly fluorescent P-polymers have been studied, but their quantum yields have not been reported.[45, 46]

Excited state lifetime measurements were performed on **4.1b**·O-**4.1e**·O and **4.2a**·O-**4.2d**·O. The decay times measured for each material were all extremely short (<4.0 ns) indicative of fluorescence rather than a phosphorescence emission mechanism. Each of the model compounds **4.2b**·O-**4.2d**·O possessed a higher quantum yield than their corresponding oxidized PPYP. The hexyl-(**4.2b**·O) and hexyloxy-(**4.2c**·O) substituted model compounds had vastly different quantum yields (Φ_{soln} = 0.86 and 0.15). Model compound **4.2a**·O**,** with no substitution on its phenyl rings was only very weakly emissive (Φ_{soln} = 0.01). Thus, the obtained quantum yield values for **4.2a**·O, **4.2b**·O and **4.2c**·O show a trend of increasing quantum yield with more electron-donating groups substituted on the di-yne aryl ring for these model

compounds. The fluorene-containing model compound **4.2d**·O had a high quantum yield (Φ_{soln} = 0.82). Similar phosphine oxide compounds containing fluorene substituents exhibit high quantum yields[272] and a patent detailing their incorporation into devices has been applied for recently.[273]

The maximum emission wavelength of each oxidized polymer (**4.1b**·O-**4.1e**·O) was red shifted when compared to its corresponding model compound (**4.2b**·O-**4.2d**·O). The smallest shift was observed for **4.1b**·O ($\Delta\lambda_{max}$ = 10 nm; i.e. λ_{max} = 339 nm for **4.1b**·O *vs.* 329 nm for **4.2b**·O). A larger red shift was seen with the hexyloxy polymer ($\Delta\lambda_{max}$ 19 nm). The two bands of the fluorene-containing polymer **4.1e**·O were red shifted a similar amount ($\Delta\lambda_{max}$ = 21 and 29 nm) compared to **4.2d**·O. A higher wavelength band (λ = 404 nm) and shoulder (λ = 430 nm) band were also seen in **4.1e**·O but not observed in **4.2d**·O. The red shift in the emission maxima of the polymers compared to their model compounds implies a decreased HOMO-LUMO gap as the chain length increases. In addition to the observed red shift in emission wavelength, each of the polymers displayed a broader onset of emission than the model compounds. This is also typical of conjugated polymers;[252] similar features are observed when comparing PPEs to their oligomers.[274] Solution state emission data for **4.1b**·O-**4.1e**·O and **4.2a**·O-**4.2d**·O are presented in Table 4.3.

Bearing in mind that luminescent polymers are more likely to be used in devices as solids rather than solutions, the emissive properties of PPYPs **4.1b**·O-**4.1e**·O and model compounds **4.2a**·O-**4.2d**·O were investigated in the solid-state. There are only a few examples of phosphorus-containing polymers that have been reported as emissive in the solid state.[260, 268] In contrast, there has been a major growth in the number of opto-electrical devices that incorporate P-based molecular materials.[56, 194, 195, 275]

Thin films of each material were made by drop casting dilute solutions of dichloromethane (**4.1b**·O-**4.1e**·O) or toluene (**4.2a**·O-**4.2d**·O) on a glass slide. Remarkably, each derivative exhibited green or yellow colored fluorescence (Figure 4.9). The emission wavelength for each material is red shifted and the emission profile is significantly broader than that observed in solution. Each of the solid-state quantum yields of the polymers (Φ = 0.04-0.08) and model compounds (Φ = 0.13-0.45) were somewhat lower than in the solution state. This may be attributed to the increased formation of aggregates and excimers in the solid state that enhance non-radiative decay processes.[276] Surprisingly, **4.2a**·O had a much higher quantum yield in the solid state (Φ = 0.39) than in solution. This may be due to emission from π stacked aggregate states that are not present in solution. Solid-state emission data is presented in Table 4.3.

Table 4.3: Emission data for model compounds 4.1b·O-4.1e·O and polymers 4.2a·O-4.2d·O

	Solution State			Solid State		
Compound	λ_{ex} / nm	λ_{em} / nm	Φ	λ_{ex} / nm	λ_{em} / nm	Φ
4.1b·O	318	339	0.12	380	520	0.08
4.1c·O	372	415	0.20	330	492	0.08
4.1d·O	370	418	0.28	324	532	0.04
4.1e·O	355	382,404	0.22	352	556	0.08
4.2a·O	298	328	0.01	364,384	432	0.39
4.2b·O	317	329	0.15	382	426	0.13
4.2c·O	368	396	0.86	364	474	0.22
4.2d·O	346	361, 375	0.82	332, 348	464,494	0.45

The magnitude of the red shift of emission from the solution state to solid state is greater for the polymers than for model compounds (for example λ_{max} = 432 nm for **4.2b**·O *vs.* 520 nm for **4.1b**·O). This increased emission red shift is attributed to increased intermolecular interactions in the solid state between the π-systems of multiple polymer molecules. Inter-chain or intra-chain mobility of excitons and excimers is considerably greater in the solid state

compared to the solution state due to the formation of aggregates. This phenomenon been observed previously with other conjugated polymers.[28, 264, 277, 278]

It was supposed that the formation of PPYP aggregates would be encouraged by increasing the concentration of **4.1b**·O in THF and/or by the addition of a nonsolvent to a THF solution of **4.1b**·O. By concentrating a THF solution of **4.1b**·O the maximum wavelength of emission was significantly red-shifted (for example c = 0.020 mM λ_{max} = 339; c = 8.0 mM λ_{max} = 450 nm). We also investigated the fluorescence properties of a THF solution of **4.1b**·O (8.0 mM) with varying amounts of the nonsolvent water (Figure 4.11). As expected, increasing the fraction of water in the THF/water mixture lowered the overall emission intensity and red shifted the emission wavelength maxima (from 450 to 480 nm). The emission was also substantially broadened with increased water concentration, and the solutions appeared to emit from a blue to a green color as the water content was increased. We therefore conclude that the emission red shift of PPYPs is aggregation induced. This aggregation behavior is consistent with that of other conjugated polymers[28, 264, 277, 278] and is highly relevant to the development of solid-state optoelectronic devices incorporating this materials.

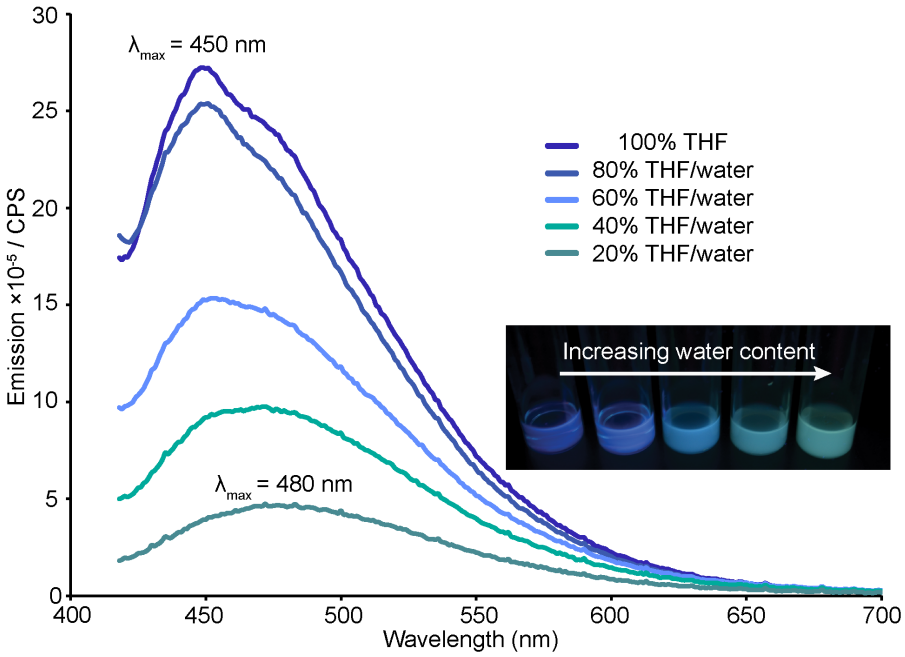

Figure 4.11: Emission of 4.1b·O upon varying the solution solvent from THF to a mixture of THF/water. Concentration of THF solution = 8 mM.

4.3 Conclusion

In summary, we have disclosed the synthesis and characterization of the first examples of poly(*p*-phenylenediethynylene phosphine)s and their respective molecular model compounds. PPYPs are an exciting new class of phosphorus-containing macromolecule bearing functional phosphine and alkyne groups. Although the study of the fascinating photophysical properties is at an early stage, preliminary evidence for σ-π- conjugation within the polymer backbone has been obtained. Another intriguing property of PPYPs is the "turn on" of emission upon oxidation of phosphine moieties within the polymer, and the solid state emission exhibited from these materials. Future work will further explore the novel electronic properties of PPYPs and their potential application as sensor materials. Additionally, we will attempt to exploit the fascinating prospect of post-polymerization modification of PPYPs at either the alkyne and/or the phosphine functional groups.

4.4 Experimental

4.4.1 Materials and Methods

All manipulations of air- and/or water-sensitive compounds were performed under a nitrogen atmosphere by using standard Schlenk or glovebox techniques. Hexanes, dichloromethane and toluene were deoxygenated with nitrogen and dried by passing through a column containing activated alumina. Tetrahydrofuran (THF) was dried over sodium and benzophenone, and was distilled prior to use. Methanol and ethanol were degassed before use. Triethylamine was dried over calcium hydride and was distilled before use. Nickel(II) acetylacetonate (Aldrich) and anthracene (Fisher) were sublimed before use. Phenylacetylene (Aldrich) and 1,4-diethylnylbenzene (Acros) were used as received. Phenyldichlorophosphine was purchased from Fisher and was distilled before use. Diphenylchlorophosphine was purchased from Strem and was used as received. Hydrogen peroxide was purchased as a 50% aqueous solution (w/w) from BDH. 1,4-diethylnyl-2,5-di-*n*-hexylbenzene,[247] 1,4-diethynyl-2,5-bis(*n*-hexyloxy)benzene,[248] 1,4-bis(*n*-dodecyloxy)-2,5-diethynylbenzene and 2,7-diethynyl-9,9-dihexyl-9H-fluorene[68] were made following literature procedures.

4.4.2 Equipment

^{1}H, $^{31}P\{^{1}H\}$, $^{13}C\{^{1}H\}$ NMR spectra were recorded at 25 °C on Bruker Avance 300, 400 or 600 MHz spectrometers. H_3PO_4 (85%) was used as an external standard ($\delta = 0$ for ^{31}P). ^{1}H NMR spectra were referenced to the residual protonated solvent signal and $^{13}C\{^{1}H\}$ NMR spectra were referenced to the deuterated solvent signal. Elemental analyses were performed in the University of British Columbia Chemistry Microanalysis Facility. Mass spectra were recorded on a Kratos MS 50 instrument in EI mode (70 eV). Polymer molecular weights were determined by gel permeation chromatography (GPC) using an Agilent liquid chromatograph equipped with an

Agilent 1200 series isocratic pump, Agilent 1200 series standard autosampler, Phenomenex Phenogel 5 mm narrow bore columns (4.6 × 300 mm) 10^4 Å (5000–500,000 g mol^{-1}), 500 Å (1000–15 000 g mol^{-1}), and 10^3 Å (1000–75,000 g mol^{-1}), Wyatt Optilab T-rEx differential refractometer (λ = 658 nm, 40 °C). A flow-rate of 0.5 mL min^{-1} was used and samples were dissolved in THF (ca. 2 mg mL^{-1}). Molecular weights were determined in comparison to polystyrene standards.

Absorption spectra were obtained in THF on a Varian Cary 5000 UV-Vis-near-IR spectrophotometer using a 1 cm quartz cuvette. Fluorescence and excitation spectra were obtained in THF on a Horiba scientific Fluoromax-4 spectrofluorometer using a 1 cm quartz cuvette. Solid state emission spectra and quantum yield measurements were recorded on a Photon Technology International QuantaMaster 50 fluorimeter fitted with an integrating sphere, double monochromator and utilizing a 75W Xe arc lamp as the source. Emission lifetime data for solution and solid state were collected using a Horiba Yvon Fluorocube TCSPC apparatus. A 370 nm NanoLED source pulsing at a repetition rate of 50 - 100 kHz was used for excitation. Broadband emission was monitored by a CCD detector at wavelengths > 400 nm using a low pass filter. Data were fitted using the DAS6 Data Analysis software package.

MALDI-TOF mass spectra were obtained on Bruker Autoflex MALDI-TOF. The samples were dissolved in chloroform where possible. For insoluble **4.1a**, the sample was mixed with the matrix as a dry powder. DHB was used as the matrix. The solutions of the sample (~1 mg/mL) and matrix (20 mg/mL) were mixed in the ratio of between 1:1 to 1:10 and 1 µl of final mixture was deposited onto the sample target. MALDI mass spectra were acquired in the positive linear mode and the spectra normally represent the average of ca. 2000 lasershots. X-ray data and collection parameters is given in Appendix A, Table A2.

4.4.3 Computational Details

Density functional theory calculations were performed in Gaussian 09 (Revision D.01).[226] Initial geometry optimizations were performed using the 6-31g*+ basis set and the B3LYP functional.[227-229] MO mapping and TD-DFT[230] calculations were performed as single point calculations with the 6-311g**++ basis set and B3LYP functional, with a solvation correction using the Polarizable Continuum Model[232] using THF ($\varepsilon = 7.43$) as solvent.

4.4.4 Synthesis

4.4.4.1 Preparation of 4.1a

A Schlenk flask was charged with phenyldichlorophosphine (0.70 g, 4.0 mmol), 1,4-diethynyl-benzene (0.50 g, 4.0 mmol), triethylamine, nickel (II) acetylacetonate (50 mg, 0.20 mmol) and toluene (100 mL). The reaction mixture was stirred at 85 °C and turned a dark red-brown colour. After *ca.* 30 minutes a dark powder precipitated from the reaction mixture. The reaction mixture was stirred for a further 24 hours, whereupon it was analyzed by $^{31}P\{^{1}H\}$ NMR spectroscopy. The spectrum revealed that the starting material had been completely consumed but only a weak signal was observed at –61 ppm. The solvent was removed *in vacuo* leaving a dark red solid that was washed with degassed water, degassed methanol, degassed ethanol, toluene, THF, DMSO and dichloromethane (consecutively, all 20 mL) to afford a fine light red-yellow powder, deemed to be **4.1a**. Yield = 0.38 g (42%).

$^{31}P\{^{1}H\}$ NMR (121 MHz, $CDCl_3$): δ –61. MALDI TOF MS (DHB Matrix) spectrum is shown in Appendix D (Figure D1) .

4.4.4.2 Preparation of 4.1b.

A Schlenk flask was charged with phenyldichlorophosphine (0.30 g, 1.7 mmol), 1,4 diethynyl 2,5 dihexylbenzene (0.50 g, 1.7 mmol), triethylamine (2.5 mL, 18 mmol), nickel (II)

acetylacetonate (8.7 mg, 34 μmol) and toluene (4.0 mL). The reaction mixture was heated to 85 °C and was stirred vigorously for 24 h. After this time 20 mL (2 × 10 mL) toluene and 30 mL degassed water was added. The organic layer was taken and solvent was removed *in vacuo* to leave a dark red sticky solid. To this solid was added THF (*ca.* 1.5 mL) to decrease the viscosity of the residue, followed by degassed methanol (300 mL) to precipitate the polymer. This precipitation process was repeated twice more to leave a dark red gum. Yield = 0.48 g (71%). ^{31}P NMR (121MHz, $CDCl_3$): δ –61 (br). ^{1}H NMR (300MHz, $CDCl_3$): δ 7.93-7.81 (br, 2H, aryl H), 7.49-7.21 (br, 5H, aryl H), 3.31 (s, 0.16H, C≡C*H*), 2.75-2.63 (br, 4H, CH_2), 1.71-1.45 (br, 4H, CH_2), 1.45-1.05 (br, 12H, CH_2), 0.95-0.72 (br, 6H, CH_3). ^{13}C{^{1}H} NMR (75 MHz, $CDCl_3$): δ 142.8 ($^{ipso}C_{Ar}$-CH_2), 134.1-132.5 (br,m, aryl C), 131.0 (aryl C), 129.5 (aryl C), 128.5 (br, aryl C), 122.3 (br, C_{Ar}-C≡C), 104.9 (br, P-C≡*C*), 87.6 (br, m, P-*C*≡C), 82.2 (ArC-*C*≡CH), 81.8 (C_{Ar}-C≡*C*H), 34.1 (*C*H_2), 31.6 (*C*H_2), 30.6 (*C*H_2), 29.0 (*C*H_2), 22.6 (*C*H_2), 14.0 (*C*H_3). GPC (THF, vs. Polystyrene): M_n = 6,600 g mol^{-1}, Đ = 1.8. Elem. Anal. calcd for $[C_{28}H_{33}P]_n$: C 84.0, H 8.3; found: C 79.7, H 8.1.

4.4.4.3 Preparation of 4.1c

A Schlenk flask was charged with phenyldichlorophosphine (0.60 g, 3.4 mmol), 1,4-diethynyl-2,5-bis(hexyloxy)benzene (1.1 g, 3.4 mmol), triethylamine (1.2 mL, 17 mmol), nickel (II) acetylacetonate (0.020 g , 78 μmol) and toluene (5.8 mL). The reaction mixture was heated to 85 °C and was stirred vigorously for 24 hours. After this time 20 mL (2 × 10 mL) toluene and 30 mL degassed water were added. The organic layer was taken and solvent was removed *in vacuo* to leave a dark red sticky solid. To this solid was added THF (*ca.* 3 mL) to decrease the viscosity of the residue, followed by degassed methanol (300 mL) to precipitate the polymer. This precipitation process was repeated twice more to leave a dark red gum. Yield = 1.10 g (75%).

^{31}P NMR (121 MHz, $CDCl_3$): δ -59 (br); ^{1}H NMR (600 MHz, $CDCl_3$): δ 7.99-7.88 (br, 2H, aryl H), 7.62-7.34 (br, 3H, aryl H), 7.05-6.89 (br, 2H, aryl H), 4.06-3.81 (br, 4H O-C*H*$_2$), 3.36 (s, C≡C*H* end group), 1.86-1.66 (br m, 4H, O-CH_2C*H*$_2$), 1.56-1.38 (br, 4H, C*H*$_2$), 1.37-1.16 (br, 8H, C*H*$_2$) 1.00-0.75 (br, 6H, C*H*$_3$); ^{13}C{^{1}H} NMR (151 MHz, $CDCl_3$): δ 153.9 ($^{ipso}C_{Ar}$OCH$_2$), 132.2 (aryl C), 132.1 (aryl C), 129.3 (aryl C), 128.7 (aryl C), 128.7 (aryl C) 117.7 (aryl C), 117.6 (aryl C), 117.0 (aryl C), 116.8 (aryl C) 113.8 (P-C≡C-C_{Ar}), 113.7 (P-C≡C-C_{Ar}), 113.4 (P-C≡C-C_{Ar}), 102.5 (d, *J* = 30.0 Hz, P-C≡*C*), 88.4 (d, *J* = 40.7 Hz), 82.6 (-C≡*C*H) 79.8 (*C*≡CH end group), 69.6 (br,$^{ipso}C_{Ar}$-O), 31.5 (*C*H$_2$), 29.2 (*C*H$_2$), 29.0 (*C*H$_2$) 25.5 (*C*H$_2$), 14.0 (*C*H$_3$). GPC (THF, vs. Polystyrene): M_n = 4,800 g mol^{-1}, Đ = 1.4.

4.4.4.4 Preparation of 4.1d.

To a stirred suspension of 1,4-bis(dodecyloxy)-2,5-diethynylbenzene (0.53 g, 1.1 mmol), phenyldichlorophosphine (0.19 g, 1.1 mmol), triethylamine (1.0 mL, 7.2 mmol), and nickel (II) acetylacetonate (10 mg, 39 μmol) in toluene (3.0 mL) was heated at 85 °C overnight. After 20 h, an additional 3.0 mL of toluene was added to dissolve some of the formed precipitate and to encourage stirring. The reaction was stirred for a further 48 h. At this point the reaction mixture was cooled to RT and 6 mL of toluene was added. Upon dissolution the majority of the brown colored residue, degassed methanol (50 mL) was added. This precipitation method was repeated twice more to yield a dark red solid that was dried *in vacuo*. Yield = 0.27 g (42%).

^{31}P{^{1}H} NMR (121 MHz, $CDCl_3$): δ –59 (br); ^{1}H NMR (300 MHz, $CDCl_3$): δ 8.04-7.80 (br, 2H, aryl H), 7.60-7.36 (br, 3H, aryl H), 7.04-6.86 (br, 2H, aryl H), 4.04-3.89 (br m, 4H, O-C*H*$_2$), 3.35 (-C≡C*H*), 1.88-1.71 (br, 4H, C*H*$_2$), 1.60 – 1.09 (br, 40H, C*H*$_2$), 1.00-0.80 (br, 6H, C*H*$_3$).

$^{13}C\{^{1}H\}$ NMR (151 MHz, $CDCl_3$): δ 153.9 ($^{ipso}C_{Ar}OCH_2$), 132.2 (aryl C), 132.0 (aryl C), 128.7 (aryl C), 128.6 (aryl C), 117.7 (aryl C), 116.9 (aryl C), 113.9 (aryl C), 113.7(aryl C),113.6 (br, P-C≡C-C_{Ar}), 102.6 (br, P-C≡*C*), 88.2 (br, P-*C*≡C), 82.7 (C_{Ar}-C≡*C*H), 79.8 (C_{Ar}-*C*≡CH), 69.7 (br, O-*C*H_2) 31.9 (*C*H_2), 30.1-29.1 (br, *C*H_2), 25.9 (br, *C*H_2), 22.7 (*C*H_2), 14.1 (*C*H_3). GPC (THF, vs. Polystyrene): M_n = 5,700 g mol^{-1}, Đ = 1.7.

4.4.4.5 Preparation of 4.1e

A Schlenk flask was charged with phenyldichlorophosphine (0.56 g, 3.1 mmol), nickel (II) acetylacetonate (20 mg, 77 μmol), 2,7-diethynyl-9,9-dihexyl-9H-fluorene (1.19 g, 3.1 mmol) and toluene (2.5 mL). Triethylamine (3.5 mL) was subsequently added to the reaction mixture. The deep red reaction mixture was stirred vigorously at 85 °C for 72 h. After this time the reaction mixture was extremely viscous and upon cooling to room temperature a dark coloured precipitate formed. To this mixture was added chlorobenzene (50 mL) and the reaction mixture was heated to 70 °C to enhance solubility of the precipitate. To this mixture was added degassed ethanol (300 mL) and the mixture was stirred for *ca.* 30 mins while it cooled to RT. Upon filtering an orange dusty solid was obtained. To this solid was added THF (5 mL) to make a liquid with high viscosity. To this residue was added degassed H_2O (80 mL). The resulting orange dusty solid was filtered and heated to 60 °C *in vacuo* for 8 h to remove any residual moisture. The isolated material has limited solubility in THF, dichloromethane, chloroform and benzene. Yield = 1.12 g (74%).

$^{31}P\{^{1}H\}$ NMR (121 MHz, $CDCl_3$): δ –60 (br); ^{1}H NMR (300 MHz, $CDCl_3$): δ 7.96 (br. t, *J* = 8.0 Hz, 2H, aryl H), 7.64 (br, 3H, aryl H), 7.50 (br, 6H, aryl H), 3.16 (s, C≡C*H* end group), 1.93 (br, 4H, CH_2), 1.07 (br, 12H, CH_2), 0.77 (t, *J* = 6.3 Hz, CH_3), 0.55 (br, 4H, CH_2). $^{13}C\{^{1}H\}$ NMR (101

MHz, $CDCl_3$): δ 151.1 (aryl C), 141.3 (aryl C), 133.3 (aryl C), 132.4 (aryl C), 132.2 (aryl C), 131.3 (aryl C), 129.6 (aryl C), 129.0 (aryl C), 128.9 (aryl C), 126.6 (aryl C), 126.4 (aryl C), 121.3 (aryl C), 120.1 (aryl C), 107.6 (br, P-C≡*C*), 84.5 (C_{Ar}-*C*≡CH), 83.0 (br, P-*C*≡C), 77.2 (C_{Ar}-C≡*C*H), 55.3 (*C*-CH_2), 40.3 (*C*H_2), 31.5 (*C*H_2), 29.6 (*C*H_2), 23.7 (*C*H_2), 22.6 (*C*H_2), 14.0 (*C*H_3). assignments are tentative. GPC (THF, vs. polystyrene): M_n = 3,400 g mol^{-1}, Đ = 2.1.

4.4.4.6 Preparation of 4.1b·O.

To a rapidly stirred solution of a sample of **4.1b** (0.14 g, 0.35 mmol P, M_n = 6,000 g mol^{-1}, Đ = 2.0) in CH_2Cl_2 (10 mL), H_2O_2 (50% in water, 15 mL) was added at room temperature. The reaction was stirred rigorously for 1 h, at which time a $^{31}P\{^1H\}$ NMR spectrum of the reaction mixture revealed quantitative conversion to a new product. The organic layer was taken and the solvent was removed *in vacuo* to leave a dark red solid. This solid was dried in a vacuum oven for 3 h. Yield 0.12 g (76%).

$^{31}P\{^1H\}$ NMR (121 MHz, $CDCl_3$): δ –20. ^1H NMR (300MHz, $CDCl_3$): δ 8.22-7.97 (br, 2H, aryl H), 7.70-7.29 (br, 5H, aryl H), 3.36 (s, 0.32H, C≡C*H* end gp), 2.77-2.55 (br, 4H, CH_2), 1.70-0.59 (br, 18H, CH_2 + CH_3). $^{13}C\{^1H\}$ NMR (75 MHz, $CDCl_3$): δ 144.5-142.8 (m, $^{ipso}C_{Ar}$-CH_2), 134.1-131.3 (br,m, aryl C), 130.2(m, aryl C), 128.7 (br, aryl C), 122.0 (m, C_{Ar}-C≡C), 102.5 (m, P-C≡*C*), 88.0 (br, m, P-*C*≡C), 82.9 (C_{Ar}-*C*≡CH), 81.7 (C_{Ar}-C≡*C*H), 33.7 (*C*H_2), 31.5 (*C*H_2), 30.4 (*C*H_2), 28.9 (*C*H_2), 22.4 (s, *C*H_2), 13.9 (s, *C*H_3). GPC (THF, vs. Polystyrene): M_n = 3,300 g mol^{-1}, Đ = 2.6. Elem. Anal. calcd (%) for $[C_{28}H_{33}PO]_n$: C 80.23, H 8.21; found: C 78.64, H 8.25

4.4.4.7 Preparation of 4.1c·O

To a rapidly stirred solution of a sample of **4.1c** (0.11 g, 0.25 mmol P, M_n = 4,780 g mol^{-1}, Đ = 1.4) in CH_2Cl_2 (50 mL), H_2O_2 (50% in water, 15 mL) was added at room temperature. The reaction was stirred rigorously for 1 h, at which time a $^{31}P\{^1H\}$ NMR spectrum of the reaction mixture revealed quantitative conversion to a new product. The organic layer was taken. Some red coloured material had precipitated out of solution. This material was filtered and combined with the organic layer. The solvent was removed *in vacuo* to leave a dark red solid. This solid was dried in a vacuum oven for 3 h. Yield 0.094 g (84%).

$^{31}P\{^1H\}$ NMR (121 MHz, $CDCl_3$): δ –19. ^1H NMR (300 MHz, $CDCl_3$): δ 8.24-8.02 (br, 2H, aryl H), 7.68-7.47 (br, 3H aryl H), 7.10-6.93 (br, 2H, aryl H), 4.10-3.76 (br, 4H, OC*H*$_2$), 3.40 (-C≡C*H*), 1.89-1.61 (br, 4H, C*H*$_2$), 1.56-0.99 (br, 12H, C*H*$_2$), 0.97-0.69 (br, 6H, CH_3). $^{13}C\{^1H\}$ NMR (75 MHz, $CDCl_3$): δ 154.8 (br, aryl C), 153.8 (br, aryl C), 151.5 (br, aryl C), 135.7 (aryl C), 132.5 (aryl C), 130.6 (aryl C), 130.4 (aryl C), 128.7 (aryl C), 128.5 (aryl C), 125.5 (aryl C), 117.4 (aryl C), 117.2 (aryl C), 117.1 (aryl C), 104.3 (P-C≡*C*), 89.2 (P-*C*≡C), 83.6 (C≡*C*H), 79.4 (*C*≡CH), 69.7 (O*C*H$_2$), 69.5 (O*C*H$_2$), 34.2 (*C*H$_2$), 31.4 (*C*H$_2$), 29.0 (*C*H$_2$), 25.4 (*C*H$_2$), 22.5 (*C*H$_2$), 14.0 (*C*H$_3$). Assignments are tentative due to low resolution of spectrum due to low solubility. GPC (THF, vs. Polystyrene): M_n = 2,100 g mol^{-1} Đ = 1.9. Much of the material could not be dissolved in THF for GPC analysis.

4.4.4.8 Preparation of 4.1d·O

To a rapidly stirred solution of a sample of **4.1d** (0.071 g, 0.12 mmol P, M_n = 5,700 g mol^{-1}, Đ = 1.7) in CH_2Cl_2 (10 mL), H_2O_2 (50% in water, 15 mL) was added at room temperature. The reaction was stirred rigorously for 1 h, at which time a $^{31}P\{^1H\}$ NMR spectrum of the reaction

mixture revealed quantitative conversion to a new product. The organic layer was taken and the solvent was removed *in vacuo* to leave a dark red solid. This solid was dried in a vacuum oven for 3 h. Yield 0.050 g (70%).

^{31}P {^{1}H} NMR (121 MHz, $CDCl_3$): δ –19. ^{1}H NMR (300 MHz, $CDCl_3$): δ 8.19-8.06 (br, 2H, aryl H), 7.64-7.45 (br, 3H, aryl H), 7.02 (br, 1H, aryl H), 6.95 (br, 1H, aryl H), 4.05-3.87 (br, 4H, O-C*H*$_2$), 3.39 (-C≡C*H*), 1.88-1.67 (br, 4H, C*H*$_2$), 1.44-1.16 (br, 40H, C*H*$_2$), 0.93-0.84 (br, 6H, C*H*$_3$). ^{13}C{^{1}H} NMR (101 MHz, $CDCl_3$): δ 155.0 (br, aryl C), 154.7 (br, aryl C), 153.8 (br, aryl C), 132.6 (br, aryl C), 130.6 (br, aryl C), 130.5 (br aryl C), 128.7 (br, aryl C), 128.5 (br, aryl C), 117.4 (br, aryl C), 117.3(br, aryl C), 117.1 (br, aryl C), 100.4 (P-C≡*C*), 88.7 (P-*C*≡C), 83.6 (*C*≡CH), 79.5 (*C*≡CH), 69.5 (O-*C*H$_2$), 31.9 (*C*H$_2$), 29.7 (br, *C*H$_2$), 29.6 (*C*H$_2$), 29.4 (*C*H$_2$), 29.1 (*C*H$_2$), 25.8 (*C*H$_2$), 22.7 (*C*H$_2$), 14.1 (*C*H$_3$) assignments are tentative. GPC (THF, vs. Polystyrene): M_n = 5,100 g mol^{-1} Đ = 2.0.

4.4.4.9 Preparation of 4.1e·O

To a rapidly stirred solution of a sample of **4.1e** (0.12 g, 0.25 mmol P, M_n = 3,400 g mol^{-1}, Đ = 2.1) in CH_2Cl_2 (10 mL), H_2O_2 (50% in water, 15 mL) was added at room temperature. The reaction was stirred rigorously for 1 h, at which time a ^{31}P{^{1}H} NMR spectrum of the reaction mixture revealed quantitative conversion to a new product. The organic layer was taken and the solvent was removed *in vacuo* to leave a dark red solid. This solid was dried in a vacuum oven for 3 h. Yield 0.11 g (94%).

^{31}P{^{1}H} NMR (121 MHz, $CDCl_3$): δ –19 (br), ^{1}H NMR (400 MHz, $CDCl_3$): 8.24-8.10 (br, 2H, aryl H), 7.77-7.46 (br, 7H, aryl H), 3.19 (C≡C*H*), 2.04-1.86 (br, 4H, C*H*$_2$), 1.18-0.92 (br, 12H, C*H*$_2$), 0.83-0.65 (br t, 6H, C*H*$_3$) 0.62-0.45 (br, 4H, CH_2). GPC (THF, vs. Polystyrene): M_n = 3,400 g mol^{-1}, Đ = 1.9.

4.4.4.10 Preparation of 4.2a·O

To solution of 1,4-diethynylbenzene (0.38 g, 3.0 mmol) was added potassium bis(trimethylsilyl) amide (0.23 g, 1.4 mmol). The reaction mixture was warmed to RT and was stirred for 20 minutes. The reaction mixture was cooled to -78 °C and phenyl dichlorophosphine (0.23 g, 1.3 mmol) was added dropwise over 1 minute. Immediately the reaction mixture turned an orange colour. The reaction was warmed to room temperature and left overnight. An extract of the reaction mixture was taken and analyzed by $^{31}P\{^{1}H\}$ NMR spectroscopy which revealed complete consumption of the starting material (161 ppm), placed by 2 new singlets at -59.2 and -59.3 ppm. The solvent was removed under reduced pressure and the solid residue extracted with dichloromethane (2 × 20 mL) and water (20 mL). The organic fraction was taken and washed with brine. To the organic fraction was added hydrogen peroxide (5 mL, 30% in water) and water (20 mL) and the reaction mixture was stirred vigorously. After 10 min the organic layer was taken and dried with magnesium sulfate. The mixture was filtered and the solvent was removed from the filtrate, leaving a brown residue. The product was isolated by flash chromatography (3:1 hexanes:ethyl acetate) leaving a pale yellow solid. Yield = 55 mg (11%)

^{31}P NMR (121 MHz, $CDCl_3$): δ –19 (t, J = 15.3 Hz); ^{1}H NMR (300 MHz, $CDCl_3$): δ 8.07 (m, 2H, aryl H), 7.60 (m, 2H, aryl H), 7.58 (m, 2H, aryl H), 7.55 (m, 3H, aryl H), 7.51 (m, 3H, aryl H), 7.48 (m, 1H, aryl H), 3.25 (s, 2H C≡C*H*); $^{13}C\{^{1}H\}$ NMR (75 MHz, $CDCl_3$): δ 132.6 (d, J = 3.1 Hz, aryl C), 132.2 (aryl C), 132.1 (d, J = 140 Hz, P-C_{Ar}) 131.9 (aryl C), 130.2 (aryl C), 130.0 (aryl C), 128.6 (aryl C), 128.5 (aryl C), 124.8, (HC≡C-C_{Ar}), 119.9 (d, J = 4.7 Hz, P-C≡C-C_{Ar}), 103.0 (d, J = 38 Hz, P-C≡*C*), 84.8 (d, J = 201 Hz, P-*C*≡C), 82.6 (*C*≡CH), 80.5 (C≡*C*H), MS (70

eV): 375 (1.5, 4.5, 0.4) [M^+], 250 (100, 22, 3) [M^+- $C_{10}H_5$+1], 125 (8, 2,1) [$C_{10}H_5$], HRMS calcd for $C_{26}H_{15}PO$ Expected 374.08605, Found: 374.08618.

4.4.4.11 Preparation of 4.2b·O

To solution of 1,4-diethynyl-2,5-dihexylbenzene (0.75 g, 2.5 mmol) was added potassium bis(trimethylsilyl) amide (0.56 g, 2.8 mmol). The reaction mixture was warmed to RT and was stirred for 20 min. The reaction mixture was cooled to –78 °C and phenyl dichlorophosphine (0.23 g, 1.3 mmol) was added dropwise over 1 min. Immediately, the reaction mixture turned an orange colour. The reaction was warmed to room temperature and left overnight. An extract of the reaction mixture was taken and analyzed by $^{31}P\{^1H\}$ NMR spectroscopy which revealed complete consumption of the starting material (161 ppm), placed by a broad singlet at –60 ppm. The solvent was removed under reduced pressure and the solid residue extracted with dichloromethane (2 x 20 mL) and water (20 mL). The organic fraction was taken and washed with brine. To the organic fraction was added hydrogen peroxide (5 mL, 30% in water) and water (20 mL) and the reaction mixture was stirred vigorously. After 10 min the organic layer was taken and dried with magnesium sulfate. The mixture was filtered and the solvent was removed from the filtrate, leaving a brown residue. The product was isolated by flash chromatography (3:1 hexanes:ethyl acetate) and was isolated as a yellow oil. Yield = 0.16 g (18%).

^{31}P NMR (121 MHz, $CDCl_3$): δ –19 (t, J = 15.7 Hz); ^1H NMR (300 MHz, $CDCl_3$): δ 8.09 (m, 2H, aryl H), 7.59 (m, 3H, aryl H), 7.40 (s, 2H, aryl H), 7.33 (s, 2H, aryl H), 3.37 (s, 2H, C≡C*H*), 2.71 (m, 8H, Ar-CH_2) 1.67-1.50 (m, 8H, CH_2) 1.55-1.42 (m, 4H, CH_2), 1.41-1.13 (m, 20H, CH_2), 0.90 (t, J = 6.8 Hz, 6H, CH_3) 0.82 (t, J = 6.6 Hz, 6H, CH_3). $^{13}C\{^1H\}$ NMR (75 MHz, $CDCl_3$): δ 143.9 ($^{ipso}C_{Ar}CH_2$), 143.9 ($^{ipso}C_{Ar}CH_2$), 143.1 ($^{ipso}C_{Ar}CH_2$), 133.3 (aryl C), 133.2 (aryl C), 133.2

(aryl C), 132.7 (aryl C), 130.4 (aryl C), 130.2 (aryl C), 128.9 (aryl C), 128.7 (aryl C), 124.2 (C_{Ar}-C≡CH), 119.4 (d, J = 4.5 Hz, P-C≡C-C_{Ar}) 102.7 (d, J =38 Hz, P-C≡C), 87.5 (d, J = 202 Hz, P-C≡C) 82.8 (C≡CH), 81.8 (C≡CH), 34.0 (CH$_2$), 33.7 (CH$_2$), 31.6 (CH$_2$), 31.5 (CH$_2$), 30.7 (CH$_2$), 30.3 (CH$_2$), 29.0 (CH$_2$), 29.0 (CH$_2$), 22.5 (CH$_2$), 22.5 (CH$_2$) 14.1 (CH$_3$), 14.0 (CH$_3$). MS (70 eV): 710 (100, 55, 14) [M^+], 653 (61, 30, 11) [M^+ - C_4H_9], 639 (10) [M^+ - C_5H_{11}]. HRMS Expected: 710.46166, found 710.46221.

4.4.4.12 Preparation of 4.2c·O

To solution of 1,4-diethynyl-2,5-bis(*n*-hexyloxy)benzene (0.75 g, 2.3 mmol) was added lithium bis(trimethylsilyl)amide at –78 °C, premade from the reaction of bis(trimethylsilyl)amine (0.37 g, 2.3 mmol) and *n*-BuLi (1.4 mL, 1.6 M) in THF. The reaction mixture was warmed to RT and was stirred for 20 min. The reaction mixture was cooled to –78 °C and phenyl dichlorophosphine (0.21 g, 1.2 mmol) was added dropwise over 1 min. Immediately the reaction mixture turned an orange colour. The reaction was warmed to room temperature and left overnight. An extract of the reaction mixture was taken and analyzed by $^{31}P\{^1H\}$ NMR spectroscopy which revealed complete consumption of the starting material (δ = 161), placed by a broad singlet at δ = –59. The solvent was removed under reduced pressure and the solid residue extracted with dichloromethane (2 x 20 mL) and water (20 mL). The organic fraction was taken and washed with brine. To the organic fraction was added hydrogen peroxide (5 mL, 30% in water) and water (20 mL) and the reaction mixture was stirred vigorously. After 10 minutes the organic layer was taken, dried with magnesium sulfate. The mixture was filtered and the solvent was removed from the filtrate, leaving a brown residue. The product was isolated by flash chromatography (2:1 hexanes:ethyl acetate) to give a pale orange solid. Yield = 0.46 g (51%).

^{31}P NMR (121 MHz, $CDCl_3$): δ = –19 (t, *J* = 15.6 Hz); ^{1}H NMR (300 MHz, $CDCl_3$): δ 8.14 (m, 2H, aryl H), 7.57 (m, 3H, aryl H), 7.03 (s, 2H, aryl H), 6.96 (s, 2H, aryl H), 3.97 (t, *J* = 6.5, O-C*H*$_2$), 3.93 (t, *J* = 6.5, O-C*H*$_2$), 3.40 (s, 2H, C≡C*H*), 1.80-1.66 (m, 8H, C*H*$_2$) 1.55-1.42 (m, 4H, C*H*$_2$), 1.41-1.29 (m, 12H, C*H*$_2$), 1.23 (m, 8H, C*H*$_2$), 0.91 (t, 6H, C*H*$_3$) 0.84 (t, 6H, C*H*$_3$). ^{13}C{^{1}H} NMR (75 MHz, $CDCl_3$, δ): 154.9 ($^{ipso}C_{Ar}CH_2$), 154.9 ($^{ipso}C_{Ar}CH_2$), 153.8 ($^{ipso}C_{Ar}CH_2$), 133.2 (d, 142 Hz, P-C_{Ar}), 132.6 (aryl C), 132.5 (aryl C), 130.7 (aryl C), 130.5 (aryl C), 128.7 (aryl C), 128.5 (aryl C), 117.5 (aryl C), 117.3 (aryl C), 115.6, (HC≡C-C_{Ar}), 110.1 (d, *J* = 4.6 Hz, P-C≡C-C_{Ar}) 100.4 (d, *J* = 39 Hz, P-C≡*C*) 88.1 (d, *J* = 203 Hz, P-*C*≡C) 83.6 (C≡*C*H), 79.4 (*C*≡CH), 69.7 (O-*C*H$_2$), 69.4 (O-*C*H$_2$), 31.5 (*C*H$_2$), 31.4 (*C*H$_2$), 29.1 (*C*H$_2$), 29.0 (*C*H$_2$), 25.6 (*C*H$_2$), 25.4 (*C*H$_2$), 22.5 (*C*H$_2$), 22.5 (*C*H$_2$) 14.0 (*C*H$_3$), 14.0 (*C*H$_3$). MS (70 eV): 774 (12, 7, 2) [M$^+$], 704 (4, 2) [M$^+$-C_5H_{11}], 689 (1,8,4) [M$^+$- C_6H_{13}], 605 (6,4, 2) [M$^+$-$C_{12}H_{26}$], Elem. Anal. Calcd for $C_{29}H_{34}$: C 77.49, H 8.19; found C 77.16, H 8.24.

4.4.4.13 Preparation of 4.2d·O

To solution of 2,7-diethynyl-9,9-dihexyl-9*H*-fluorene (0.75 g, 2.0 mmol) was added potassium bis(trimethylsilyl)amide (0.39 g, 2.0 mmol) at –78 °C in THF (10 mL). The reaction mixture was warmed to RT and was stirred for 20 minutes. The reaction mixture was cooled to –78 °C and phenyl dichlorophosphine (0.18 g, 1.0 mmol) was added dropwise over 1 min. Immediately, the reaction mixture turned a dark red colour. The reaction was warmed to room temperature and left overnight. An extract of the reaction mixture was taken and analyzed by ^{31}P{^{1}H} NMR spectroscopy which revealed complete consumption of the starting material (161 ppm), placed by a broad singlet at –60 ppm. The solvent was removed under reduced pressure and the solid residue was extracted with dichloromethane (2 × 75 mL) and water (20 mL). The organic

fraction washed with brine. To the organic fraction was added hydrogen peroxide (5 mL, 30% in water) and water (20 mL) and the reaction mixture was stirred vigorously. After 10 minutes the organic layer was taken, dried with magnesium sulfate and the solvent removed, leaving a red coloured residue. The product was isolated by flash chromatography (2:1 hexanes:ethyl acetate) to give a pale orange solid. Yield = 0.21 g (24%).

^{31}P NMR (121 MHz, $CDCl_3$): δ –19 (t, *J* = 16 Hz); 1H NMR (300 MHz, CDCl3): δ 8.18 (m, 2H, aryl H), 7.71 (s, 1H, aryl H), 7.69 (s, 2H, aryl H), 7.65 (m, 5H, aryl H) 7.60 (s, 3H, aryl H), 7.52 (s, 1H, aryl H), 7.50 (s, 3H, aryl H) 3.19 (s, 2H, C≡CH), 1.97 (m, 8H, ArCH_2) 1.18-0.97 (m, 24H, CH_2) 0.78 (t, *J* = 6.9 Hz, 12H, CH_3), 0.57 (m, 8H, CH_2). $^{13}C\{^1H\}$ NMR (75 MHz, $CDCl_3$): δ 151.3 (aryl C), 151.2 (aryl C), 143.0 (aryl C), 140.4 (aryl C), 133.0 (d, *J* = 143 Hz, P-C_{Ar}), 132.7 (aryl C), 132.2 (aryl C), 131.9 (aryl C), 131.3 (aryl C), 130.5 (d, *J* = 13 Hz, aryl C), 128.8 (d, *J* = 15 Hz, aryl C), 127.1 (aryl C), 126.6 (aryl C), 121.6 (aryl C), 120.4 (aryl C), 120.2 (aryl C), 118.20 (d, *J* = 4.5 Hz, P-C≡C-C_{Ar}) 104.8 (d, *J* = 38 Hz, P-C≡*C*), 84.3 (*C*≡CH), 83.3 (d, *J* = 196 Hz, P-*C*≡C), (*C*≡CH), 77.8 (C≡*C*H), 55.37 (*C*-CH_2), 40.14 (*C*H_2), 31.43 (*C*H_2), 29.54 (*C*H_2), 23.63 (*C*H_2), 22.51 (*C*H_2), 13.93 (*C*H_3). MS (70 eV): 886 [1, 0.4; M^+], 801 [0.5; M^+ - C_6H_{13}], 554 [1; M^+ -3 x C_6H_{13} – Ph], 56 [100, 11; C_4H_8], HRMS Expected 886.52426, found 886.52406.

4.4.4.14 Preparation of 4.2e·O

A solution of phenyldichlorophosphine (3.0 g, 17 mmol) in toluene (50 mL) was added to a mixture of nickel (II) acetylacetonate (0.22 g, 0.83 mmol) and phenylaceylene (4.3 g, 4.6 mL, 42 mmol) in toluene (50 mL). Triethylamine (13 mL, 9.7 mmol) was subsequently added to the reaction mixture. The reaction mixture was stirred vigorously at 80 °C. The reaction was

monitored after 2 h by ^{31}P NMR spectroscopy, which revealed a single resonance (–60 ppm). The solvent was removed *in vacuo* leaving a dark yellow-red coloured solid. To the solid was added dichloromethane (3 × 30 mL) and the suspension was filtered. To the filtrate was added hydrogen peroxide (30 mL, 50% in water) and the reaction mixture was stirred vigorously for 1 h. After this time an aliquot of the reaction mixture was analysed by ^{31}P NMR spectroscopy revealing complete consumption of starting material, replaced by a single resonance (–19 ppm). The organic layer was dried with magnesium sulfate and filtered. The solvent was removed *in vacuo* and the product was purified by column chromatography (eluent: hexanes:ethyl acetate, 1:1, rf ≈ 0.4). Pale yellow crystals suitable for analysis by x-ray crystallography were grown from a saturated ethyl acetate solution upon standing at room temperature. Yield: 1.71 g (31%). ^{31}P NMR ($CDCl_3$, 162 MHz): δ –19 (t, J = 16 Hz), ^{1}H NMR ($CDCl_3$, 300MHz): δ 8.15-8.05 (m, 2H, aryl H), 7.67-7.52 (m, 7H, aryl H), 7.49-7.32(m, 6H, aryl H), ^{13}C{^{1}H} NMR ($CDCl_3$, 75 MHz): δ 133.8 (aryl C), 132.7 (aryl C), 132.5 (aryl C), 131.9 (aryl C), 130.8 (aryl C), 130.3 (aryl C), 128.9 (aryl C), 128.5 (aryl C), 119.6 (d, J = 5 Hz, P-C≡C-C_{Ar}), 103.7 (d, J = 38 Hz, P-C≡C), 83.2 (d, J = 202 Hz, P-C≡C). EI-MS (70 eV): 326 [M^+], 249 [M^+-Ph], 202 (100) [M^+-PhPO], 178 (10) [$C_{14}H_{10}$]. Elem. Anal. calcd for $C_{22}H_{15}PO$: C 80.97, H 4.63; found C 80.70 H 4.65.

4.4.4.15 Preparation of 4.3a·O

A Schlenk flask was charged with diphenylchlorophosphine (1.8 g, 7.9 mmol), nickel (II) acetylacetonate (0.051 g, 0.20 mmol), 1,4-diethynylbenzene (0.50 g, 4.0 mmol) and toluene (20 mL). Triethylamine (2.8 mL, 20 mmol) was subsequently added to the reaction mixture. The deep red reaction mixture was stirred vigorously at 85 °C. After 30 min, the ^{31}P NMR spectrum of an aliquot removed from the reaction mixture showed only new signal at –33 ppm. The

solvent was removed *in vacuo* to afford a red solid that was subsequently dissolved in dichloromethane and washed with water. The organic layer was taken and dried with magnesium sulfate. The product was dissolved in dichloromethane and run through a silica plug. To the yellow solution that was collected was added hydrogen peroxide (15 mL, 50% in water) and water (10 mL). The organic layer was separated, dried with magnesium sulfate, and filtered. Yield 0.35 g (18%).

^{31}P NMR (121 MHz, $CDCl_3$): δ 9.4 (t, J = 12 Hz); ^{1}H (300 MHz, $CDCl_3$): 7.88 (m, 8H, aryl H), 7.59 (s, 4H, aryl H), 7.51 (br m, aryl H) 13C{^{1}H} NMR (75 MHz, $CDCl_3$): δ 132.4 (m, aryl C), 132.2 (d, J =122 Hz, P-C_{Ar}), 130.9 (aryl C), 130.7 (aryl C), 128.7 (aryl C), 128.5 (aryl C) 121.9 (d, J = 4 Hz, P-C≡C-C_{Ar}), 103.6 (d, J = 29 Hz, P-C≡C) 85.6 (d, J =166 Hz, PC≡C).

4.4.4.16 Preparation of 4.3b·O

A Schlenk flask was charged with diphenylchlorophosphine (0.82 g, 3.7 mmol), nickel (II) acetylacetonate (0.048 g, 0.19 mmol), 1,4-diethynyl-2,5-dihexylbenzene (0.54 g, 1.8 mmol) and toluene (25 mL). Triethylamine (3.1 mL, 22 mmol) was subsequently added to the reaction mixture. The deep red reaction mixture was stirred vigorously at 85 °C. After 30 min, the ^{31}P NMR spectrum of an aliquot removed from the reaction mixture showed only new signal at –33 ppm. The solvent was removed *in vacuo* to afford a red solid that was subsequently dissolved in dichloromethane (15 mL) oxidized with hydrogen peroxide (15 mL, 50% in water). After 10 minutes TLC confirmed reaction completion. The organic layer was separated, dried with magnesium sulfate, and filtered. Upon removal of the solvent *in vacuo*, ethanol (10 mL) was added to dissolve, and the resulting solution was cooled in a freezer (–40 °C) overnight. At this time a pale pink solid precipitated and was isolated by filtration. Pale pink crystals suitable of X-

ray crystallography were grown from a saturated 1:1 hexanes/ethyl acetate mixture upon cooling. Yield 0.58 g (45%).

^{31}P NMR ($CDCl_3$, 162MHz): δ 8 (t, J = 13 Hz). ^{1}H NMR ($CDCl_3$, 400 MHz): δ 7.95-7.85 (m, 4H, aryl H), 2.70 (m, 2H, CCH_2), 1.54 (m, 2H, CH_2), 1.29-1.13 (m, 6H, C_3H_6), 0.84 (t, 3H, CH_3), ^{13}C{^{1}H} NMR ($CDCl_3$, 100MHz): δ 143.7 (aryl C), 133.2 (aryl C), 132.0 (aryl C), 132.0 (aryl C), 130.6 (aryl C), 130.5 (aryl C), 128.4 (aryl C), 128.3 (aryl C), 121.3 (d, J = 4 Hz, P-C≡C-C_{Ar}), 103.1 (d, J = 29 Hz, P-C≡C), 88.1 (d, J = 167 Hz, P-C≡C), 33.7 (CH$_2$), 31.2 (CH$_2$), 30.3 (CH$_2$), 28.6 (CH$_2$), 22.1 (CH$_2$), 13.65 (CH$_3$). MS (70 eV): 694 (44) [M$^+$], 494 (37) [M$^+$-POPh$_2$], 201 (100) [M$^+$-$C_{34}H_{38}PO$], HRMS Expected: 694.31344, found 694.31296. Elemental analysis (%) calculated for $C_{64}H_{48}P_2O_2$: C 79.52, H 6.96; found C 79.61 H 6.95.

4.4.4.17 Preparation of 4.3c·O

A Schlenk flask was charged with diphenylchlorophosphine (0.68 g, 3.1 mmol), nickel (II) acetylacetonate (0.020 g, 77 μmol), 1,4-bis(hexyloxy), 2,5-diethynylbenzene (0.50 g, 1.5 mmol) and toluene (25 mL). Triethylamine (5.0 mL, 35 mmol) was subsequently added to the reaction mixture. The deep red reaction mixture was stirred vigorously at 85 °C. After 8 h, the ^{31}P NMR spectrum of an aliquot removed from the reaction mixture showed two major signals at –32 ppm. The solvent was removed *in vacuo* to afford a red solid that was subsequently dissolved in dichloromethane (15 mL) and oxidized with hydrogen peroxide (15 mL, 50% in water). After 10 minutes TLC confirmed that the starting material had been consumed. The organic layer was separated, dried with magnesium sulfate, and filtered. Upon removal of the solvent *in vacuo*, crystals suitable for X-ray crystallography were grown from column yield = 0.33 g (30%).

^{31}P NMR (121 MHz, $CDCl_3$): δ 9 (t, J = 13 Hz); ^{1}H NMR (300 MHz, $CDCl_3$): δ 8.14 (m, 2H, aryl H), 7.57 (m, 3H, aryl H), 7.02 (s, 2H, aryl H), 6.95 (s, 2H, aryl H), 3.97 (t, J = 6.5 Hz, O-

CH_2), 3.93 (t, J = 6.5 Hz, O-CH_2), 3.39 (s, 2 H, C≡CH), 1.80-1.66 (m, 8H, CH_2) 1.55-1.42 (m, 4H, CH_2), 1.41-1.29 (m, 12H, CH_2), 1.23 (m, 8H, CH_2), 0.91 (t, J = 6.2 Hz, 6H, CH_3) 0.84 (t, 6H, CH_3). $^{13}C\{^1H\}$ NMR (75 MHz, $CDCl_3$): δ 154.9 ($^{ipso}C_{Ar}OCH_2$), 133.7 (aryl C), 132.1 (aryl C), 132.1 (aryl C), 130.9 (d, J = 11 Hz, aryl C) 128.5 (d, J = 14 Hz, aryl C), 116.6 (aryl C) 112.5 (d, J = 4.2 Hz, P-C≡C-C_{Ar}) 101.2 (d, J = 30 Hz, P-C≡C) 88.6 (d, J = 169 Hz, P-C≡C), 69.7 (O-CH$_2$), 69.4 (O-CH$_2$) 31.5 (CH$_2$), 31.4 (CH$_2$), 29.1 (CH$_2$), 29.0 (CH$_2$), 25.6 (CH$_2$), 25.4 (CH$_2$), 22.5 (CH$_2$), 22.5 (CH$_2$), 14.0 (CH$_3$), 14.0 (CH$_3$). MS (70 eV): 726 (22, 12, 6) [M^+], 525 (12,16,13) [M^+-$POPh_2$], 201 (100, 22, 4) [PPh_2O].

4.4.4.18 Preparation of 4.3d·O

A Schlenk flask was charged with diphenylchlorophosphine (0.55 g, 2.50 mmol), nickel acetylacetonate (31 mg, 0.12 mmol), 1,4-bis(dodecyloxy), 2,5-diethynylbenzene (0.59 g, 1.2 mmol), and toluene (25 mL). Triethylamine (3.0 mL, 22 mmoL) was subsequently added to the reaction mixture. The deep red reaction mixture was stirred vigorously overnight. The reaction was monitored by ^{31}P NMR which revealed a single peak at –33 ppm. The solution was purified by filter cannulation and solvent was removed *in vacuo* to afford a brown solid. The product was subsequently dissolved in dichloromethane (20 mL) and oxidized by stirring with a solution of 30% hydrogen peroxide in water (10 mL) and water (10 mL). After 10 minutes TLC confirmed reaction completion. The organic layer was separated, dried with magnesium sulfate, and filtered. Upon removal of the solvent *in vacuo*, the crude product was isolated as a brown solid. The crude was purified by column chromatography (1:1 ethyl acetate:hexanes) to give **4.3d**·O as a yellow solid. Yield = 0.17 g (49%).

^{31}P NMR (121 MHz, $CDCl_3$): δ 9 (t, *J* = 13 Hz); ^{1}H NMR (300 MHz, $CDCl_3$): δ 7.95 (m, 8H, aryl H), 7.49 (m, 12H, aryl H), 7.05 (s, 2H, aryl H), 3.96 (t, *J* = 6.5 Hz, 4H, O-C*H*$_2$), 1.81 (m, 4H, OCH_2CH_2), 1.42 (m, 4H, C*H*$_2$), 1.24 (m, 28H, C*H*$_2$), 0.89 (t, *J* = 6.9 Hz, 6H, C*H*$_3$). ^{13}C{^{1}H} NMR (75 MHz, $CDCl_3$): δ 154.6 ($^{ipso}C_{Ar}OCH_2$), 133.1 (d, *J* = 122 Hz, P-C_{Ar}), 132.2 (d, *J* = 2.7 Hz, aryl C), 131.0 (d, *J* = 11 Hz, aryl C) 128.6 (d, *J* = 14 Hz, aryl C), 116.8 (aryl C), 112.7 (d, *J* = 4.0 Hz, P-C≡C-C_{Ar}), 101.3 (d, *J* = 30 Hz, P-C≡*C*), 88.7 (d, *J* = 168 Hz, P-*C*≡C), 69.4 (O-*C*H_2), 31.9 (*C*H_2), 29.6 (*C*H_2), 29.6 (*C*H_2), 29.5 (*C*H_2), 29.3 (*C*H_2), 29.2 (*C*H_2), 25.9 (*C*H_2), 14.1 (*C*H_3).

4.4.4.19 Reaction of PhC≡CLi with $PhPCl_2$ (excess) – NMR evidence for PhP(C≡CPh)Cl

To a diethyl ether (10 mL) solution of phenyl acetylene (0.50 g, 4.9 mmol) was added *n*-butyl lithium (3.1 mL, 4.9 mmol) at -78 °C. The cooling bath was removed and, once the solution reached room temperature, it was added dropwise over a period of 20 min to a cooled (–78 °C) solution of phenyl dichlorophosphine in diethyl ether (10 mL). An aliquot was removed from the reaction mixture and analyzed by ^{31}P NMR spectroscopy. Two new signals at 53 ppm and –60 ppm were observed in a ratio of 5:6, in addition to starting material (161 ppm). The new signals are assigned to the mono and disubstituted reaction products, respectively.

Chapter 5: A Fluorenyl Phosphine Polymer as a Selective "Turn-On" Fluorescent Sensor for Gold and Mercury ions.

5.1 Introduction

Gold metal salts and ions are being increasingly studied across many different fields of chemistry. The use of gold catalysts for a variety of organic transformations has received increased attention over the previous two decades.[279-282] Historically, gold compounds are of considerable interest because of their anti-inflammatory properties and have been used commonly in the treatment of rheumatoid arthritis.[283] Gold based drugs have also been shown to have anti-cancer properties[284] and, recently, their use as anti-HIV agents has been investigated.[285] Gold nanoparticles are used extensively in the fields of drug delivery (especially chemotherapy),[286, 287] catalysis[288-291] and sensors.[292, 293]

As their use is becoming more common, there is a growing concern regarding the safety of gold reagents. Au(I) compounds show cytotoxicity *in vivo* as part of their anti-tumour characteristics whereas Au(III) ions have also been shown to be toxic as they bind strongly to DNA.[294-296] Given these considerations the ability to detect the presence of gold ions is of increasing importance and has recently received specific attention in the literature.[297-300] The majority of gold ion sensors reported to date have a mechanism of action that involves an intramolecular facilitated reaction by the activation of an alkyne moiety by Au(I)[301-305] or Au(III)[302-317] ions. The product of these organic transformations are detectable fluorescent species. Given that soft phosphine-based ligands have a very high affinity to bind soft gold ions, it is perhaps suprising that there are very limited examples of sensors based on phosphine ligand coordination to gold ions,[122] especially as many of these coordination complexes are fluorescent.[172, 301, 318-324] As mentioned in Chapter 1, phosphine sensors have previously been

reported for the detection of peroxides[109-113, 118-120, 325] and other heavy metals.[124] In these cases the coordination or oxidation of the phosphine moities in these compounds inhibit photoinduced electron transfer (PET) which quenches fluorescence from the attached fluorescent chromophores.

As a group we are interested in synthesis and properties of novel phosphine polymers.[43, 71] The incorporation of P atoms within macromolecules gives rise to polymers with unique functionality, imparted by the chemical reactivity of the phosphine moieties within the polymers. As discussed in Chapter 4 of this thesis, we recently reported the synthesis of poly(*p*-phenylene diethynylene phosphine), PPYP, the first di-yne substituted phosphine macromolecule.[193] Notably, oxidation of the phosphine moieties imparted a significant change in the emissive properties of the polymer. The oxidized polymer emitted blue coloured fluorescence whereas the non-functionalized polymer was non emissive. It was envisaged that these polymers could be utilized for the detection of analytes to make a highly fluorescent polymeric sensor. This is because the coordination of the P-lone pair within PPYPs to analytes may block the PET quenching pathway (Scheme 5.1). Herein we report the synthesis of a fluorene-containing PPYP and its use in the sensing of Au and Hg ions.

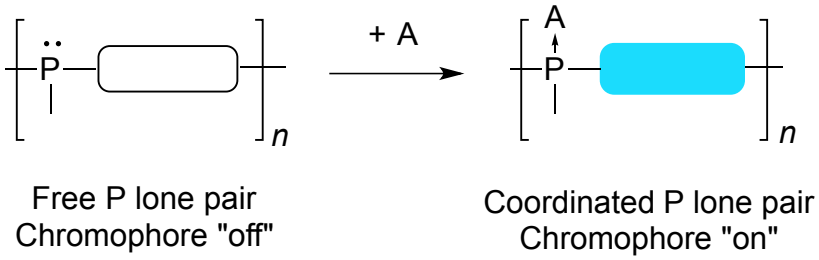

Scheme 5.1: Coordination of the P lone pair to analytes resulting in turn on fluorescence of chromophores within the polymer.

5.2 Results and Discussion

In order to realize a highly fluorescent macromolecular sensor, a PPYP that incorporated fluorene moieties was targeted. A nickel coupling procedure[245] was utilized to synthesize the target polymer. According to our previous published procedure (and as in Chapter 4),[193] polymer **5.1** was prepared (Scheme 5.2). By reacting a mixture of di-ynes, 2,7-diethynyl-9,9-di-*n*-hexylfluorene[249] (0.25 equiv) with 1,4-diethynyl-2,5-di-*n*-hexylbenzene[247] (0.75 equiv) with phenyldichlorophosphine under the standard conditions, incorporation of fluorene moieties within the polymer was achieved. A $^{31}P\{^{1}H\}$ NMR spectrum of the reaction mixture was taken after 16 h contained three distinct resonances at –59.6, –60.0 and –60.5 ppm with relative intensities of 1:7:8 (Figure 5.1). The polymer was precipitated from a concentrated THF solution into degassed ethanol and was isolated as a deep red coloured solid (yield 64 %).

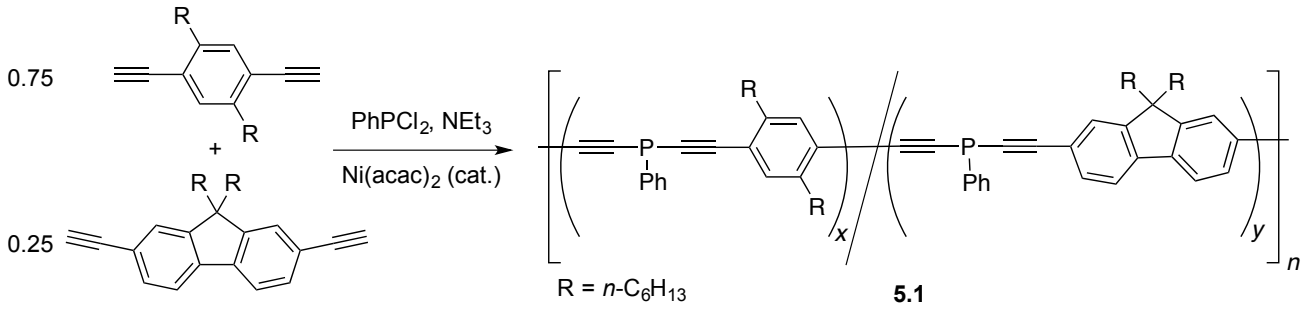

Scheme 5.2: Synthesis of polymer 5.1

The aforementioned three signals in the $^{31}P\{^{1}H\}$ NMR spectrum were also observed in the isolated polymer of **5.1**. A MALDI-TOF MS (dithranol matrix) of the isolated solid was obtained with a series of fragment ions that contain spacing of both 504/505 and 416/417 g mol^{-1} that corresponds to two different polymer repeat units, each incorporating fluorene and phenyl moieties. This spectrum can be found in the Appendix E, Figure E1. Polymer **5.1** was also characterized by gel permeation chromatography (GPC), which revealed a number molecular

weight average, M_n, of 3,600 g mol^{-1}, $DP_n \approx 9$ (*vs.* polystyrene) and a dispersity of 2.2. The polymer has also been characterized by ^{1}H, $^{13}C\{^{1}H\}$, HSQC and APT NMR spectroscopy.

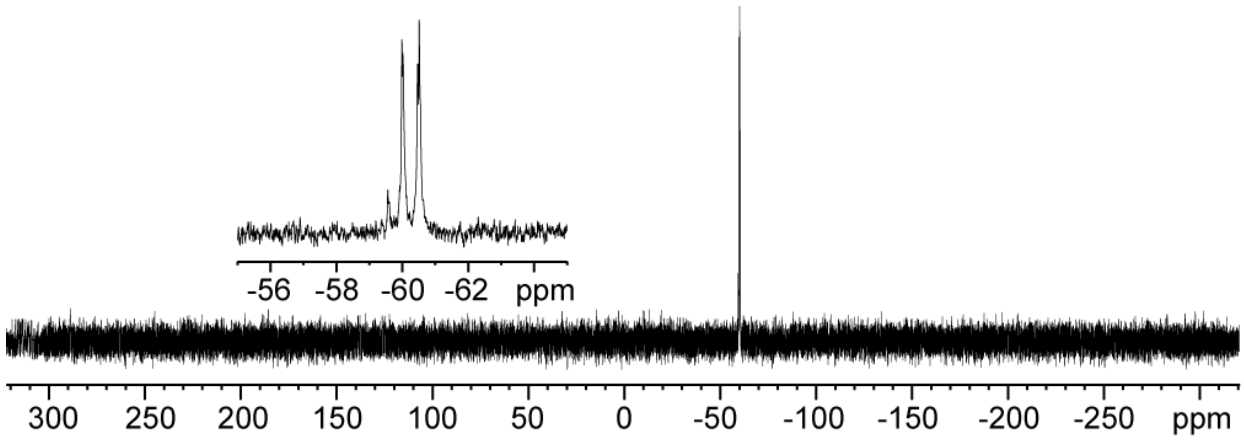

Figure 5.1: $^{31}P\{^{1}H\}$ NMR (121 MHz, Toluene) spectrum of the reaction mixture of 5.1

With polymer **5.1** in hand, we were interested is exploring the chemical functionality of the phosphorus atoms within the polymer. To this end, we prepared the highly metallated polymer **5.1**·AuCl, which was prepared by adding equimolar amounts of **5.1** and Au(tht)Cl (tht = tetrahydrothiophene) together in a THF solution at RT. After 30 min a $^{31}P\{^{1}H\}$ NMR spectrum of the reaction mixture revealed complete consumption of the starting material and two new signals were observed at –28.0 and –28.2 ppm, assigned to phosphine moieties coordinated to AuCl. After removal of the solvent and byproducts (e.g. tht) under reduced pressure, the polymer was dissolved in 1 mL of THF and precipitated into degassed MeOH (50 mL). GPC analysis of the isolated material revealed that the molecular weight of the polymer had increased (M_n = 5,000 g mol^{-1}) compared to **5.1** (M_n = 3,600 g mol^{-1}), consistent with gold incorporation within the polymer. The GPC trace also revealed a shoulder at shorter retention times (higher molecular weight) that was not present in the GPC trace of **5.1** (Figure 5.2). This high molecular weight

shoulder increased the dispersity of **5.1**·AuCl (Đ = 3.1, M_w = 16,500 g mol^{-1}) compared to **5.1**. The presence of high molecular weight material was perhaps due to aggregation of multiple chains of **5.1**·AuCl. This aggregation is potentially due to aurophillic interactions, which are commonly observed in the crystal structures of gold(I) compounds[326, 327] and are of interest for supramolecular self assembly applications.[328] Furthermore, additional evidence for aggregation within **5.1** was gathered by analyzing the crystal structure for alkynyl phosphine model compound (Ph-C≡C)$_2$PPh·AuCl, (**5.2**·AuCl, Figure 5.3) that showed close Au-Au contacts (3.11 Å), characteristic of aurophillic interactions.

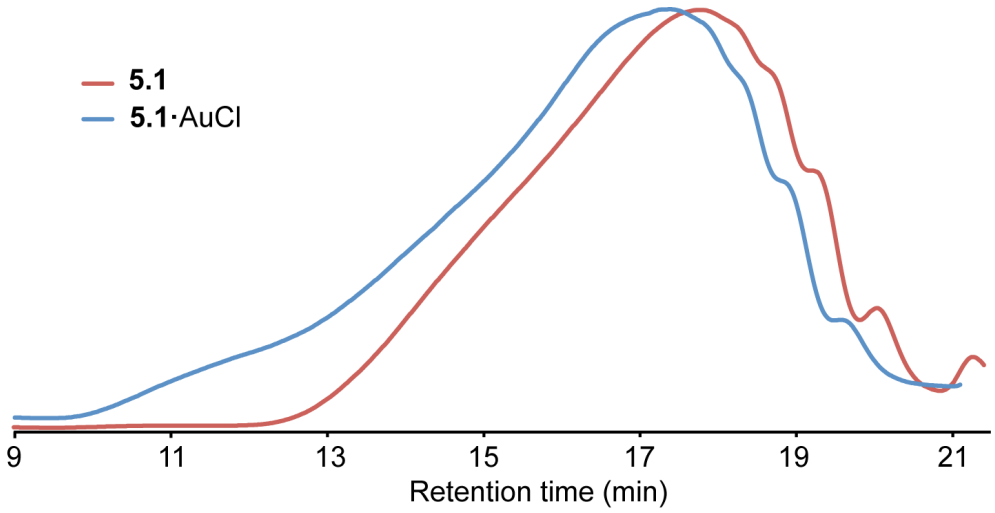

Figure 5.2: GPC traces of 5.1 and 5.1·AuCl

The polymer derived from the reaction of **5.1** and $HAuCl_4$ was also of interest. Reacting equimolar amounts of **5.1** and $HAuCl_4$ resulted in a product that gave a chemical shift of –27 and –22 ppm in the $^{31}P\{^1H\}$ NMR spectrum of the reaction mixture. Since these resonances were significantly shifted from the starting material, the phosphine atoms were likely coordinated to the gold ions. Unfortunately, characterization of this material was difficult, as upon removal of solvent the polymer could not be redissolved in common organic solvents (e.g. THF, DCM,

DMSO, toluene). The insolubility of this material was potentially due to crosslinking of phosphine ligands from different polymer chains around the Au(III) ions.

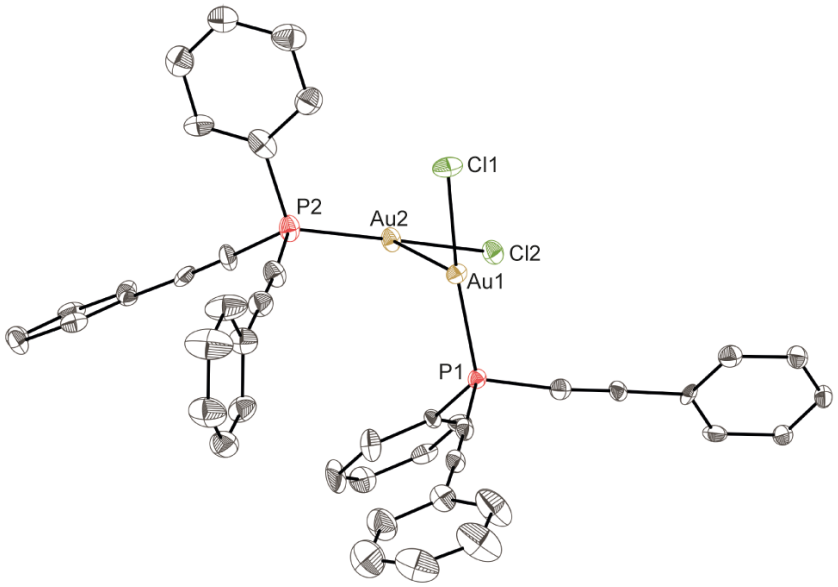

Figure 5.3: Molecular structure of two 5.2·AuCl molecules.

Aurophillic interactions are clearly present, Au(1)-Au(2) 3.11 Å. Hydrogen atoms have been removed for clarity. Ellipsoids are displayed at 50% probably level. Crystals were grown from deuterated chloroform.

Being satisfied that it was possible to bind gold atoms to **5.1** we were interested in exploring reactivity of alkynyl phosphines to other analytes. A series of test reactions were performed where alkynyl phosphine model compound $(PhC{\equiv}C)_2PPh$, **5.2**, was mixed with a equimolar amount of a variety of metal salts. Each reaction was monitored by $^{31}P\{^1H\}$ NMR spectroscopy. The reaction of **5.2** with transition metal ions [Fe(III), Ni(II), Cu(I), Rh(I), Pd(0), Pd(II), Ag(I), Pt(II), Au(I) and Au(III)] and Hg(I)/Hg(II) ions resulted in a change in the $^{31}P\{^1H\}$ NMR spectrum (typically a down field shift compared to **5.2** *cf.* –60 ppm), indicative of complex formation. The reaction of **5.2** with alkali and alkali earth metals ions [K(I), Na(I) and Ca(II)]

and heavy metal ions[Cd(II), Pb(II) and Bi(III)] resulted in no change of the ^{31}P NMR spectrum suggesting that complexes could not be formed or the rate of complex formation was slow.

Given that we had established that alkynyl phosphines bind readily to transition metals, we were interested in exploring the changing photophysical properties of the polymer upon functionalization of the P centres. Like other PPYPs polymer **5.1** also exhibits turn on fluorescence upon oxidation (see experimental section for synthetic details and characterization of **5.1**·O). We were interested to learn if a similar effect could be observed upon the coordination of the phosphine substituents in **5.1** to metal analytes.

To this end, a solution of **5.1** (c = 20 μM) was distributed into vials and an excess (10 mol equiv) of different metal ions were added to each. After 10 min the fluorescence spectra of each solution was recorded (Fig. 5.4, top). A bar chart of relative emission intensity at λ_{max} for each trial is shown in Fig. 5.4 (bottom). Remarkably, an extremely large fluorescence increase was seen with the trials that involved Au(I) and Au(III) ions [17 and 32 times that of **5.1;** λ_{max} = 387 nm for Au(I) and 383 nm for Au(III)]. Modest fluorescence increases were observed in the trial that involved Hg(I) and Hg(II) ions (7 and 3 times that of **5.1**; λ_{max} = 382 nm for both). Trials that involved other heavy metals [Bi(III) and Pb(II)] or group 1/2 metals [Na(I), K(I), Ca(II), Cs(I), Ba(II)] groups showed no such response under the reaction conditions. This is potentially due to no reaction occurring between the phosphine moieties in the polymer and the metal ions, similar to results observed when reacting **5.2** with heavy metals and group 1/2 metals.

The emission spectra recorded after reacting **5.1** with $PtCl_2$ showed a change of emission maxima wavelength (433 nm vs. 381 nm for **5.1**) suggesting that complex formation had occurred, however only a very small increase in fluorescence was observed. A mild fluorescence increase was observed in the trial involving $PdCl_2$ and no emission increase was seen for other

the other Pd or Pt derivatives that were tested ([$Pd(PPh_3)_4$], [$Pd(PPh_3)_2Cl_2$], [$Pd(OAc)_2$] and K_2PtCl_4). This may be due to the slower kinetics of complex formation in the presence of competing ligands. Leaving the reactions of **5.1** and $PdCl_2$/$PtCl_2$ for an extended period of time, or adding a larger excess of metal resulted in complete fluorescence quenching. Reactions involving **5.1** and Y(III), Ru(III), Rh(I), Ag(I), Cd(I), Ir(I) or the first row transition metal ions [Fe(III), Ni(II), and Cu(I)] resulted in solutions that were not emissive.

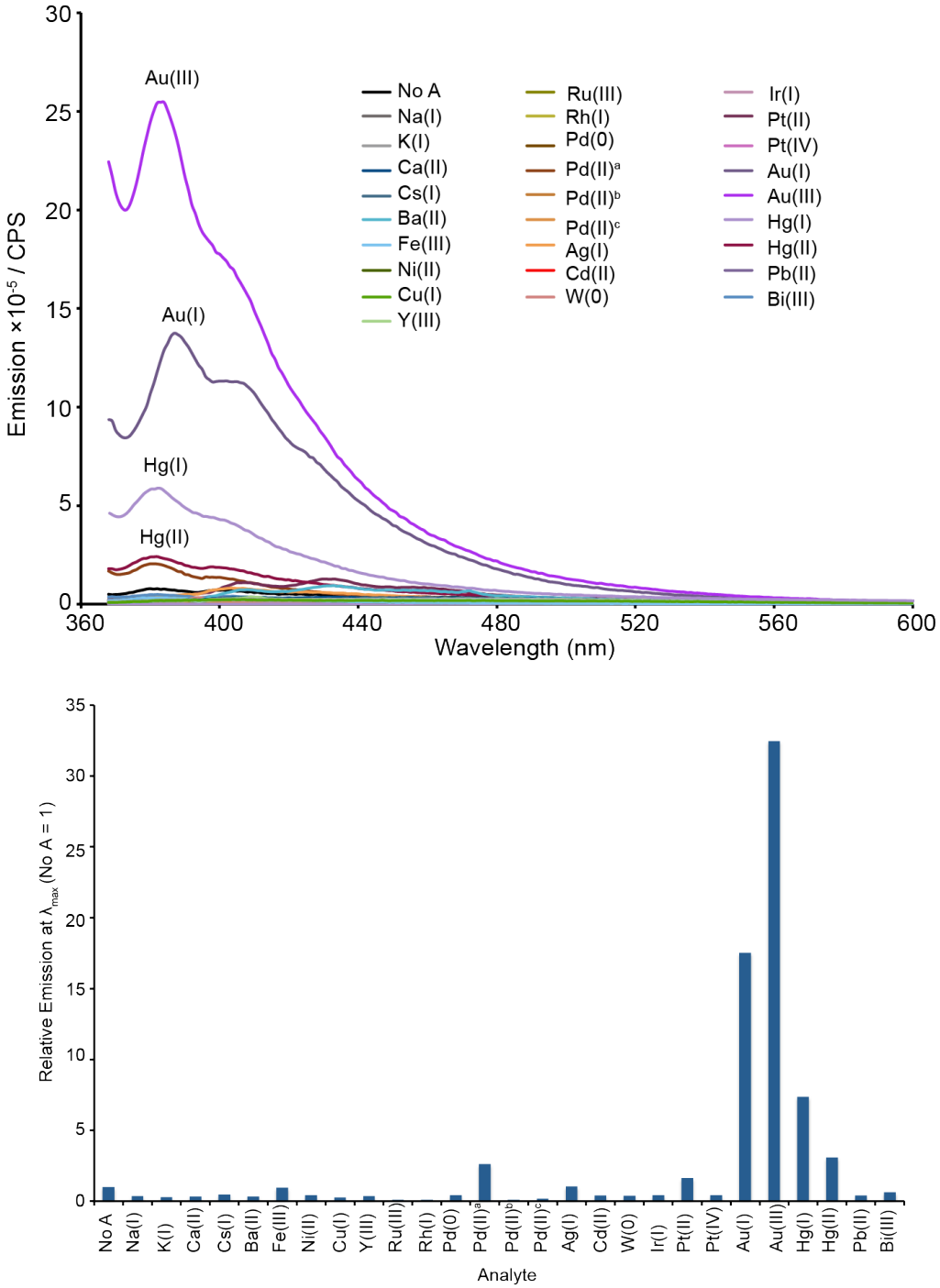

Figure 5.4 (top): Emission spectra (λ_{ex} = 353 nm) of the reaction mixture of 5.1 (20 µM) + metal analytes (200 µM, 10 equiv) in THF after 10 min. Figure 5.4 (bottom): A bar chart displaying the relative emission intensity at λ_{max} for each reaction compared to 5.1 (20 µM). [a]$PdCl_2$, [b]$Pd(PPh_3)_2Cl_2$, [c]$Pd(OAc)_2$

Summarizing the results above, **5.1** appeared to be a selective turn on fluorescence sensor for Au(I) and Au(III) ions. In order to learn about the sensitivity of **5.1** towards gold analytes an experiment was performed where substoichiometric amounts of Au(I) or Au(III) ions were added to a solution of **5.1** and the fluorescence was measured (Figure 5.5). When Au(I) was used as an analyte full emission intensity was only observed when near stoichiometric amounts of metal were added. Maximum fluorescence may only occur at full, or close to full coordination of phosphine atoms within the polymer). This observation suggests that small amounts of free phosphine moieties within the polymer can dramatically affect its emissive properties. We have observed a similar effect when undertaking similar experiments with fluorescent poly(methylenephosphine)s as described in Chapter 3.

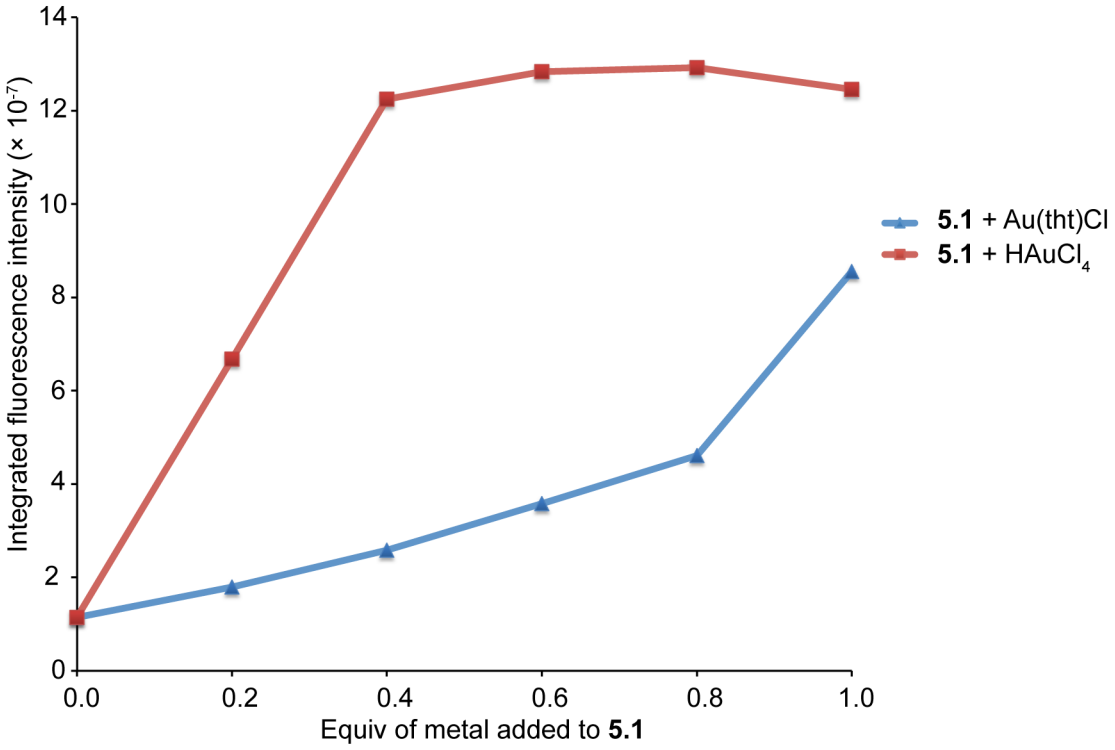

Figure 5.5 A plot of integrated emission intensity (λ_{ex} = 353 nm) upon addition of Au(I) and Au(III) to 5.1.

Performing a similar experiment with **5.1** with Au(III) ions resulted in a substantial increase in emission upon addition of far less equivalents of analyte. The maximum emission

from the polymer was reached upon the addition of 0.4 equiv of $HAuCl_4$ to **5.1**. As less analyte is required to fully "turn on" the emission from the polymer likely that multiple phosphine moieties can coordinate to each Au(III) ion. To test this, polymer **5.1** was reacted with 0.5 equiv $HAuCl_4$ in THF. After 10 min, the ^{31}P NMR spectrum showed only two signals at –24 and –28 ppm. As no resonances corresponding to the starting material was observed it appears that each Au(III) ion was coordinated to at least two phosphorus centres, and no uncoordinated phosphorus atoms were present throughout the polymer.

5.3 Summary

In closing, a fluorene-containing PPYP was synthesized and was fully characterized. It was shown that phosphorus atoms within the polymer could readily coordinate to Au(I) or Au(III) ions to make highly metallated polymers. When exploring the photophysical properties of **5.1** in the presence of analytes from across the periodic table, turn on emission was observed selectively in the presence of gold and mercury ions. By reacting **5.1** with substoichiometric amounts of Au(I) ions it was realized that maximum fluorescence only occurred at high levels of phosphine coordination to the metal. Maximum fluorescence was observed using lower stoichiometric amounts of Au(III) ions compared to Au(I) ions as this metal can accommodate multiple phosphine atoms.

Further studies will be focused on developing our understanding regarding the turn-on fluorescence mechanism within these systems with the aim of increasing the sensitivity of these intriguing polymeric sensors.

5.4 Experimental

5.4.1 Materials and Methods

All manipulations of air- and/or water-sensitive compounds were performed under a nitrogen atmosphere by using standard Schlenk or glovebox techniques. Hexanes, dichloromethane and toluene were deoxygenated with nitrogen and dried by passing through a column containing activated alumina. Tetrahydrofuran (THF) was dried over sodium and benzophenone, and was distilled prior to use. Ethanol and methanol was degassed before use. Triethylamine was dried over calcium hydride and was distilled before use. Nickel (II) acetylacetonate (Aldrich) and anthracene (Fisher) were sublimed before use. $HAuCl_4 \cdot 3H_2O$ was purchased from STREM and was used as received. Au(tht)Cl,[175] 1,4-diethynyl-2,5-*n*-hexylbenzene,[247] and 2,7-diethynyl-9,9-di-*n*-hexyl-9H-fluorene[68] were made following literature procedures.

5.4.2 Equipment

^1H, $^{31}P\{^1H\}$, $^{13}C\{^1H\}$ NMR spectra were recorded at 25 °C on Bruker Avance 300, 400 or 600 MHz spectrometers. H_3PO_4 (85%) was used as an external standard ($\delta = 0$ for ^{31}P). ^1H NMR spectra were referenced to the residual protonated solvent signal and $^{13}C\{^1H\}$ NMR spectra were referenced to the deuterated solvent signal. Elemental analyses were performed in the University of British Columbia Chemistry Microanalysis Facility. Mass spectra were recorded on a Kratos MS 50 instrument in EI mode (70 eV). Polymer molecular weights were determined by gel permeation chromatography (GPC) using an Agilent liquid chromatograph equipped with an Agilent 1200 series isocratic pump, Agilent 1200 series standard autosampler, Phenomenex Phenogel 5 mm narrow bore columns (4.6 × 300 mm) 10^4 Å (5,000–500,000 g mol^{-1}), 500 Å (1,000–15,000 g mol^{-1}), and 10^3 Å (1,000–75,000 g mol^{-1}) and Wyatt Optilab T-rEx

differential refractometer (λ = 658 nm, 40 °C). A flow-rate of 0.5 mL min^{-1} was used and samples were dissolved in THF (ca. 2 mg mL^{-1}). Molecular weights were determined in comparison to polystyrene standards. Absorption spectra were obtained in THF on a Varian Cary 5000 UV-Vis-near-IR spectrophotometer using a 1 cm quartz cuvette. Solution state fluorescence and excitation spectra were obtained in THF on a Horiba scientific Fluoromax-4 spectrofluorometer using a 1 cm quartz cuvette. MALDI-TOF mass spectra were obtained on Bruker Autoflex MALDI-TOF. Dithranol was used as the matrix. The solutions of the sample (~1 mg/mL) and matrix (20 mg/mL) were mixed in the ratio of between 1:1 to 1:10 and 1 μl of final mixture was deposited onto the sample target. MALDI mass spectra were acquired in the positive linear mode and the spectra normally represent the average of ca. 2000 lasershots.

5.4.3 Synthesis

5.4.3.1 Preparation of 5.1

A Schlenk flask was charged with phenyldichlorophosphine (0.56 g, 3.1 mmol), 1,4 diethynyl 2,5 di-*n*-hexylbenzene (0.69 g, 2.4 mmol), 2,7-diethynyl-9,9-di-*n*-hexyl-9*H*-fluorene (0.30 g, 0.78 mmol), triethylamine (2.6 mL, 19 mmol), nickel (II) acetylacetonate (20 mg, 78 μmol) and toluene (10 mL) (concentration of reaction mixture = 0.24 M). The reaction mixture was heated to 85 °C and was stirred vigorously for 16 h. After this time volatiles were removed under reduced pressure. THF (2.0 mL) was added to the deep red solid to make a viscous liquid. To this residue was added 200 mL of degassed methanol to precipitate the polymer. The solvent was removed and the precipitation method was repeated with ethanol (200 mL degassed ethanol into 2 mL THF solution of polymer). Finally the polymer residue was dissolved in THF (*ca.* 5 mL)

and 200 mL methanol was added, leaving a deep red solid that was dried under vacuum overnight. Yield = 0.84 g (64%).

$^{31}P\{^{1}H\}$ NMR (121 MHz, $CDCl_3$): δ –59.6 (br, 1 P), –60.0 (7 P), –60.5 (8 P); ^{1}H NMR (400 MHz, $CDCl_3$): δ 8.02-7.80 (br, 1H, aryl H), 7.68-7.61 (br, 1H, aryl H) 7.57-7.36 (br, 3H, aryl H) 7.37-7.29 (br, 2H, aryl H), 3.31 (s, C≡C*H* end group), 2.79-2.60 (br, 2H, ^{Ph}C-CH_2,), 2.00-1.88 (br, ^{Flu}C-CH_2,), 1.67-1.46 (br, 2H, CH_2), 1.40-1.16 (br, 8H, CH_2), 1.12-0.95 (br, 4H), 0.94-0.65 (br m, 4.5H, CH_3), 0.61-0.49 (br, 1.5H CH_3). $^{13}C\{^{1}H\}$ NMR (151 MHz, $CDCl_3$): δ 151.1 (Fluorene aryl C) 142.9 (aryl C), 141.2 (aryl C) 132.4 (br, aryl C), 131.3 (aryl C), 129.6 (aryl C), 128.8 (br, aryl C), 126.3 (aryl C), 122.5 (br, P-C≡C-C_{Ar}), 122.2 (br, P-C≡C-C_{Ar}), 121.3 (br, P-C≡C-C_{Ar}), 122.0 (br, P-C≡C-C_{Ar}), 107.3 (br, P-C≡*C*-C_{Ar}), 104.9 (br, P-C≡*C*-C_{Ar}), 87.8 (br, m, P-*C*≡C-C_{Ar}), 83.0 ($^{Flu}C_{Ar}$-*C*≡CH) 82.2 (s, $^{Ph}C_{Ar}$-*C*≡CH), 81.8 (s, $^{Ph}C_{Ar}$-C≡*C*H), 55.3 ($^{Flu}C_{Ar}$-*C*$(CH_2)_2$) , 40.3 (*C*H_2), 34.0 (*C*H_2) 33.8 (*C*H_2), 31.6 (*C*H_2), 31.5 (*C*H_2), 30.6 (*C*H_2), 29.6 (*C*H_2), 29.1 (*C*H_2), 23.6 (*C*H_2), 22.6 (*C*H_2), 14.1 (*C*H_3). GPC (vs. Polystyrene): M_n = 3,600 g mol^{-1}, Đ = 2.2.

5.4.3.2 Preparation of 5.1·O

To a rapidly stirred solution of a sample of **5.1** (0.16 g, 0.37 mmol P, M_n = 3,600 g mol^{-1}, Đ = 2.2) in CH_2Cl_2 (50 mL), H_2O_2 (20% in water, 20 mL) was added at room temperature. The reaction was stirred rigorously for 1 h, at which time a $^{31}P\{^{1}H\}$ NMR spectrum of the reaction mixture was taken and all the starting material had been consumed. The organic layer was taken and the solvent was removed *in vacuo* to leave a dark red solid. This solid was dried in a vacuum oven for 3 h. Yield 0.14 g (87%).

$^{31}P\{^{1}H\}$ NMR (121 MHz, $CDCl_3$): δ –18.6 (br, 1 P), –19.0 (br, 4.7 P), –19.5 (br, 6.2 P); ^{1}H NMR (600 MHz, $CDCl_3$): δ 8.09 (br, 2H, aryl H), 7.62 (br, 4H, aryl H) 7.47 (br, 3H, aryl H) 7.41 (br, 2H, ary; H), 3.38 (s, C≡C*H* end group), 2.70 (br, 2.5H, $^{Ph}C_{ipso}$-CH_2,), 1.96 (br, 0.80H, $^{Flu}CH_2$,), 1.56 (br, 2.40H), 1.14 (br m, 13H), 1.12-0.95 (br m, 4H), 0.84 (br m, 6H, CH_3), 0.55 (br, 2H CH_2).$^{13}C\{^{1}H\}$ NMR (151 MHz, $CDCl_3$): δ 151.4, (Fluorene aryl C), 144.2 (aryl C), 143.8 (aryl C), 143.0 (aryl C), 142.3 (aryl C), 133.4 (aryl C), 133.1 (aryl C), 132.8 (aryl C), 131.9 (aryl C), 131.2 (aryl C), 130.3 (aryl C), 130.2 (aryl C), 130.2 (aryl C), 130.1 (aryl C), 127.0 (aryl C), 126.5 (aryl C), 124.2 (aryl C), 121.4 (aryl C), 120.5 (aryl C), 120.0 (aryl C), 119.8 (aryl C). 119.0 (m, aryl C) 104.7 (P-C≡*C*-C_{Ar}), 101.8 (P-C≡*C*-C_{Ar}), 89.1 (br, P-*C*≡C-C_{Ar}), 87.8 (br), 86.6 (br, P-*C*≡C-C_{Ar}), 84.2 (br, $^{Flu}C_{Ar}$-*C*≡CH) 82.9 ($^{Ph}C_{Ar}$-C≡*C*H), 81.6 ($^{Ph}C_{Ar}$-*C*≡CH), 55.5 (^{Flu}C-CH_2), 40.0 (*C*H_2), 34.0 (*C*H_2) 33.8 (*C*H_2), 33.6 (*C*H_2), 31.4 (*C*H_2), 31.3 (*C*H_2), 30.6 (*C*H_2), 30.5 (*C*H_2), 30.2 (*C*H_2), 29.4 (*C*H_2), 28.9 (*C*H_2), 23.5 (*C*H_2), 22.4 (*C*H_2), 13.86 (*C*H_3), 13.82 (*C*H_3). GPC (*vs*. Polystyrene, THF): M_n = 3,200 g mol^{-1}, Đ = 1.7.

5.4.3.3 Preparation of 5.1·AuCl

This reaction was carried out in a glovebox. THF (10 mL) was added to a vial containing **5.1** (60 mg, 140 μmol) and the mixture was stirred at RT until the polymer had dissolved (*ca*. 30 min). To the solution was added Au(tht)Cl (49 mg, 150 μmol) and the solution was stirred at RT for 30 min. After this time a $^{31}P\{^{1}H\}$ NMR spectrum was taken which revealed complete consumption of the starting material and the presence of a two new signals at —28.0 ppm and —28.2 ppm. The reaction vessel was removed from the glovebox and the solvent was removed under reduced pressure, leaving an orange residue. To this residue was added THF (1 mL) and the polymer was

precipitated into degassed methanol (25 mL). The resulting orange solid was isolated and dried under reduced pressure at RT for 2 h. Yield 92 mg (99%).

$^{31}P\{^{1}H\}$ NMR (162 MHz, $CDCl_3$) δ –28.0 (br), 28.2 (br); ^{1}H NMR (400 MHz, $CDCl_3$): δ 8.25-7.97 (br, 2H, aryl H), 7.80-7.51 (br, 3H, aryl H), 7.49-7.30 (br, 2H, aryl H) 3.58-3.25 (br, 1H, C*H*$_2$), 2.79-2.50 (br, 2H, C*H*$_2$), 2.31-1.78 (br, 2H, C*H*$_2$), 1.68-1.43 (br, 2H, C*H*$_2$) 1.36-0.94 (br, 12H, C*H*$_2$+C*H*$_3$), 0.95-0.33 (br, 10H, C*H*$_2$+C*H*$_3$); $^{13}C\{^{1}H\}$ NMR (151 MHz, $CDCl_3$): δ 151.8-151.3 (Fluorene aryl C), 144.3 (aryl C), 143.9 (aryl C), 143.3 (aryl C), 142.5 (aryl C), 133.8-132.7 (m, aryl C), 132.0 (aryl C), 129.9-129.3 (m, aryl C), 127.0 (aryl C), 122.0-121.3 (m, aryl C), 120.7 (aryl C), 119.5-118.8 (m, aryl C), 107.9-105.9 (br, P-C≡*C*-C$_{Ar}$), 83.2 (P-*C*≡C-C$_{Ar}$), 81.7 (C≡*C*H), 55.7 (^{Flu}*C*-CH$_2$), 40.1(*C*H$_2$), 34.1(*C*H$_2$), 33.7(*C*H$_2$), 31.6(*C*H$_2$), 30.7 (*C*H$_2$), 30.3 (*C*H$_2$), 29.6 (*C*H$_2$), 29.1 (*C*H$_2$), 23.7 (*C*H$_2$), 22.5 (*C*H$_2$), 14.0 (*C*H$_3$). GPC (*vs*. Polystyrene, THF): M_n = 5,000 g mol^{-1}, Đ = 3.12.

5.4.3.4 Attempted preparation of 5.1·Au(III) polymer

THF (10 mL) was added to a vial containing **5.1** (65 mg, 140 μmol) and the mixture was stirred at RT until the polymer had dissolved (*ca*. 30 min). To this solution was added $HAuCl_4 \cdot 3H_2O$ (55 mg, 140 μmol), and the mixture was stirred at RT for 20 min. After this time a $^{31}P\{^{1}H\}$ NMR spectrum was taken which revealed complete consumption of the starting material and the presence of a two new signals at –27 and –22 ppm. The reaction vessel was removed from the glovebox and the solvent was removed. Unfortunately the red solid residue that was isolated could not be dissolved in organic solvents (THF, DCM, DMSO, toluene etc). Yield 116 mg (99%).

$^{31}P\{^{1}H\}$ NMR (162 MHz, $CDCl_3$) δ –22 (br), –27 (br).

5.4.3.5 Preparation of 5.2

A solution of phenyldichlorophosphine (3.6 g, 20 mmol) in toluene (50 mL) was added to a mixture of nickel (II) acetylacetonate (0.16 g, 0.60 mmol) and phenylaceylene (5.1 g, 5.5 mL, 50 mmol) in toluene (50 mL). Triethylamine (12 g, 17 mL, 0.12 mol) was subsequently added to the reaction mixture. The reaction mixture was stirred vigorously at 80 °C. The reaction was monitored after 2 h by ^{31}P NMR spectroscopy that revealed a single resonance at –60 ppm. The solvent was removed *in vacuo* leaving a dark yellow-red coloured solid. To the solid was added dichloromethane (3 × 30 mL) and the suspension was filtered, leaving a brown residue. This brown residue was redissolved in dichloromethane and run through a silica plug. The solvent was removed to leave a yellow coloured crystalline solid that matched literature characterization.[245] Yield 3.4 g (55%).

^{31}P NMR (122 MHz, $CDCl_3$): δ –60 (t, J = 8 Hz); ^{1}H NMR ($CDCl_3$, 300 MHz): δ 7.97-7.88 (m, 2H), 7.61-7.32 (m, 13H); $^{13}C\{^{1}H\}$ NMR ($CDCl_3$, 75 MHz): δ 133.3 (aryl C), 132.3 (aryl C), 132.0 (aryl C), 129.5 (aryl C), 122.8 (d, J = 8 Hz, P-C≡C-C_{Ar}), 106.3 (d, J = 7 Hz, P-C≡C-C_{Ar}), 82.8 (d, J = 3 Hz, P-C≡C-C_{Ar}).

5.4.3.6 Preparation of 5.2·AuCl

Compound **5.2** (0.10 g, 0.32 mmol) and chloro(tetrahydrothiophene)gold(I) (0.11 g, 0.33 mmol) were added to a vial in the glovebox. To this vial was added 5 ml of THF and the resulting solution was stirred at room temperature for 10 min. The reaction mixture was taken outside of the glovebox and the solvent was removed under vacuum. Yield = 0.16 g (91%). A crystal suitable for X-ray analysis was grown from a saturated $CDCl_3$ solution.

^{31}P NMR (121 MHz, $CDCl_3$): δ –28 (t, *J* = 17 Hz). ^{1}H NMR (300 MHz, $CDCl_3$): δ 8.20-7.91 (br, 2H, aryl H) 7.76-7.31 (br, 13H, aryl H). $^{13}C\{^{1}H\}$ NMR (101 MHz, $CDCl_3$): δ 133.0 (aryl C), 132.7 (aryl C), 132.6 (aryl C), 131.1 (aryl C), 129.7 (aryl C), 129.5 (aryl C), 128.7 (aryl C), 119.7 (d, *J* = 3.5 Hz, P-C≡C-C_{Ar}), 108.4 (d, *J* = 26 Hz, P-C≡C-C_{Ar}), 76.6 (d, *J* = 135 Hz, P-C≡C-C_{Ar}). MS (70 eV): 309 (58, 69, 14) $[M–AuCl]^+$, 233 (51, 9) $[AuCl]^+$. Elem. Anal. (%) calcd for $C_{22}H_{15}PAuCl$: C 48.69, H 2.79; found C 48.61 H 3.05.

General Procedure for Sensing Tests involving polymer 5.1.

A stock THF solution of **5.1** (c = 20 μM) was prepared in a glovebox. 3 mL aliquots (60 nmol) were taken from this stock solution and 75 μL of a EtOH solution (c = 8.0 mM, 600 nmol, 10 equiv) of metal ion were added to these aliquots outside of the glovebox. Each reaction was swirled initially and left for 10 min without stirring. The fluorescence spectra were taken after this time using 353 nm as an excitation wavelength. The metal salts used were $NaNO_3$ KNO_3, $Fe(NO_3)_3·9H_2O$, $Ni(NO_3)_2·6H_2O$, $Cu(OAc)_2$, $YNO_3·6H_2O$, $RuCl_3$, $[Rh(cod)Cl]_2$, $PdCl_2$, $Pd(PPh_3)_2Cl_2$, $Pd(OAc)_2$, $Pd(PPh_3)_4$, $AgNO_3$, $Cd(NO_3)·4H_2O$, $BaNO_3$, $W(CO)_5MeCN$, $[Ir(cod)Cl]_2$, $PtCl_2$, K_2PtCl_4, Au(tht)Cl, $HAuCl_4·3H_2O$, $HgCl_2$, $Hg_2(NO_3)_2$, $Hg(NO_3)_2·H_2O$, $Pb(NO_3)$, $Bi(NO_3)_3·5H_2O$. Due to solubility $PdCl_2$, $Pd(PPh_3)_2Cl_2$, $PtCl_2$, Au(tht)Cl, $[Rh(cod)Cl]_2$, $RuCl_3$, $[Ir(cod)Cl]_2$ $Pd(PPh_3)_4$ and $W(CO)_5MeCN$ were added as THF solutions and $YNO_3·6H_2O$, $BaNO_3$ and K_2PtCl_4, were added as an aqueous solutions.

5.4.3.7 General Procedure for Sensing Tests reactions involving model compound 5.2

These experiments were carried out in a golvebox. Compound **5.2** (100 mg, 0.32 mmol) was dissolved in THF (5 mL). To this solution was added a metal salt or complex (0.35 mmol, 1.1

equiv) and the solution was stirred for 20 min. After this time a $^{31}P\{^{1}H\}$ NMR spectrum was taken of the reaction mixture. The chemical shifts observed are in Table 5.1

Table 5.1: $^{31}P\{^{1}H\}$ NMR (121MHz,THF): Chemical shifts of products of 5.2 + metal salt or complex

Metal Used	$^{31}P\{^{1}H\}$ NMR δ
No analyte (control)	–60
$NaNO_3$	–60[a]
KNO_3	–60[a]
$Ca(NO_3)_2 \cdot 4H_2O$	–60[a]
$Fe(NO_3)_3 \cdot 9H_2O$	–20 (br)[b]
$Ni(NO_3)_2 \cdot 6H_2O$	–60 (br)[b]
$Cu(OAc) \cdot H_2O$	–60 major, -20 (br)[b] minor
$Cu(NO_3)_2 \cdot 2.5H_2O$	–40 (br)[b]
$[Rh(cod)Cl]_2$[c]	–20 (minor), –16 (major), –14 (major)
$Pd(PPh_3)_4$	9, –44
$AgNO_3$	–51
$Cd(NO_3)_2 \cdot 4H_2O$	–60[a]
$PtCl_2$	–36[d]
Au(tht)Cl	–28
$HAuCl_4 \cdot 3H_2O$	–44, –24
$Hg_2(NO_3)_2 \cdot H_2O$	–21
$Hg(NO_3)_2$	–21, –49 (br)
$Pb(NO_3)_2$	–60[a]
$Bi(NO_3)_3 \cdot 5H_2O$	–60[a]

[a]No reaction deemed, [b]Broad signals potentially due to paramagnetic complex formed with first row transition metal. [c]0.55 equiv added.[d] Satellite Pt-P coupling observed (J = 3800Hz).

Chapter 6: Conclusion and Future Work

6.1 Introduction

The incorporation of phosphorus atoms into polymers can give rise to materials with intriguing properties due to the functionality of the phosphine lone pair. This thesis has focused on the synthesis of novel phosphine polymers with photophysically active substituents in order to investigate their emissive properties as the phosphine environment is modified. Prior to this work, limited examples of such materials were known, and most examples were non- or very weakly fluorescent. Crucially, many of the polymers presented in this thesis are fluorescent (some even in the solid state) and their emissive properties are dependent on the chemical environment at phosphorus. From this work, the potential of P-containing polymers as sensory materials may soon be realized.

6.2 Poly(methylenephosphine)s (PMPs)

Chapter 2 described the synthesis and characterization of three phosphaalkenes bearing UV-active substituents (**2.1a-2.1c**) and the anionic polymerization of two of these to make PMPs **2.2a** and **2.2b**. The chemistry of the C-naphthyl-containing PMP (**2.2a**) was investigated by functionalizing the phosphorus lone pair to make four different derivatives; **2.2a**·O, **2.2a**·S, **2.2a**·BH_3 and **2.2a**·AuCl. The photophysics of these materials were investigated, and it was discovered that only the oxidized polymer (**2.2a**·O) was emissive.

A drawback of the work detailed in Chapter 2 was that the emission exhibited from **2.2a**·O occurred in the UV region and was therefore invisible to the naked eye. The work presented in Chapter 3 featured a C-pyrenyl PMP, **3.2**. The incorporation of pyrene groups within the

polymer gave rise to a polymer that showed "turn on" fluorescence upon oxidation (Figure 6.1), similar to **2.2a**, however, the emission was blue in colour ($\Phi = 0.05$).

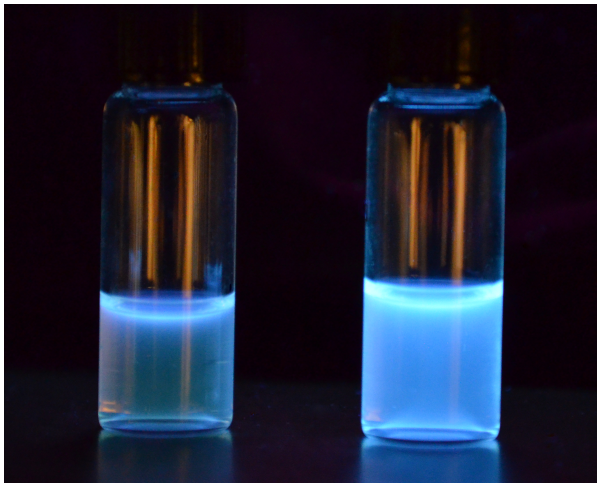

Figure 6.1: Polymers 3.2 (left) and 3.2·O (right) under a UV light ($\lambda = 365$ nm)

The emissive properties of **3.2** were measured as the polymer was partially oxidized by the substoichiometric amounts of H_2O_2. It was observed that an increase in fluorescence intensity was only observed upon very high degrees of oxidation. The presence of phosphorus lone pairs within the polymer quenched the emission from the pyrene substituents through intramolecular photo-induced electron transfer. Polymer **3.2**·O also emitted green-blue light in the solid state, which was assigned to emission from pyrene excimers.

The sensory behaviour of PMPs is of interest and may be investigated further. It appears that the fluorophore and the phosphorus atoms do not need to be adjacent to each other within the polymer for fluorescence quenching to occur. It therefore may be possible to incorporate large fluorophores into a PMP without the need to make challenging new phosphaalkenes. A copolymer of MesP=CPh_2 with a highly fluorescent vinyl polyaromatic may provide a more facile route to PMP polymers (Scheme 6.1) and may fashion materials which still exhibit sensory behaviour. This strategy has multiple benefits. Firstly, MesP=CPh_2 can be synthesized and purified on a multi-gram scale and its polymerization is far more understood compared with that

of **2.1a, 2.1b** and **3.1**. Secondly, vinyl-substituted polyaromatics are straightforward to synthetize and in some cases, such as 2-vinylnapthalene, are commercially available. The polymerization of some vinyl polyaromatics have previously been reported and is well understood.[329, 330] The fluorescence/sensing properties of the polymer could be probed by varying comonomer ratios (and therefore the amount of phosphine moieties in the polymer) or by making block or random copolymers. It should be possible to manipulate the physical properties (for example T_g or T_m) of such materials by the incorporation of other comonomers (e.g. acrylate or isoprene) within the polymer. The coordination chemistry of PMPs is also largely unexplored. Should these polymers be made in large quantities, the chemistry and photophysical responses to more analytes can be examined.

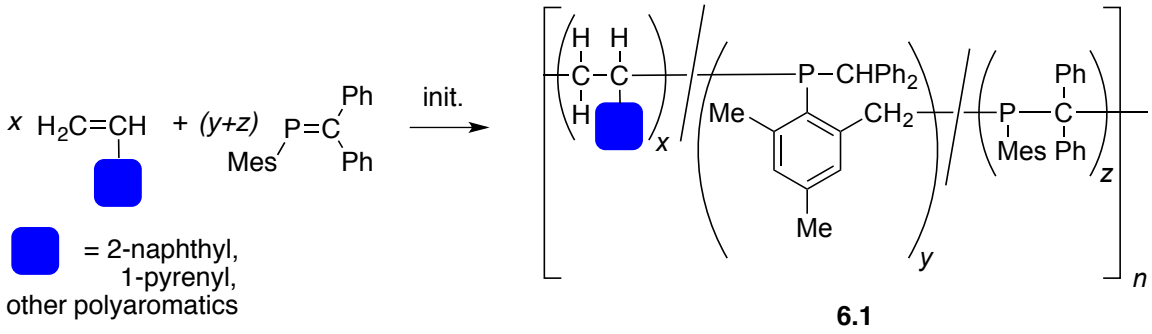

6.1

Scheme 6.1. Synthesis of a PMP copolymer with fluorescent derivatives

6.3 Poly(*p*-phenylenediethynylene phosphine)s (PPYPs)

Chapter 4 presented the synthesis and photophysical properties of the first examples of PPYPs, a novel type of phosphorus-containing macromolecule. Utilizing a nickel catalyzed P-C bond forming reaction, polymers **4.1a-4.1e** were synthesized (Scheme 6.2). Polymer **4.1a** was isolated as a red/brown dusty solid, insoluble in organic solvents, whereas **4.1b-4.1e** were solution processable. With reference of the absorption spectra and crystal structures of model compounds, it was determined that **4.1b-4.1e** and their corresponding oxidized polymers have electronic characteristics that are consistent with a degree of electronic communication throughout the

backbone. Remarkably, polymers **4.1b-4.1e** were non-fluorescent in solution, however upon oxidation blue coloured emission was observed in each case in dilute solutions. The wavelength of emission **4.1b** was substantially red-shifted by increasing the THF solution concentration or by the addition of a non-solvent that encouraged emission from an aggregation state. Each of the oxidized polymers **4.1b**·O-**4.1e**·O also exhibited green/yellow emission in the solid state.

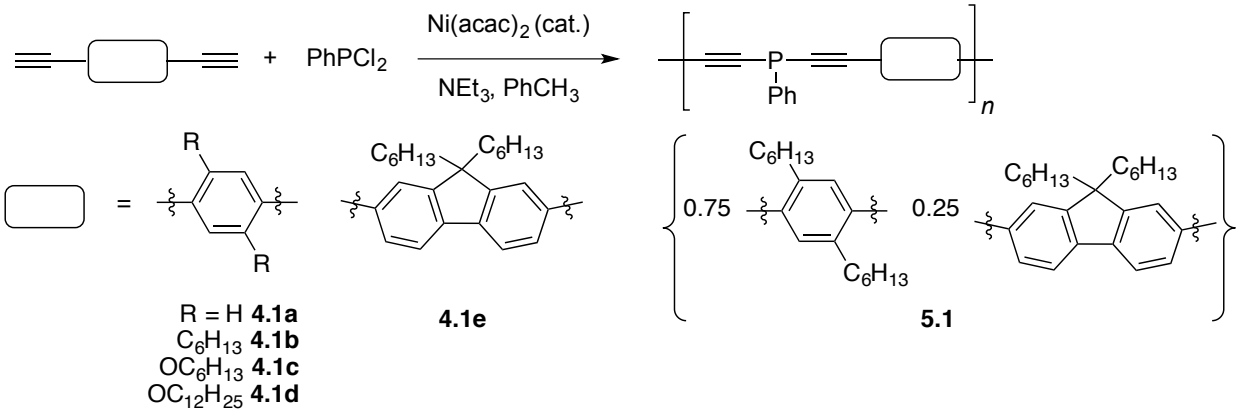

Scheme 6.2. PPYPs presented in this thesis

Chapter 5 presented an initial investigation into the use of PPYPs to sense metal analytes. Polymer **5.1** was synthesized as a more soluble version of **4.1e** as its structure incorporated 2 different di-yne linkers. Turn on fluorescence was observed when Au(I), Au(III), Hg(I) and Hg(II) ions were added to a solution of **5.1** whereas other metal ions did not yield such a response.

The discovery of PPYPs in this thesis has opened a new avenue of phosphine materials and there are many potential directions for further investigation. An obvious first direction would be to further explore the sensing capabilities of PPYPs. Given the growing number of gold-based drugs[331-333] in the pharmaceutical industry and the inability for traditional analytical techniques to detect gold *in vivo*, fluorescence based sensors for gold ions are highly desirable,[297] especially for bio-imaging applications.[334] Intriguingly, molecular alkynyl phosphine gold complexes have

been investigated for their biological properties[301, 318, 324, 335] and have shown potential as chemotherapeutics. Bioinorganic chemistry is beyond the scope of investigation in our research group but the compounds and polymers presented in this thesis may be of interest to medicinal chemists for their biological properties or as biosensors.

The PPYPs introduced in this work exhibited blue fluorescence in the solution state with moderate quantum yields upon oxidation (Φ up to 0.30). Although these efficiencies are amongst the highest for phosphorus-containing polymers, it is of interest to develop PPYPs with higher quantum yields for their use as chemosensors. Derivatives that undergo emission with alternative colours may be useful for optical devices (such as OLEDs, for example). There are a couple of obvious strategies to accomplish these goals. The first would involve the incorporation of different di-yne linkers that have high quantum yields. PPYPs incorporating 2,1,3-benzothiadiazole or BODIPY substituents (such as in **6.2** or **6.3,** Scheme 6.3) would likely be highly fluorescent and exhibit colours from blue to yellow. The high quantum yields of the di-yne monomers (up to 0.92) suggest that the resulting PPYPs may be highly emissive.[336, 337] An alternative strategy would be to synthesize an oligomeric PPE polymer with alkyne end groups and use the nickel coupling strategy (used to make **4.1a-4.1e** and **5.1**) as the method to incorporate phosphine moieties within the polymer. This would make a polymer with the structure of **6.4**. This route would distribute P atoms sparsely within the polymer but hopefully the materials may exhibit sensor-like behaviour due long range intramolecular quenching from P lone pairs within the polymer. The emission colour of the resulting polymers could also be varied by either the length of- or by the identity of the substituents on the oligomeric PPE backbone.

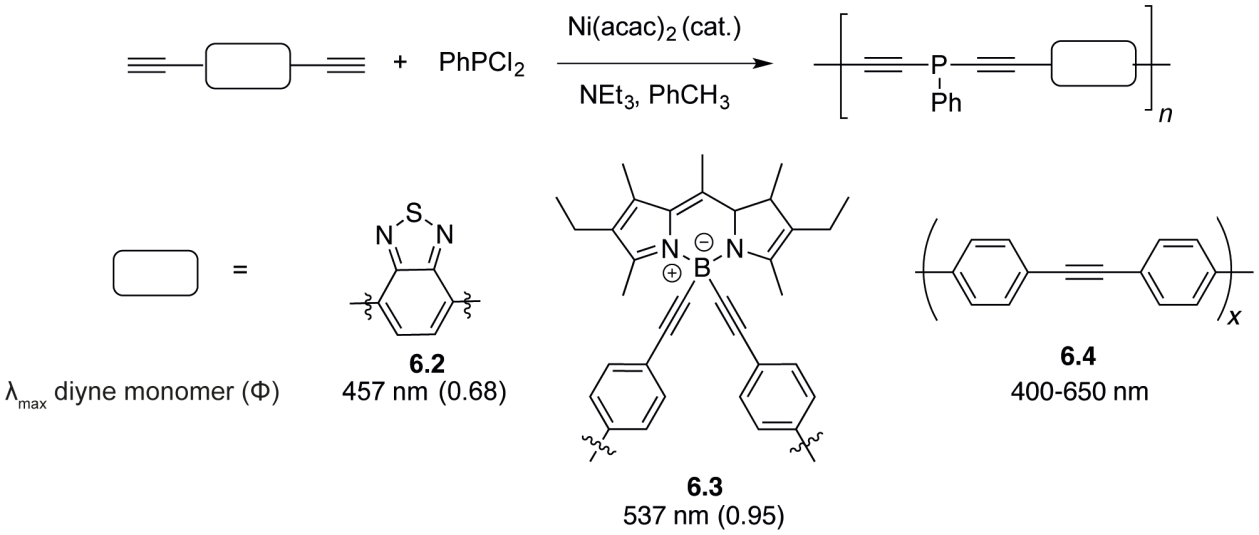

Scheme 6.3. Future PPYP targets featuring dialkyne linkers that have high quantum yields.

Another avenue of exploration within PPYPs is the chemistry of the alkyne groups within the polymer. Preliminary experiments have been performed which show that Br_2 can be added across the alkyne bonds of the polymer. It may be possible to reduce the alkynes to alkenes (or alkanes) with standard conditions (H_2/Pd). Alternatively, it has recently been reported that the reduction of alkynyl phosphines to alkenyl phosphines can be achieved by zirconium catalysis using a stoichiometric amount of triethylaluminium.[338] While these transformations are of interest, the resulting materials may have limited conjugation and thus may be less fluorescent. This is because the π framework throughout the polymer is disrupted.

Instead of reducing the alkynes within PPYPs, the chemistry of the phosphinoalkyne moieites could be explored. A few reactions have appeared in the literature involving phosphinoalkynes where a conjugated system is maintained. One intriguing example is the synthesis of phospholes via the 1,1-carboboration of bis(alkynyl)phosphines (Scheme 6.4a).[237] The reaction of $B(C_6F_5)_3$ with the bis alkyne results in the installation of a borane on the 3-position of the phosphole, which can be reacted further using a Suzuki coupling to make a new

C-C bond. If this reaction can be replicated with a PPYP (Scheme 6.4b), the resulting polyphospholes would be of interest for their electronic and photophysical properties.[194, 339]

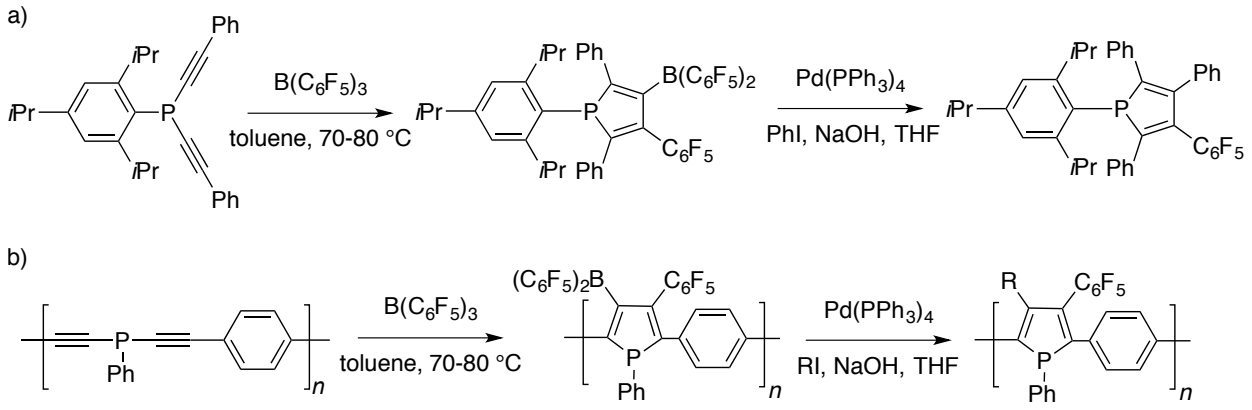

Scheme 6.4a). 1,1 carboration route to phospholes b) Proposed analogous carboration reaction with PPYP to form phosphole-containing polymers.

6.4 Concluding remarks

The work contained in this thesis has increased the knowledge base of organophosphorus polymer chemistry. While the field is far from mature, it is the hope that the fascinating properties of these materials will ignite the imagination of future researchers and push this field to ever more fruitful levels.

As you have reached the end of this, I hope you got as excited as I did, in between the blood, sweat and tears of my Ph. D.

References

(1) Baekeland, L. H. Method of Making Insoluble Products of Phenol and Formaldehyde. U.S. Patent 942699, Jul 13, 1907.

(2) Neufeld, L.; Stassen, F.; Sheppard, R.; Gilman, T. *The New Plastics Economy: Rethinking the future of plastics*; Research agenda for the World Economic Forum: Cologny, Switzerland, January 2016.

(3) Chanda, M.; Roy, S. K. Industrial Polymers, Specialty Polymers, and their Applications; CRC Press: Boca Raton, FL, 2008;

(4) Allcock, H. R. *Chemistry and Applications of Polyphosphazenes*, John Wiley & Sons: Hoboken, NJ, 2002.

(5) Mark, J. E.; Schäfer, D. W.; Lin, G. *The Polysiloxanes*, Oxford University Press: New York, 2015.

(6) Mark, J. E.; Allcock, H. R.; West, R. *Inorganic Polymers*, 2nd ed.; Oxford University Press: New York, 2005.

(7) Ma, J.; Li, S.; Jiang, Y. *Macromolecules* **2002,** *35*, 1109-1115.

(8) Shirakawa, H.; Louis, E. J.; MacDiarmid, A. G.; Chiang, C. K.; Heeger, A. J. *J. Chem. Soc., Chem. Commun.* **1977**, 578-580.

(9) Adamec, V.; Calderwood, J. H. *J. Phys. D: Appl. Phys.* **1981,** *14*, 1487.

(10) Saxman, A. M.; Liepins, R.; Aldissi, M. *Prog. Polym. Sci.* **1985,** *11*, 57-89.

(11) The Nobel Prize in Chemistry, 2000. http://www.nobelprize.org/nobel_prizes/chemistry/laureates/2000/ (23rd May 2017),

(12) Friend, R. H.; Gymer, R. W.; Holmes, A. B.; Burroughes, J. H.; Marks, R. N.; Taliani, C.; Bradley, D. D. C.; Santos, D. A. D.; Bredas, J. L.; Logdlund, M.; Salaneck, W. R. *Nature* **1999,** *397*, 121-128.

(13) De Paoli, M.-A.; Nogueira, A. F.; Machado, D. A.; Longo, C. *Electrochim. Acta* **2001,** *46*, 4243-4249.

(14) Jiang, H.; Taranekar, P.; Reynolds, J. R.; Schanze, K. S. *Angew. Chem., Int. Ed.* **2009,** *48*, 4300-4316.

(15) Burroughes, J. H.; Bradley, D. D. C.; Brown, A. R.; Marks, R. N.; Mackay, K.; Friend, R. H.; Burns, P. L.; Holmes, A. B. *Nature* **1990,** *347*, 539-541.

(16) Gustafsson, G.; Cao, Y.; Treacy, G. M.; Klavetter, F.; Colaneri, N.; Heeger, A. J. *Nature* **1992,** *357*, 477-479.

(17) Li, G.; Shrotriya, V.; Huang, J.; Yao, Y.; Moriarty, T.; Emery, K.; Yang, Y. *Nat. Mater.* **2005,** *4*, 864-868.

(18) Kim, Y. H.; Sachse, C.; Machala, M. L.; May, C.; Müller-Meskamp, L.; Leo, K. *Adv. Funct. Mater.* **2011,** *21*, 1076-1081.

(19) Marks, R. N.; Halls, J. J. M.; Bradley, D. D. C.; Friend, R. H.; Holmes, A. B. *J. Phys. Condens. Matter* **1994,** *6*, 1379.

(20) Huang, J.; Virji, S.; Weiller, B. H.; Kaner, R. B. *Chem. Eur. J.* **2004,** *10*, 1314-1319.

(21) Gao, J. B.; Sansinena, J. M.; Wang, H. L. *Synth. Met.* **2003,** *135*, 809-810.

(22) Martins, C. R.; De Paoli, M.-A. *Eur. Polym. J.* **2005,** *41*, 2867-2873.

(23) Soto-Oviedo, M. A.; Araújo, O. A.; Faez, R.; Rezende, M. C.; De Paoli, M.-A. *Synth. Met.* **2006,** *156*, 1249-1255.

(24) Trivedi, D. C.; Dhawan, S. K. *Polymer. Adv. Tech.* **1993,** *4*, 335-340.

(25) Wang, D.-W.; Li, F.; Zhao, J.; Ren, W.; Chen, Z.-G.; Tan, J.; Wu, Z.-S.; Gentle, I.; Lu, G. Q.; Cheng, H.-M. *ACS Nano* **2009,** *3*, 1745-1752.
(26) Wang, Z.-L.; Guo, R.; Li, G.-R.; Lu, H.-L.; Liu, Z.-Q.; Xiao, F.-M.; Zhang, M.; Tong, Y.-X. *J. Mater. Chem.* **2012,** *22*, 2401-2404.
(27) Ge, J.; Cheng, G.; Chen, L. *Nanoscale* **2011,** *3*, 3084-3088.
(28) Bunz, U. H. *Chem. Rev.* **2000,** *100*, 1605-1644.
(29) Montali, A.; Smith, P.; Weder, C. *Synth. Met.* **1998,** *97*, 123-126.
(30) Pourghaz, Y.; Dongare, P.; Thompson, D. W.; Zhao, Y. *Chem. Commun.* **2011,** *47*, 11014-11016.
(31) Wosnick, J. H.; Mello, C. M.; Swager, T. M. *J. Am. Chem. Soc.* **2005,** *127*, 3400-3405.
(32) Cumming, C. J. Explosives Detection based on Amplifying Fluorescence Polymers. In *Trace Chemical Sensing of Explosives*; Woodfin, R. L., Ed.; Wiley: Hoboken, NJ, 2006; pp 195-210.
(33) Lucht, B. L.; St Onge, N. O. *Chem. Commun.* **2000**, 2097-2098.
(34) Jin, Z.; Lucht, B. L. *J. Organomet. Chem.* **2002,** *653*, 167-176.
(35) Jin, Z.; Lucht, B. L. *J. Am. Chem. Soc.* **2005,** *127*, 5586-5595.
(36) Katsyuba, S. A.; Burganov, T. I. *Phosphorus, Sulfur Silicon Relat. Elem.* **2016,** *191*, 417-422.
(37) Inagaki, S.; Yoshikawa, K.; Hayano, Y. *J. Am. Chem. Soc.* **1993,** *115*, 3706-3709.
(38) Gilheany, D. G. *Chem. Rev.* **1994,** *94*, 1339-1374.
(39) Power, P. P. *Chem. Rev.* **1999,** *99*, 3463-3504.
(40) Fischer, R. C.; Power, P. P. *Chem. Rev.* **2010,** *110*, 3877-3923.
(41) Orpen, A. G.; Connelly, N. G. *Organometallics* **1990,** *9*, 1206-1210.
(42) Wang, S.; Samedov, K.; Serin, S. C.; Gates, D. P. *Eur. J. Inorg. Chem.* **2016,** *2016*, 4144-4151.
(43) Wright, V. A.; Gates, D. P. *Angew. Chem., Int. Ed.* **2002,** *41*, 2389-2392.
(44) Wright, V. A.; Patrick, B. O.; Schneider, C.; Gates, D. P. *J. Am. Chem. Soc.* **2006,** *128*, 8836-8844.
(45) Smith, R. C.; Chen, X. F.; Protasiewicz, J. D. *Inorg. Chem.* **2003,** *42*, 5468-5470.
(46) Smith, R. C.; Protasiewicz, J. D. *J. Am. Chem. Soc.* **2004,** *126*, 2268-2269.
(47) Schäfer, B.; Öberg, E.; Kritikos, M.; Ott, S. *Angew. Chem., Int. Ed.* **2008,** *47*, 8228-8231.
(48) Geng, X.-L.; Hu, Q.; Schäfer, B.; Ott, S. *Org. Lett.* **2010,** *12*, 692-695.
(49) Geng, X.-L.; Ott, S. *Chem. Eur. J.* **2011,** *17*, 12153-12162.
(50) Ghassemi, H.; McGrath, E. *Polymer* **1997,** *38*, 3139-3143.
(51) Chen, X. T.; Sun, H.; Tang, X. D.; Wang, C. Y. *J. Appl. Polym. Sci.* **2008,** *110*, 1304-1309.
(52) Shao, S. Y.; Ding, J. Q.; Ye, T. L.; Xie, Z. Y.; Wang, L. X.; Jing, X. B.; Wang, F. S. *Adv. Mater.* **2011,** *23*, 3570-3574.
(53) Han, L. B.; Huang, Z. X.; Matsuyama, S.; Ono, Y.; Zhao, C. Q. *J. Polym. Sci. A Polym. Chem.* **2005,** *43*, 5328-5336.
(54) Vanderark, L. A.; Clark, T. J.; Rivard, E.; Manners, I.; Slootweg, J. C.; Lammertsma, K. *Chem. Commun.* **2006**, 3332-3333.
(55) Naka, K.; Umeyama, T.; Nakahashi, A.; Chujo, Y. *Macromolecules* **2007,** *40*, 4854-4858.

(56) Duffy, M. P.; Delaunay, W.; Bouit, P. A.; Hissler, M. *Chem. Soc. Rev.* **2016,** *45*, 5296-5310.
(57) Mao, S. S. H.; Tilley, T. D. *Macromolecules* **1997,** *30*, 5566-5569.
(58) Morisaki, Y.; Aiki, Y.; Chujo, Y. *Macromolecules* **2003,** *36*, 2594-2597.
(59) Hay, C.; Fischmeister, C.; Hissler, M.; Toupet, L.; Réau, R. *Angew. Chem., Int. Ed.* **2000,** *39*, 1812-1815.
(60) Hay, C.; Hissler, M.; Fischmeister, C.; Rault-Berthelot, J.; Toupet, L.; Nyulászi, L.; Réau, R. *Chem. Eur. J.* **2001,** *7*, 4222-4236.
(61) Sebastian, M.; Hissler, M.; Fave, C.; Rault-Berthelot, J.; Odin, C.; Réau, R. *Angew. Chem., Int. Ed.* **2006,** *45*, 6152-6155.
(62) de Talance, V. L.; Hissler, M.; Zhang, L. Z.; Kárpáti, T.; Nyulászi, L.; Caras-Quintero, D.; Bäuerle, P.; Réau, R. *Chem. Commun.* **2008**, 2200-2202.
(63) Baumgartner, T.; Neumann, T.; Wirges, B. *Angew. Chem., Int. Ed.* **2004,** *43*, 6197-6201.
(64) Romero-Nieto, C.; Durben, S.; Kormos, I. M.; Baumgartner, T. *Adv. Funct. Mater.* **2009,** *19*, 3625-3631.
(65) Baumgartner, T.; Bergmans, W.; Karpati, T.; Neumann, T.; Nieger, M.; Nyulászi, L. *Chem. Eur. J.* **2005,** *11*, 4687-4699.
(66) Baumgartner, T.; Wilk, W. *Org. Lett.* **2006,** *8*, 503-506.
(67) Durben, S.; Dienes, Y.; Baumgartner, T. *Org. Lett.* **2006,** *8*, 5893-5896.
(68) Chen, R. F.; Zhu, R.; Fan, Q. L.; Huang, W. *Org. Lett.* **2008,** *10*, 2913-2916.
(69) Saito, A.; Matano, Y.; Imahori, H. *Org. Lett.* **2010,** *12*, 2675-2677.
(70) Matano, Y.; Ohkubo, H.; Honsho, Y.; Saito, A.; Seki, S.; Imahori, H. *Org. Lett.* **2013,** *15*, 932-935.
(71) Tsang, C. W.; Yam, M.; Gates, D. P. *J. Am. Chem. Soc.* **2003,** *125*, 1480-1481.
(72) Tsang, C. W.; Baharloo, B.; Riendl, D.; Yam, M.; Gates, D. P. *Angew. Chem., Int. Ed.* **2004,** *43*, 5682-5685.
(73) Gillon, B. H.; Gates, D. P. *Chem. Commun.* **2004**, 1868-1869.
(74) Noonan, K. J. T.; Gates, D. P. *Angew. Chem., Int. Ed.* **2006,** *45*, 7271-7274.
(75) Noonan, K. J. T.; Gates, D. P. *Macromolecules* **2008,** *41*, 1961-1965.
(76) Noonan, K. J. T.; Patrick, B. O.; Gates, D. P. *Chem. Commun.* **2007**, 3658-3660.
(77) Dugal-Tessier, J.; Dake, G. R.; Gates, D. P. *Angew. Chem., Int. Ed.* **2008,** *47*, 8064-8067.
(78) Dugal-Tessier, J.; Serin, S. C.; Castillo-Contreras, E. B.; Conrad, E. D.; Dake, G. R.; Gates, D. P. *Chem. Eur. J.* **2012,** *18*, 6349-6359.
(79) Serin, S. C.; Dake, G. R.; Gates, D. P. *Dalton Trans.* **2016,** *45*, 5659-5666.
(80) Gillon, B. H.; Patrick, B. O.; Gates, D. P. *Chem. Commun.* **2008**, 2161-2163.
(81) Noonan, K. J. T.; Feldscher, B.; Bates, J. I.; Kingsley, J. J.; Yam, M.; Gates, D. P. *Dalton Trans.* **2008**, 4451-4457.
(82) Noonan, K. J. T.; Gillon, B. H.; Cappello, V.; Gates, D. P. *J. Am. Chem. Soc.* **2008,** *130*, 12876-12877.
(83) Priegert, A. M.; Siu, P. W.; Hu, T. Q.; Gates, D. P. *Fire Mater.* **2015,** *39*, 647.
(84) Siu, P. W.; Serin, S. C.; Krummenacher, I.; Hey, T. W.; Gates, D. P. *Angew. Chem., Int. Ed.* **2013,** *52*, 6967-6970.

(85) Cumming, C. J.; Aker, C.; Fisher, M.; Fok, M.; Grone, M. J. l.; Reust, D.; Rockley, M. G.; Swager, T. M.; Towers, E.; Williams, V. *IEEE T. Geosci. Remote* **2001,** *39*, 1119-1128.
(86) Salinas, Y.; Martinez-Manez, R.; Marcos, M. D.; Sancenon, F.; Costero, A. M.; Parra, M.; Gil, S. *Chem. Soc. Rev.* **2012,** *41*, 1261-1296.
(87) Colton, R. J.; Russell, J. N. *Science* **2003,** *299*, 1324-1325.
(88) Kim, H. N.; Ren, W. X.; Kim, J. S.; Yoon, J. *Chem. Soc. Rev.* **2012,** *41*, 3210-3244.
(89) Tracey, M. P.; Pham, D.; Koide, K. *Chem. Soc. Rev.* **2015,** *44*, 4769-4791.
(90) Feng, X. L.; Liu, L. B.; Wang, S.; Zhu, D. B. *Chem. Soc. Rev.* **2010,** *39*, 2411-2419.
(91) Chen, X. Q.; Pradhan, T.; Wang, F.; Kim, J. S.; Yoon, J. *Chem. Rev.* **2012,** *112*, 1910-1956.
(92) Basabe-Desmonts, L.; Reinhoudt, D. N.; Crego-Calama, M. *Chem. Soc. Rev.* **2007,** *36*, 993-1017.
(93) Kim, H. N.; Guo, Z. Q.; Zhu, W. H.; Yoon, J.; Tian, H. *Chem. Soc. Rev.* **2011,** *40*, 79-93.
(94) McQuade, D. T.; Pullen, A. E.; Swager, T. M. *Chem. Rev.* **2000,** *100*, 2537-2574.
(95) Zhou, Q.; Swager, T. M. *J. Am. Chem. Soc.* **1995,** *117*, 12593-12602.
(96) Zhou, Q.; Swager, T. M. *J. Am. Chem. Soc.* **1995,** *117*, 7017-7018.
(97) Thomas, S. W.; Joly, G. D.; Swager, T. M. *Chem. Rev.* **2007,** *107*, 1339-1386.
(98) Fatah, A. A.; Arcilesi, R. D.; McClintock, J. A.; Lattin, C. H.; Helinski, M.; Hutchings, M. *Guide for the Selection of Explosives Detection and Blast Mitigation Equipment for Emergency First Responders;* Guide 105-07; Department of Homeland Security, U.S. Government Printing Office: Washington, DC, 2008.
(99) de Silva, A. P.; Gunaratne, H. Q. N.; Gunnlaugsson, T.; Huxley, A. J. M.; McCoy, C. P.; Rademacher, J. T.; Rice, T. E. *Chem. Rev.* **1997,** *97*, 1515-1566.
(100) *Phosphorus(III) Ligands in Homogeneous Catalysis: Design and Synthesis;* Karner, P. C. J., van Leeuwen, P. W. N. M., Eds.; John Wiley & Sons: Chichester, UK, 2012.
(101) Carter, K. P.; Young, A. M.; Palmer, A. E. *Chem. Rev.* **2014,** *114*, 4564-4601.
(102) Schindlbauer, H.; Hagen, H. *Monatsh. Chem. Verw. Teile Anderer Wiss.* **1965,** *96*, 285-299.
(103) Rozanel'skaya, N. A.; Bokanov, A. I.; Uzhinov, B. M.; Stepanov, B. I. *Zh. Obshch. Khim.* **1975,** *45*, 277.
(104) Akasaka, K.; Suzuki, T.; Ohrui, H.; Meguro, H. *Anal. Lett.* **1987,** *20*, 731-745.
(105) Akasaka, K.; Ohrui, H. *J. Chromatogr. A* **2000,** *881*, 159-170.
(106) Papkovsky, D. B.; Ponomarev, G. V.; Trettnak, W.; O'Leary, P. *Anal. Chem.* **1995,** *67*, 4112-4117.
(107) Lee, S.-K.; Okura, I. *Anal. Commun.* **1997,** *34*, 185-188.
(108) Ast, C.; Schmälzlin, E.; Löhmannsröben, H.-G.; van Dongen, J. T. *Sensors* **2012,** *12*, 7015-7032.
(109) Okimoto, Y.; Watanabe, A.; Niki, E.; Yamashita, T.; Noguchi, N. *FEBS Lett.* **2000,** *474*, 137-140.
(110) Morita, M.; Naito, Y.; Yoshikawa, T.; Niki, E. *Anal. Bioanal. Chem.* **2016,** *408*, 265-270.
(111) Santas, J.; Guardiola, F.; Rafecas, M.; Bou, R. *Anal. Biochem.* **2013,** *434*, 172-177.
(112) Okimoto, Y.; Warabi, E.; Wada, Y.; Niki, E.; Kodama, T.; Noguchi, N. *Free Radic. Biol. Med.* **2003,** *35*, 576-585.

(113) Santas, J.; Guzman, Y. J.; Guardiola, F.; Rafecas, M.; Bou, R. *Food Chem.* **2014,** *162*, 235-241.
(114) Chotimarkorn, C.; Nagasaka, R.; Ushio, H.; Ohshima, T.; Matsunaga, S. *Biochem. Biophys. Res. Commun.* **2005,** *338*, 1222-1228.
(115) Chotimarkorn, C.; Ohshima, T.; Ushio, H. *Lipids* **2006,** *41*, 295-300.
(116) Chotimarkorn, C.; Ohshima, T.; Ushio, H. *J. Agric. Food Chem.* **2005,** *53*, 7361-7366.
(117) Gomes, A.; Fernandes, E.; Lima, J. *J. Biochem. Biophys. Methods* **2005,** *65*, 45-80.
(118) Onoda, M.; Uchiyama, S.; Endo, A.; Tokuyama, H.; Santa, T.; Imal, K. *Org. Lett.* **2003,** *5*, 1459-1461.
(119) Soh, N.; Sakawaki, O.; Makihara, K.; Odo, Y.; Fukaminato, T.; Kawai, T.; Irie, M.; Imato, T. *Bioorg. Med. Chem.* **2005,** *13*, 1131-1139.
(120) Inoue, N.; Suzuki, Y.; Yokoyama, K.; Karube, I. *Biosci. Biotechnol. Biochem.* **2009,** *73*, 1215-1217.
(121) Pan, J.; Downing, J. A.; McHale, J. L.; Xian, M. *Mol. Biosyst.* **2009,** *5*, 918-920.
(122) Christianson, A. M.; Gabbaï, F. P. *Inorg. Chem.* **2016,** *55*, 5828-5835.
(123) Vasiuta, R.; Plenio, H. *Chem. Eur. J.* **2016,** *22*, 6353-6360.
(124) Cai, S.; Lu, Y.; He, S.; Wei, F.; Zhao, L.; Zeng, X. *Chem. Commun.* **2013,** *49*, 822-824.
(125) Sainz-Gonzalo, F. J.; Casimiro, M.; Popovici, C.; Rodriguez-Dieguez, A.; Fernandez-Sanchez, J. F.; Fernandez, I.; Lopez-Ortiz, F.; Fernandez-Gutierrez, A. *Dalton Trans.* **2012,** *41*, 6735-6748.
(126) Sainz-Gonzalo, F. J.; Elosua, C.; Fernandez-Sanchez, J. F.; Popovici, C.; Fernandez, I.; Ortiz, F. L.; Arregui, F. J.; Matias, I. R.; Fernandez-Gutierrez, A. *Sens. Actuators B: Chem.* **2012,** *173*, 254-261.
(127) Baumgartner, T.; Reau, R. *Chem. Rev.* **2006,** *106*, 4681-4727.
(128) Wang, X.; Cao, K.; Liu, Y.; Tsang, B.; Liew, S. *J. Am. Chem. Soc.* **2013,** *135*, 3399-3402.
(129) Patra, S. K.; Whittell, G. R.; Nagiah, S.; Ho, C.-L.; Wong, W.-Y.; Manners, I. *Chem. Eur. J.* **2010,** *16*, 3240-3250.
(130) Cao, L.; Manners, I.; Winnik, M. A. *Macromolecules* **2001,** *34*, 3353-3360.
(131) Mizuta, T.; Onishi, M.; Miyoshi, K. *Organometallics* **2000,** *19*, 5005-5009.
(132) Foucher, D. A.; Honeyman, C. H.; Nelson, J. M.; Tang, B. Z.; Manners, I. *Angew. Chem., Int. Ed. Engl.* **1993,** *32*, 1709-1711.
(133) Withers, H. P.; Seyferth, D.; Fellmann, J. D.; Garrou, P. E.; Martin, S. *Organometallics* **1982,** *1*, 1283-1288.
(134) Matano, Y.; Ohkubo, H.; Miyata, T.; Watanabe, Y.; Hayashi, Y.; Umeyama, T.; Imahori, H. *Eur. J. Inorg. Chem.* **2014**, 1620-1624.
(135) Greenberg, S.; Gibson, G. L.; Stephan, D. W. *Chem. Commun.* **2009**, 304-306.
(136) Greenberg, S.; Stephan, D. W. *Inorg. Chem.* **2009,** *48*, 8623-8631.
(137) Dorn, H.; Rodezno, J. M.; Brunnhöfer, B.; Rivard, E.; Massey, J. A.; Manners, I. *Macromolecules* **2003,** *36*, 291-297.
(138) Marquardt, C.; Jurca, T.; Schwan, K. C.; Stauber, A.; Virovets, A. V.; Whittell, G. R.; Manners, I.; Scheer, M. *Angew. Chem., Int. Ed.* **2015,** *54*, 13782-13786.
(139) Dorn, H.; Singh, R. A.; Massey, J. A.; Nelson, J. M.; Jaska, C. A.; Lough, A. J.; Manners, I. *J. Am. Chem. Soc.* **2000,** *122*, 6669-6678.
(140) Simpson, M. C.; Protasiewicz, J. D. *Pure Appl. Chem.* **2013,** *85*, 801-815.

(141) Wang, Y.; Robinson, G. H. *Chem. Commun.* **2009**, 5201-5213.
(142) Worch, J. C.; Chirdon, D. N.; Maurer, A. B.; Qiu, Y.; Geib, S. J.; Bernhard, S.; Noonan, K. J. T. *J. Org. Chem.* **2013,** *78*, 7462-7469.
(143) Laughlin, F. L.; Rheingold, A. L.; Deligonul, N.; Laughlin, B. J.; Smith, R. C.; Higham, L. J.; Protasiewicz, J. D. *Dalton Trans.* **2012,** *41*, 12016-12022.
(144) Laughlin, F. L.; Deligonul, N.; Rheingold, A. L.; Golen, J. A.; Laughlin, B. J.; Smith, R. C.; Protasiewicz, J. D. *Organometallics* **2013,** *32*, 7116-7121.
(145) Floch, P. L. *Coord. Chem. Rev.* **2006,** *250*, 627-681.
(146) Öberg, E.; Schäfer, B.; Geng, X.-L.; Pettersson, J.; Hu, Q.; Kritikos, M.; Rasmussen, T.; Ott, S. *J. Org. Chem.* **2009,** *74*, 9265-9273.
(147) Oberg, E.; Geng, X.-L.; Santoni, M.-P.; Ott, S. *Org. Biomol. Chem.* **2011,** *9*, 6246-6255.
(148) Dugal-Tessier, J.; Conrad, E. D.; Dake, G. R.; Gates, D. P. Phosphaalkenes. In *Phosphorus(III) Ligands in Homogeneous Catalysis: Design and Synthesis*; John Wiley & Sons: Chichester, UK, 2012; pp 321-341.
(149) Magnuson, K. W.; Oshiro, S. M.; Gurr, J. R.; Yoshida, W. Y.; Gembicky, M.; Rheingold, A. L.; Hughes, R. P.; Cain, M. F. *Organometallics* **2016,** *35*, 855-859.
(150) Dillon, K. B.; Mathey, F.; Nixon, J. F. *Phosphorus: The Carbon Copy: From Organophosphorus to Phospha-organic Chemistry*, Wiley: 1998.
(151) Mathey, F. *Angew. Chem., Int. Ed.* **2003,** *42*, 1578-1604.
(152) Bates, J. I.; Dugal-Tessier, J.; Gates, D. P. *Dalton Trans.* **2010,** *39*, 3151-3159.
(153) Yam, M.; Chong, J. H.; Tsang, C. W.; Patrick, B. O.; Lam, A. E.; Gates, D. P. *Inorg. Chem.* **2006,** *45*, 5225-5234.
(154) Yasunami, M.; Ueno, T.; Yoshifuji, M.; Okamoto, A.; Hirotsu, K. *Chem. Lett.* **1992**, 1971-1974.
(155) Takita, R.; Takada, Y.; Jensen, R. S.; Okazaki, M.; Ozawa, F. *Organometallics* **2008,** *27*, 6279-6285.
(156) Yoshifuji, M.; Toyota, K.; Inamoto, N. *Tetrahedron Lett.* **1985,** *26*, 1727-1730.
(157) Van Der Does, T.; Bickelhaupt, F. *Phosphorus Sulfur Relat. Elem.* **1987,** *30*, 515-518.
(158) Yoshifuji, M.; Toyota, K.; Inamoto, N.; Hirotsu, K.; Higuchi, T. *Tetrahedron Lett.* **1985,** *26*, 6443-6446.
(159) Appel, R. Multiple Bonds and Low Coordination in Phosphorus Chemistry. In *Phosphaalkenes, Phosphacarbaoligoenes, Phosphaalllenes*; Regitz, M.; Scherer, O. J., Eds.; Thieme: Stuttgart, 1990; pp 157-219.
(160) Van Der Knaap, T. A.; Klebach, T. C.; Visser, F.; Bickelhaupt, F.; Ros, P.; Baerends, E. J.; Stam, C. H.; Konijn, M. *Tetrahedron* **1984,** *40*, 765-776.
(161) Mundt, O.; Becker, G.; Uhl, W.; Massa, W.; Birkhahn, M. *Z. Anorg. Allg. Chem.* **1986,** *540*, 319-335.
(162) *"Characteristic Bond Lengths in Free Molecules", CRC Handbook of Chemistry and Physics*, 84th Edition: 2003.
(163) Trotter, J. *Acta Crystallogr.* **1963,** *16*, 605.
(164) Yoshifuji, M.; Takahashi, H.; Shimura, K.; Toyota, K.; Hirotsu, K.; Okada, K. *Heteroatom Chem.* **1997,** *8*, 375-382.
(165) Oddon, Y.; Darbon, N.; Reboul, J. P.; Cristau, B.; Soyfer, J. C.; Pepe, G. *Acta Crystallogr. Sect. C-Cryst. Struct. Commun.* **1984,** *40*, 524-526.

(166) Friedel, R. A.; Orchin, M. *Ultraviolet Spectra of Aromatic Compounds*, Wiley: New York, 1951.
(167) Klebach, T. C.; Lourens, R.; Bickelhaupt, F. *J. Am. Chem. Soc.* **1978,** *100*, 4886-4888.
(168) Smith, R. C.; Protasiewicz, J. D. *Eur. J. Inorg. Chem.* **2004**, 998-1006.
(169) Fife, D. J.; Morse, K. W.; Moore, W. M. *J. Photochem.* **1984,** *24*, 249-263.
(170) Bourson, J.; Oliveros, L. *Phosphorus Sulfur Relat. Elem.* **1986,** *26*, 75-81.
(171) Yamaguchi, S.; Akiyama, S.; Tamao, K. *J. Organomet. Chem.* **2002,** *652*, 3-9.
(172) Osawa, M.; Hoshino, M.; Akita, M.; Wada, T. *Inorg. Chem.* **2005,** *44*, 1157-1159.
(173) Burchat, A. F.; Chong, J. M.; Nielsen, N. *J. Organomet. Chem.* **1997,** *542*, 281-283.
(174) Becker, G.; Mundt, O.; Rössler, M.; Schneider, E. *Z. Anorg. Allg. Chem.* **1978,** *443*, 42-52.
(175) Uson, R.; Laguna, A.; Laguna, M.; Briggs, D. A.; Murray, H. H.; Fackler, J. P. *Inorg. Synth.* **1989,** *26*, 85-91.
(176) Krasovskiy, A.; Knochel, P. *Angew. Chem., Int. Ed.* **2004,** *43*, 3333-3336.
(177) Dubois, J.-E.; Boussu, M. *Tetrahedron Lett.* **1970,** *11*, 2523-2526.
(178) Sheldrick, G. M. *SHELXL-97 (Release 97-2)*, University of Göttingen, Germany, 1997.
(179) Sheldrick, G. *Acta Crystallogr. Sect. A* **2008,** *64*, 112-122.
(180) Farrugia, L. *J. Appl. Crystallogr.* **1999,** *32*, 837-838.
(181) Priegert, A. M.; Rawe, B. W.; Serin, S. C.; Gates, D. P. *Chem. Soc. Rev.* **2016,** *45*, 922-953.
(182) Parke, S. M.; Boone, M. P.; Rivard, E. *Chem. Commun.* **2016,** *52*, 9485-9505.
(183) Jäkle, F. Recent Advances in the Synthesis and Applications of Organoborane Polymers. In *Synthesis and Application of Organoboron Compounds*; Fernández, E.; Whiting, A., Eds.; Springer International Publishing: Cham, 2015; pp 297-325.
(184) Tanaka, K.; Chujo, Y. *Macromol. Rapid Commun.* **2012,** *33*, 1235-1255.
(185) Chivers, T.; Manners, I. *Inorganic Rings and Polymers of the P-Block Elments: from Fundermentals to Applications*, RSC Publishing: Cambridge, 2009.
(186) Reus, C.; Baumgartner, T. *Dalton Trans.* **2016,** *45*, 1850-1855.
(187) Baumgartner, T. *Acc. Chem. Res.* **2014,** *47*, 1613-1622.
(188) Hobbs, M. G.; Baumgartner, T. *Eur. J. Inorg. Chem.* **2007,** *2007*, 3611-3628.
(189) Hissler, M.; Dyer, P. W.; Reau, R. *Coord. Chem. Rev.* **2003,** *244*, 1-44.
(190) He, X. M.; Woo, A. Y. Y.; Borau-Garcia, J.; Baumgartner, T. *Chem. Eur. J.* **2013,** *19*, 7620-7630.
(191) Stolar, M.; Baumgartner, T. *New J. Chem.* **2012,** *36*, 1153-1160.
(192) Fadhel, O.; Benko, Z.; Gras, M.; Deborde, V.; Joly, D.; Lescop, C.; Nyulaszi, L.; Hissler, M.; Reau, R. *Chem. Eur. J.* **2010,** *16*, 11340-11356.
(193) Rawe, B. W.; Gates, D. P. *Angew. Chem., Int. Ed.* **2015,** *54*, 11438-11442.
(194) Joly, D.; Bouit, P. A.; Hissler, M. *J. Mater. Chem. C* **2016,** *4*, 3686-3698.
(195) Stolar, M.; Baumgartner, T. *Chem. Asian J.* **2014,** *9*, 1212-1225.
(196) He, X.; Baumgartner, T. *RSC Adv.* **2013,** *3*, 11334-11350.
(197) Jeon, S. O.; Lee, J. Y. *J. Mater. Chem.* **2012,** *22*, 4233-4243.
(198) Yasunami, M.; Ueno, T.; Yoshifuji, M.; Okamoto, A.; Hirotsu, K. *Chem. Lett.* **1992,** *21*, 1971-1974.
(199) Gudimetla, V. B.; Rheingold, A. L.; Payton, J. L.; Peng, H.-L.; Simpson, M. C.; Protasiewicz, J. D. *Inorg. Chem.* **2006,** *45*, 4895-4901.

(200) Kumar, N. S. S.; Gujrati, M. D.; Wilson, J. N. *Chem. Commun.* **2010,** *46*, 5464-5466.
(201) Liu, F.; Tang, C.; Chen, Q.-Q.; Shi, F.-F.; Wu, H.-B.; Xie, L.-H.; Peng, B.; Wei, W.; Cao, Y.; Huang, W. *J. Phys. Chem. C* **2009,** *113*, 4641-4647.
(202) Berlman, I. B. *Handbook of Fluorescence Spectra of Aromatic Molecules*, 2nd ed.; Academic Press: New York, 1971.
(203) Martinho, J. M. G. *J. Phys. Chem.* **1989,** *93*, 6687-6692.
(204) Förster, T. *Angew. Chem., Int. Ed. Engl.* **1969,** *8*, 333-343.
(205) Birks, J. B.; Dyson, D. J.; Munro, I. H. *Proc. R. Soc. A* **1963,** *275*, 575-588.
(206) Forster, T.; Kasper, K. *Z. Elektrochem.* **1955,** *59*, 976-980.
(207) Ramos Chagas, G.; Xie, X.; Darmanin, T.; Steenkeste, K.; Gaucher, A.; Prim, D.; Méallet-Renault, R.; Godeau, G.; Amigoni, S.; Guittard, F. *J. Phys. Chem. C* **2016,** *120*, 7077-7087.
(208) Abd-El-Aziz, A. S.; Abdelghani, A. A.; Wagner, B. D.; Pearson, J. K.; Awad, M. K. *Polymer* **2016,** *98*, 210-228.
(209) Matsui, J.; Mitsuishi, M.; Miyashita, T. *J. Phys. Chem. B* **2002,** *106*, 2468-2473.
(210) Baker, L. A.; Crooks, R. M. *Macromolecules* **2000,** *33*, 9034-9039.
(211) Figueira-Duarte, T. M.; Simon, S. C.; Wagner, M.; Drtezhinin, S. I.; Zachariasse, K. A.; Müllen, K. *Angew. Chem., Int. Ed.* **2008,** *47*, 10175-10178.
(212) Vilbrandt, N.; Gassmann, A.; von Seggern, H.; Rehahn, M. *Macromolecules* **2016,** *49*, 1674-1680.
(213) Mikroyannidis, J. A. *Chem. Mater.* **2003,** *15*, 1865-1871.
(214) Mikroyannidis, J. A. *Macromolecules* **2002,** *35*, 9289-9295.
(215) Ahn, T.; Song, S.-Y.; Shim, H.-K. *Macromolecules* **2000,** *33*, 6764-6771.
(216) Miyata, M.; Matsumi, N.; Chujo, Y. *Polym. Bull.* **1999,** *42*, 505-510.
(217) Nagata, Y.; Chujo, Y. *Macromolecules* **2008,** *41*, 2809-2813.
(218) Wang, X.-d.; Wolfbeis, O. S. *Chem. Soc. Rev.* **2014,** *43*, 3666-3761.
(219) Krawczyk, T.; Baj, S. *Anal. Lett.* **2014,** *47*, 2129-2147.
(220) Roberts, L.; Lines, R.; Reddy, S.; Hay, J. *Sens. Actuators B: Chem.* **2011,** *152*, 63-67.
(221) Germain, M. E.; Knapp, M. J. *Chem. Soc. Rev.* **2009,** *38*, 2543-2555.
(222) Schulte-Ladbeck, R.; Vogel, M.; Karst, U. *Anal. Bioanal. Chem.* **2006,** *386*, 559-565.
(223) Mills, A. *Chem. Soc. Rev.* **2005,** *34*, 1003-1011.
(224) Amao, Y. *Microchimica Acta* **2003,** *143*, 1-12.
(225) SADABS, *V2008/1. Bruker AXS Inc.*, Madison, WI, 2008.
(226) Frisch, M. J.; Trucks, G. W.; Schlegel, H. B.; Scuseria, G. E.; Robb, M. A.; Cheeseman, J. R.; Scalmani, G.; Barone, V.; Mennucci, B.; Petersson, G. A.; Nakatsuji, H.; Caricato, M.; Li, X.; Hratchian, H. P.; Izmaylov, A. F.; Bloino, J.; Zheng, G.; Sonnenberg, J. L.; Hada, M.; Ehara, M.; Toyota, K.; Fukuda, R.; Hasegawa, J.; Ishida, M.; Nakajima, T.; Honda, Y.; Kitao, O.; Nakai, H.; Vreven, T.; Montgomery Jr., J. A.; Peralta, J. E.; Ogliaro, F.; Bearpark, M. J.; Heyd, J.; Brothers, E. N.; Kudin, K. N.; Staroverov, V. N.; Kobayashi, R.; Normand, J.; Raghavachari, K.; Rendell, A. P.; Burant, J. C.; Iyengar, S. S.; Tomasi, J.; Cossi, M.; Rega, N.; Millam, N. J.; Klene, M.; Knox, J. E.; Cross, J. B.; Bakken, V.; Adamo, C.; Jaramillo, J.; Gomperts, R.; Stratmann, R. E.; Yazyev, O.; Austin, A. J.; Cammi, R.; Pomelli, C.; Ochterski, J. W.; Martin, R. L.; Morokuma, K.; Zakrzewski, V. G.; Voth, G. A.; Salvador, P.; Dannenberg, J. J.; Dapprich, S.; Daniels, A. D.; Farkas, Ö.; Foresman, J.

B.; Ortiz, J. V.; Cioslowski, J.; Fox, D. J. *Gaussian 09, Revision D.01*, Gaussian, Inc.: Wallingford, CT, USA, 2009.
(227) Becke, A. D. *Physical Review A* **1988,** *38*, 3098-3100.
(228) Becke, A. D. *The Journal of Chemical Physics* **1993,** *98*, 5648-5652.
(229) Hehre, W. J.; Ditchfield, R.; Pople, J. A. *The Journal of Chemical Physics* **1972,** *56*, 2257-2261.
(230) Bauernschmitt, R.; Ahlrichs, R. *Chemical Physics Letters* **1996,** *256*, 454-464.
(231) Yanai, T.; Tew, D. P.; Handy, N. C. *Chemical Physics Letters* **2004,** *393*, 51-57.
(232) Tomasi, J.; Mennucci, B.; Cammi, R. *Chemical Reviews* **2005,** *105*, 2999-3094.
(233) Schäfer, A.; Jurca, T.; Turner, J.; Vance, J. R.; Lee, K.; Du, V. A.; Haddow, M. F.; Whittell, G. R.; Manners, I. *Angew. Chem., Int. Ed.* **2015,** *54*, 4836-4841.
(234) For an excellent overview of poly(aryleneethynylenes), see: U. H. F. Bunz, *Macromol. Rapid Commun.* 2009, **30**, 772, and references therein.
(235) Kreienbrink, A.; Sarosi, M. B.; Kuhnert, R.; Wonneberger, P.; Arkhypchuk, A. I.; Lonnecke, P.; Ott, S.; Hey-Hawkins, E. *Chem. Commun.* **2015,** *51*, 836-838.
(236) Öberg, E.; Orthaber, A.; Lescop, C.; Réau, R.; Hissler, M.; Ott, S. *Chem. Eur. J.* **2014,** *20*, 8421-8432.
(237) Moebus, J.; Bonnin, Q.; Ueda, K.; Froehlich, R.; Itami, K.; Kehr, G.; Erker, G. *Angew. Chem., Int. Ed.* **2012,** *51*, 1954-1957.
(238) Appelt, C.; Westenberg, H.; Bertini, F.; Ehlers, A. W.; Slootweg, J. C.; Lammertsma, K.; Uhl, W. *Angew. Chem., Int. Ed.* **2011,** *50*, 3925-3928.
(239) Ekkert, O.; Kehr, G.; Frohlich, R.; Erker, G. *Chem. Commun.* **2011,** *47*, 10482-10484.
(240) Westenberg, H.; Slootweg, J. C.; Hepp, A.; Kösters, J.; Roters, S.; Ehlers, A. W.; Lammertsma, K.; Uhl, W. *Organometallics* **2010,** *29*, 1323-1330.
(241) van Assema, S. G. A.; Kraikivskii, P. B.; Zelinskii, S. N.; Saraev, V. V.; de Jong, G. B.; de Kanter, F. J. J.; Schakel, M.; Chris Slootweg, J.; Lammertsma, K. *J. Organomet. Chem.* **2007,** *692*, 2314-2323.
(242) Märkl, G.; Zollitsch, T.; Kreitmeier, P.; Prinzhorn, M.; Reithinger, S.; Eibler, E. *Chem. Eur. J.* **2000,** *6*, 3806-3820.
(243) Huc, V.; Balueva, A.; Sebastian, R. M.; Caminade, A. M.; Majoral, J. P. *Synthesis-Stuttgart* **2000**, 726-730.
(244) Scott, L. T.; Unno, M. *J. Am. Chem. Soc.* **1990,** *112*, 7823-7825.
(245) Beletskaya, I. P.; Afanasiev, V. V.; Kazankova, M. A.; Efimova, I. V. *Org. Lett.* **2003,** *5*, 4309-4311.
(246) Hengefeld, A.; Nast, R. *Chem. Ber.* **1983,** *116*, 2035-2036.
(247) Gao, H.-Y.; Wagner, H.; Zhong, D.; Franke, J.-H.; Studer, A.; Fuchs, H. *Angew. Chem., Int. Ed.* **2013,** *52*, 4024-4028.
(248) Liu, B.; Bao, Y.; Du, F.; Wang, H.; Tian, J.; Bai, R. *Chem. Commun.* **2011,** *47*, 1731-1733.
(249) Thomas, K. R. J.; Lin, J. T.; Lin, Y.-Y.; Tsai, C.; Sun, S.-S. *Organometallics* **2001,** *20*, 2262-2269.
(250) Odian, G. *Principles of Polymerization*, 4th ed.; John Wiley & Sons: Hoboken, NJ, 2004.
(251) Bozolyubov, G. M.; Petrov, A. A. *Zhurnal Obshchei Khimii* **1967,** *37*, 229-231.
(252) Mössinger, D.; Jester, S.-S.; Sigmund, E.; Müller, U.; Höger, S. *Macromolecules* **2009,** *42*, 7974-7978.

(253) Hinderer, F.; May, R.; Jester, S.-S.; Höger, S. *Macromolecules* **2016,** *49*, 1816-1821.
(254) Schumm, J. S.; Pearson, D. L.; Tour, J. M. *Angew. Chem., Int. Ed. Engl.* **1994,** *33*, 1360-1363.
(255) Hu, J.; Zhao, N.; Yang, B.; Wang, G.; Guo, L.-N.; Liang, Y.-M.; Yang, S.-D. *Chem. Eur. J.* **2011,** *17*, 5516-5521.
(256) Mootz, D.; Sassmannshausen, G. *Z. Anorg. Allg. Chem.* **1967,** *355*, 200-208.
(257) Ekkert, O.; Tuschewitzki, O.; Daniliuc, C. G.; Kehr, G.; Erker, G. *Chem. Commun.* **2013,** *49*, 6992-6994.
(258) Alvarez, S. *Dalton Trans.* **2013,** *42*, 8617-8636.
(259) Davies, L. H.; Stewart, B.; Harrington, R. W.; Clegg, W.; Higham, L. J. *Angew. Chem., Int. Ed.* **2012,** *51*, 4921-4924.
(260) Rawe, B. W.; Brown, C. M.; MacKinnon, M. R.; Patrick, B. O.; Bodwell, G. J.; Gates, D. P. *Organometallics* **2017**.
(261) Pei, Q.; Yang *J. Am. Chem. Soc.* **1996,** *118*, 7416-7417.
(262) Lee, S. H.; Nakamura, T.; Tsutsui, T. *Org. Lett.* **2001,** *3*, 2005-2007.
(263) Melhuish, W. H. *J. Phys. Chem.* **1961,** *65*, 229-235.
(264) Halkyard, C. E.; Rampey, M. E.; Kloppenburg, L.; Studer-Martinez, S. L.; Bunz, U. H. F. *Macromolecules* **1998,** *31*, 8655-8659.
(265) Monkman, A.; Rothe, C.; King, S.; Dias, F. Polyfluorene photophysics. In *Polyfluorenes*; Scherf, U.; Neher, D., Eds.; Springer-Verlag Berlin: Berlin, 2008; Vol. 212, pp 187-225.
(266) Koziar, J. C.; Cowan, D. O. *Acc. Chem. Res.* **1978,** *11*, 334-341.
(267) Solovyov, K. N.; Borisevich, E. A. *Physics-Uspekhi* **2005,** *48*, 231-253.
(268) Durben, S.; Nickel, D.; Krüger, R. A.; Sutherland, T. C.; Baumgartner, T. *J. Polym. Sci. A Polym. Chem.* **2008,** *46*, 8179-8190.
(269) Dienes, Y.; Durben, S.; Kárpáti, T.; Neumann, T.; Englert, U.; Nyulászi, L.; Baumgartner, T. *Chem. Eur. J.* **2007,** *13*, 7487-7500.
(270) Lemau de Talance, V.; Hissler, M.; Zhang, L.-Z.; Karpati, T.; Nyulaszi, L.; Caras-Quintero, D.; Bauerle, P.; Reau, R. *Chem. Commun.* **2008**, 2200-2202.
(271) Matsumura, Y.; Ueda, M.; Fukuda, K.; Fukui, K.; Takase, I.; Nishiyama, H.; Inagi, S.; Tomita, I. *ACS Macro Lett.* **2015,** *4*, 124-127.
(272) Padmaperuma, A. B.; Sapochak, L. S.; Burrows, P. E. *Chem. Mater.* **2006,** *18*, 2389-2396.
(273) Goelfert, U.; Rothe, C.; Vygintas, J. Light-Emitting Device Comprising Polar Matrix, Metal Dopant, and Silver Cathode. Internat. Pat. Appl. EP2016064448, June 22, 2016.
(274) Li, H.; Powell, D. R.; Hayashi, R. K.; West, R. *Macromolecules* **1998,** *31*, 52-58.
(275) Shameem, M. A.; Orthaber, A. *Chem. Eur. J.* **2016,** *22*, 10718-10735.
(276) Lemmer, U.; Heun, S.; Mahrt, R. F.; Scherf, U.; Hopmeier, M.; Siegner, U.; Göbel, E. O.; Müllen, K.; Bässler, H. *Chem. Phys. Lett.* **1995,** *240*, 373-378.
(277) Murali, M. G.; Udayakumar, D. Thiophene-Based Conjugated Polymers: Synthesis, Linear, and Third-Order Nonlinear Optical Properties. In *Advances in Polymer Materials and Technology*; Srinivasan, A.; Bandyopadhyay, S., Eds.; CRC Press: Boca Raton, FL, 2016; pp 467-503.
(278) Andrew, T. L.; Swager, T. M. *J. Polym. Sci. B Polym. Phys.* **2011,** *49*, 476-498.
(279) Liu, X.; He, L.; Liu, Y. M.; Cao, Y. *Acc. Chem. Res.* **2014,** *47*, 793-804.
(280) Belmont, P.; Parker, E. *Eur. J. Org. Chem.* **2009**, 6075-6089.

(281) Jimenez-Nunez, E.; Echavarren, A. M. *Chem. Commun.* **2007**, 333-346.
(282) Min, B. K.; Friend, C. M. *Chem. Rev.* **2007,** *107*, 2709-2724.
(283) Block, W. D.; Knapp, E. L. *J. Pharm. Exp. Ther.* **1945,** *83*, 275-278.
(284) Che, C. M.; Sun, R. W. Y. *Chem. Commun.* **2011,** *47*, 9554-9560.
(285) Berners-Price, S. J.; Filipovska, A. *Metallomics* **2011,** *3*, 863-873.
(286) Boisselier, E.; Astruc, D. *Chem. Soc. Rev.* **2009,** *38*, 1759-1782.
(287) Giljohann, D. A.; Seferos, D. S.; Daniel, W. L.; Massich, M. D.; Patel, P. C.; Mirkin, C. A. *Angew. Chem., Int. Ed.* **2010,** *49*, 3280-3294.
(288) Stratakis, M.; Garcia, H. *Chem. Rev.* **2012,** *112*, 4469-4506.
(289) Hvolbaek, B.; Janssens, T. V. W.; Clausen, B. S.; Falsig, H.; Christensen, C. H.; Norskov, J. K. *Nano Today* **2007,** *2*, 14-18.
(290) Corma, A.; Garcia, H. *Chem. Soc. Rev.* **2008,** *37*, 2096-2126.
(291) Daniel, M. C.; Astruc, D. *Chem. Rev.* **2004,** *104*, 293-346.
(292) Luo, X. L.; Morrin, A.; Killard, A. J.; Smyth, M. R. *Electroanalysis* **2006,** *18*, 319-326.
(293) Pingarron, J. M.; Yanez-Sedeno, P.; Gonzalez-Cortes, A. *Electrochim. Acta* **2008,** *53*, 5848-5866.
(294) Habib, A.; Tabata, M. *J. Inorg. Biochem.* **2004,** *98*, 1696-1702.
(295) Nyarko, E.; Hanada, N.; Habib, A.; Tabata, M. *Inorg. Chim. Acta* **2004,** *357*, 739-745.
(296) Nyarko, E.; Hara, T.; Grab, D. J.; Habib, A.; Kim, Y.; Nikolskaia, O.; Fukuma, T.; Tabata, M. *Chem. Biol. Interact.* **2004,** *148*, 19-25.
(297) Singha, S.; Kim, D.; Seo, H.; Cho, S. W.; Ahn, K. H. *Chem. Soc. Rev.* **2015,** *44*, 4367-4399.
(298) Zhang, J. F.; Zhou, Y.; Yoon, J.; Kim, J. S. *Chem. Soc. Rev.* **2011,** *40*, 3416-3429.
(299) Eun Jun, M.; Roy, B.; Han Ahn, K. *Chem. Commun.* **2011,** *47*, 7583-7601.
(300) Zhao, Q. A.; Li, F. Y.; Huang, C. H. *Chem. Soc. Rev.* **2010,** *39*, 3007-3030.
(301) Balasingham, R. G.; Williams, C. F.; Mottram, H. J.; Coogan, M. P.; Pope, S. J. A. *Organometallics* **2012,** *31*, 5835-5843.
(302) Patil, N. T.; Shinde, V. S.; Thakare, M. S.; Hemant Kumar, P.; Bangal, P. R.; Barui, A. K.; Patra, C. R. *Chem. Commun.* **2012,** *48*, 11229-11231.
(303) Wang, J.-B.; Wu, Q.-Q.; Min, Y.-Z.; Liu, Y.-Z.; Song, Q.-H. *Chem. Commun.* **2012,** *48*, 744-746.
(304) Egorova, O. A.; Seo, H.; Chatterjee, A.; Ahn, K. H. *Org. Lett.* **2010,** *12*, 401-403.
(305) Emrullahoglu, M.; Karakus, E.; Ucuncu, M. *Analyst* **2013,** *138*, 3638-3641.
(306) Seo, H.; Jun, M. E.; Ranganathan, K.; Lee, K.-H.; Kim, K.-T.; Lim, W.; Rhee, Y. M.; Ahn, K. H. *Org. Lett.* **2014,** *16*, 1374-1377.
(307) Dong, M.; Wang, Y.-W.; Peng, Y. *Org. Lett.* **2010,** *12*, 5310-5313.
(308) Do, J. H.; Kim, H. N.; Yoon, J.; Kim, J. S.; Kim, H.-J. *Org. Lett.* **2010,** *12*, 932-934.
(309) Wang, J.; Lin, W.; Yuan, L.; Song, J.; Gao, W. *Chem. Commun.* **2011,** *47*, 12506-12508.
(310) Yuan, L.; Lin, W.; Yang, Y.; Song, J. *Chem. Commun.* **2011,** *47*, 4703-4705.
(311) Cao, X.; Lin, W.; Ding, Y. *Chem. Eur. J.* **2011,** *17*, 9066-9069.
(312) Wang, B.; Fu, T.; Yang, S.; Li, J.; Chen, Y. *Anal. Methods* **2013,** *5*, 3639-3641.
(313) Young Choi, J.; Kim, G.-H.; Guo, Z.; Yeon Lee, H.; Swamy, K. M. K.; Pai, J.; Shin, S.; Shin, I.; Yoon, J. *Biosens. Bioelectron.* **2013,** *49*, 438-441.
(314) Yang, Y.-K.; Lee, S.; Tae, J. *Org. Lett.* **2009,** *11*, 5610-5613.

(315) Jung Jou, M.; Chen, X.; Swamy, K. M. K.; Na Kim, H.; Kim, H.-J.; Lee, S.-g.; Yoon, J. *Chem. Commun.* **2009**, 7218-7220.
(316) Ucuncu, M.; Emrullahoglu, M. *Chem. Commun.* **2014,** *50*, 5884-5886.
(317) Seo, H.; Jun, M. E.; Egorova, O. A.; Lee, K.-H.; Kim, K.-T.; Ahn, K. H. *Org. Lett.* **2012,** *14*, 5062-5065.
(318) Arcau, J.; Andermark, V.; Aguilo, E.; Gandioso, A.; Moro, A.; Cetina, M.; Lima, J. C.; Rissanen, K.; Ott, I.; Rodriguez, L. *Dalton Trans.* **2014,** *43*, 4426-4436.
(319) Camara, J.; Crespo, O.; Gimeno, M. C.; Koshevoy, I. O.; Laguna, A.; Ospino, I.; Smirnova, E. S.; Tunik, S. P. *Dalton Trans.* **2012,** *41*, 13891-13898.
(320) Fernández-Moreira, V.; Cámara, J.; Smirnova, E. S.; Koshevoy, I. O.; Laguna, A.; Tunik, S. P.; Blanco, M. C.; Gimeno, M. C. *Organometallics* **2016,** *35*, 1141-1150.
(321) Koshevoy, I. O.; Lin, C.-L.; Hsieh, C.-C.; Karttunen, A. J.; Haukka, M.; Pakkanen, T. A.; Chou, P.-T. *Dalton Trans.* **2012,** *41*, 937-945.
(322) Koshevoy, I. O.; Lin, C.-L.; Karttunen, A. J.; Jänis, J.; Haukka, M.; Tunik, S. P.; Chou, P.-T.; Pakkanen, T. A. *Inorg. Chem.* **2011,** *50*, 2395-2403.
(323) Koshevoy, I. O.; Ostrova, P. V.; Karttunen, A. J.; Melnikov, A. S.; Khodorkovskiy, M. A.; Haukka, M.; Janis, J.; Tunik, S. P.; Pakkanen, T. A. *Dalton Trans.* **2010,** *39*, 9022-9031.
(324) Robilotto, T. J.; Deligonul, N.; Updegraff, J. B.; Gray, T. G. *Inorg. Chem.* **2013,** *52*, 9659-9668.
(325) Rawe, B. W.; Chun, C. P.; Gates, D. P. *Chem. Sci.* **2014,** *5*, 4928-4938.
(326) Schmidbaur, H. *Gold Bull.* **2000,** *33*, 3-10.
(327) Schmidbaur, H.; Schier, A. *Chem. Soc. Rev.* **2012,** *41*, 370-412.
(328) Katz, M. J.; Sakai, K.; Leznoff, D. B. *Chem. Soc. Rev.* **2008,** *37*, 1884-1895.
(329) Natori, I.; Natori, S.; Ogino, K. *J. Appl. Polym. Sci.* **2015,** *132*, 41901-41902.
(330) Wang, J.; Leung, L. M.; So, S.-K.; Chan, C. Y. H.; Wong, M. Y. *Polym. Int.* **2014,** *63*, 1797-1805.
(331) Best, S. L.; Sadler, P. J. *Gold Bull.* **1996,** *29*, 87-93.
(332) Parish, R. V.; Cottrill, S. M. *Gold Bull.* **1987,** *20*, 3-12.
(333) Křikavová, R.; Hošek, J.; Vančo, J.; Hutyra, J.; Dvořák, Z.; Trávníček, Z. *PLoS ONE* **2014,** *9*, e107373.
(334) Langdon-Jones, E. E.; Pope, S. J. A. *Chem. Commun.* **2014,** *50*, 10343-10354.
(335) Meyer, A.; Bagowski, C. P.; Kokoschka, M.; Stefanopoulou, M.; Alborzinia, H.; Can, S.; Vlecken, D. H.; Sheldrick, W. S.; Wölfl, S.; Ott, I. *Angew. Chem., Int. Ed.* **2012,** *51*, 8895-8899.
(336) Nagai, A.; Miyake, J.; Kokado, K.; Nagata, Y.; Chujo, Y. *J. Am. Chem. Soc.* **2008,** *130*, 15276-15278.
(337) Ruan, Y.-B.; Yu, Y.; Li, C.; Bogliotti, N.; Tang, J.; Xie, J. *Tetrahedron* **2013,** *69*, 4603-4608.
(338) Ramazanov, I. R.; Kadikova, R. N.; Saitova, Z. R.; Dzhemilev, U. M. *Asian J. Org. Chem.* **2015,** *4*, 1301-1307.
(339) Matano, Y.; Imahoria, H. *Org. Biomol. Chem.* **2009,** *7*, 1258-1271.

Appendices

Appendix A: Crystallographic Data

Table A1: Crystallographic parameters for crystal structures in Chapter 2 and Chapter 3

	***E*-2.1a**	***Z*-2.1b**	**2.1c**	***Z*-3.1**
Empirical formula	$C_{26}H_{23}P$	$C_{30}H_{25}P$	$C_{24}H_{21}P$	$C_{32}H_{25}P$
FW	366.41	416.47	340.38	440.49
Crystal system	Monoclinic	Monoclinic	Monoclinic	triclinic
Space group	$P2_1/n$	$C2/c$	$P2_1/c$	P –1
a [Å]	12.054(5)	19.514(2)	7.6281(5)	8.5160(4)
b [Å]	9.298(5)	13.3010(14)	29.8493(19)	11.6325(5)
c [Å]	18.724(5)	20.028(2)	8.0370(5)	12.4299(5)
α [°]	90	90	90	86.573(2)
β [°]	99.348(5)	119.5190(10)	95.421(4)	72.136(2)
γ [°]	90	90	90	83.904(2)
V [Å^3]	2070.7(15)	4523.6(8)	1821.79	1164.86(9)
T [K]	173(2)	173(2)	173(2)	293(2)
Z	4	8	4	2
F (000)	776	1760	720	464
No. of reflections collected	13929	47661	2381	44052
Goodness of fit on F^2	1.01	1.054	1.198	1.07
R_1 [I > 2σ(I)][a]	0.042	0.049	0.056	0.050
wR_2 [all data][b]	0.104	0.137	0.137	0.119
CCDC	1013550	1013551	1013549	1530414

[a] $R_1 = \Sigma||F_o| - |F_c||/\Sigma|F_o|$. [b] $wR_2(F^2[\text{all data}]) = \{\Sigma[w(F_o^2 - F_c^2)^2]/\Sigma[w(F_o^2)^2]\}^{1/2}$

Table A2: Crystallographic parameters for crystal structures in Chapter 4 and Chapter 5

	4.2a·O	**4.2e·O**	**4.3b·O**	**5.2·AuCl**
Empirical formula	$C_{26}H_{15}PO$	$C_{22}H_{15}PO$	$C_{48}H_{48}P_2O_2$	$C_{22}H_{15}PAuCl$
FW	374.38	323.31	694.78	542.76
Crystal system	Orthorhomic	Orthorhombic	Triclinic	Triclinic
Space group	Pna21	P $ca2_1$	P–1	P–1
a [Å]	13.2917 (18)	19.497(3)	5.975(2)	9.124(4)
b [Å]	7.5342(10)	7.603(1)	9.973(5)	11.140(5)
c [Å]	19.659(3)	11.664(2)	16.775(7)	19.624(9)
α [°]	90	90	89.62(1)	98.178(7)
β [°]	90	90	81.30(1)	95.095(7)
γ [°]	90	90	76.86(1)	96.374(7)
V [$Å^3$]	1968.7	1729.0(5)	961.8(7)	1951.0(15)
T [K]	100	100	90	296
Z	4	4	1	4
F (000)	776	680	370	1026.3
No. of reflections collected	22859	16758	15730	7954
Goodness of fit on F^2	1.03	1.02	1.06	1.06
R_1 [$I > 2\sigma(I)$][a]	0.054	0.062	0.033	0.0445
wR_2 [all data][b]	0.105	0.107	0.111	0.111
CCDC	N/A	1400994	1400995	N/A

[a] $R_1 = \Sigma||F_o| - |F_c||/\Sigma|F_o|$. [b] $wR_2(F^2[\text{all data}]) = \{\Sigma[w(F_o^2 - F_c^2)^2]/\Sigma[w(F_o^2)^2]\}^{1/2}$

Appendix B: Supplementary Spectra for Chapter 2

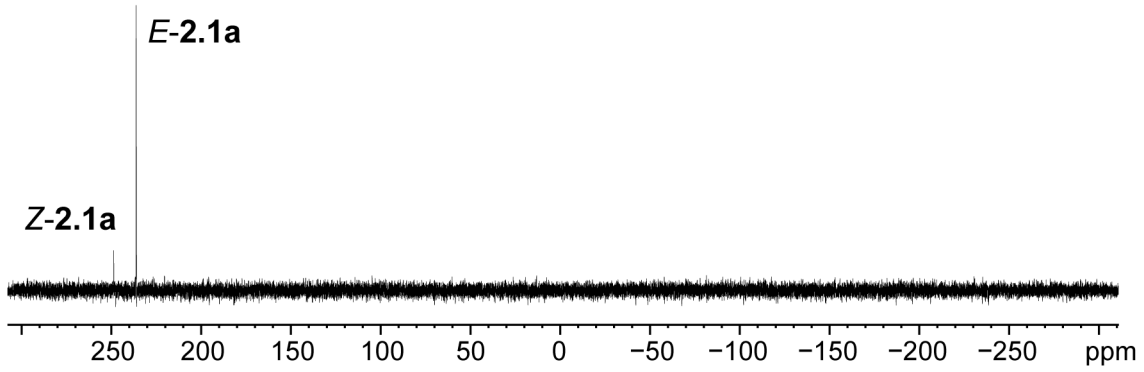

Figure B1: $^{31}P\{^{1}H\}$ NMR (121 MHz, $CDCl_3$) spectrum of *E*-2.1a after recrystallization in hexanes

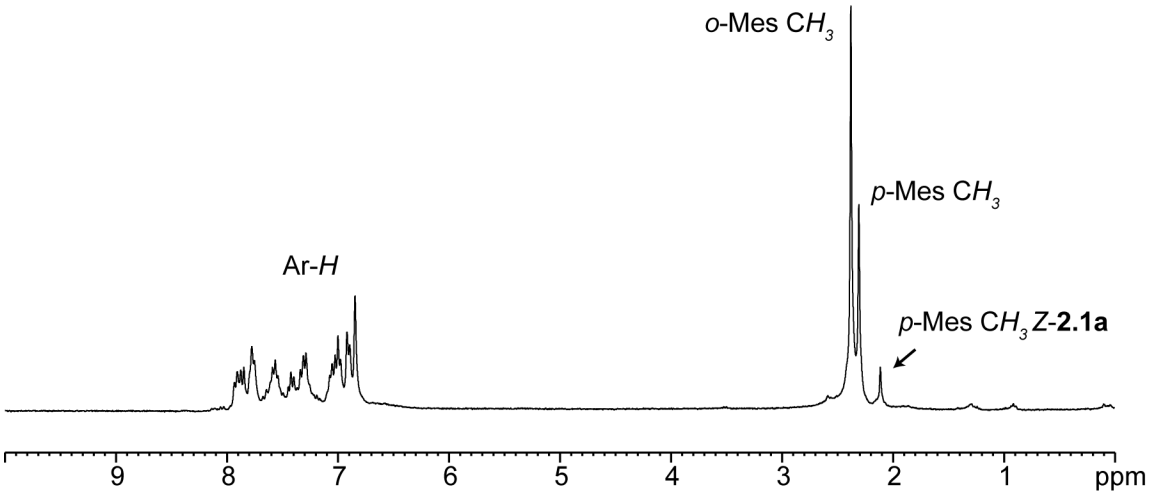

Figure B2: ^{1}H NMR (300 MHz, $CDCl_3$) spectrum of *E*-2.1a after recrystallization in hexanes

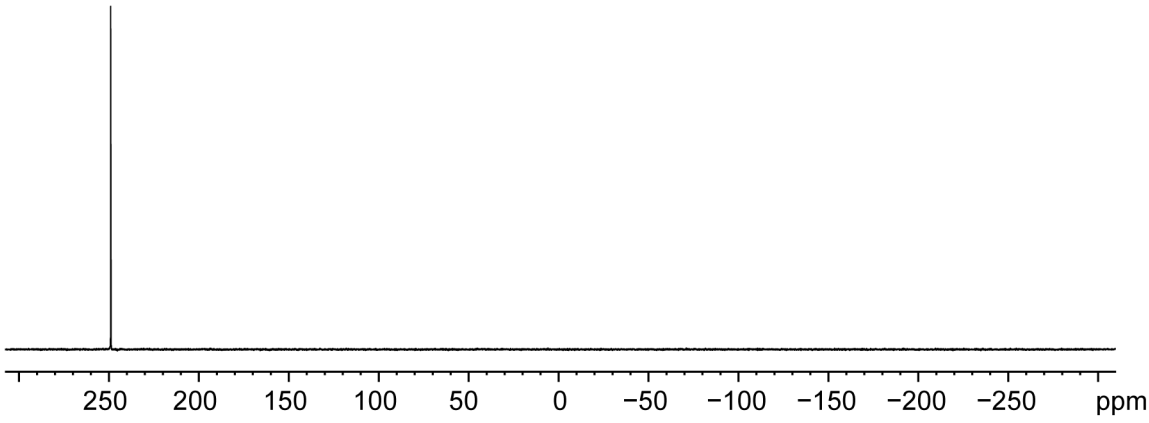

Figure B3: $^{31}P\{^{1}H\}$ NMR (121 MHz, C_6D_6) spectrum of 2.1c

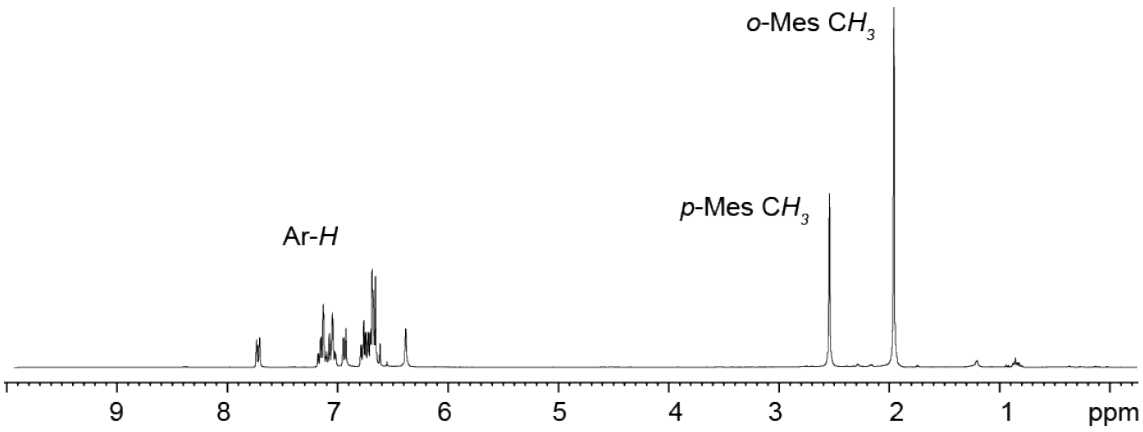

Figure B4: ^{1}H NMR (300 MHz, C_6D_6) spectrum of 2.1c

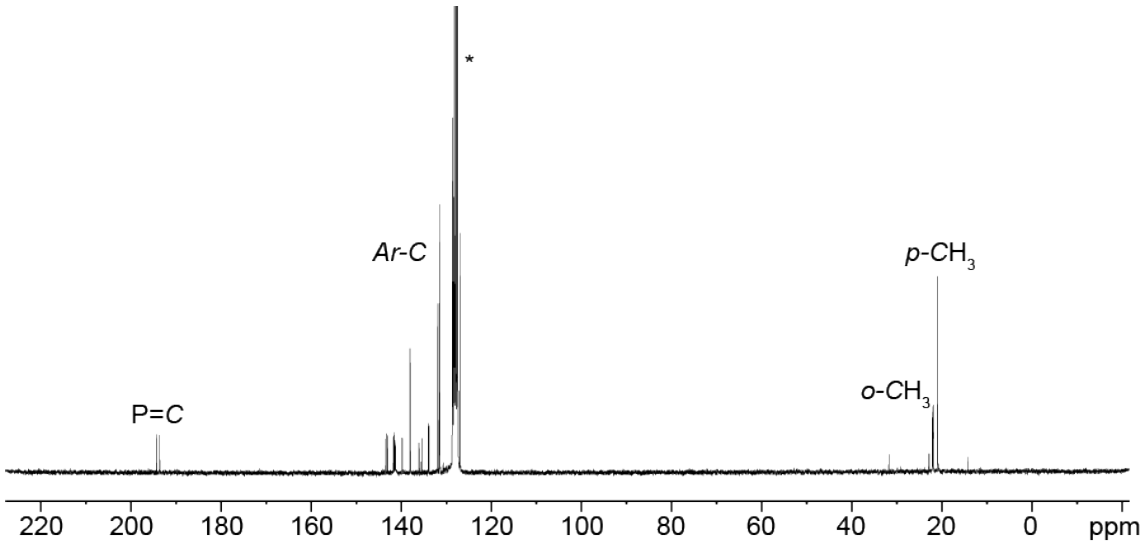

Figure B5: ^{13}C{^{1}H} NMR (75 MHz, C_6D_6) NMR spectrum of 2.1c. *C_6D_6

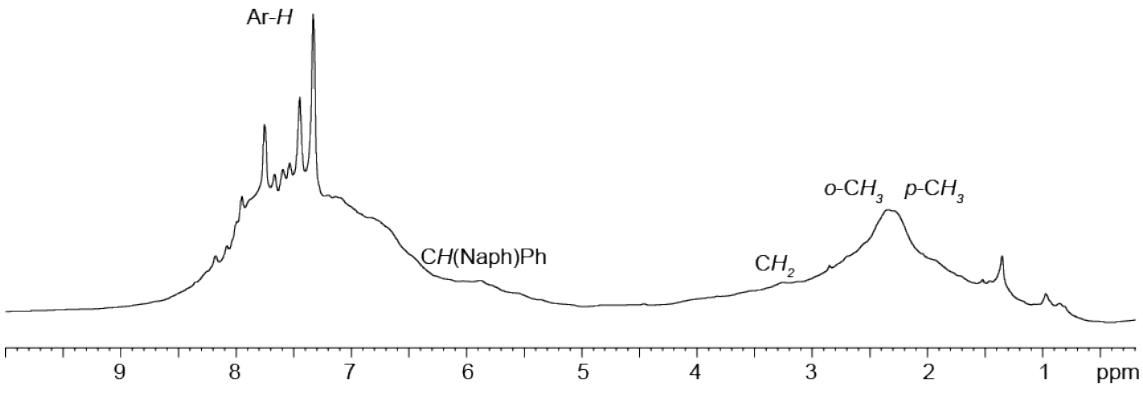

Figure B6: ^{1}H NMR (600 MHz, $CDCl_3$) of 2.2a

Appendix C: Supplementary Spectra for Chapter 3

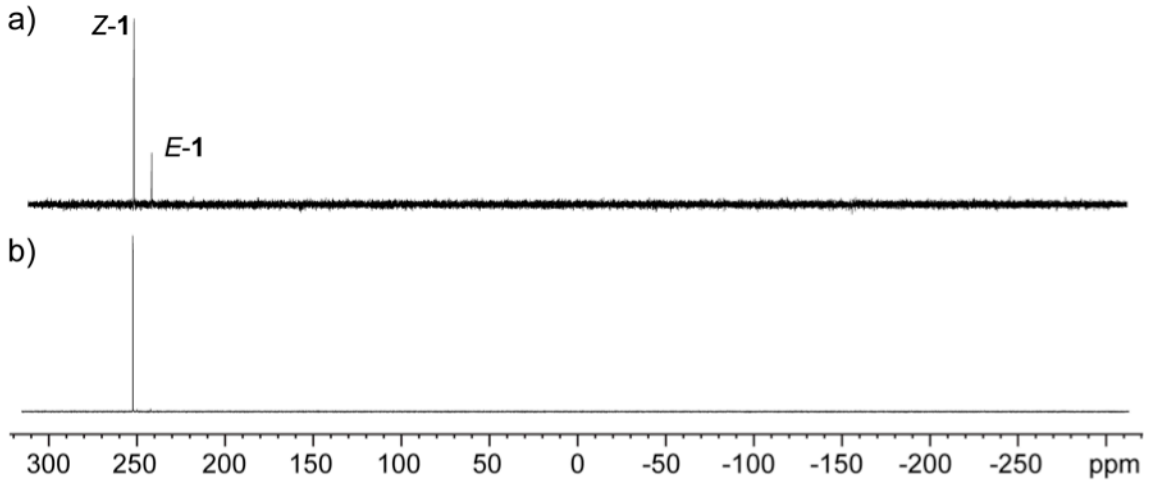

Figure C1: ^{31}P NMR (121 MHz, $CDCl_3$) spectra of a) crude reaction mixture of *E/Z*-3.1. b) *Z*-3.1 (121 MHz, C_6D_6) selectively crystalized from a saturated toluene solution.

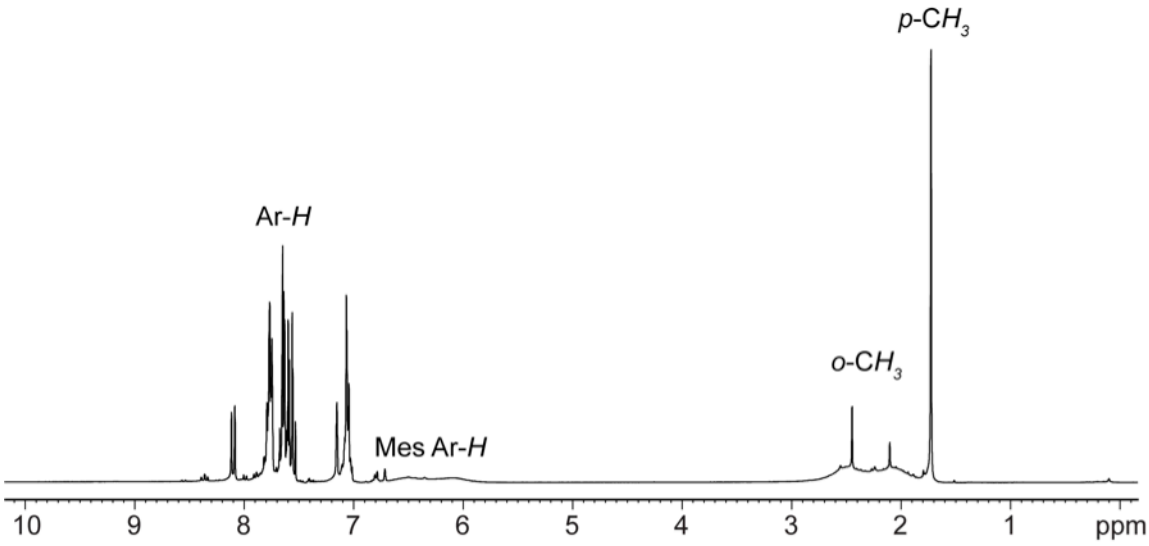

Figure C2: ^{1}H NMR (300 MHz, C_6D_6) spectrum of *Z*-3.1.

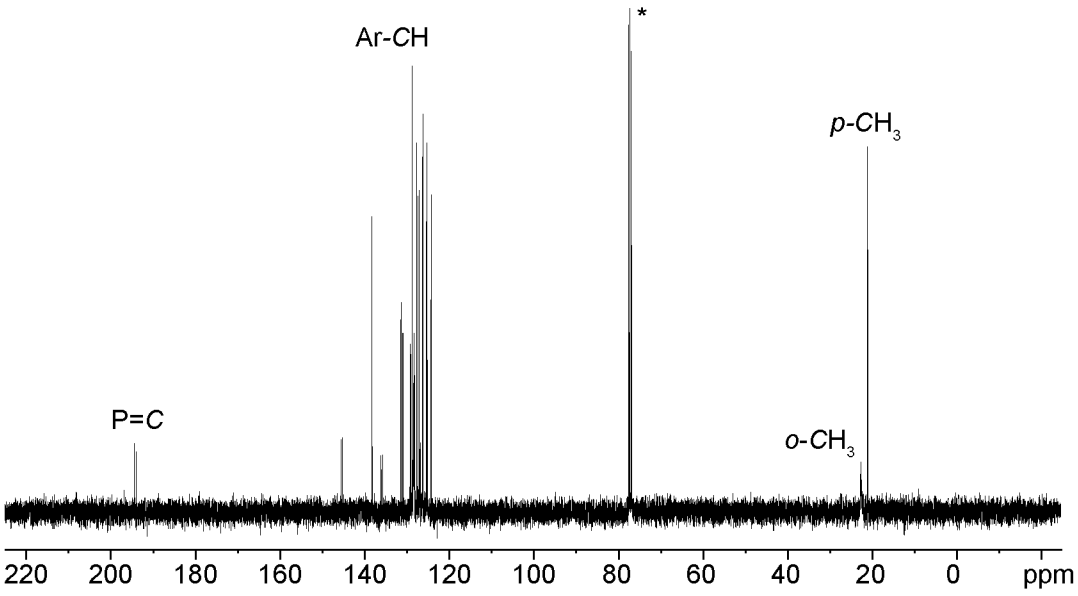

Figure C3: $^{13}C\{^{1}H\}$ NMR (101 MHz, $CDCl_3$) of *Z*-3.1, * = $CDCl_3$

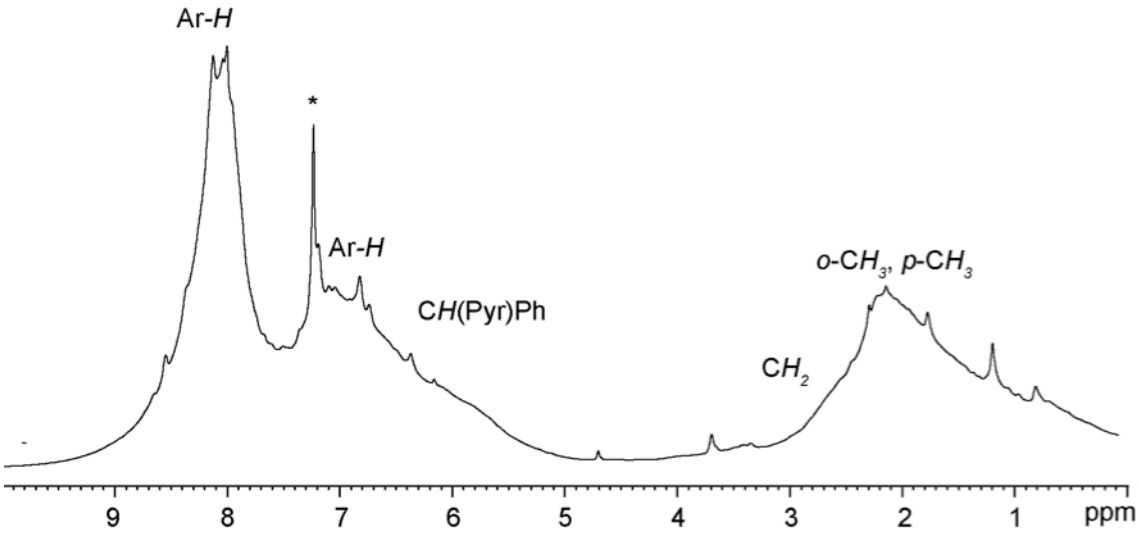

Figure C4: ^{1}H NMR (600 MHz, $CDCl_3$) spectrum of 3.2. * = residual $CHCl_3$

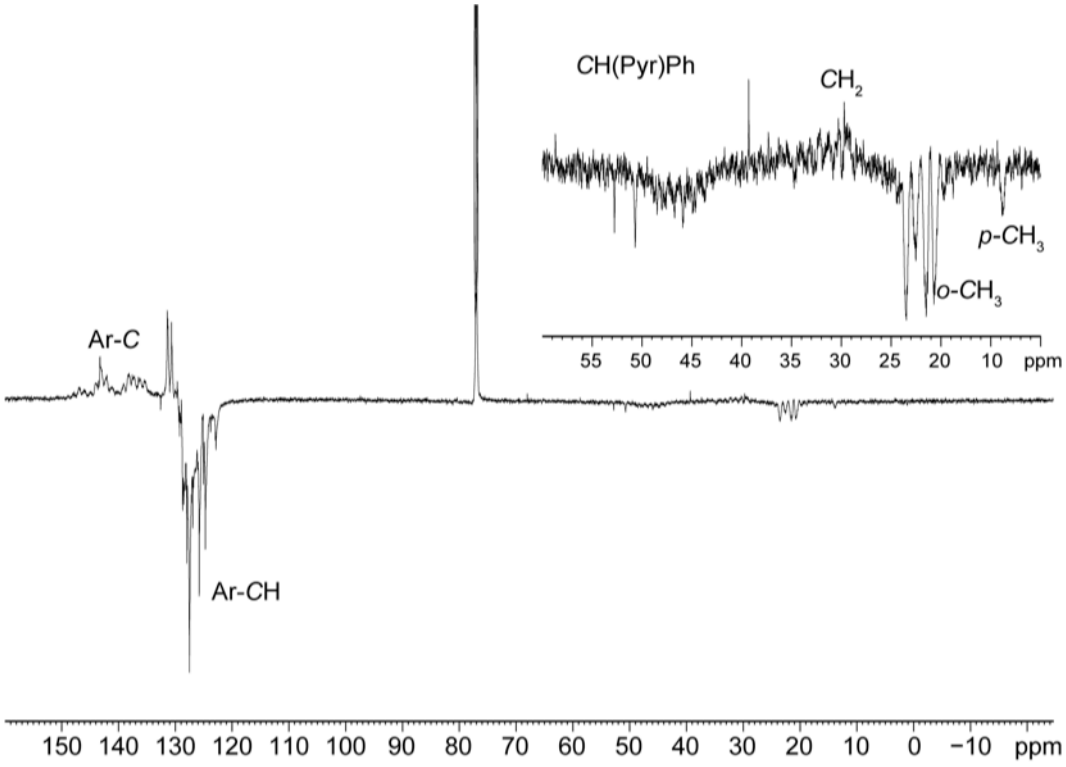

Figure C5: $^{13}C\{^{1}H\}$ NMR (151 MHz, $CDCl_3$) APT spectrum of 3.2.

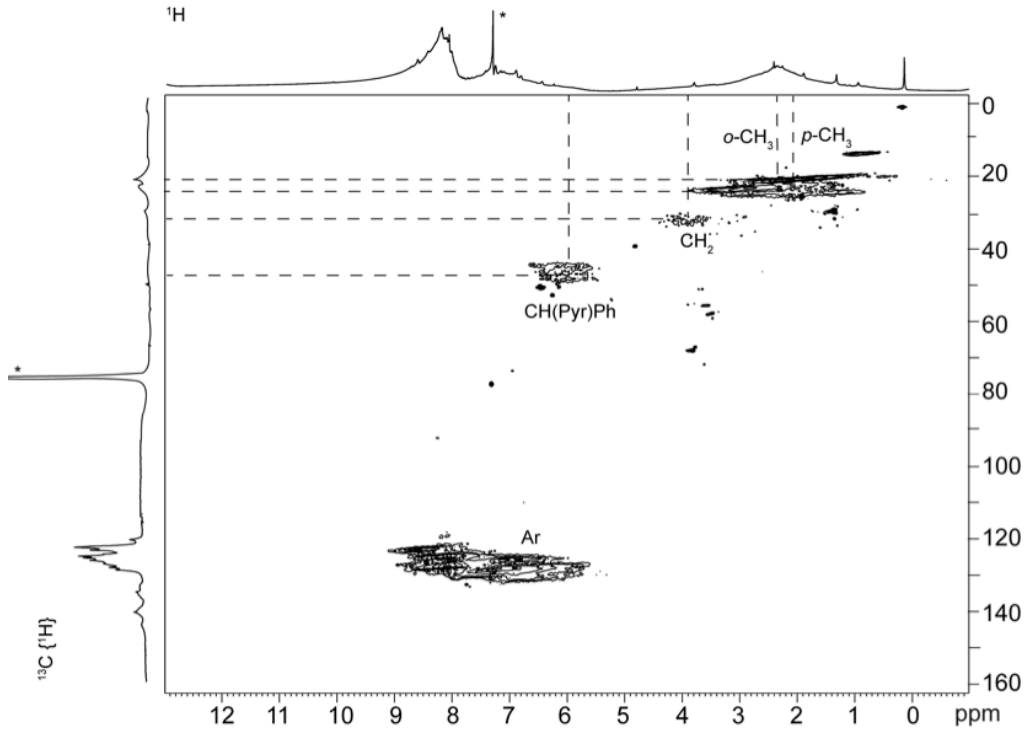

Figure C6: ^{1}H-^{13}C HSQC NMR (600 MHz for ^{1}H, $CDCl_3$) spectrum of 3.2.The ordinate shows the ^{13}C axis and the abscissa shows the ^{1}H axis.

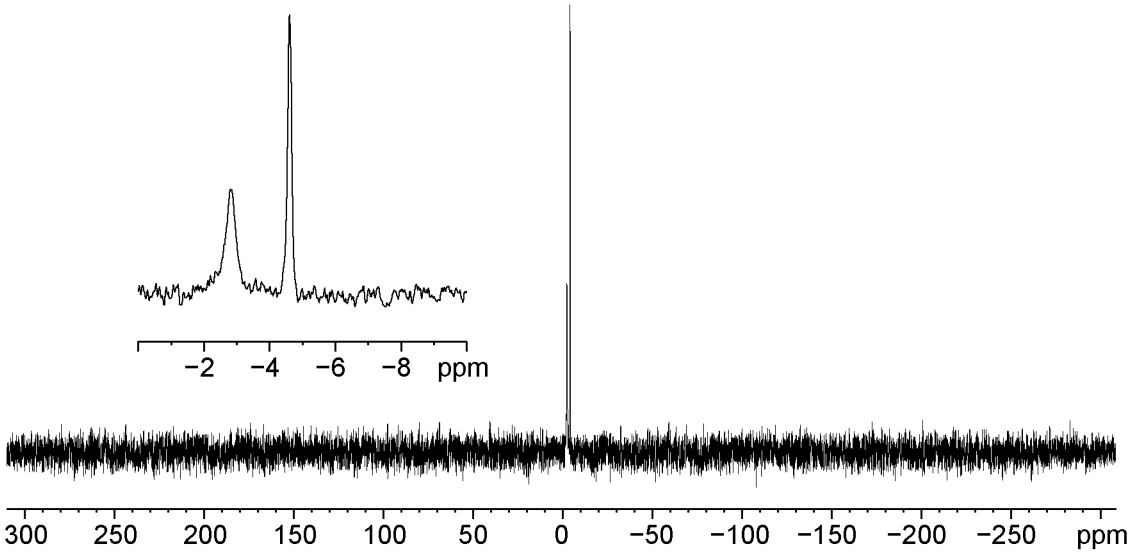

Figure C7: $^{31}P\{^{1}H\}$ NMR (121 MHz, $CDCl_3$) spectrum of Bn(Mes)P-CH(Pyr)Ph.

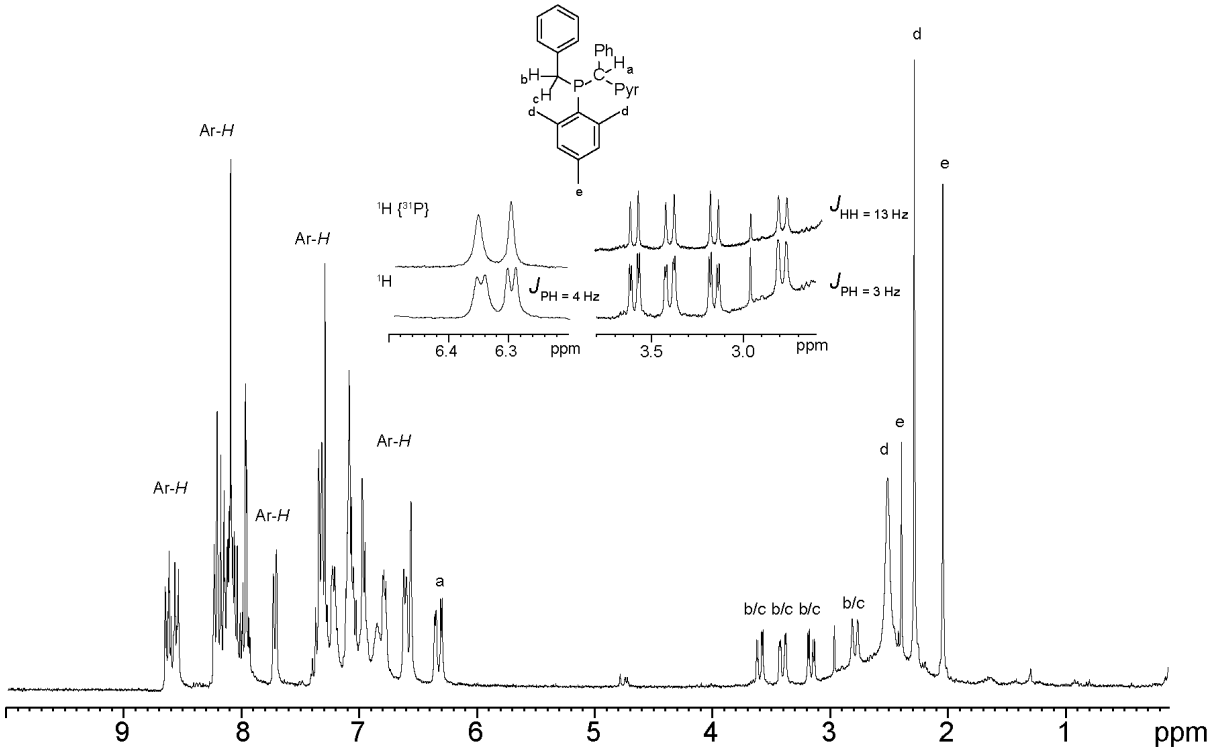

Figure C8: ^{1}H NMR (300 MHz, $CDCl_3$) spectrum of Bn(Mes)P-CH(Pyr)Ph, Assignments are tentative.

Appendix D: Supplementary Spectra for Chapter 4

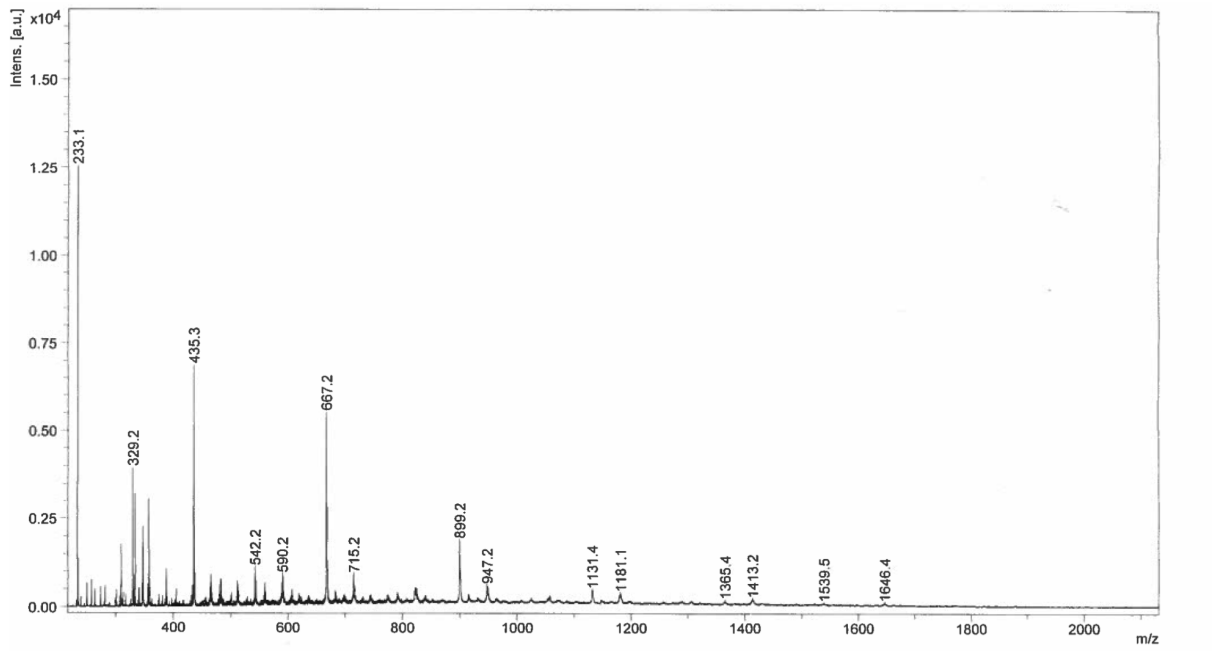

Figure D1: MALDI-TOF MS (DHB matrix) of 4.1a.

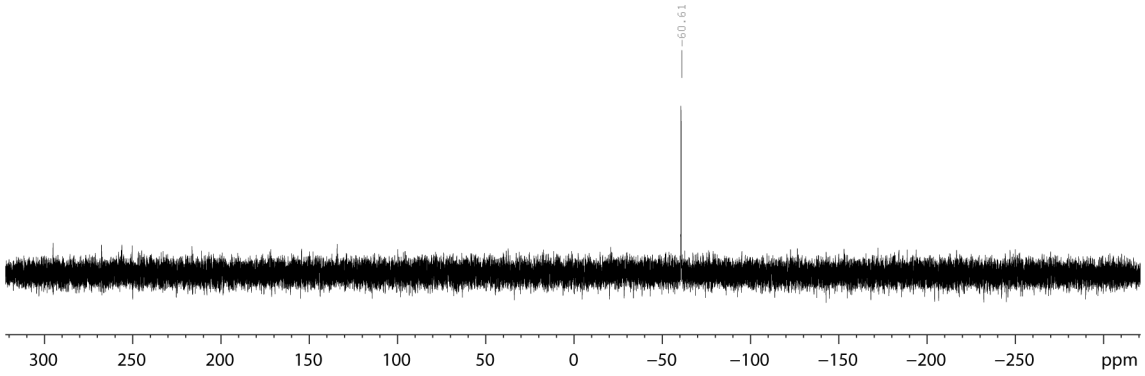

Figure D2. $^{31}P\{^{1}H\}$ NMR (121 MHz, $CDCl_3$) spectrum of soluble fraction from the synthesis of 4.1a (the majority is insoluble).

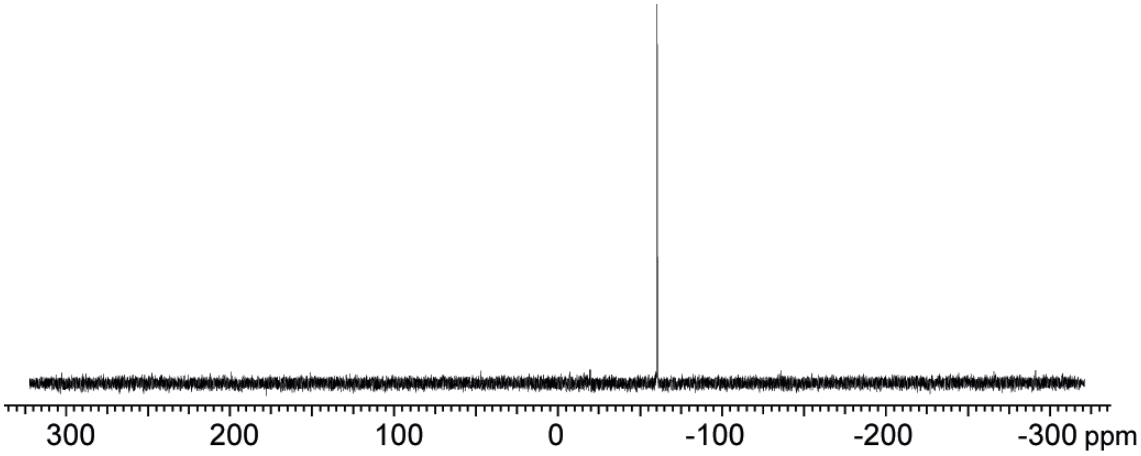

Figure D3: $^{31}P\{^{1}H\}$ NMR (121 MHz, $CDCl_3$) spectrum of 4.1b

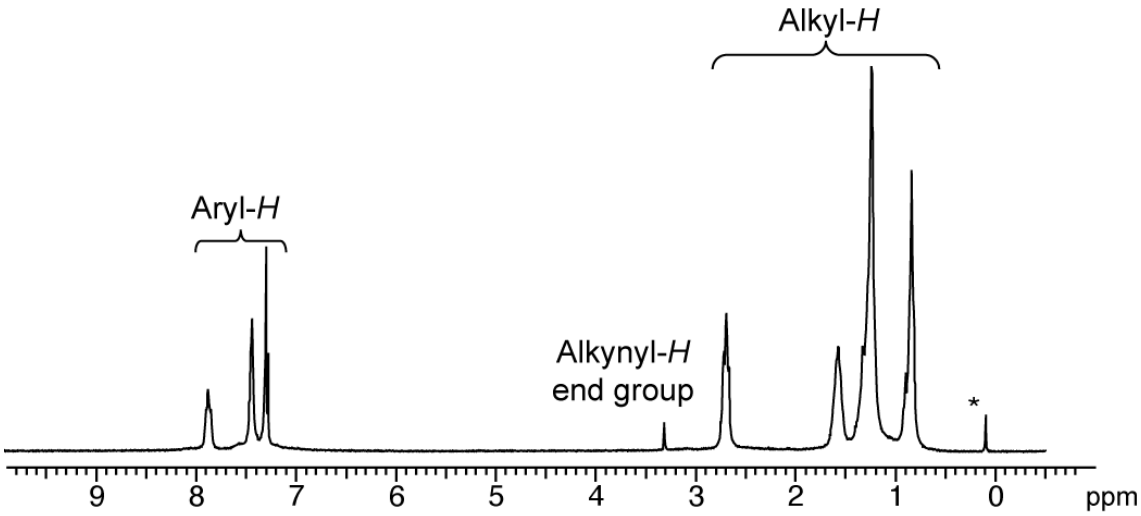

Figure D4. ^{1}H NMR (300 MHz, $CDCl_3$) spectrum of 4.1b (M_n = 6,600 g mol^{-1}, Đ = 1.8)

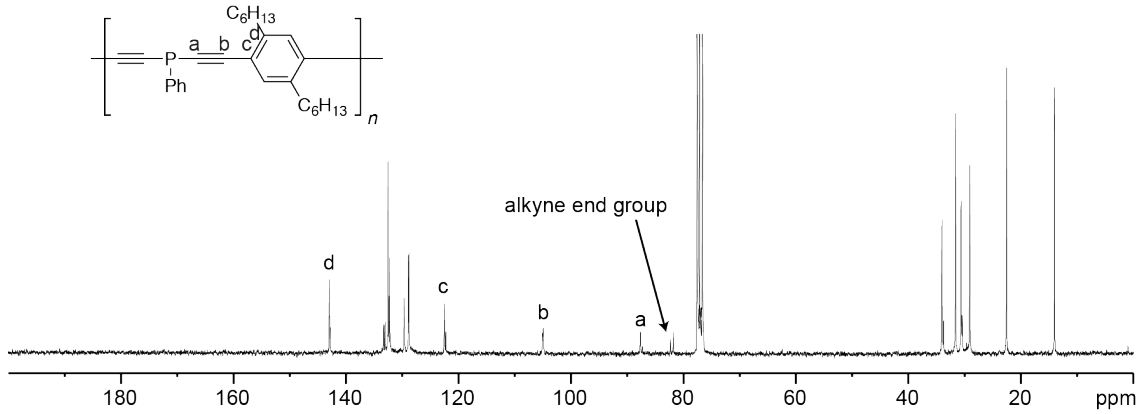

Figure D5: $^{13}C\{^{1}H\}$ NMR (75 MHz, $CDCl_3$) spectrum of 4.1b.

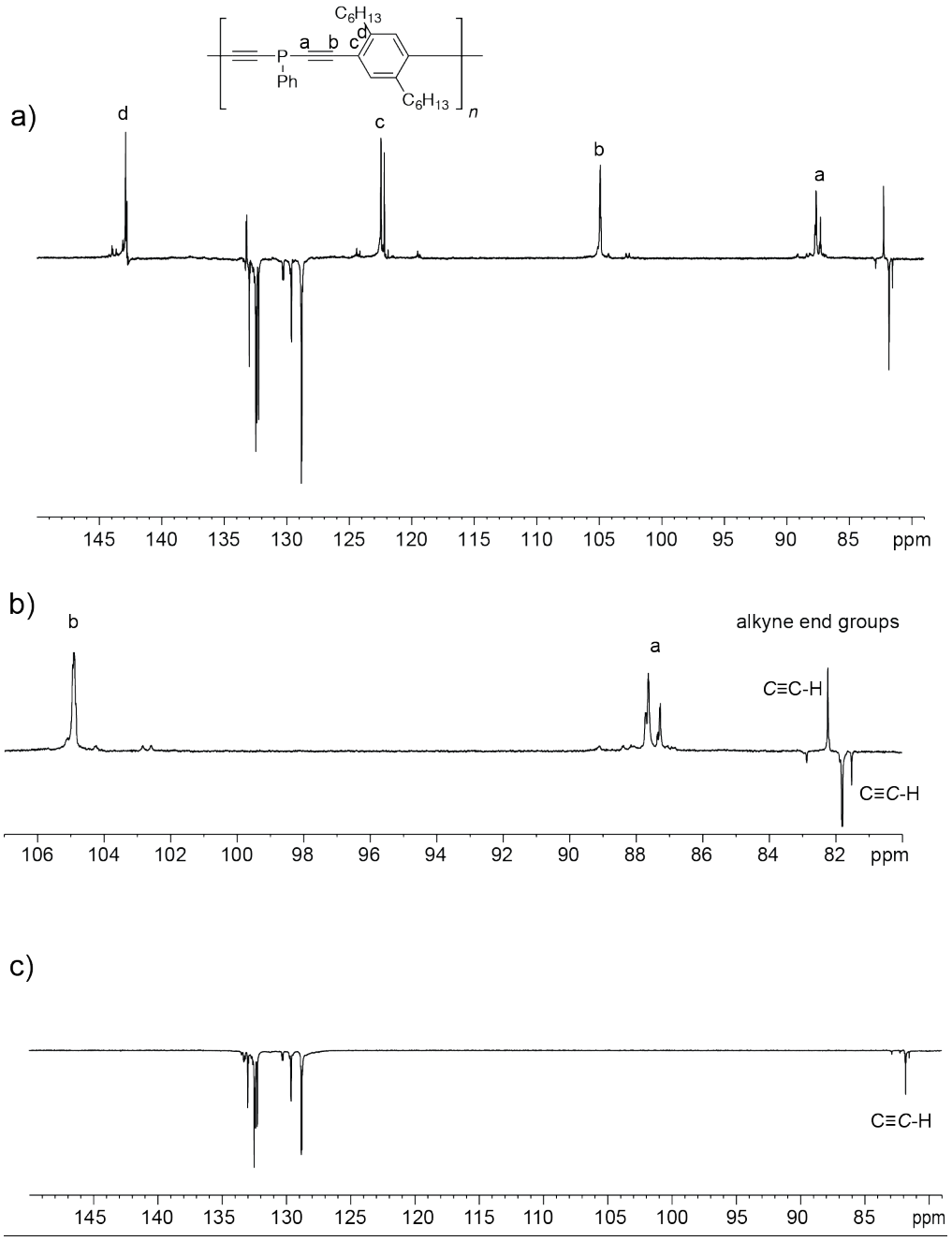

Figure D6: a) and b) ^{13}C APT NMR (151 MHz, $CDCl_3$) spectrum of 4.1b. c) DEPT 135 NMR (151 MHz, $CDCl_3$) spectrum of 4.1b.

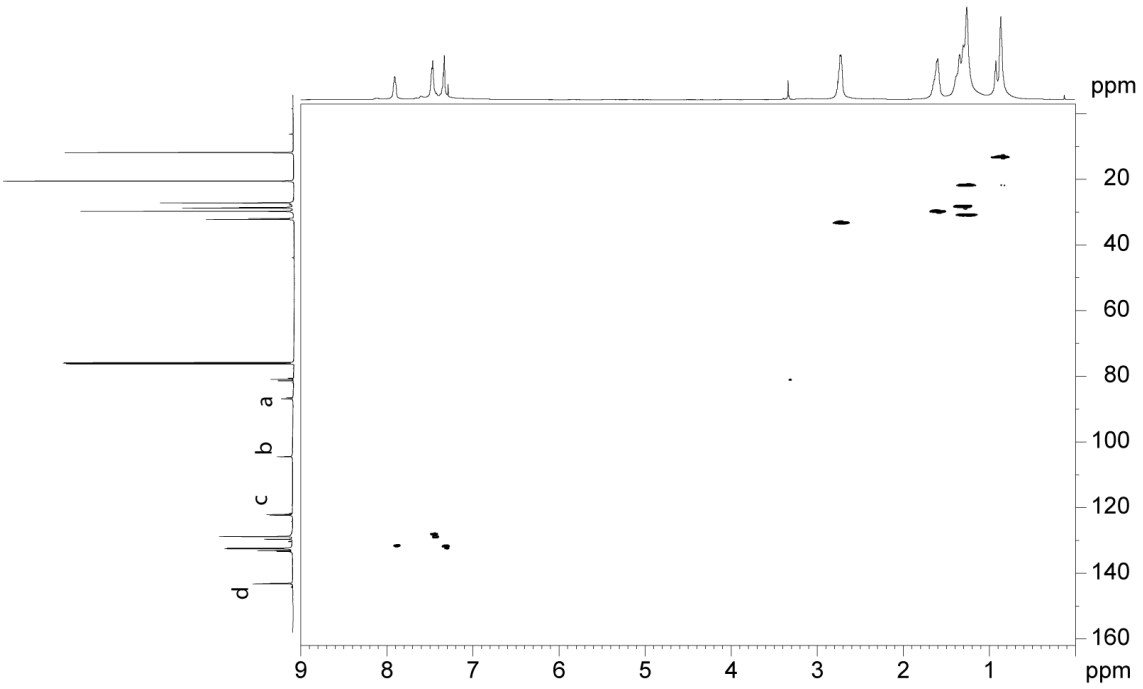

Figure D7: ^{1}H-^{13}C HSQC NMR (600 MHz for ^{1}H, $CDCl_3$) spectrum of 4.1b.

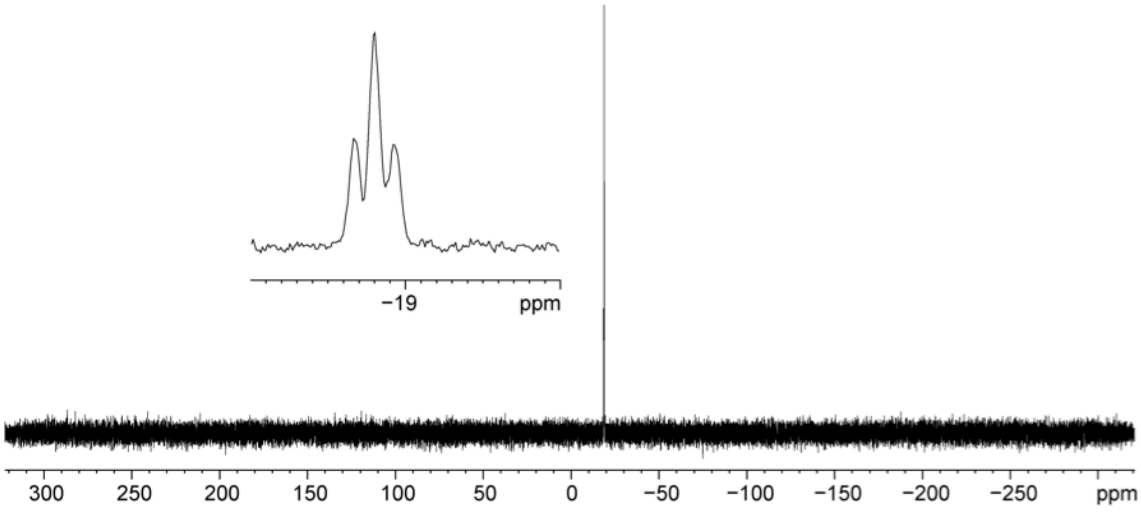

Figure D8: ^{31}P NMR (121 MHz, $CDCl_3$) spectrum of 4.2a·O.

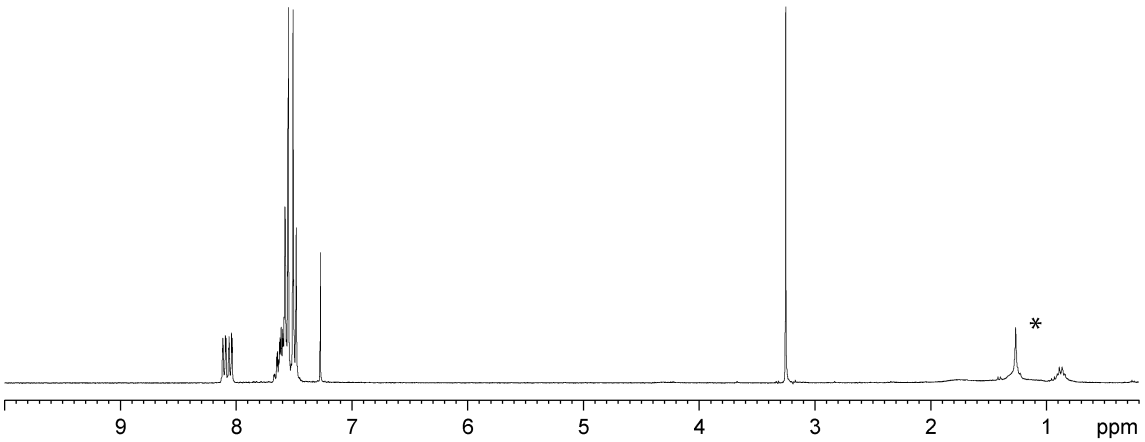

Figure D9: ^{1}H NMR (300 MHz, $CDCl_3$) spectrum of 4.2a·O. * = residue hexanes.

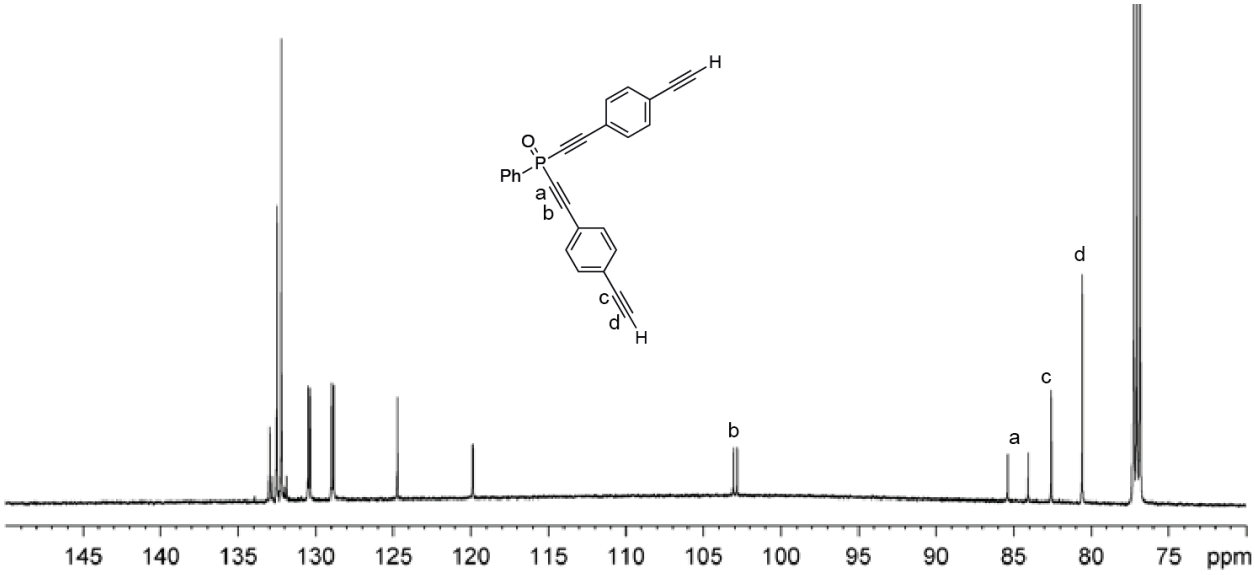

Figure D10: $^{13}C\{^{1}H\}$ NMR (75 MHz, $CDCl_3$) spectrum of 4.2a·O.

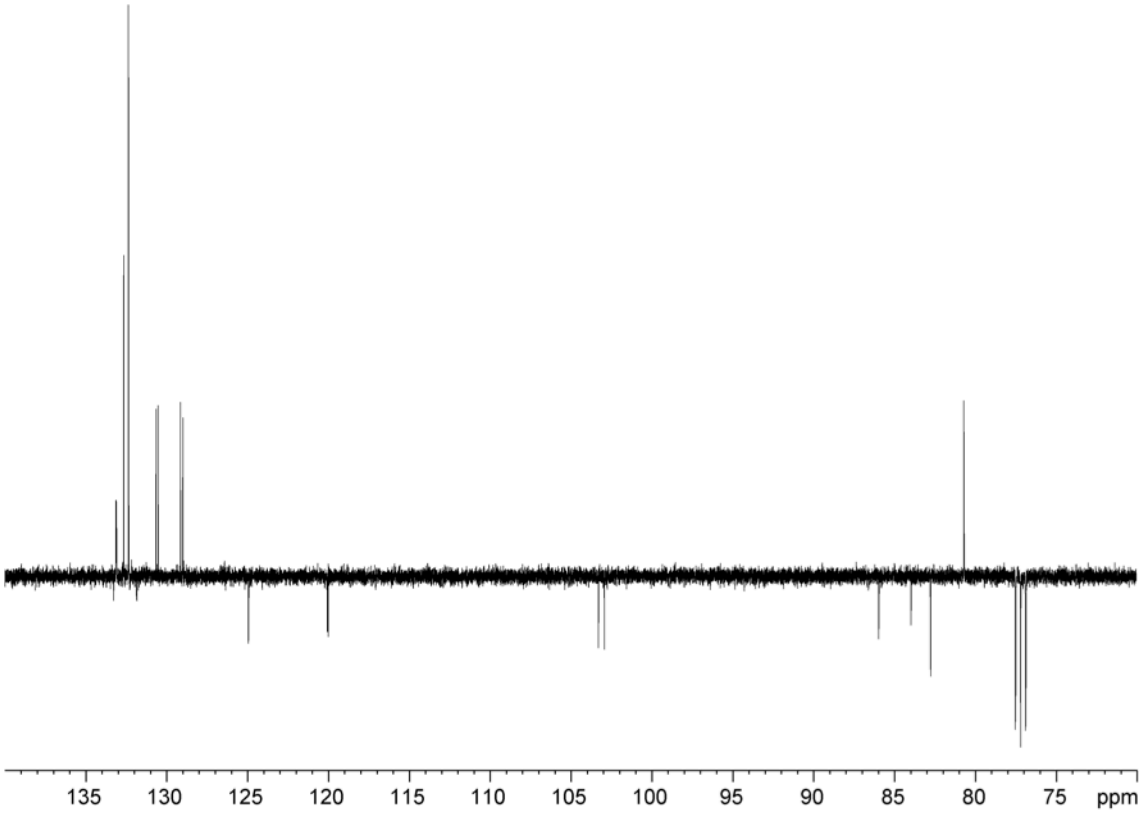

Figure D11: $^{13}C\{^{1}H\}$ APT (75 MHz, $CDCl_3$) spectrum of 4.2a·O.

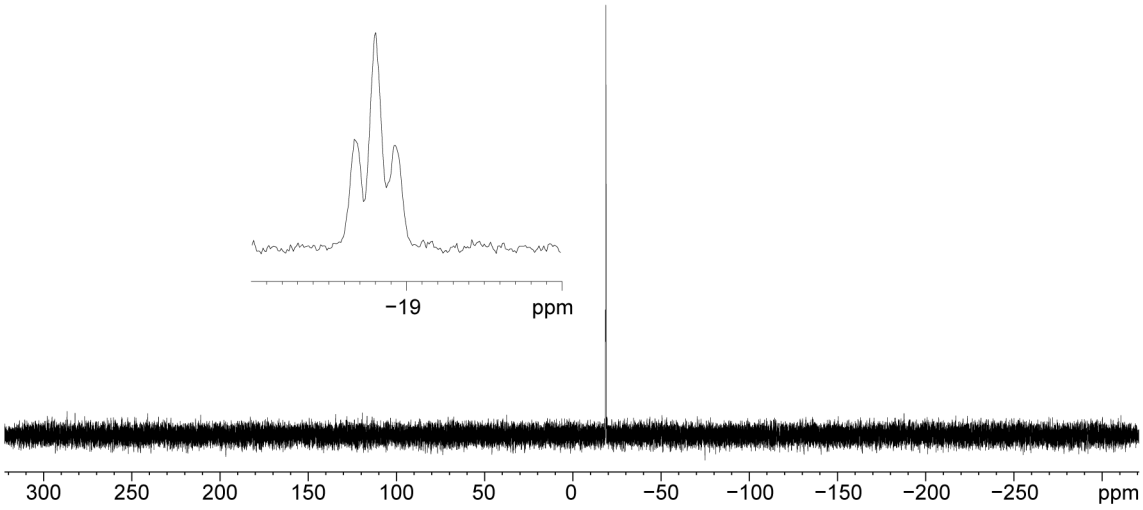

Figure D12: ^{31}P NMR (121 MHz, $CDCl_3$) spectrum of 4.2c·O

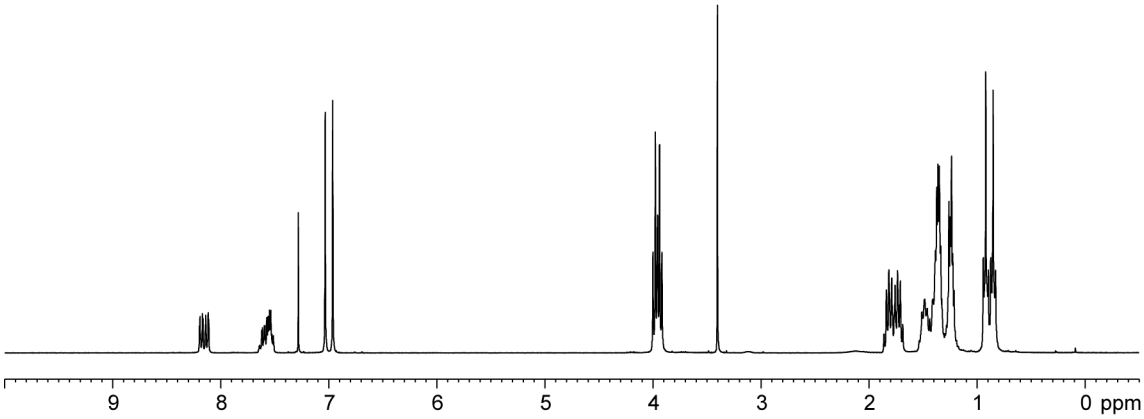

Figure D13: ^{1}H NMR (300 MHz, $CDCl_3$) spectrum of 4.2c·O.

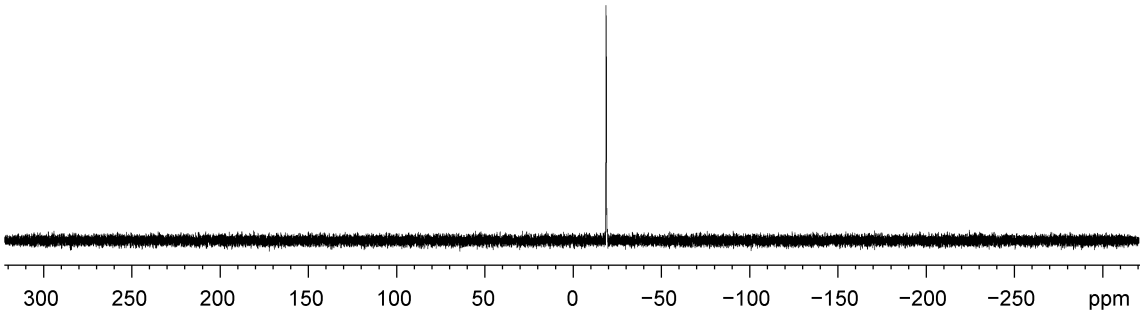

Figure D14: ^{31}P{^{1}H} NMR (162 MHz, $CDCl_3$) spectrum of 4.2d·O.

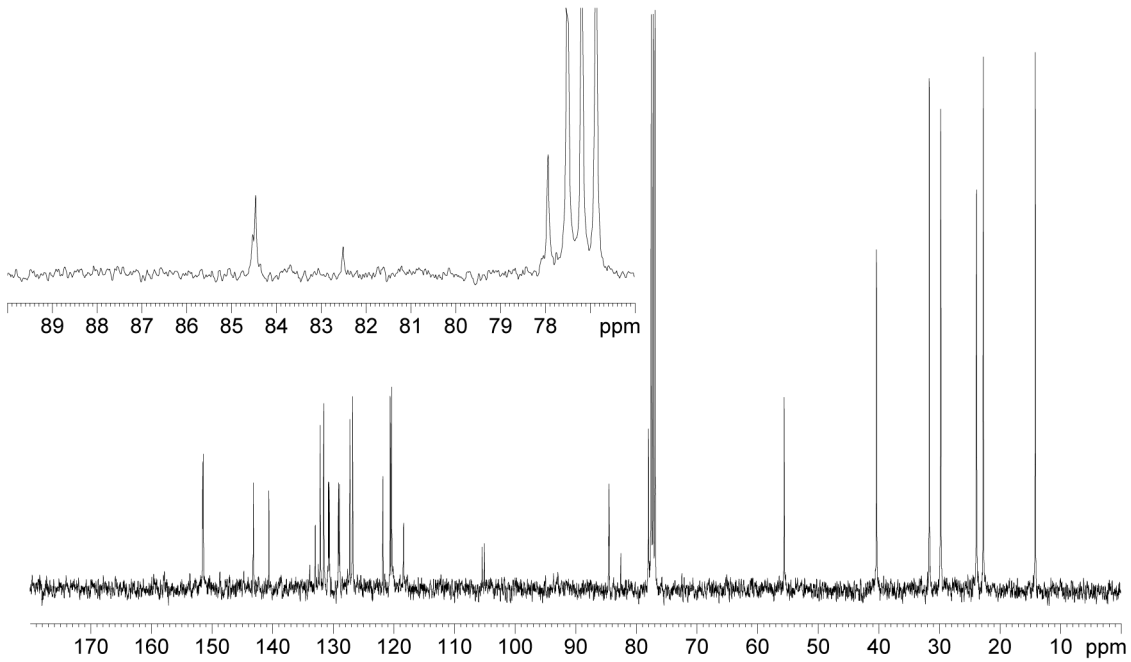

Figure D15. $^{13}C\{^{1}H\}$ NMR (101 MHz, $CDCl_3$) spectrum of 4.2d·O.

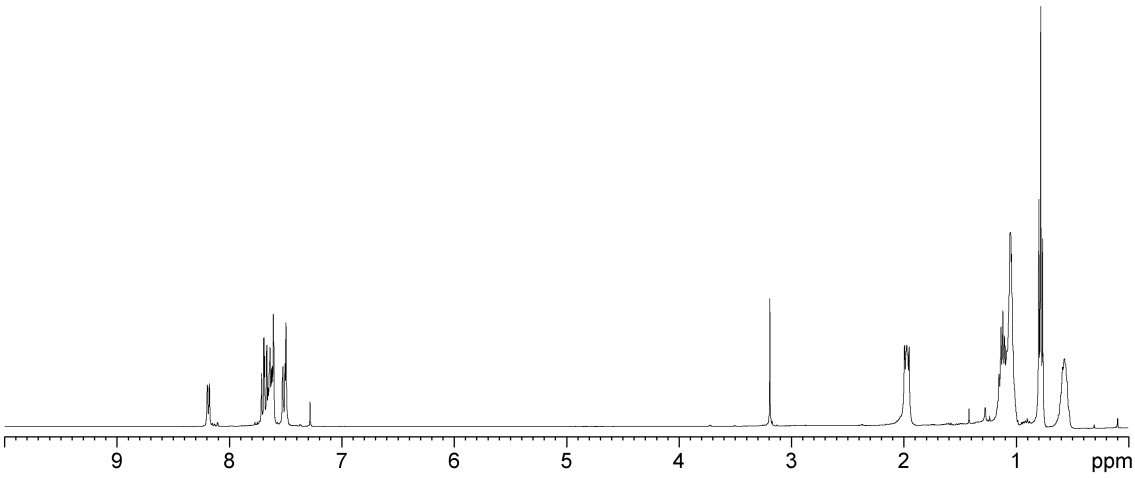

Figure D16. ^{1}H NMR (400 MHz, $CDCl_3$) spectrum of 4.2d·O.

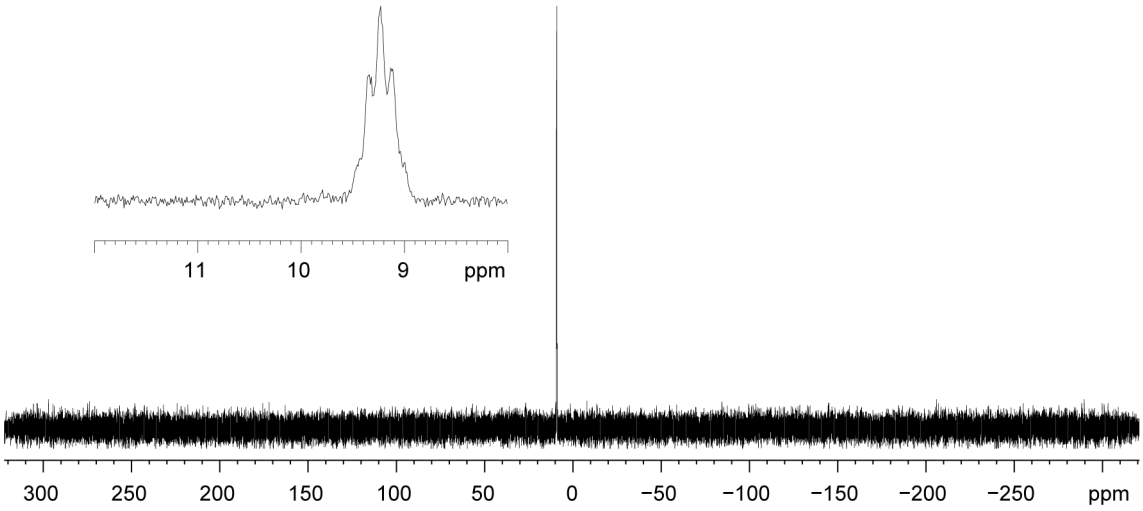

Figure D17: $^{31}P\{^{1}H\}$ NMR (121 MHz, $CDCl_3$) spectrum of 4.3c

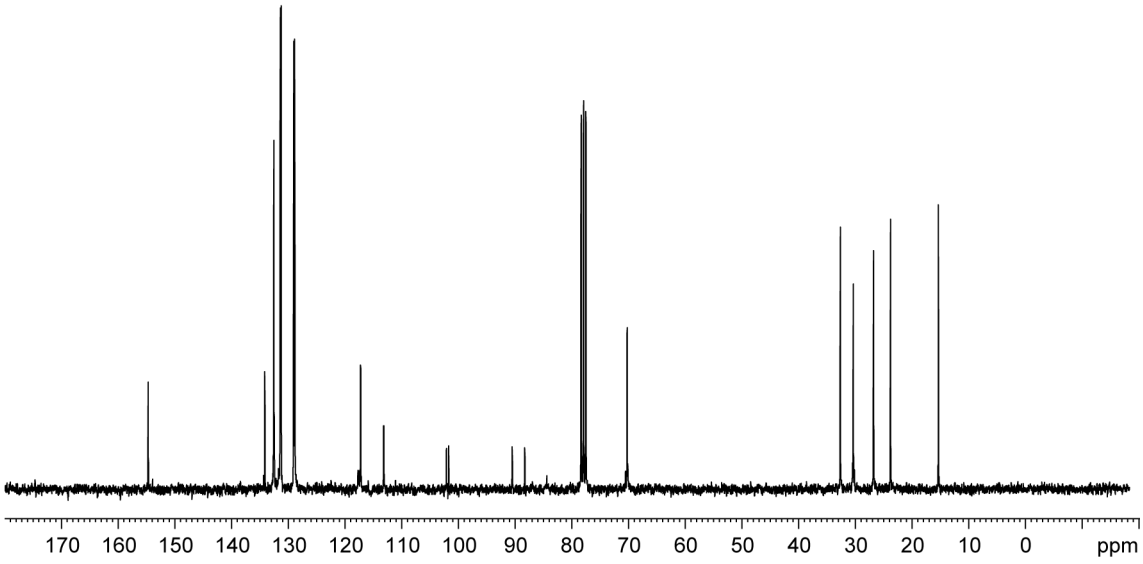

Figure D18: $^{13}C\{^{1}H\}$ NMR (75 MHz, $CDCl_3$) spectrum of 4.3c.

Appendix E: Supplementary Spectra for Chapter 5

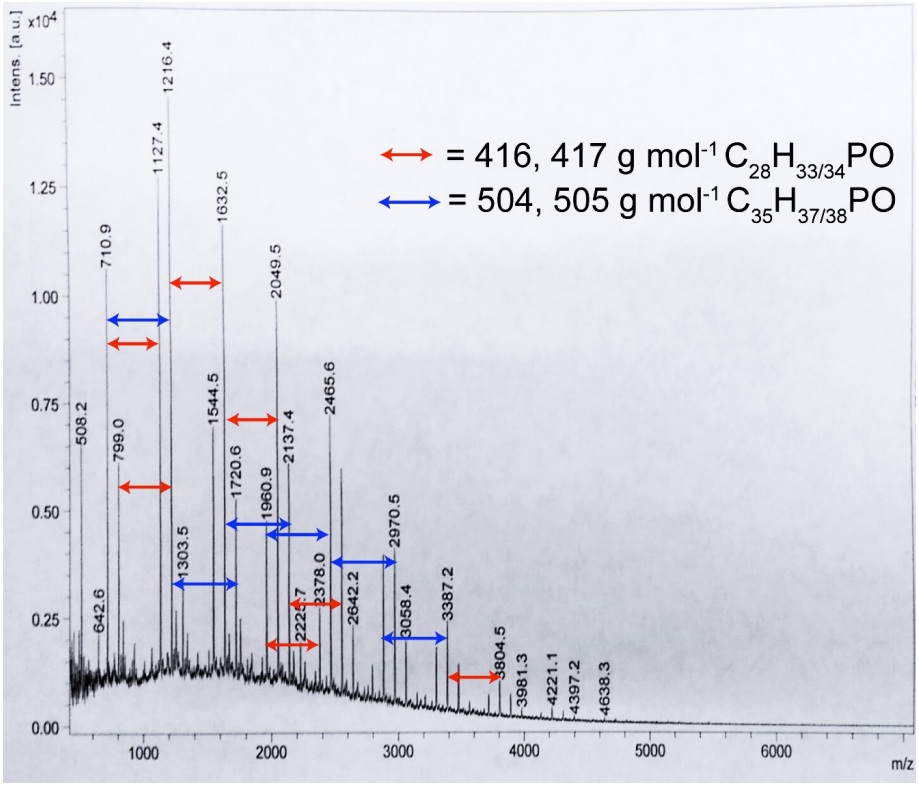

Figure E1: MALDI-TOF spectrum (dithranol matrix) of 5.1·O

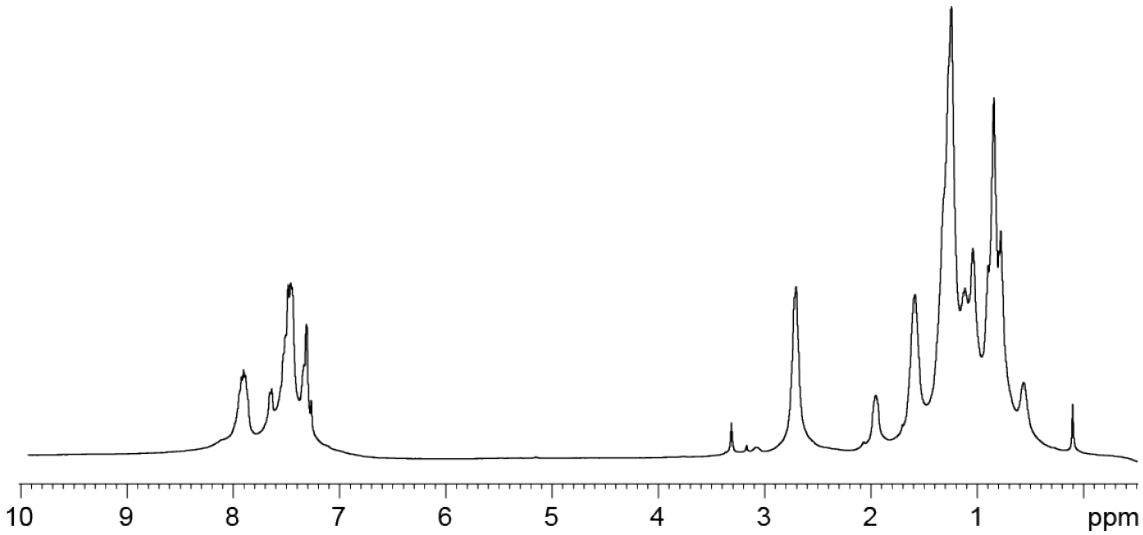

Figure E2: ^{1}H NMR (600 MHz, $CDCl_3$) spectrum of 5.1

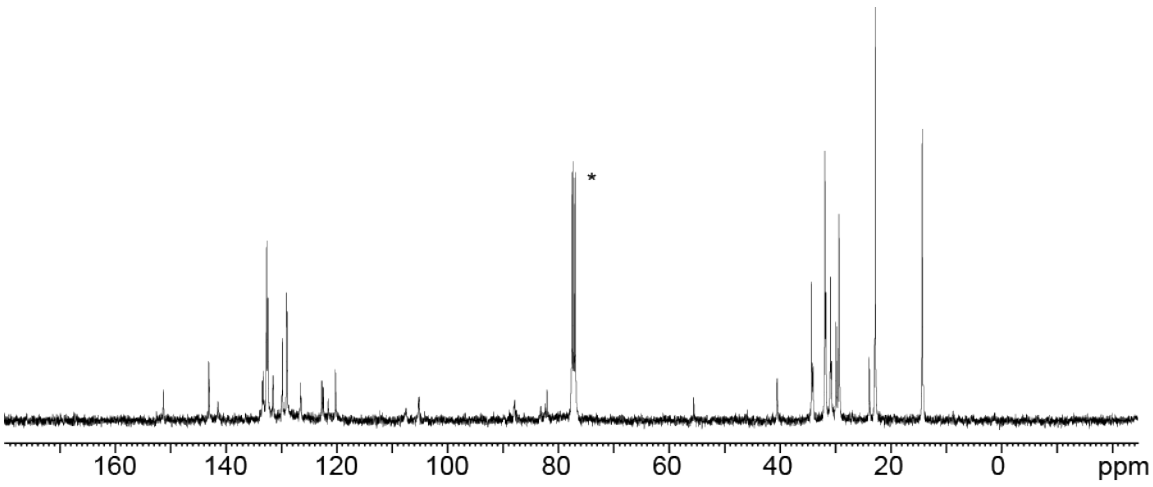

Figure E3: $^{13}C\{^{1}H\}$ NMR (151 MHz, $CDCl_3$) spectrum of 5.1. *$CDCl_3$

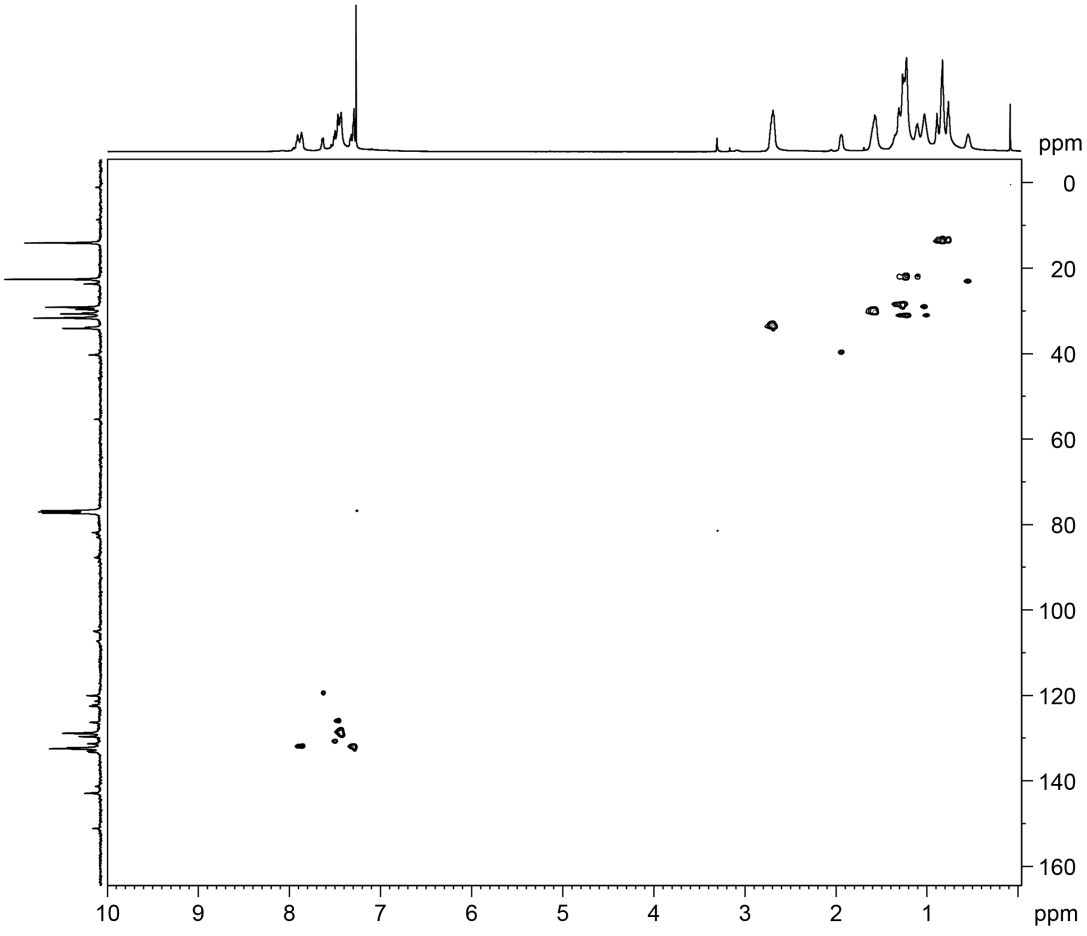

Figure E4: ^{1}H-^{13}C HSQC NMR (600 MHz for ^{1}H, $CDCl_3$) spectrum of 5.1.

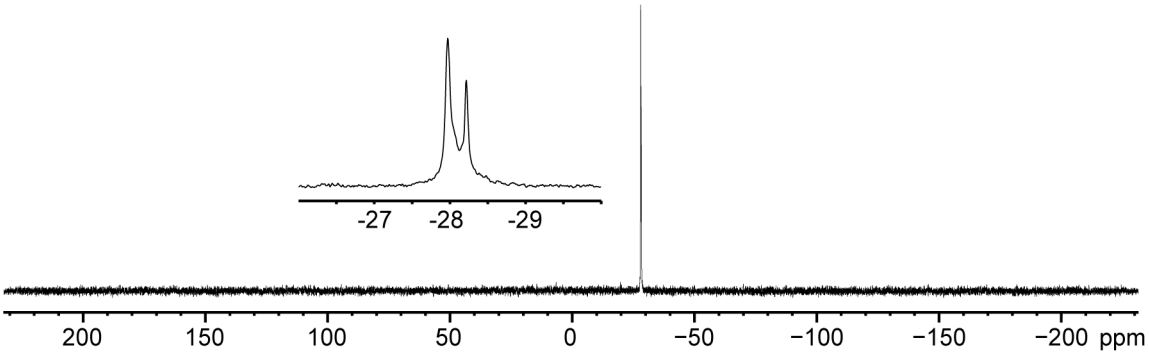

Figure E5: $^{31}P\{^{1}H\}$ NMR (162 MHz, $CDCl_3$) spectrum of 5.1·AuCl

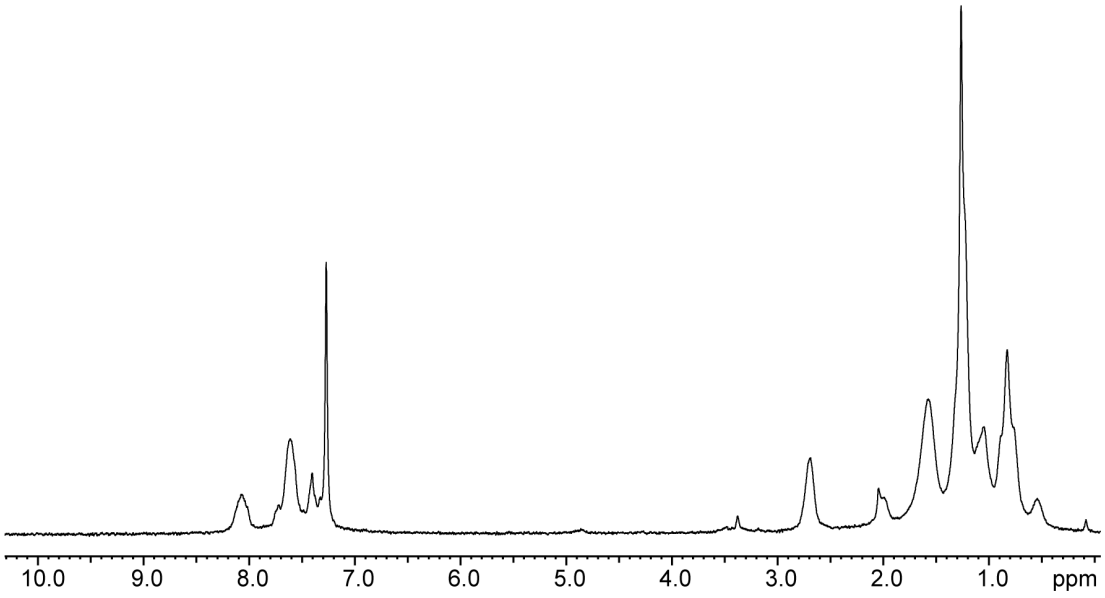

Figure E6: ^{1}H NMR (300 MHz, $CDCl_3$) spectrum of 5.1·AuCl